

Journal of Polymer Science

Part A-1: Polymer Chemistry

Contents

YUZO YAMAZAWA, TADASHI IWAI, AKIHIKO ITO, and KOICHIRO HAYASHI: Radiation-Induced Solid-State Polymerization of Trioxane under High Pressure	257
J. M. HAMMOND, J. F. HOOPER, and W. G. P. ROBERTSON: Cationic Copolymerization of Tetrahydrofuran with Epoxides. I. Polymerization Mechanism in the Presence of a Glycol	265
J. M. HAMMOND, J. F. HOOPER, and W. G. P. ROBERTSON: Cationic Copolymerization of Tetrahydrofuran with Epoxides. II. Characterization and Gel-Permeation Chromatography of By-Products Formed during Polymerization	281
J. M. HAMMOND, J. F. HOOPER, and W. G. P. ROBERTSON: Cationic Copolymerization of Tetrahydrofuran with Epoxides. III. Synthesis of Block Copolymers	295
JUNJI FURUKAWA, TOSHIO KITAO, SHINZO YAMASHITA, and SEIGO OHYA: Orientation of Polymer Molecules during Melt Spinning. I. Estimation of Degree of Orientation By Retraction above T_m	299
R. D. GLAUZ: Transient Analysis of a Viscoelastic Torsion Pendulum: Error Analysis	311
S. R. RICCIETIELLO, G. M. FOHLEN, and J. A. PARKER: Thermal Reactions of <i>N,N'</i> Bis(<i>p</i> -nitrophenyl)sulfamide and <i>p</i> -Benzoquinone Dioxime-Acid Mixtures	317
T. KONOMI and H. TANI: Al(Cap) ₃ as Initiator in the Anionic Polymerization of ϵ -Caprolactam at High Temperature	325
HIROYOSHI KAMOGAWA: Syntheses and Properties of Photochromic Polymers of the Mercury Thiocarbonates Series	335
V. D. MOCHEL and W. E. CLAXTON: Reduction of Composite NMR Spectra by Using an Analog Computer	345
H. F. HAMIL, L. D. ADAMS, W. W. HARLOWE, JR., and E. C. MARTIN: Irradiation-Grafted Polymeric Films. I. Preparation and Properties of Acrylic Acid-Grafted Polyethylene Films	363
F. LAUTENSCHLAGER: Structure of Polymers Obtained from Sulfur Monochloride and Olefins Containing Sulfonium Salt Structures	377
HAJIME SUZUKI: Sequence Distribution of Poly(ether)urethane Elastomer	387
PRANAB C. BANDYOPADHYAY and ASOKE K. DAS: Some Studies on a Polymer from Urea	395
J. SZITA and C. S. MARVEL: Partial Ladder Polymers with Anthraquinone Units. Reaction of 1,2,5,6-Tetraaminoanthraquinone with <i>p</i> -Benzoquinone Derivatives	415
KENKICHI MURAKAMI and SABURO TAMURA: Chemorheological Treatment of Crosslinked EPT	423
YOSHIKI KOBUKE, KATSUMI HANJI, JUNJI FURUKAWA, and TAKAYUKI FUENO: Hydrogen-Transfer Polymerization of <i>cis</i> - and <i>trans</i> -Crotonamides	431

(continued inside)

Journal of Polymer Science: **Part A-1: Polymer Chemistry**

Board of Editors: H. Mark • C. G. Overberger • T. G. Fox

Advisory Editors:

R. M. Fuoss • J. J. Hermans • H. W. Melville • G. Smets

Editor: C. G. Overberger **Associate Editor:** E. M. Pearce

Advisory Board:

T. Alfrey, Jr.	N. D. Field	R. W. Lenz	C. C. Price
W. J. Bailey	F. C. Foster	Eloisa Mano	B. Rånby
John Boor, Jr.	H. N. Friedlander	C. S. Marvel	J. H. Saunders
F. A. Bovey	K. C. Frisch	F. R. Mayo	C. Schuerch
J. W. Breitenbach	N. G. Gaylord	R. B. Mesrobian	W. H. Sharkey
W. J. Burlant	W. E. Gibbs	Donald Metz	V. T. Stannett
G. B. Butler	A. R. Gilbert	H. Morawetz	J. K. Stille
S. Bywater	M. Goodman	M. Morton	M. Szwarc
W. L. Carrick	J. E. Guillet	James Mulvaney	A. V. Tobolsky
H. W. Coover, Jr.	George Hulse	S. Murahashi	E. J. Vandenberg
W. H. Daly	Otto Kauder	G. Natta	Herbert Vogel
F. Danusso	J. P. Kennedy	K. F. O'Driscoll	L. A. Wall
F. R. Eirich	W. Kern	S. Okamura	O. Wichterle
E. M. Fettes	J. Lal	P. Pino	F. H. Winslow

Contents (continued)

R. C. POTTER and D. J. METZ: γ -Radiation-Induced Ionic Polymerization of Pure Liquid Styrene. III. Effect of Temperature.....	441
YOSHIKI NAKASE, MASARU YOSHIDA, AKIHIKO ITO, and KOICHIRO HAYASHI: Radiation-Induced Polymerization of Tetraoxane in the Solid State.....	465
KIICHIRO MATSUMURA and OSAMU FUKUMOTO: Copolymerization of Propylene with Acrylate by a Ziegler-Natta Type Catalyst.....	471
KIICHIRO MATSUMURA, YUJI ATARASHI, and OSAMU FUKUMOTO: Polymerization of Propylene by the Three-Component System Comprising Titanium(III) Chloride, Ethylaluminum Sesquichloride, and Sodium Sulfate.....	485
EMMANUEL J. ZAGANARIS: Thermoplastic Elastomers via Radical Polymerization. II.....	497
O. F. SOLOMON, M. CORCIOVEI, I. GABE and E. BERAL: Polymerization of Asymmetric Polyfunctional Monomers. III. Ionic Polymerization of Acrylic and Methacrylic Esters of 2-Allylphenol.....	509

(continued on inside back cover)

The Journal of Polymer Science is published in four sections as follows: Part A-1, Polymer Chemistry, monthly; Part A-2, Polymer Physics, monthly; Part B, Polymer Letters, monthly; Part C, Polymer Symposia, irregular.

Published monthly by Interscience Publishers, a Division of John Wiley & Sons, Inc., covering one volume annually. Publication Office at 20th and Northampton Sts., Easton, Pa. 18042. Executive, Editorial, and Circulation Offices at 605 Third Avenue, New York, N. Y. 10016. Second-class postage paid at Easton, Pa. Subscription price, \$325.00 per volume (including Parts A-2, B, and C). Foreign postage \$15.00 per volume (including Parts A-2, B, and C).

Copyright © 1971 by John Wiley & Sons, Inc. All rights reserved. No part of this publication may be reproduced by any means, nor transmitted, or translated into a machine language without the written permission of the publisher.

Radiation-Induced Solid-State Polymerization of Trioxane under High Pressure

YUZO YAMAZAWA, TADASHI IWAI, AKIHIKO ITO, and KOICHIRO HAYASHI, *Takasaki Radiation Chemistry Research Establishment, Japan Atomic Energy Research Institute, Takasaki, Gunma, Japan*

Synopsis

The in-source polymerization of trioxane in the solid state was investigated over a wide range of temperature and pressure, i.e., from 30 to 140°C and up to 7000 kg/cm², respectively. In the polymerization that was carried out slightly below the melting point under pressure, the higher the pressure, the higher the rate of polymerization. It was confirmed that the maximum rate of solid-state polymerization of trioxane occurs near the melting points, even under elevated pressure. The rate of polymerization decreased with increasing pressure at constant temperature. The shape of the time-conversion curves may be classified into two types, i.e., one which is typical of high pressure and low temperature, and the other which is typical of low pressure and high temperature. Changes in the shape of the conversion-intrinsic viscosity curves occurred coincidentally. Thus, three regions for the different "polymerization characteristic" were determined as functions of polymerization temperature and pressure. Explanations are given for the above-mentioned polymerization characteristic.

Introduction

Two papers have been published on the radiation-induced solid-state polymerization of trioxane under high pressure,^{1,2} but the polymerization temperatures were kept in the range in which trioxane is solid under atmospheric pressure, i.e., 45 and 55°C. It was reported that the radiation-induced polymerization of trioxane and some other cyclic ethers and esters can be accomplished only in the solid state and that the maximum conversion rate occurs at a temperature slightly below the melting point.³⁻⁶ Since the melting point may be raised considerably as the pressure increases, it was of interest to examine the polymerization of trioxane under high pressure. In the present study, melting points of trioxane under various pressures were measured, and the in-source polymerization in the solid state was investigated over a comparatively wide range of temperature and pressure.

Experimental

The polymerization of trioxane was carried out in a cylinder to which pressures up to 15,000 kg/cm² could be applied by a piston. The pressure

calibration was made by observing transitions for benzene,⁷ *n*-octane,⁸ *n*-decane,⁸ and chloroform.⁹ The following method was used. Transition pressures were determined by measuring the volume change of the standard materials which were pressurized at the constant temperatures. The temperature of the apparatus was regulated by circulating through a jacket water of known temperature, or by controlling the current through a heating mantle. The temperature of the cylinder was measured with a thermister which was inserted into the wall.

Trioxane contained 24 ppm of water, 21 ppm of formaldehyde, and 47 ppm of formic acid. It was subjected to γ -ray irradiation from a Co⁶⁰ source of 9000 Ci placed under the cylinder. The irradiation dose rate was always 5.6×10^4 R/hr, determined by ferrous sulfate dosimetry. The trioxane was placed directly in the cylinder kept at a given temperature and irradiated after pressurization for 10–30 min. The polymer was washed with methanol or acetone, and the percentage conversion was determined after drying *in vacuo*. The intrinsic viscosities of the polymers were measured at 60°C after the polymer samples had been dissolved in *p*-chlorophenol containing 2% α -pinene at 115°C for 20 min.

Results and Discussion

The melting points of trioxane under high pressure (Fig. 1) were determined by observing the volume change as mentioned above. It was reported that the radiation-induced polymerization of trioxane and some other cyclic ethers and esters such as 3,3-bis(chloromethyl)cycloxabutane, β -propiolactone can be accomplished only in the solid state and that the

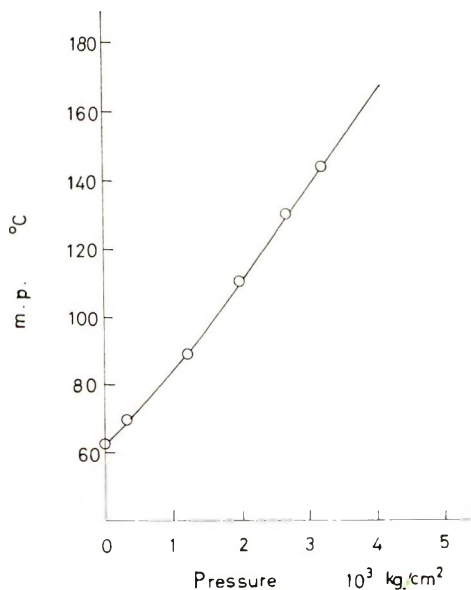


Fig. 1. Melting point of trioxane.

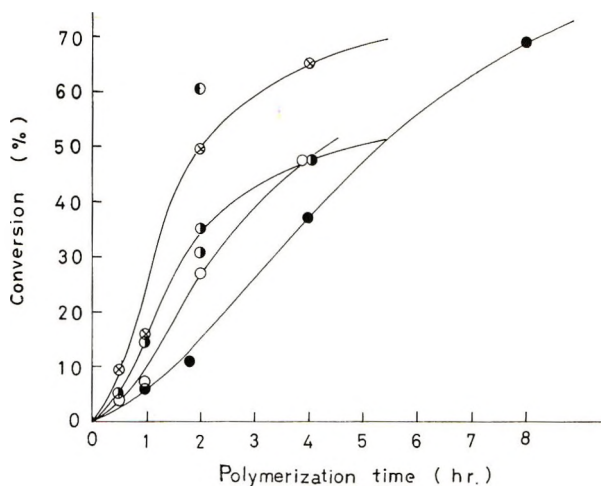


Fig. 2. Radiation-induced polymerization of trioxane at temperatures slightly below melting points under various pressures: (●) 1 kg/cm², 55°C; (○) 1000 kg/cm², 70°C; (●) 2000 kg/cm², 100°C; (⊗) 2500 kg/cm², 115°C; (●) 3500 kg/cm², 140°C.

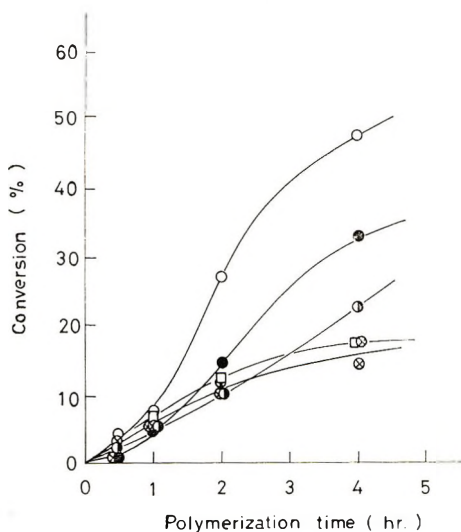


Fig. 3. Radiation-induced polymerization of trioxane under various pressures at 70°C: (○) 1000 kg/cm²; (●) 2000 kg/cm²; (●) 3500 kg/cm²; (⊗) 5000 kg/cm²; (□) 7000 kg/cm².

maximum conversion rate occurs at a temperature slightly below the melting point. Therefore, it is interesting to examine if the relationship between the polymerization temperature and the rate under high pressures is similar to that under atmospheric pressure and whether the above mentioned maximum conversion rate increases or decreases when the pressure is increased. Figure 2 shows the results of polymerization that was carried out at temperatures slightly below the melting points under various pressures.

The higher the pressure, the higher the rate of the polymerization. This fact may indicate that the effect of temperature that activates the motion of monomer molecules predominates over the effect of pressure that suppresses the motion. Trioxane was scarcely polymerized without irradiation under

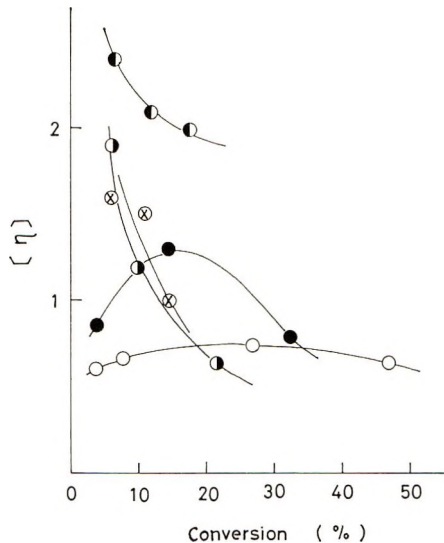


Fig. 4. Relationship between conversion and intrinsic viscosity of polyoxymethylene obtained by radiation-induced polymerization of trioxane at 70°C under various pressures: (○) 1000 kg/cm²; (●) 2000 kg/cm²; (●) 3500 kg/cm²; (⊗) 5000 kg/cm²; (●) 7000 kg/cm².

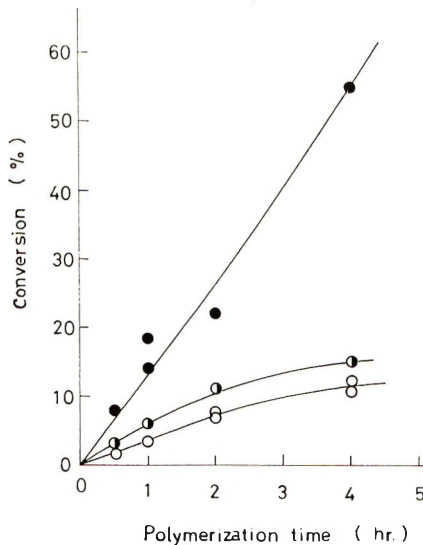


Fig. 5. Radiation-induced polymerization of trioxane under 5000 kg/cm² pressure at various temperatures: (○) 55°C; (●) 70°C; (●) 105°C.

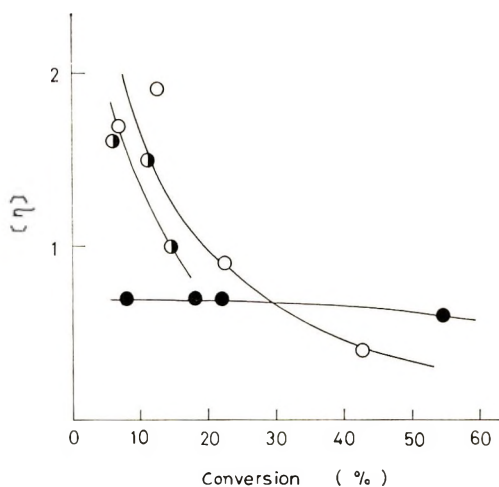


Fig. 6. Relationship between conversion and intrinsic viscosity of polyoxymethylene obtained by radiation-induced polymerization of trioxane under 5000 kg/cm^2 pressure at various temperatures: (O) 55°C ; (◐) 70°C ; (●) 105°C .

these conditions. Attempts to polymerize trioxane in the liquid state under high pressure, e.g., 2000 kg/cm^2 , at 140°C were unsuccessful. Thus, it is confirmed that the maximum rate of the solid-state polymerization occurs near the melting point even under high pressure.

The in-source polymerization of trioxane was also investigated at constant temperature, 70°C , on varying the pressure in the range between 1000 and 7000 kg/cm^2 . As shown in Figure 3, the rate of polymerization was decreased by increasing pressure. This decrease is attributed to the elevation of the melting point due to the pressure, i.e., the pressure suppresses the motion of monomer molecules that is essential for the polymerization reaction.

However, it should be noted that the shape of the curve changed as the pressure was varied. The curves were S-shaped under low pressures, i.e., 1000 and 2000 kg/cm^2 , similar to the curve obtained at atmospheric pressure. On the other hand, at high pressures, i.e., 5000 and 7000 kg/cm^2 , the initial rates of polymerization were high and gradually leveled off. The intrinsic viscosities of the polymers were almost independent of conversion under low pressure, whereas under high pressure the intrinsic viscosities were extremely high at low conversion and fell off rapidly with increasing conversion (Fig. 4). This change coincides with the variation in the shape of time-conversion curves. The rapid decrease in the intrinsic viscosity cannot be explained by degradation due to irradiation alone, since the maximum dose was only $2.2 \times 10^5 \text{ R}$. In fact, the intrinsic viscosity was almost constant in the case of polymerization near the melting point.

Similarly, plots of percentage conversion versus the polymerization time (Fig. 5) and of conversion versus intrinsic viscosity (Fig. 6) at various temperatures under constant pressure, 5000 kg/cm^2 , were obtained. The

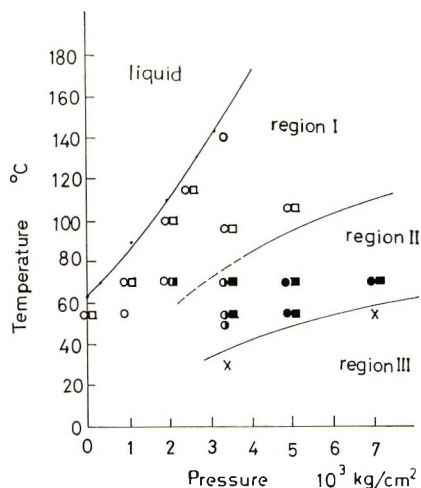


Fig. 7. Diagram of polymerization characteristic as a function of temperature and pressure in the radiation-induced polymerization of trioxane: (○) the time-conversion curve was S-shaped and reached high conversion; (●) the time-conversion curve attained saturation at low conversion; (◐) the intermediate between the above two cases; (×) no polymerization took place; (□) intrinsic viscosity of the polymer was almost constant over the whole conversion range; (■) the intrinsic viscosity of the polymer was extremely high at low conversion and fell off rapidly with increasing conversion; (◑) the intermediate between the above two cases, i.e., the intrinsic viscosity passed through a maximum.

rate increased with increasing temperature, and the variation in the shape of the time-conversion curves and the viscosity-conversion curves was similar to those in Figures 3 and 4, respectively. In other words, the polymerization characteristic under high pressure at constant temperature corresponds to that at low temperature under constant pressure and that under low pressure corresponds to that at high temperature.

From these results we may distinguish a region I near the melting point where the time-conversion curves are S-shaped and the intrinsic viscosities are independent of conversion, and region II with temperatures at some distance from the melting points where the initial rates of polymerization are high but attain saturation at low conversion and the intrinsic viscosities rapidly decrease with increasing conversion. Finally, there is a region III where polymerization of trioxane cannot take place, since little polymer was obtained at 30°C, 3500 kg/cm² and 55°C, 7000 kg/cm². These three regions with different "polymerization characteristics" are illustrated in Figure 7.

The initial polymerization rate was higher in region II than in region I, e.g., in Figure 3 the conversion at 5000 kg/cm² was higher than that at 3500 kg/cm² or 2000 kg/cm² up to 1 hr. The results are explained as follows. (1) The crystalline state of region II is originally favorable to polymerization. As polymerization proceeds, however, the polymer formed disorders the crystal lattice and the polymerization rate falls rapidly, since rearrange-

ment of the monomer molecules (annealing) hardly occurs in this region. Alternatively, there are two parts in the crystal, a well-ordered part where polymerization proceeds easily and a disorder part where polymerization is very slow. (2) It is probable that a crystal transition occurs between region I and II, and this should be clarified by further study.

Rao and Ballantine¹ pressurized trioxane prior to irradiation and carried out in-source polymerization at 45 or 55°C. They found that the yield and the intrinsic viscosity was increased by pre-pressurization. Their results are, however, inconsistent with their contention that pressure inhibits initiation by removing defect sites, but that the order imposed favors the propagation of the chains before termination. This interpretation can better be applied to the present results.

The authors should like to express cordial thanks to Prof. S. Okamura of Kyoto University for his encouragement of this work. They are also grateful to Mr. N. Morishita for his assistance in measuring intrinsic viscosity of the polymer. A part of this work was presented before the 17th annual meeting of the Society of Polymer Science, Tokyo, May, 1968.

References

1. H. Rao and D. S. Ballantine, *J. Polym. Sci. A*, **3**, 2579 (1965).
2. Y. Tabata, T. Suzuki, and K. Oshima, *J. Macromol. Chem.*, **1**, 817 (1966).
3. S. Okamura, K. Hayashi, and Y. Nakamura, *Isotopes Radiation (Tokyo)* **3**, 416 (1960).
4. S. Okamura, K. Hayashi, Y. Kitanishi, and M. Nishii, *Isotopes Radiation*, **3**, 510 (1960).
5. S. Okamura, K. Hayashi, and Y. Nakamura, *Isotopes Radiation*, **3**, 346 (1960).
6. S. Okamura, K. Hayashi, and Y. Nakamura, *J. Polym. Sci.*, **58**, 925 (1962).
7. J. Osugi, K. Shimizu, A. Onodera, *Rev. Phys. Chem. Japan*, **34**, 97 (1964).
8. P. W. Bridgman, *Proc. Amer. Acad. Arts Sci.*, **77**, 129 (1949).
9. P. W. Bridgman, *Phys. Rev.*, **3**, 153 (1914).

Received April 21, 1970

Cationic Copolymerization of Tetrahydrofuran with Epoxides. I. Polymerization Mechanism in the Presence of a Glycol

J. M. HAMMOND, J. F. HOOPER, and W. G. P. ROBERTSON,
*Australian Defence Scientific Service, Department of Supply,
Weapons Research Establishment, Salisbury, South Australia*

Synopsis

Polymerization of several epoxides and their copolymerization with tetrahydrofuran have been studied. The polymerizations were carried out by use of $\text{BF}_3 \cdot \text{O}(\text{C}_2\text{H}_5)_2$ as catalyst in the presence of 1,4-butanediol. Variations of catalyst and 1,4-butanediol ratio and concentration affect polymerization rate, molecular weight, and the formation of cyclic oligomers. The latter is also influenced by monomer feed ratio in the case of the copolymerizations. These effects are discussed, and some observations are made concerning the mechanism, particularly with respect to the role of the 1,4-butanediol. Mayo-Lewis monomer reactivity ratios were determined. The ratios found differed from previously published figures.

INTRODUCTION

Polymerizations and copolymerizations of epoxides and other cyclic oxides catalyzed by $\text{BF}_3 \cdot \text{O}(\text{C}_2\text{H}_5)_2$ have been studied fairly extensively.¹⁻⁸ While there may be some doubt about the precise steps involved in the initiation, it is generally accepted that the propagating species involves an oxonium ion.^{4,6,8-13}

Arising from the use of polyether glycols for the formulation of castable rubbers there has been a particular interest in copolymerizations of this type carried out in the presence of small amounts of a low molecular weight glycol.^{1-5,10,14} The use of this glycol facilitates control of polymer molecular weight, particularly where fairly low molecular weight is desired, while maintaining the formation of dihydroxyl-terminated polymer. It seems to be generally agreed that the glycol becomes incorporated in the polymer but some statements which have been made concerning the mechanism of glycol incorporation appear to be erroneous.^{1,5}

Initially we were interested simply in determining reactivity ratios for the monomer pairs propylene oxide (PO)-tetrahydrofuran (THF), 1,2-butylene oxide (1,2-BO)-THF, and *n*-propyl glycidyl ether (*n*-PGE)-THF in connection with the synthesis of copolymers for possible use in the formulation of castable polyurethane rubbers. During the course of

preliminary experiments to determine suitable polymerization conditions concentrations of catalyst, glycol [1,4-butanediol (1,4-BD)], and monomers were varied fairly widely. Several effects of these variations on the course of the polymerizations were noted which seemed to have a significant bearing on the mechanism and to warrant further examination.

In these polymerizations the formation of polymer is attended by the formation of low molecular weight nonhydroxylic cyclic by-products. In addition to controlling molecular weight, the inclusion of the glycol in the polymerization mixture substantially reduces the formation of cyclic by-products. The molecular weight of the polymer formed depends upon the concentration of initial glycol and the monomer conversion.

EXPERIMENTAL

Reagents

PO. Commercial reagent was refluxed over potassium hydroxide pellets for 6 hr., decanted and dried over calcium hydride overnight. The purified monomer was obtained by fractionation through a small column as a middle cut, bp 34–34.5°C.

1,2-BO. Commercial reagent was purified by the same procedure used for PO giving the monomer as a fraction, bp 63–63.5°C.

THF. Commercial reagent was refluxed over sodium hydroxide pellets for 6 hr, dried overnight over lithium aluminum hydride, and distilled, yielding the purified monomer as a fraction, bp 65–65.5°C.

***n*-PGE.** *n*-Propanol and epichlorohydrin were condensed in the presence of sulfuric acid as catalyst to give 1-propoxy-2-hydroxy-3-chloropropane, bp 96–99°C/20 mm (yield 52%), which was subsequently treated with sodium hydroxide in ether giving *n*-PGE, bp 72–73°C/55 mm (yield 68%), as previously described by Flores-Gallardo and Pollard.¹⁵

BF₃·O(C₂H₅)₂. The commercial reagent was distilled in a dry nitrogen atmosphere, bp 126–127°C. The catalyst discolors on standing and was freshly prepared for each polymerization.

1,4-BD. Laboratory grade reagent was dried over Linde Molecular Sieve No. 5A and distilled, bp 82–84°C/0.25 mm.

***n*-Butanol.** Laboratory-grade reagent was dried over Linde Molecular Sieve No. 5A and distilled through a small column, bp 117.5–118°C.

Ethylene Dichloride. Analytical grade reagent was refluxed over phosphorus pentoxide for 6 hr and distilled through a small fractionating column, bp 83.5–84°C.

Polymerization Procedure

The polymerizations were carried out in a 50-ml three-necked flask fitted with a stirrer, thermometer, gas inlet, and self-sealing rubber septum for reagent addition. The reagents were measured out in a dry box by use of Hamilton gas-tight syringes previously calibrated for each reagent.

The apparatus was assembled in the dry box, which was continually flushed with a stream of dry nitrogen, and the flask was charged with the monomer mixture, 1,4-BD, and ethylene dichloride. The apparatus, with gas inlet closed, was then removed from the dry box and connected to the dry nitrogen supply. The gas inlet was opened and a continual stream of nitrogen admitted to the flask to maintain a slight positive pressure and exclude moisture. The flask was immersed in a cooling bath and the temperature of the stirred mixture cooled to 0°C. $\text{BF}_3 \cdot \text{O}(\text{C}_2\text{H}_5)_2$ dissolved in ethylene dichloride (2 ml) was added slowly (5 min) through the rubber septum from a Hamilton gas-tight syringe. The polymerization mixture was stirred and maintained at 0°C throughout the polymerization.

Polymerization was stopped by quenching with water. The contents of the flask together with more ethylene dichloride (20 ml) used to rinse the flask were shaken vigorously with water for several minutes and then separated. The organic layer was washed twice with water (10 ml) to remove all traces of catalyst. Solvent and unreacted monomers were removed under reduced pressure in a rotating evaporator and the product finally dried by heating at 55°C/1 mm for 4 hr.

The polymers were obtained as clear, colorless liquids. Their infrared spectra showed strong hydroxyl absorption and indicated that they were substantially free from the unsaturation encountered in some commercial polyether glycols.¹⁶ This was confirmed by analysis for unsaturation by the mercuric acetate method (ASTM D1638-61T), where, for example, a PO-THF copolymer having a molecular weight of approximately 2000 gave a result of 0.002 meq/g, compared with 0.020 meq/g for a commercial polyoxypropylene glycol of similar molecular weight (Union Carbide Niox Diol PPG 2000).

For the determinations of reactivity ratios polymerizations were carried out at nine monomer mole ratios, viz., 9:1, 8:2, 7:3, 6:4, 1:1, 4:6, 3:7, 2:8 and 1:9, for each of the three monomer pairs. The reactions were stopped at 7-8% conversion, appropriate reaction times having been established by preliminary runs in each case. The proportions of reactants and solvent used in all the reactivity ratio runs were as follows: total monomers, 0.40 mole; 1,4-BD, 0.0064 mole (1.60 mole-% with respect to total monomers); $\text{BF}_3 \cdot \text{O}(\text{C}_2\text{H}_5)_2$, 0.00032 mole (0.08 mole-% with respect to total monomers); ethylene dichloride, 20 ml.

Molecular Weight Determination

Number-average molecular weights by vapor pressure osmometry, \bar{M}_n (VPO), were determined with a Mechrolab Model 302 vapor pressure osmometer with benzene as solvent at 37°C.

\bar{M}_n (OH) was determined from endgroup analysis, by acetylation with acetic anhydride in pyridine assuming 100% bifunctionality, perchloric acid being used as catalyst.¹⁷

Neither of these figures represents number-average molecular weight of the linear polymer. Since all the polymer samples were found to contain

some nonhydroxylic cyclic oligomer, \bar{M}_n (VPO) is lower than and \bar{M}_n (OH) higher than the \bar{M}_n of the linear polymer present. In the absence of cyclic oligomer, \bar{M}_n (VPO) and \bar{M}_n (OH) should be equal. If one could determine accurately the proportions of polymer and oligomer, one could calculate \bar{M}_n values for these two species from \bar{M}_n (OH) and \bar{M}_n (VPO). However, their molecular weight ranges frequently overlap, and volatility, solubility, and other characteristics are similar, so that complete separation has not been achieved. We were able to isolate only the cyclic tetramers quantitatively.

Polymer Analysis

From NMR spectra one may determine the amount of 1,4-BD incorporated in an epoxide homopolymer and the epoxide/THF ratio in copolymers.

The NMR spectra of the copolymers had a characteristic absorption at τ 8.46 which increased with increasing THF content. The 1,4-BD residue (oxybutylene) present in the polymers is the same as the THF unit in the copolymers. The NMR spectra of commercial polyoxypropylene glycols do not have an absorption peak at τ 8.46 (C—CH₂), but the NMR spectra of homopolymers of PO produced by using BF₃·O(C₂H₅)₂ as catalyst in the presence of 1,4-BD do have a small absorption peak at τ 8.46, thus confirming that 1,4-BD is incorporated in the polymer.

Polymer analyses also indicated that all the 1,4-BD present initially in the reaction mixture becomes incorporated into the polymer at fairly low conversion. For example, in one particular case of PO homopolymerization the amount of 1,4-BD present initially was 0.0064 mole, and at 27.3% conversion the yield of polymer was 6.5 g. From the NMR spectrum the mole ratio of PO/1,4-BD [given by (C—CH₃/3)/(C—CH₂/4)] was 14.9/1. If y is the number of moles of 1,4-BD incorporated in the polymer and the molecular weights of PO and 1,4-BD are 58.08 and 90.12, respectively, we have

$$\text{Polymer yield} = 14.9 y (58.08) + y (90.12) = 6.5$$

whence

$$y = 0.0068$$

In the monomer reactivity ratio determinations, accurate determination of the mole ratio of THF/epoxide in the polymers is necessary. From NMR the mole ratio of (THF + 1,4-BD)/epoxide is obtained. Correction for the mole ratio of 1,4-BD/epoxide is achieved independently from a knowledge of the hydroxyl content of the polymer (by endgroup analysis) and the assumption that each polymer chain contains one 1,4-BD unit.

The infrared spectra of the PO = THF copolymers were very similar to those of low molecular weight commercial PO homopolymers, except for a peak at 1200 cm⁻¹ which is attributed to the presence of the THF unit.^{18,19} The BF₃·O(C₂H₅)₂ = 1,4-BD system will not initiate the homopolymeriza-

tion of THF, thus the THF units in the copolymerization products must be present as copolymer. Solubility characteristics confirmed the absence of epoxide homopolymer in the copolymerization products. For example, PO-THF copolymers are insoluble in cold water, whereas polyoxypropylenes of molecular weight below 1000 are soluble. In a specific instance, a PO = THF copolymer of molecular weight of about 1000 was prepared. This polymer was found to contain PO units, which must have been present as copolymer rather than as homopolymer which, being of molecular weight less than 1000, would have been water-soluble and would have been removed during polymer workup. No polymer was recovered from the aqueous washings.

Infrared and NMR Spectra

Infrared spectra were recorded on a Perkin-Elmer grating spectrophotometer, Model 521, with films of polymer between rock-salt plates. NMR spectra were determined with solutions of polymer in carbon tetrachloride on a Varian HA-60 NMR spectrometer.

RESULTS

Initially a series of polymerizations was run at various concentrations and proportions of reactants in order to determine conditions suitable for reactivity ratio determination and the formation of polymer of the molecular weight required for castable rubber preparation. Details of these experiments are summarized in Table I. From the results of these experiments a number of conclusions may be drawn.

Under the conditions used, the three epoxides will each homopolymerize (Table I, runs 2, 4, 5, 11, 12, and 13) and each will copolymerize with THF (Table I, runs 26, 27, 29).

THF does not homopolymerize under the conditions used in this work (Table I, run 14). Homopolymerization of THF by BF_3 requires much higher concentrations of initiator.²⁰ With the addition of small amounts of PO, polymerization starts under the influence of $\text{BF}_3 \cdot \text{O}(\text{C}_2\text{H}_5)_2$ in the presence of excess 1,4-BD but stops at low conversion when all the PO has been used. The polymerization can be reinitiated by the addition of a further portion of PO but again terminates after consumption of the PO added (Table I, runs 14-18). From this it follows that at high THF/epoxide feed ratios copolymer yields are limited to low conversion.

All the 1,4-BD becomes incorporated in the polymer at conversions above about 30%. This is shown by the absence of 1,4-BD from the aqueous washings obtained during work-up and, in the case of epoxide homopolymer, by the NMR spectrum of the polymer.

Nonhydroxylic cyclic oligomers are formed during these polymerizations. They are discussed in greater detail in Part II.²¹ Cyclic oligomers (mainly tetramer but also pentamer and hexamer) are formed during both the homopolymerizations and the copolymerizations and may under certain

TABLE I
 Polymerizations and Copolymerization of Cyclic Oxides in Ethylene Dichloride at Various Catalyst and 1,4-Butanediol Concentrations

Run no.	Monomer feed	1,4-Butane-diol mole-%	Catalyst $\text{BF}_3 \cdot \text{O}(\text{C}_2\text{H}_5)_2$, mole-%	Con- version, %	Bulk viscosity at 30°C., poise ^b	Hydroxyl equivalents ^c		Molecular weight		Remarks
						[OH] ₁ × 10 ²	[OH] _P × 10 ²	\bar{M}_n (OH)	\bar{M}_n (VPO)	
1	PO/THF (1:1)	0	1	92	26	—	—	—	—	High molecular weight in absence of 1,4-butanediol
2	PO	0	1	68	—	—	—	310	—	Mainly cyclic tetramer of PO
3	PO/THF (1:1)	1	1	98	9.6	0.40	0.56	4630	—	[OH] in product ≫ initial cocatalyst [OH]
4	PO	1	1	82	0.59	0.40	1.77	1083	—	
5	PO	0.08	0.08	17	0.15	0.03	0.07	—	283	Mainly cyclic tetramer
6	PO/THF (1:1)	2	1	93	—	0.80	0.81	3084	—	} Good agreement between duplicate runs
7	PO/THF (1:1)	1.65	0.086	25	—	0.66	0.62	1058	—	
8	PO/THF (1:1)	1.65	0.086	3	26	0.66	0.61	1149	—	} Good agreement between duplicate runs
9	PO/THF (1:1)	1.65	0.086	6	49	0.66	0.72	1807	—	
10	PO/THF (1:1)	1.65	0.086	24	87	0.66	0.76	3055	—	} Good agreement between duplicate runs
11	PO	1.60	0.08	3	26	0.64	0.58	1070	—	
12	1,2-BO	1.60	0.08	3	25	0.64	0.72	1032	—	} Good agreement between duplicate runs
13	n-PGE	1.60	0.08	3	16	—	—	—	—	
14	THF	1.65	0.086	3	—	—	—	—	—	No reaction
15	THF + 5 mole-% PO	1.65	0.086	3	7	0.66	0.31	642	—	[OH] in product ≪ initial cocatalyst [OH]
16	THF + 5-mole-% PO	1.65	0.086	24	19	0.66	0.55	1051	—	} Reaction stops at 19% conversion
17	THF + 5 mole-% PO	1.65	0.086	72	19	0.66	0.60	961	—	

18	THF + 2(5 mole-% PO)	1.65	0.086	24 + 24	38	0.66	0.75	1610	Addition of second portion of PO after 24 hr doubles conversion from 19% to 38% (cf. runs 16 and 17)
19	PO/THF (1:1)	1.60	0.08	3	22	1.7	0.58	984	
20	PO/THF (1:1)	0.80	0.08	3	21	2.5	0.36	1546	
21	PO/THF (1:1)	1.60	0.08	24	82	5.2	0.64	2934	
22	PO/THF (1:1)	0.80	0.08	24	83	8.0	0.32	4616	
23	PO/THF (1:1)	<i>n</i> -Butanol ^d 1.60	0.08	3	23		0.32	1021 ^e	Monohydroxyl terminated polymer
24	PO/THF (9:1)	1.60	0.08	0.5	11	1.28	0.67	779	426
25	PO/THF (1:1)	1.60	0.08	0.5	5	1.28	0.41	628	
26	PO/THF (1:9)	1.60	0.08	1.5	3	1.28	0.26	620	457
27	1,2-BO/THF (9:1)	1.60	0.08	0.5	9			698	378
28	1,2-BO/THF (1:9)	1.60	0.08	1	3			558	458
29	<i>n</i> -PGE/THF (9:1)	1.60	0.08	1	4			674	443
30	<i>n</i> -PGE/THF (1:9)	1.60	0.08	2	5			613	490
	Commercial poly(oxypropylene glycol), NIAX DIOL PPG 2000				2.5			2180	

^a Ethylene dichloride concentration of 64 mole-% (based on total monomers) was employed throughout.

^b Ferranti-Shirley cone-and-plate viscometer.

^c [OH]₁ = gram-equivalents of hydroxyl (present at 1,4-BD) in the initial reactants; [OH]₂ = gram-equivalents of hydroxyl (by analysis) in the product isolated.

^d *n*-Butanol used instead of 1,4-BD in run 23.

^e Calculated for monofunctional polymer.

conditions predominate in the product. The reaction of $\text{BF}_3 \cdot \text{O}(\text{C}_2\text{H}_5)_2$ with PO in the absence of any added glycol has been reported²² as a preparative method for the cyclic tetramer of PO, while an earlier reference²³ states that as many as five cyclic oligomers, ranging from dimer to hexamer, may be isolated from the products of this reaction.

It seems that this report, which is not mentioned in *Chemical Abstracts*, has been frequently overlooked as no other reference to it appears in subsequent published literature.

In copolymerizations carried out in the presence or absence of 1,4-BD at the higher ratios of THF to epoxide co-oligomers containing both alkylene oxide and THF units are formed. The co-oligomers were found (NMR) to be mixtures of cotetramers of epoxide and THF with each cotetramer containing at least two epoxide units. Tetramers containing three or four THF units were not detected. At the same time increasing THF in the monomer feed ratio increasingly suppresses the extent of cyclic tetramer formation during polymerization (see Table II).

TABLE II
Effect of Tetrahydrofuran on Cyclic Tetramer Formation^a

Monomer feed	Conversion, %	Yield, %	
		Polymer	Cyclic tetramer
PO	50	29	21
PO/THF (1:1)	88	83	5
PO/THF (1:4)	84	83	1
THF	0	0	0

^a 1,4-BD concentration = 0; $\text{BF}_3 \cdot \text{O}(\text{C}_2\text{H}_5)_2$ concentration = 1 mole-%.

The presence of 1,4-BD in the reaction mixture reduces the amount of cyclic oligomers formed and the suppression of cyclic oligomer formation increases as 1,4-BD/catalyst ratio increases. Cyclic oligomer is formed early in the reaction. It is present in low conversion products (e.g. Table I, runs 26, 28) and the ratio of linear polymer to cyclic oligomer (by gel-permeation chromatography²¹) is not a function of conversion.

In general the hydroxyl content of the polymerization products (as isolated) remains constant for conversions between 30% and 90% at a level about 10% higher than that present in the initial reactants as 1,4-BD (Fig. 1). At least part of this increase may be attributed to the traces of water present in the initial mixture of solvents and monomers (0.009% w/w by Karl Fischer). This water content is equivalent to 0.07 mole % of 1,4-BD in the units of Table I. Some additional hydroxyl must also be introduced in the final quenching. The low hydroxyl content in the low-conversion products results from the fact that during these earlier stages of reaction not all of the glycol has been incorporated into the polymer prod-

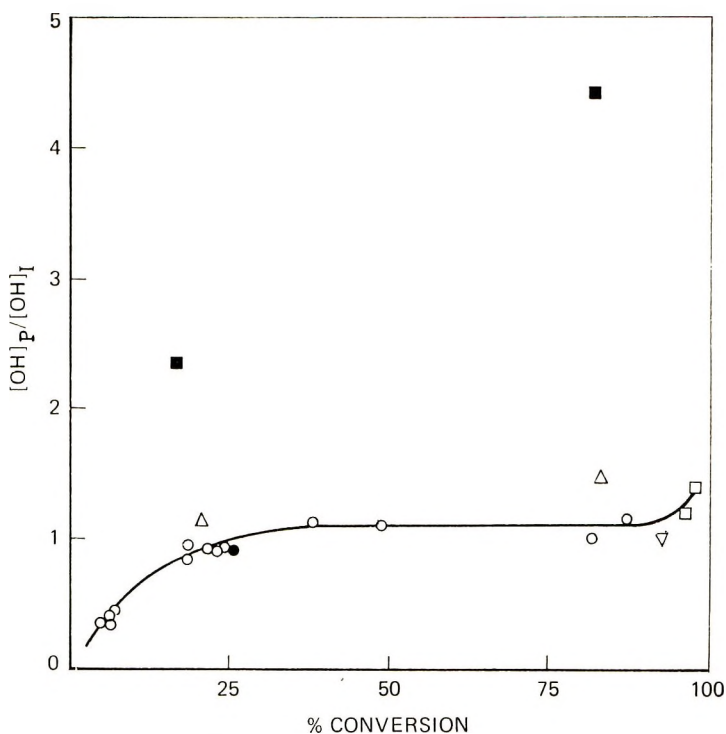


Fig. 1. Plot of $[\text{OH}]_P/[\text{OH}]_I$ vs. conversion for (●, ■) PO polymerizations and (○, △, ▽, □) PO-THF copolymerizations at various 1,4-butanediol/ $\text{BF}_3 \cdot \text{O}(\text{C}_2\text{H}_5)_2$ ratios: (●, ○) 20:1; (△) 10:1; (▽) 2:1; (■, □) 1:1.

uct. In these cases of low conversion, unreacted 1,4-BD was removed during polymer workup and found to be present in the aqueous washings. Adherence to this behavior was best at high 1,4-BD/catalyst ratios (20:1). Two cases of marked departure were homopolymerizations of PO at 1:1 ratios of 1,4-BD to catalyst (Table I, runs 4, 5). In one case (run 5) the initial 1,4-BD concentration was very low, and the discrepancy is presumably due to the combined effects of traces of water in the reaction mixture and the final water quenching predominating in determining the hydroxyl content of the product. In the other case (run 4) a satisfactory explanation of the discrepancy is not so readily apparent. At the low glycol/catalyst ratio (1:1) it might be expected that the final water quenching should contribute as much to the hydroxyl content of the product as does the glycol. However the results indicate a factor of 4 rather than 2. It is also puzzling why in run 3 the ratio of product hydroxyl to initial hydroxyl should be less than 1.5 instead of about 2.

The difficulty of separating the ever-present cyclic tetramers and higher oligomers quantitatively from these relatively low molecular weight polymers and copolymers makes it difficult to determine with certainty the molecular weights of the latter. Nevertheless the available evidence

strongly suggests that, at a given catalyst concentration, increasing the 1,4-BD content proportionately decreases polymer molecular weight (e.g., runs 19, 20, 21, 22) and that, for the same initial 1,4-BD concentration, polymer molecular weight increases with conversion. Moreover the system remains alive until deliberately quenched, and increased conversion (and molecular weight) may be achieved by stepwise addition of further portions of monomer when the previous portion is exhausted.

When 1,4-BD is replaced by *n*-butanol in the copolymerization of PO and THF, monohydroxyl-terminated copolymer is formed, as indicated by hydroxyl analysis (c.f. runs 19 and 23 in Table I).

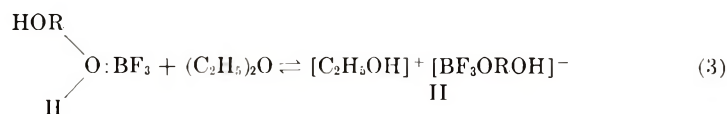
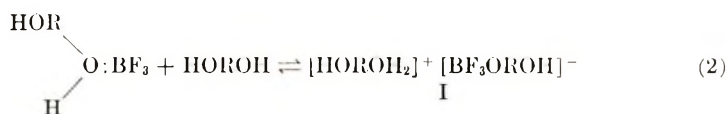
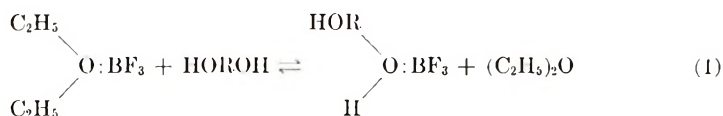
DISCUSSION

Polymerization Mechanism

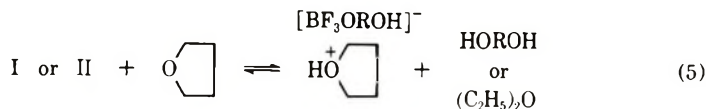
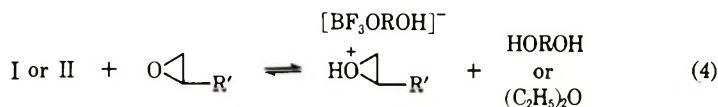
A previous postulation^{1,3} of dication propagation to give dihydroxyl terminated polymers seems to be quite erroneous. In particular it does not account for the facts that complete incorporation of glycol (1,4-BD) into the polymer is achieved at 30% conversion even at glycol/catalyst ratios of 20:1 whilst at the same time molecular weight is a function of conversion.

In our view a mechanism, as outlined below, in which the essential features are (a) preinitiation, (b) initiation, (c) propagation, (d) intramolecular transfer to polymer (cyclic oligomer formation), (e) transfer to hydroxyl (transfer to initial glycol and repetitive transfer to polymer glycol), is more plausible and accounts for the known experimental facts. The scheme should be applicable with slight modifications to similar polymerizations carried out in the presence of alcohols and polyols.

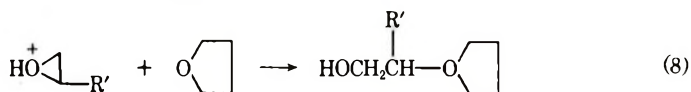
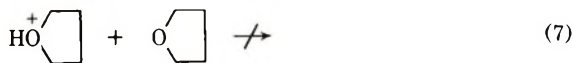
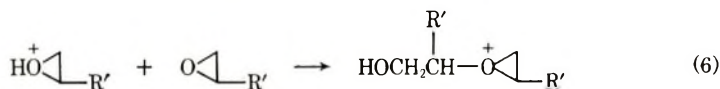
Preinitiation.



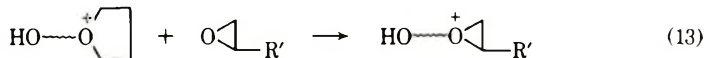
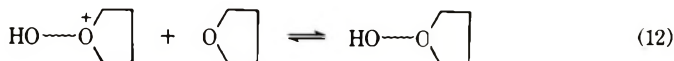
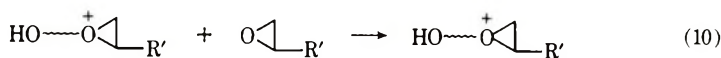
Either reaction (2) or (3) or both may occur. Water (HOH) or polymer glycol may replace HOROH, which represents a glycol such as 1,4-BD.

Initiation.


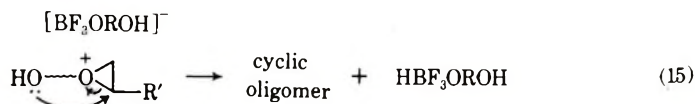
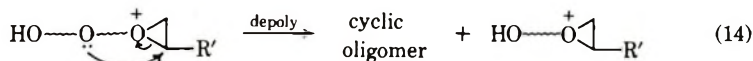
Propagation. The possible initial reactions are:



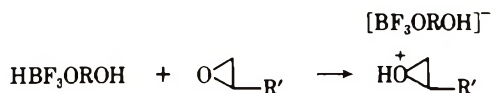
followed by



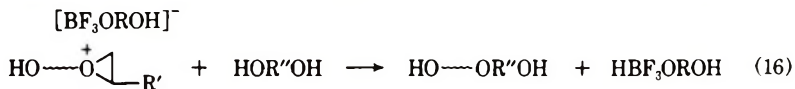
Cyclic Oligomer Formation by Intramolecular Transfer. There are two possibilities, reaction with oxygen atoms in the body of the polymer chain (14), or at the end of the polymer chain (15).



followed by



Transfer to Hydroxyl. This may occur with hydroxyl attached to the glycol which is initially present or with polymer hydroxyl end group.



where $\text{HOR}''\text{OH}$ may be original glycol or polymer glycol of the types $\text{HO} \sim \text{OROH}$ and $\text{HO} \sim \text{ORO} \sim \text{OH}$.

The full sequence of reactions (1) to (16) describes the copolymerization of epoxides with THF. Epoxide homopolymerization is described by reactions (1)–(4), (6), (10), (14), (15), and (16).

The reactions postulated for preinitiation, initiation and propagation are based on the work of others^{10–12,14,24} and we have not attempted to prove them. Other preinitiation steps are feasible and possible⁸ but those suggested here are likely to predominate with high glycol/catalyst ratios. In this scheme incorporation of glycol into polymer does not stem from glycol participation in these initiating steps.

Cyclic oligomer formation could occur either by intramolecular transfer attack on the initial hydroxyl of a (short) growing polymer chain [eq. (15)] or by intramolecular transfer to ether oxygen a few units back from the oxonium ion [eq. (14)]. Substantial amounts of cyclic oligomer are formed in the early stages of polymerization and there is no evidence of intermolecular chain transfer with ether oxygen in another molecule at least in the case of systems containing THF, PO, 1,2-BO, and *n*-PGE although it can occur with the ether oxygen atoms of polyethylene oxide (see part III²⁵). It is believed therefore that intramolecular transfer to hydroxyl is the preferred process for cyclic oligomer formation.

The transfer to hydroxyl reaction (16) leads to incorporation of initial glycol into polymer and to increasing polymer molecular weight with conversion by repetitive intermolecular transfer to polymer hydroxyl. From this it follows that at high 1,4-BD/catalyst ratios the amount of 1,4-BD will predominantly control the number of hydroxyl groups present in the polymer.

With *n*-butanol instead of 1,4-BD as transfer agent, similar transfer to hydroxyl reactions will occur, but the polymers formed will be terminated at one end with $-\text{O}(\text{CH}_2)_3\text{CH}_3$. Dreyfuss and Dreyfuss in their review²⁶ on polytetrahydrofuran have suggested that alcohol in small amounts would behave like water as a transfer agent and lead to polymers with $-\text{OR}$ endgroups. It appeared to them also that the ethylene glycol used by Murbach and Adicoff² in their copolymerization of THF and ethylene oxide functions as a transfer agent and not merely as a cocatalyst.

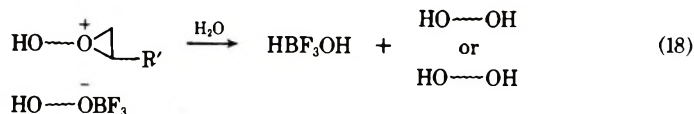
Since experimental results show that all the initial glycol becomes incorporated in the polymer it is necessary to postulate a means whereby the initial glycol does not remain locked up in the counterion in reactions (2)–(5). One possibility is an exchange reaction:



Another possibility is that counterions may participate equally well in intermolecular transfer to hydroxyl [eq. (16)] as initial glycol and polymer glycol. Probably both of these reactions occur. They imply that the size of the counter ion increases as polymerization proceeds.

Since glycol begins to be incorporated into the polymer at quite low conversion and since the presence of glycol suppresses cyclic oligomer formation it follows that the transfer reactions leading to glycol incorporation and cyclic oligomer formation are competitive processes in the early stages of the polymerization and that suppression of cyclic oligomer formation should be most effective at high 1,4-BD/catalyst ratios as was found experimentally.

There is no termination step. If the conversion of monomer proceeds to completion active end groups remain and polymerization will proceed further on the addition of more monomer. The reaction is stopped by quenching with excess water which destroys the catalyst and deactivates chain ends by conversion to hydroxyl-containing endgroups:



Failure of reaction (7) to proceed is a more likely reason than failure of reaction (5) for the failure of THF to homopolymerize under the conditions used in this work. Cyclic oligomers are formed in THF copolymerizations but the amounts formed are smaller than in the case of epoxide homopolymerization and decrease as the proportion of THF in the monomer feed increases. This is consistent with the observation that cyclic co-oligomers always contain at least two epoxide units implying cyclization reactions cannot take place where THF units predominate in the chain.

Reactivity Ratio Determinations

Table III gives the reactivity ratios obtained during the early part of our work. The reactivity ratios were determined at low conversion (ca. 5%) by using both the Fineman-Ross²⁷ and Mayo-Lewis²⁸ equations. Copolymer composition analyses (Fig. 2) were corrected for 1,4-BD content in every case.²⁻⁴

The ratios given in Table III differ from those previously published.^{2,3} The differences arise from the 1,4-BD correction which is quite large for these low molecular weight polymers. Murbach and Adicoff² in their determination of reactivity ratios for the ethylene oxide-THF monomer pair used elemental analysis to determine copolymer composition and made

TABLE III
 Monomer Reactivity Ratios

	PO/THF		1,2-BO/THF		<i>n</i> -PGE/THF	
	r_1	r_2	r_1	r_2	r_1	r_2
Fineman-Ross	0.29	0.57	0.58	0.56	0.24	0.42
Mayo-Lewis	0.34 ± 0.05	0.63 ± 0.05	0.58 ± 0.02	0.58 ± 0.02	0.27 ± 0.03	0.46 ± 0.03

no correction for the ethylene glycol (employed as "cocatalyst") content. Maine and Levesque³ saw the need to correct for the 1,4-BD "cocatalyst" content in their work but were unable to do so in every case. Thus their so called "corrected" values are not fully corrected.

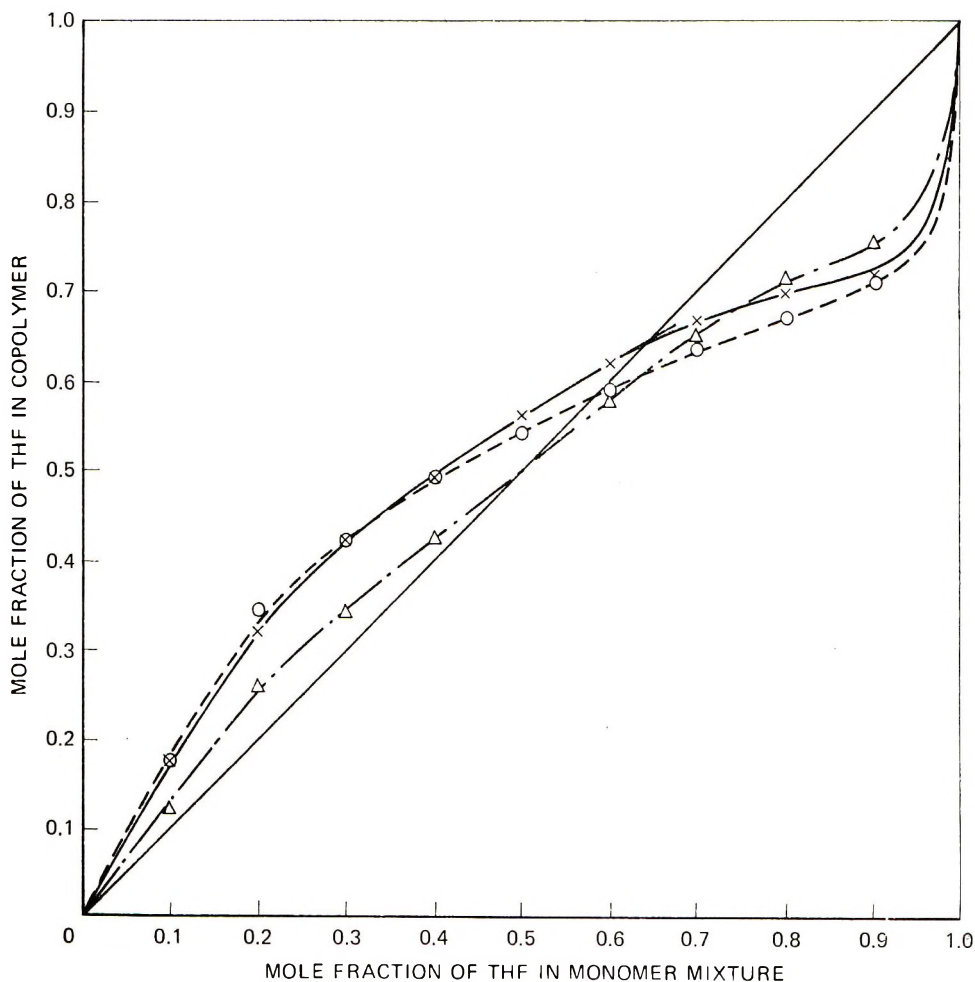


Fig. 2. Copolymer composition curves for (X) PO-THF, (Δ) 1,2-BO-THF, (O) *n*-PGE-THF systems.

While these reactivity ratios may be meaningful as a reflection of relationships between monomer feed ratio and copolymer composition one must conclude that in view of the complications arising from facile and repetitive chain transfer processes their significance, in terms of the original Mayo-Lewis concept and derivation of the copolymerization equation, is obscure.

The authors wish to thank Dr. R. G. Gillis and Dr. A. G. Moritz, of Defence Standards Laboratories, Melbourne, for determining the NMR spectra, and Mr. P. E. Rogasch of Weapons Research Establishment, for recording the infrared spectra.

References

1. L. A. Dickinson, *J. Polym. Sci.*, **58**, 857 (1962).
2. W. J. Murbach and A. Adicoff, *Ind. Eng. Chem.*, **52**, 772 (1960).
3. F. W. Maine and R. J. Levesque, paper presented to the Division of Rubber Chemistry, American Chemical Society Meeting, Chicago, Illinois, September 1964.
4. L. P. Blanchard, J. Singh, and M. D. Baijal, *Can. J. Chem.*, **44**, 2679 (1966).
5. M. D. Baijal and L. P. Blanchard, in *Macromolecular Chemistry, Kyoto-Tokyo 1966* (*J. Polym. Sci. C*, **23**), I. Sakurada and S. Okamura, Eds., Interscience, New York, 1968, p. 157.
6. T. Saegusa, H. Imai, and J. Furukawa, *Makromol. Chem.*, **56**, 55 (1962).
7. A. Ishigaki, T. Shono, and Y. Hachihama, *Makromol. Chem.*, **79**, 170 (1964).
8. A. M. Eastham, *Fortschr. Hochpolym.-Forsch.*, **2**, 18 (1960).
9. H. Meerwein, D. Delfs, and H. Morschel, *Angew. Chem.*, **72**, 927 (1960).
10. J. B. Rose, *J. Chem. Soc.*, **1956**, 542, 547.
11. S. Iwatsuki, N. Takigawa, M. Okada, Y. Yamashita, and Y. Ishii, *J. Polym. Sci. B*, **2**, 549 (1964).
12. S. Iwatsuki, N. Takigawa, M. Okada, Y. Yamashita, and Y. Ishii, *Kogyo Kagaku Zasshi*, **67**, 1236 (1964).
13. I. Penczek and S. Penczek, *Makromol. Chem.*, **67**, 203 (1963).
14. G. A. Latremouille, G. T. Merrall, and A. M. Eastham, *J. Amer. Chem. Soc.*, **82**, 120 (1960).
15. H. Flores-Gallardo and C. B. Pollard, *J. Org. Chem.*, **12**, 831 (1947).
16. D. M. Simons and J. J. Verbanc, *J. Polym. Sci.*, **44**, 303 (1960).
17. J. S. Fritz and G. H. Schenk, *Anal. Chem.*, **31**, 1808 (1959).
18. A. Kawasaki, J. Furukawa, T. Tsuruta, T. Saegusa, G. Kakogawa, and R. Sakata, *Polymer*, **1**, 315 (1960).
19. Y. Matsui, T. Kubota, H. Tadokoro, and T. Yoshihara, *J. Polym. Sci. A*, **3**, 2275 (1965).
20. R. C. Burrows and B. F. Crowe, *J. Appl. Polym. Sci.*, **6**, 465 (1962).
21. J. M. Hammond, J. F. Hooper, and W. G. P. Robertson, *J. Polym. Sci. A-1*, **9**, 281 (1971) (Part II).
22. J. L. Down, J. Lewis, B. Moore, and G. Wilkinson, *J. Chem. Soc.*, **1959**, 3771.
23. R. F. Holden, in *Glycols*, G. O. Curme and F. Johnston, Eds., Reinhold, New York, 1952, p. 274.
24. D. J. Worsfold and A. M. Eastham, *J. Amer. Chem. Soc.*, **79**, 897, 900 (1957).
25. J. M. Hammond, J. F. Hooper, and W. G. P. Robertson, *J. Polym. Sci. A-1*, **9**, 295 (1971) (Part III).
26. P. Dreyfuss and M. P. Dreyfuss, *Fortschr. Hochpolym. Forsch.*, **4**, 556 (1967).
27. M. Fineman and S. D. Ross, *J. Polym. Sci.*, **5**, 259 (1950).
28. F. R. Mayo and F. M. Lewis, *J. Amer. Chem. Soc.*, **66**, 1594 (1944).

Received October 30, 1968

Revised June 26, 1970

Cationic Copolymerization of Tetrahydrofuran with Epoxides. II. Characterization and Gel-Permeation Chromatography of By-Products Formed during Polymerization

J. M. HAMMOND, J. F. HOOPER, and W. G. P. ROBERTSON,
*Australian Defence Scientific Service, Department of Supply, Weapons
Research Establishment, Salisbury, South Australia*

Synopsis

The cyclic oligomers formed as by-products in the polymerization of propylene oxide, 1,2-butylene oxide, and *n*-propyl glycidyl ether, and in the copolymerization of these monomers with tetrahydrofuran have been studied by gel-permeation chromatography and otherwise and their structures have been determined. Some of the physical properties of the cyclic oligomers are described.

INTRODUCTION

The homopolymerization of propylene oxide (PO), 1,2-butylene oxide (1,2-BO), and *n*-propyl glycidyl ether (*n*-PGE), and the copolymerization of these monomers with tetrahydrofuran (THF), were described in Part I.¹ Thin-layer chromatography, gel-permeation chromatography (GPC), and molecular weight measurements of the products of these polymerizations have shown that the linear polymer formed is accompanied by low molecular weight nonhydroxylic by-products. It seems likely that these by-products are cyclic oligomers, with the cyclic tetramer predominating.

This paper describes the detection of these by-products in the products of polymerization by gel-permeation chromatography and the preparation and isolation of some of them. The nature of the cyclic oligomers formed from mixed monomer feeds is also discussed.

EXPERIMENTAL

Isolation of Cyclic Oligomers

Purification of the reactants and identification of the products were carried out as previously described.¹

Cyclic Tetramer of PO

Method a. The tetramer was prepared according to the procedure of Down and co-workers² by refluxing 100 g (1.72 mole) of PO with 2.55 g

(0.018 mole) of $\text{BF}_3 \cdot \text{O}(\text{C}_2\text{H}_5)_2$. The tetramer, 10.5 g (11% yield), was obtained as a clear, colorless liquid, bp 116–118°C/4 mm (lit.² bp, 104.8–105.5°C/5 mm). The molecular weight, determined by vapor-pressure osmometry (VPO), was 242; $n_D^{30} = 1.4440$; ν_{max} 2965, 2925, 2860, 1450, 1370, 1340 and (triplet) 1150–1075 cm^{-1} . The NMR spectrum showed the following resonances: doublet τ 9.03 (12) C—CH₃; τ 6.63 (12) O—CH and O—CH₂ protons.

The bulk of the product in this reaction was linear homopolymer of PO, yield 31%. The infrared spectrum resembled that of the tetramer except for ν_{max} 3450 and (singlet) 1100 cm^{-1} .

Method b. The tetramer was prepared at 0°C by using a modification of the method of Down and coworkers. To 100 g of dry PO at 0°C was added dropwise 2.55 g of $\text{BF}_3 \cdot \text{O}(\text{C}_2\text{H}_5)_2$. Addition took 2 hr. The mixture was stirred at 0°C for a further 1 hr, and then unreacted monomer and ether were removed under vacuum at 0°C. The BF_3 in the crude product was neutralized by stirring it at 0°C with a solution of 3.41 g of sodium hydroxide in 23 ml of water for 1 hr. The reaction mixture was brought to room temperature and the product then separated, and washed twice with 15 ml of water. The product was dried at room temperature in a rotating evaporator under reduced pressure. The middle fraction boiling at 63–72°C/0.12 mm was collected and redistilled to give 21.2 g (21%) of pure cyclic tetramer of PO, bp 115–118°C/4 mm. $\bar{M}_n(\text{VPO})$ was 241.

The fraction boiling at 84–99°C/0.12 mm, which totalled 4.7 g, was redistilled and shown to be cyclic pentamer of PO, bp 80–86°C/0.05 mm.

ANAL. Calcd for $(\text{C}_3\text{H}_6\text{O})_4$: C, 62.04%; H, 10.41%; MW, 290. Found: C, 62.01%; H, 10.27%; $\bar{M}_n(\text{VPO})$, 272.

The 20 g of residue obtained was presumably linear polymer of PO.

Cyclic Tetramer of 1,2-BO

The cyclic tetramer of 1,2-BO was similarly prepared (method b) from 124 g of 1,2-BO and 2.55 g of $\text{BF}_3 \cdot \text{O}(\text{C}_2\text{H}_5)_2$. The fraction boiling at 116–126°C/0.6 mm was collected and redistilled to afford 16.5 g (13%) of cyclic tetramer of 1,2-BO, bp 118–120°C/0.7 mm; $n_D^{30} = 1.4477$; ν_{max} 2955, 2920, 2870, 1455, 1340, and (doublet) 1120–1080 cm^{-1} . The NMR spectrum showed the following resonances: triplet τ 9.11 (12) C—CH₃; τ 8.67 (8) C—CH₂; τ 6.62 (12) O—CH and O—CH₂ protons.

ANAL. Calcd for $(\text{C}_4\text{H}_8\text{O})_4$: C, 66.64%; H, 11.19%; MW, 288. Found: C, 66.43%; H, 11.14%; $\bar{M}_n(\text{VPO})$, 305.

The 20 g of residue obtained was linear polymer of 1,2-BO, ν_{max} 3450 and (singlet) 1100 cm^{-1} .

Cyclic Dimer of n-PGE

This dimer was similarly prepared (method b) from 43 g of *n*-PGE and 0.66 g of $\text{BF}_3 \cdot \text{O}(\text{C}_2\text{H}_5)_2$. Fractionation of the dried reaction product af-

forded 2 g (5%) of cyclic *n*-PGE dimer, as the only volatile product, at a head temperature of 88°C/0.45 mm (bath 220°C). $n_D^{30} = 1.4330$. Further fractionation under high vacuum (10^{-4} mm) failed to yield any other product.

ANAL. Calcd for $(C_6H_{12}O_2)_2$: C, 61.95%; H, 10.41%; MW, 232. Found: C, 61.22%; H, 10.51%; \bar{M}_n (VPO), 227.

Some 20 g of residue was obtained, which was linear polymer of *n*-PGE, ν_{\max} 3450 and 1250 cm^{-1} .

Cyclic Cotetramers of PO and THF

Method a. A 1:1 mixture of 50 g of PO and 62 g of THF was treated with 2.55 g of $\text{BF}_3 \cdot \text{O}(\text{C}_2\text{H}_5)_2$ according to the method b described above. In working up the product, 50 ml of ethylene dichloride was added to the reaction mixture to ease the separation. The ethylene dichloride was subsequently removed from the washed product by distillation under vacuum. The crude product boiling at 81–90°C/0.05 mm was collected and redistilled to give 6 g (5%) of cyclic cotetramer of PO and THF, bp 71–73°C/0.04 mm; $n_D^{30} = 1.4510$. The infrared spectrum resembled that of cyclic tetramer of PO except for band at ν_{\max} 1200 and (singlet) 1100 cm^{-1} . The NMR determination of the mole ratio of PO to THF was 2.72:1.

ANAL. Calcd for $(C_5H_8O)_3 \cdot C_4H_8O$: C, 63.4%; H, 10.6%; MW, 246. Found: C, 63.46%; H, 10.48%; \bar{M}_n (VPO), 264.

The bulk of the product in this reaction was highly viscous PO–THF copolymer ν_{\max} 3450 and 1200 cm^{-1} .

Method b. A 1:4 mixture of 20 g of PO and 99 g of THF was treated similarly with 2.55 g of $\text{BF}_3 \cdot \text{O}(\text{C}_2\text{H}_5)_2$. Distillation of the dried reaction product gave only one product, namely, cyclic cotetramer of PO and THF, at a head temperature of 84°C/0.03 mm (bath 220°C). The yield was 0.5 g (<1%); $n_D^{30} = 1.4515$. The infrared spectrum was almost identical with that of the cotetramer, prepared above. NMR determination of the mole ratio of PO to THF was 1.36:1.

The 100 g of residue obtained was again PO–THF copolymer.

Gel-Permeation Chromatography

The samples examined by GPC, were of four types.

Type 1 comprised copolymers produced during reactivity ratio determinations,¹ in which the degree of conversion was less than 10%; type 2 were copolymers with THF,¹ in which the degree of conversion ranged up to 95%. These samples were subjected to GPC examination several months after their preparation.

Type 3 included volatile fractions and residues obtained during the preparation of (a) cyclic tetramers of PO and of 1,2-BO, (b) cyclic dimer of *n*-PGE, and (c) cyclic cotetramers of PO and THF. The preparation of

these samples is described above. They were examined by GPC a few weeks after their preparation.

Type 4 comprised products from the preparation of block copolymers by polymerization of (a) PO in the presence of poly(oxyethylene glycol) and (b) 1,2-BO in the presence of poly(oxypropylene glycol). These materials were prepared as described in Part III of this series.³ They were examined by GPC a few days after their preparation.

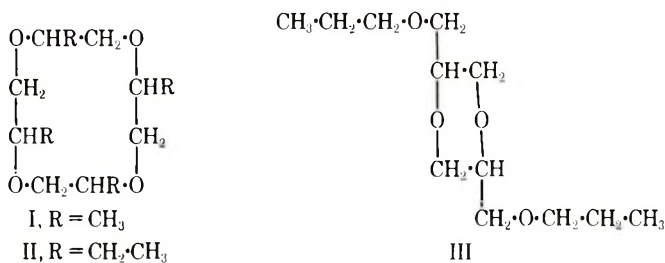
The instrument used was a Water gel-permeation chromatograph, Model 200, operated at a flow rate of 1 ml/min with THF as solvent. Two sets of columns were used: Set I, 10⁴, 10³, 250, 60 Å, operated at room temperature (about 20°C), plate count 870/ft; Set II, 10³, 250, 10², 60 Å, operated at 40°C, plate count 890/ft. Set II had greater resolution in the molecular size range of interest (see Figs. 3 and 4).

The detector fitted to the instrument is a differential refractometer, so that the chromatogram produced on the recorder chart paper is a plot of elution volume against a refractive index difference. This means that the height of the chromatogram at any point is determined by the concentration of the sample and its refractive index.

The elution volume (in milliliters) equals elution volume in counts multiplied by 5.0.

DISCUSSION OF CYCLIC OLIGOMER PREPARATIONS

The cyclic tetramer of PO (I) was prepared in 11% yield by the method of Down and co-workers.² The preparation repeated at 0°C to simulate the normal conditions used in the present polymerization studies resulted in a 21% yield of I; the overall conversion remained effectively constant the major product formed in both cases being normal linear homopolymer. In addition, a small amount of cyclic pentamer was isolated. Holden⁴



has reported the formation of as many as five cyclic oligomers in the polymerization of PO by BF₃, the tetramer being formed in highest yield. This information appears to have been completely overlooked by workers in this field as no other reference to this work appears in subsequent published literature. If any dimer or trimer was formed in the present preparation it would have been lost in the polymer work-up and drying process.

The tetramer (I) showed unusual solubility characteristics; it was readily soluble in cold water but insoluble in hot water. It was also insoluble in

cold sodium hydroxide solution. The infrared spectrum resembled that of the linear homopolymer of PO, except that in the former the band at 3450 cm^{-1} (O—H) was absent and there was a splitting of the band at 1100 cm^{-1} (C—O—C). Other examples of C—O—C splitting have been reported⁵⁻⁷ but the cause is unknown. Bellamy⁸ in his review on aliphatic ethers suggested that steric hindrance might be a possible cause.

Cyclic tetramer of 1,2-BO (II) was similarly prepared in 13% yield. It was insoluble in both hot and cold water. The tetramer showed a doublet at $1080\text{--}1120\text{ cm}^{-1}$ in the infrared spectrum compared with a broad singlet at 1100 cm^{-1} for the 1,2-BO homopolymer.

The attempted preparation of cyclic tetramer of *n*-PGE resulted in cyclic dimer (III) being formed, in 5% yield, as the only volatile product. The bulk of the reaction product was normal homopolymer. It is possible, however, that cyclic tetramer was formed, but its boiling point was such that it would not distil over under the conditions employed. The GPC studies suggest, in fact, that cyclic tetramer is formed. In addition, the GPC results indicate that cyclic pentamers and cyclic hexamers are also formed, but to a much lesser extent, in these and the other polymerizations studied.

THF in the presence of $\text{BF}_3 \cdot \text{O}(\text{C}_2\text{H}_5)_2$ failed to react.

The nature of the cyclic oligomers prepared from mixed monomer feeds at 0°C was also examined. The two cases studied were those in which the initial mole ratio of PO to THF was 1:1 and 1:4. The yield of cyclic product varied from 5% in the former to less than 1% in the latter case, while the overall conversion remained effectively constant. The bulk of the product in these reactions was normal copolymer. These cyclic compounds contained both PO and THF units and were mixtures of cyclic cotetramers of PO and THF. NMR and molecular weight measurements indicated that cotetramer contained at least two PO units. These mixtures were sparingly soluble in cold water but insoluble in hot water. The infrared spectra were similar to that of the cyclic tetramer of PO except for the band at 1200 cm^{-1} which was attributed to the presence of THF.

The cyclic oligomers are presumably all formed in the same way by attack on the oxonium ion at the end of a growing chain of oxygen atoms further back in the chain. The mode of formation of these cyclic oligomers and the effect of mixed monomer feed on cyclic oligomer formation has been discussed in Part I of this series.¹

DISCUSSION OF GPC OF POLYMERS AND OLIGOMERS

Copolymers of 1,2-BO and THF

Nine reaction products remaining from the reactivity ratio determinations with these two monomers in which the initial mole ratio of monomers varied from 9:1 to 1:9 (1,2-BO/THF), were examined by GPC by using column set I. A bimodal distribution was obtained in every case. Three of the chromatograms obtained are shown in Figure 1.

The smaller, sharper peak is attributed to the presence of the cyclic tetramer of 1,2-BO (a tetraethyl-1,4,7,10-tetraoxacyclododecane). The broad peak is, of course, due to the linear copolymer. The chromatograms show that as the monomer feed ratio increases from 9:1 to 2:8 (i.e., as THF content increases) the smaller peak decreases in height and its peak volume increases slightly. At the same time the larger peak changes its shape and its leading edge moves in the direction of greater molecular size (to the right).

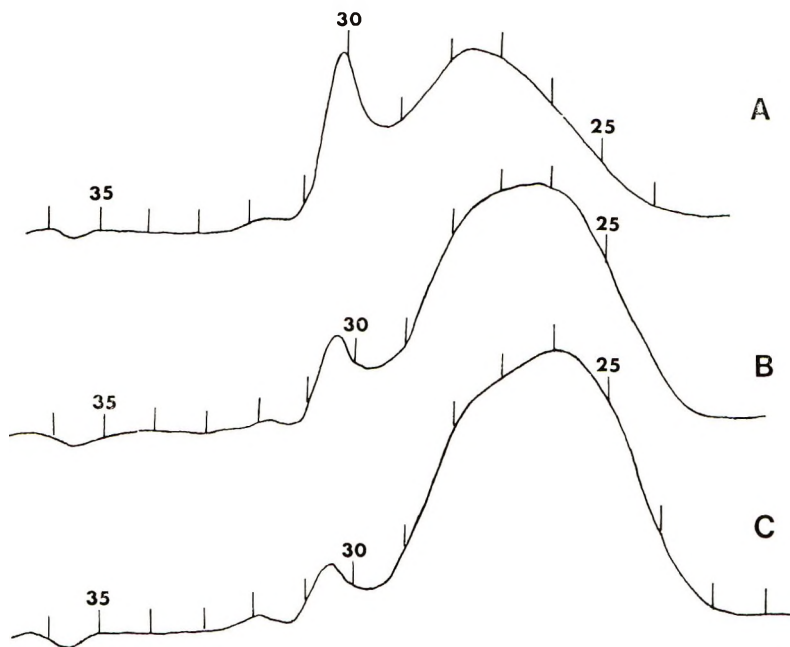


Fig. 1. Chromatograms of 1,2-BO-THF copolymers at various initial mole ratio of monomers: (A) 9:1, (B) 1:1, (C) 2:8; and various conversions (monomer to polymer): (A) 9.2%, (B) 5.8%, (C) 5.4%. Column Set I.

The GPC analyses show that in every case the formation of cyclic oligomer occurs and that the amount formed decreases steadily from about 25% of total polymerization product at low THF content in the monomer feed to about 5% at high THF content. The oligomer peak count drifts slowly and steadily to higher elution volume (smaller molecular size) with increasing THF content. This may indicate the formation of mixed cyclic cotetramers containing both 1,2-BO and THF monomer units. It is difficult to say how the replacement of a 1,2-BO unit in the oligomer ring by a THF unit would affect the volume of the tetramer molecule in solution. The presence of one THF unit would expand the ring from 12 to 14 atoms but an ethyl side-chain would be lost. The peak count drift to higher elution volumes may indicate that the volume in solution is decreased by incorporation of THF in the cotetramer.

Since our primary concern was to verify the existence of cyclic oligomers by GPC, no detailed interpretation (e.g., molecular weight calculation) of the copolymer peak was attempted. Such interpretation would be complicated by the fact that the oligomer peak and the linear polymer peak are not fully resolved and also by the fact (see Experimental Section) that the height of the chromatogram at any particular point is a function of both polymer concentration and copolymer refractive index, which is a function of the copolymer composition. In the present case, increase in the THF content of the copolymer leads to an increase in refractive index so that the shape of the broad copolymer peak changes with THF content of the copolymer (Fig. 1).

Copolymers of PO and THF

Seven of the nine copolymer samples prepared during reactivity ratio determinations¹ were examined by using column set I. The general features of the chromatograms obtained were similar to those of the 1,2-BO-THF copolymers just discussed. In this case, however, the peak ascribed to cyclic tetramer varied only very slightly in position with THF content, and this slight variation was in the opposite direction, towards greater molecular size.

Figure 2 shows the chromatogram of a sample of PO-THF copolymer, monomer-polymer conversion 25%, before and after removal of volatiles under a moderately high vacuum. The peak at 30.9 counts is assigned to

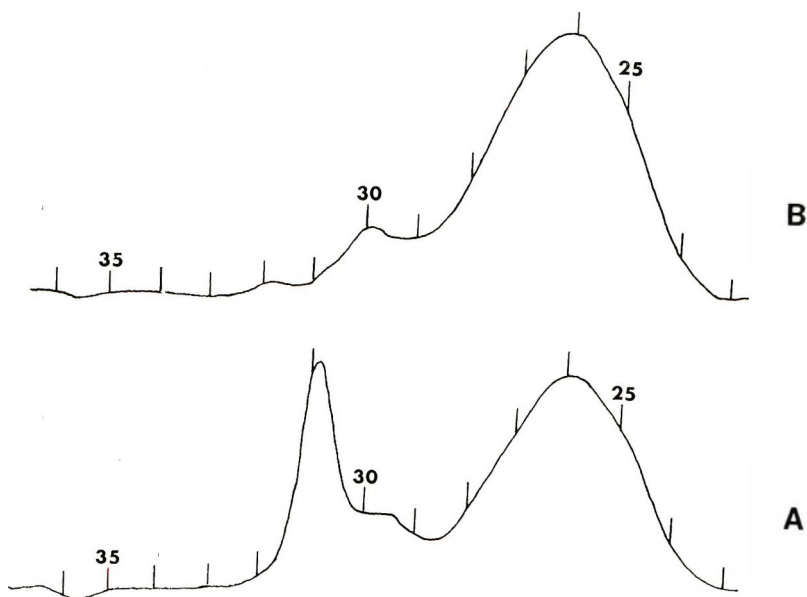


Fig. 2. Chromatograms of PO-THF copolymers: (A) sample before removal of cyclic tetramer by distillation. (B) sample after removal of cyclic tetramer. Initial mole ratio of monomers, 9:1; conversion (monomer to polymer), 25.2%; column set I.

cyclic tetramer of PO (a tetramethyl-1,4,7,10-tetraoxacyclododecane). It is apparent from Figure 2 that there is another component, with a peak near 30.0 counts, and possibly a third, with a peak in the vicinity of 29.2 counts. The compounds responsible for these peaks are probably the cyclic pentamer of PO (a pentamethyl 1,4,7,10,13-pentaoxacyclopentadecane), and the cyclic hexamer (hexamethyl-1,4,7,10,13,16-hexaoxacyclooctadecane).

Copolymers of *n*-PGE and THF

Six of the nine copolymer samples prepared during reactivity ratio determinations,¹ in which monomer to polymer conversion was about 5%, were examined, together with a homopolymer of *n*-PGE, conversion 15.8%. The chromatograms obtained were all similar to one another in general appearance, but, in contrast to the results involving 1,2-BO and PO, do not have two separately defined peaks. A typical chromatogram is shown in Figure 3 and shows a characteristic crinkled appearance on the left-hand side of the peak indicating the presence of a possible four components in addition to linear polymer. The same sample run at higher resolution, shown in Figure 4, confirms this suspicion. The peak near count 30 in Figure 4 is an artifact caused by solvent impurity. Figure 5 shows the chromatogram of a sample of the homopolymer of *n*-PGE, where two peaks are noticeable, one near 30 counts and another near 28 counts. The first

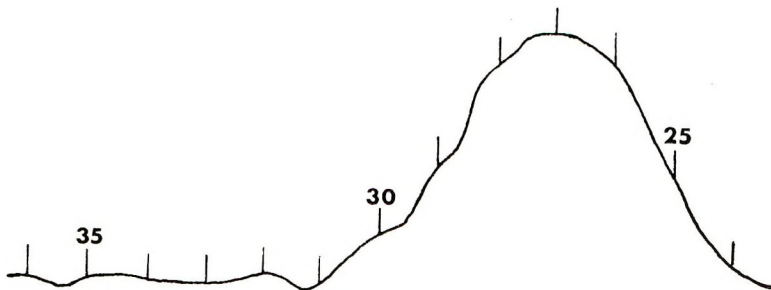


Fig. 3. Chromatogram of *n*-PGE-THF copolymer. Initial mole ratio of monomers 6:4; conversion (monomer to polymer), 5.0%; column set I.

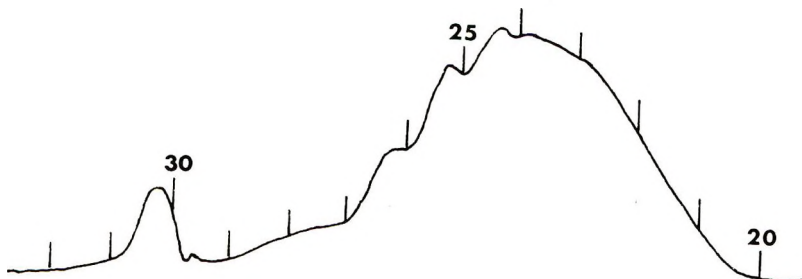


Fig. 4. Chromatogram of *n*-PGE-THF copolymer. Same sample as in Figure 3; column set II.

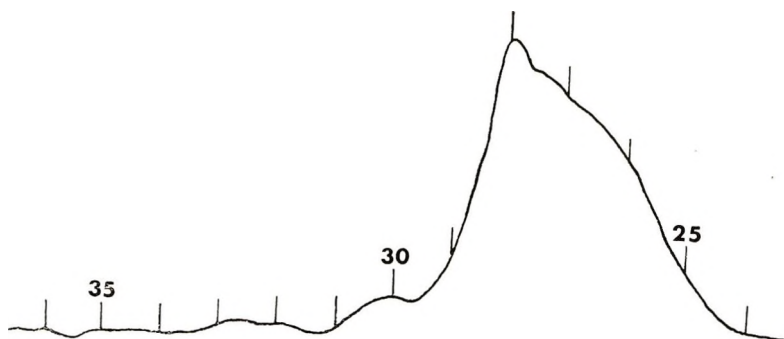


Fig. 5. Chromatogram of homopolymer of *n*-PGE. Conversion (monomer to polymer), 15.8%; column set I.

of these can be removed by vacuum distillation and is the cyclic dimer of *n*-PGE (dipropoxymethyl-1,4-dioxane), while the second is thought to be due to the cyclic tetramer (tetrapropoxymethyl-1,4,7,10-tetraoxacyclododecane). A peak at count 24.3 in Figure 4 is probably cyclic pentamer.

Cyclic Oligomers

It has been shown above that low molecular weight by-products are formed during the cationic polymerizations considered, and indications were that there was more than one such product. Chromatography of the volatile fractions obtained during large-scale preparative runs designed to make the cyclic tetramers of 1,2-BO and of PO and the cyclic dimer of *n*-PGE was carried out and resulted in the resolution of the cyclic tetramer, pentamer and hexamer of PO, the cyclic tetramer, pentamer, and hexamer of 1,2-BO and the cyclic dimer, trimer, and tetramer of *n*-PGE.

Oligomers of PO

In Figure 6 are shown the chromatograms, from a preparation of cyclic tetramer, of three volatile fractions and a residue obtained from this preparation.

Fractions 1 and 2 consist largely of cyclic tetramer with a small amount of the pentamer appearing in fraction 2. Fraction 3 consists largely of the cyclic pentamer, with a little tetramer remaining, together with a small amount of higher molecular weight material which appears to consist of two further compounds together with some linear polymer mechanically carried over during distillation. This last component is represented by the broad low peak on the right-hand side of the chromatogram of fraction 3. The chromatogram of the residue shows a peak at about 26 counts which is attributed to cyclic hexamer. The shape of this peak, however, suggests that it may represent two components imperfectly resolved. The identity of the main components in fractions 1 and 2 as cyclic tetramers, and of that of fraction 3 as cyclic pentamer, was independently established above.

The identity of the material represented by the left-hand peak in the chromatogram of the residue as cyclic hexamer was not directly established. However, the cyclic oligomers of PO, up to the hexamer, were described in

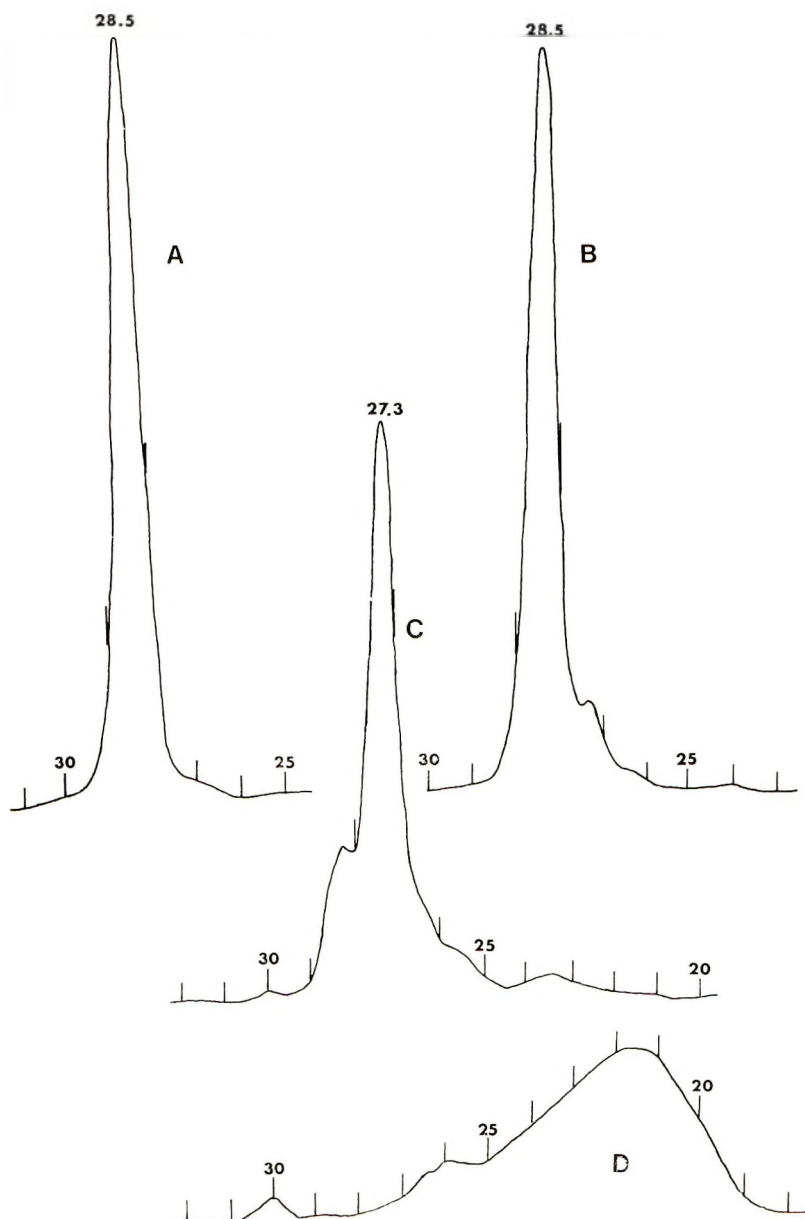


Fig. 6. Chromatograms of cyclic oligomers of PO from reaction product of PO and $\text{BF}_3 \cdot \text{O}(\text{C}_2\text{H}_5)_2$: (A) volatile fraction 1 (cyclic tetramer of PO); (B) volatile fraction 2 (cyclic tetramer of PO); (C) volatile fraction 3 (main component, cyclic pentamer of PO); (D) still-pot residue (contains linear polymer and cyclic hexamer of PO). Column set II.

1952 by Holden;⁴ these compounds, with the exception of the hexamer, are not recorded in *Chemical Abstracts*.

Recently Blanchard and Baijal published⁹ a paper on PO-THF copolymerization initiated by $\text{BF}_3 \cdot \text{O}(\text{C}_2\text{H}_5)_2$ in which they described the detection by GPC of a low molecular weight by-product which they provisionally concluded to be dimethyldioxane, the cyclic dimer of PO. It is perhaps worth pointing out that, aside from any other evidence, our product cannot be dimethyldioxane, since this molecule would certainly have too high a peak count, as may be seen by inspection of Table I. Consideration of the re-

TABLE I
Molecular Dimensions and Elution Volumes

Compound	Peak count		Dimension, Å
	Column set I	Column set II	
Toluene	35.3	32.6	7.8
Dioxane	34.75		5.8
Dimethyldioxane	33*		8.5
Trioxane	33.9		5.8
Cyclic tetramer of PO	31.3	28.45	11.8
Cyclic pentamer of PO		27.4	12.5
Cyclic hexamer of PO		26.6	13.7
Cyclic tetramer of 1,2-BO	30.7	27.35	13.8
Cyclic pentamer of 1,2-BO		26.35	14.2
Cyclic hexamer of 1,2-BO		25.0 ± 0.4	15.8
Dimer of <i>n</i> -PGE		27.9	
Trimer of <i>n</i> -PGE		26.3	
Tetramer of <i>n</i> -PGE		25.0	
Pentamer of <i>n</i> -PGE		24.2	

* Estimated value.

sults of Blanchard and Baijal in their Table I suggests that the molecule observed by them is in fact larger than dimethyldioxane; it is very likely largely cyclic tetramer.

Oligomers of 1,2-BO

Chromatograms of materials from 1,2-BO cyclic tetramer preparation clearly show peaks attributable to cyclic tetramer and cyclic pentamer. Chromatograms of fractions 4 and the still-pot residue appear in Figure 7. The tetramer was isolated and independently characterized. The pentamer peak was assigned from the observation that the distance between it and the tetramer peak was comparable with the distance between the peaks for the tetramer and pentamer of PO (see Table I). The cyclic hexamer is barely resolved in the chromatograms, but the shape of the curve in the vicinity of count 25 is considered to give a probable indication of its presence. On the basis of the figures in Table I, cyclic tetramer of 1,2-BO would be expected to peak between 25.0 and 25.5.

Oligomers of n-PGE

Four components are discernible in material from the reaction of *n*-PGE with $\text{BF}_3 \cdot \text{O}(\text{C}_2\text{H}_5)_2$. Very small amount of volatile matter was obtained. Chromatograms of fraction 2 and still-pot residue appear in Figure 8. The peak at count 30 is a solvent impurity peak. The sharp peak in the

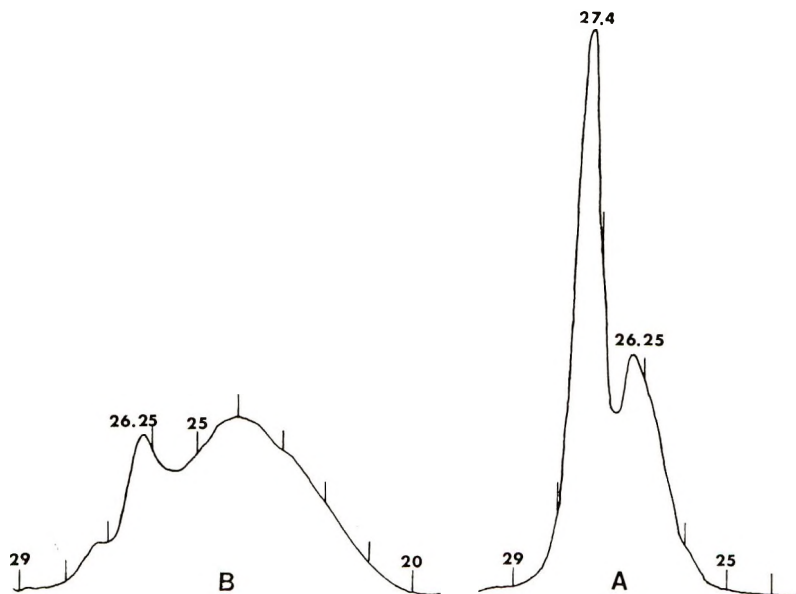


Fig. 7. Chromatograms of cyclic oligomers of 1,2-BO from reaction product of 1,2-BO and $\text{BF}_3 \cdot \text{O}(\text{C}_2\text{H}_5)_2$: (A) volatile fraction 4 (cyclic tetramer and cyclic pentamer of 1,2-BO); (B) still-pot residue (mainly linear polymer and cyclic pentamer of 1,2-BO). Column set II.

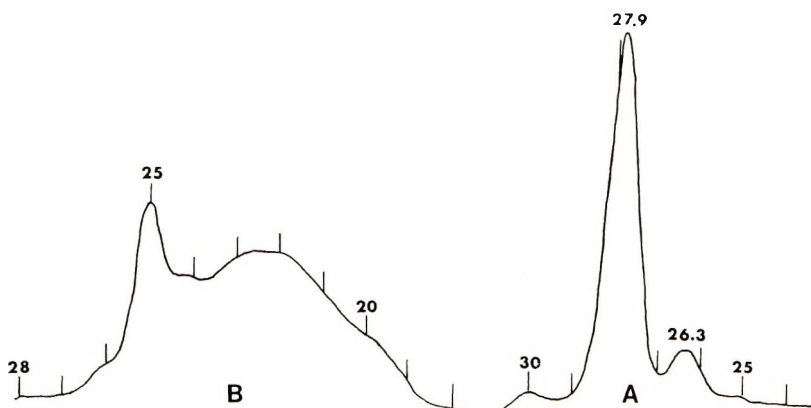


Fig. 8. Chromatograms of cyclic oligomers of *n*-PGE from reaction product of *n*-PGE and $\text{BF}_3 \cdot \text{O}(\text{C}_2\text{H}_5)_2$: (A) volatile fraction 2 (cyclic dimer and trimer of *n*-PGE); (B) still-pot residue (consisting of linear polymer and cyclic tetramer of *n*-PGE). Column set II.

chromatogram of fraction 2 arises from the presence of cyclic dimer, which was isolated and independently characterized. The smaller peak is attributed to cyclic trimer of *n*-PGE. The chromatogram of the residue shows a well defined peak at 25.0 counts; this is assigned to cyclic tetramer of *n*-PGE. The shoulder at count 24.2 may represent cyclic pentamer (cf. Fig. 4). The tetramer peak at 25 counts probably corresponds to the peak at 28 counts in the chromatogram of the homopolymer of *n*-PGE (Fig. 5). In this case, it can be seen from Figure 5 that the cyclic tetramer is produced in larger amounts than the dimer and trimer. This is in agreement with experience for PO and 1,2-BO.

Cyclic Co-oligomers of PO and THF

As was shown above, cyclic oligomers containing both PO and THF units are formed. Figure 9 shows the chromatogram of a total product of the copolymerization of PO and THF, where the linear polymer is of sufficiently high molecular weight to be well separated from the cyclic oligomers, which stand out as three small peaks corresponding to tetramer, pentamer, and hexamer.

The cyclic cotetramers which were isolated during the preparative part of this work are apparently mixtures of cyclic entities containing 0, 1, and 2 THF units, and these were not resolved during detailed GPC study of the isolated mixtures. The molecular volume of the possible compounds present is very close, for, while replacement in the ring of a PO unit by a THF unit expands the ring, at the same time a methyl side chain is lost.

In summary, these GPC studies have detected and isolated cyclic oligomers of epoxides from their polymerization products. In particular, cyclic tetramers, pentamers, and hexamers of both PO and 1,2-BO, and also cyclic

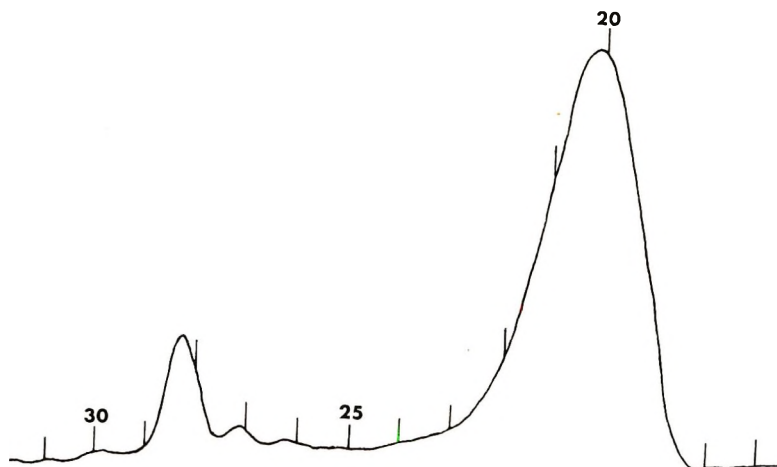


Fig. 9. Chromatogram of PO-THF copolymer containing cyclic by-products. Column set II.

dimer, trimer, tetramer, and pentamer of *n*-PGE, have been detected and isolated. The cyclic tetramer and pentamer of PO and the cyclic tetramer of 1,2-BO have been isolated and characterized.

Cyclic cotetramers containing both PO and THF monomer units have also been isolated. These materials are probably mixtures of molecules containing up to two tetrahydrofuran units. The existence of similar co-oligomers containing 1,2-BO or *n*-PGE and THF monomer units is probable.

References

1. J. M. Hammond, J. F. Hooper, and W. G. P. Robertson, *J. Polym. Sci. A-1*, **9**, 265 (1971) (Part I).
2. J. L. Down, J. Lewis, B. Moore, and G. Wilkinson, *J. Chem. Soc.*, **1959**, 3771.
3. J. M. Hammond, J. F. Hooper, and W. G. P. Robertson, *J. Polym. Sci. A-1*, **9**, 295 (1971) (Part III).
4. R. F. Holden, *Glycols*, G. O. Curme and F. Johnston, Eds., Reinhold, New York, 1952, p. 274.
5. R. B. Barnes, R. C. Gore, U. Liddel, and V. Z. Williams, *Infra-red Spectroscopy*, Reinhold, New York, 1944.
6. H. M. Randall, R. G. Fowler, N. Fuson, and J. R. Dangle, *Infra-red Determination of Organic Structures*, Van Nostrand, New York, 1949.
7. H. Tschamler and R. Leutner, *Monatsh.*, **83**, 1502 (1952).
8. L. J. Bellamy, *The Infra-red Spectra of Complex Molecules*, Wiley, New York, (Methuen, London), 1956, p. 101.
9. L. P. Blanchard and M. D. Baijal, paper presented to the Division of Polymer Chemistry, American Chemical Society, Meeting, 1966; *Polym. Preprints*, **7**, 944 (1966).

Received October 30, 1968

Revised June 26, 1970

Cationic Copolymerization of Tetrahydrofuran with Epoxides. III. Synthesis of Block Copolymers

J. M. HAMMOND, J. F. HOOPER, and W. G. P. ROBERTSON,
*Australian Defence Scientific Service, Department of Supply, Weapons
Research Establishment, Salisbury, South Australia*

Synopsis

Polymerization of various cyclic ethers by $\text{BF}_3 \cdot \text{O}(\text{C}_2\text{H}_5)_2$ in the presence of polymeric glycol leads to the formation of hydroxyl terminated block copolymers. Where poly(oxyethylene glycol) is used as the polymeric glycol, fission of the poly(oxyethylene glycol) chain occurs, and block copolymers containing shorter ethylene oxide unit sequences are obtained. With poly(oxypropylene glycol), on the other hand, the polymer chain remains intact. This may be due to the steric influence of the pendant methyl groups. The cyclic oligomers formed as by-products in the polymerizations are easily removed.

INTRODUCTION

According to the mechanism proposed in Part I of this series,¹ $\text{BF}_3 \cdot \text{O}(\text{C}_2\text{H}_5)_2$ -initiated growing polyether chains undergo facile transfer with 1,4-butanediol (1,4-BD) to give hydroxyl-terminated polymers. It seemed that a novel method of preparing block copolymers might be to carry out these polymerizations in the presence of polymeric glycols.

This paper describes such attempts by use of poly(oxyethylene glycol) (PEG) and poly(oxypropylene glycol) (PPG) as polymeric glycol with propylene oxide (PO), 1,2-butylene oxide (1,2-BO), and tetrahydrofuran (THF) as monomers.

EXPERIMENTAL

Reagents

PEG 636 and PPG 1011, both commercial grade reagents, were dried in a rotating evaporator prior to use. The numbers 636, 1011 refer to the molecular weights as determined by endgroup analysis. Other reagents were purified as described previously.¹

Polymer Syntheses

The polymerizations were carried out according to the polymerization procedure described previously.¹ In the present polymerizations, however, polymeric glycols were used in place of the 1,4-BD.

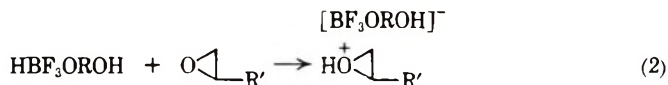
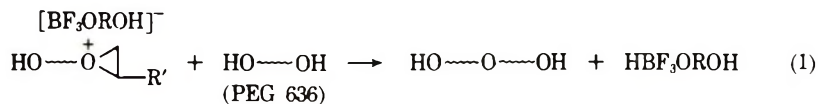
The product was worked up as described previously;¹ the process involved extraction with water. In addition to isolating the product from the organic layer, a check was made on the aqueous layer for the presence of any unreacted polyol or other products. Water and unreacted monomers were removed under vacuum in a rotating evaporator at room temperature.

The products were analyzed by NMR and GPC. Molecular weights were determined by endgroup analysis [$\bar{M}_n(\text{OH})$] and vapor pressure osmometry [$\bar{M}_n(\text{VPO})$].

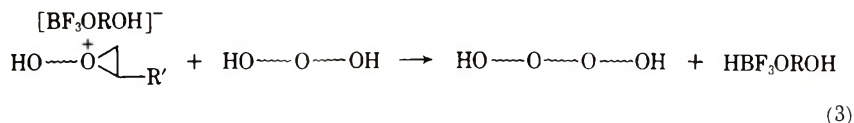
RESULTS AND DISCUSSION

Results of the polymerizations are outlined in Table I. In the polymerization of PO and copolymerization of PO with THF, block copolymers were isolated from both the organic and aqueous phases. Separation of the block copolymer products into oil-soluble and water-soluble portions reflects varying solubility characteristics depending on poly PO/poly(ethylene oxide) (poly EO) and poly (PO + THF)/poly EO ratios. The block copolymers isolated from the organic phase were shown to be contaminated with cyclic tetramers and cyclic pentamers by GPC. These cyclic oligomers were easily removed by distillation under vacuum onto a cold finger. GPC of the polymer products in each case failed to detect the presence of any unreacted PEG 636.

According to the previously proposed mechanism¹ transfer of the PEG 636 to the growing polymer chain would proceed as shown in eqs. (1) and (2):



Once formed, the polyether glycol could undergo further transfer [eq. (3)],



followed by reaction (2). Theoretically, each block copolymer chain would then contain one PEG 636 fragment.

In the case of PO polymerization, block copolymers were obtained having molecular weights of 672 and 664. If each polymer chain contained one PEG 636 molecule, as the theory suggests, there would be room for possibly only one PO unit giving a mole ratio for EO/PO of 14:1. In fact, the EO/PO ratios (Table I) were considerably lower, indicating that the PEG

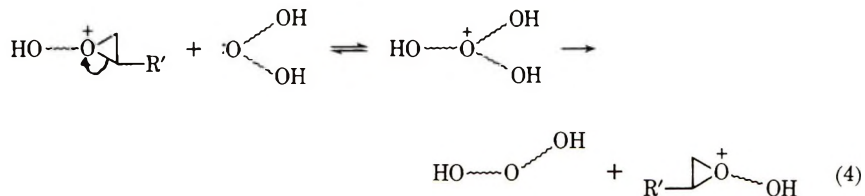
TABLE I
 Polymerization of Cyclic Oxides by $\text{BF}_3 \cdot \text{O}(\text{C}_2\text{H}_5)_2$ in the Presence of Polymeric Glycols with Ethylene Dichloride as Solvent^a

Monomers	Polymeric glycol	Reaction time, hr	Total yield, %	Fraction	Yield of cyclic by-products, %	Yield, %	Polymer	
							NMR determination of monomer unit ratios	$\bar{M}_n(\text{OH})$ $\bar{M}_n(\text{VPO})$
PO	PEG 636	3	28.8	(CH_2Cl) ₂ -soluble	6.8	7.1	EO/PO (1.29:1)	672
PO/THF (1:1)	PEG 636	3 1/2	34.5	(CH_2Cl) ₂ -soluble	6.1	14.9	EO/PO (3.73:1)	664
						20.6	EO/PO (1.19:1)	1437
1,2-BO	PPG 1011	3 1/2	31.7	(CH_2Cl) ₂ -soluble	7.5	7.8	EO/PO (6.52:1)	670
						24.2	PO/THF (1.58:1)	1250
				H ₂ O-soluble	nil	nil	PO/1,2-BO (3.18:1)	975

^a Catalyst, polymeric glycol and solvent concentrations were 0.08, 1.60, and 64 mole-%, respectively, based on total monomer.

636 chain has been split. In the case of PO-THF polymerization the differences between the theoretical and observed ratios were not so great.

Fission of the PEG chain can occur as a result of attack on the oxonium ion at the end of a growing chain by ether oxygen atoms of a PEG chain in a neighboring molecule, according to the reactions (4).



Such an attack would result in a redistribution of monomer sequences. However, the number of polymer molecules formed would remain unaltered.

The formation of cyclic oligomers in the polymerizations takes place according to the mechanism proposed for cyclic oligomer formation in Part I of this series.¹

The 1,2-BO polymerization, on the other hand, is rather different. The product isolated from the organic phase was a mixture of block copolymer and cyclic oligomers (Table I). GPC of the products failed to detect the presence of any unreacted PPG 1011. The mole ratio of PO to 1,2-BO in the block copolymer was 3.18:1, which is comparable with a theoretical value of 5.15:1 for a copolymer of molecular weight 1250. This result infers that the PPG 1011 chain in the copolymer is intact. Probably the PPG 1011 chain does not undergo fission because its pendent methyl groups hinder interaction between ether oxygen atoms in the PPG chain and neighboring oxonium ions.

Reference

1. J. M. Hammond, J. F. Hooper, and W. G. P. Robertson, *J. Polym. Sci. A-1*, **9**, 265 (1971) (Part I).

Received October 30, 1968

Revised June 26, 1970

Orientation of Polymer Molecules during Melt Spinning. I. Estimation of Degree of Orientation By Retraction above T_m

JUNJI FURUKAWA, *Faculty of Engineering, Kyoto University Yoshida, Kyoto, Japan*, and TOSHIO KITAO, SHINZO YAMASHITA, and SEIGO OHYA, *Kyoto University of Industrial Arts and Textile Fibers, Matsugasaki, Kyoto, Japan*

Synopsis

The elastic deformation ratio by spin-stretching was estimated by means of thermal retraction technique, data for a melt-spun filament from a crystalline polymer were compared with those from an amorphous one. The necessary conditions for equilibrium retraction were determined as 7 min at 170°C for amorphous polystyrene and 30 min at 180°C for high-density polyethylene. The effects of molecular weight and melt draw ratio on the retraction behavior were discussed and concluded to be negligible. The apparent activation energies of viscous flow were calculated from the temperature dependence of the retraction curves. The activation energy for polystyrene decreases with increasing temperature of retraction, as predicted by the WLF equation, and that of polyethylene obeys Arrhenius law (about 12 kcal/mole). This may be attributed to the difference in glass transition temperatures of the two polymers. By measuring the effective melt draw ratio of the resultant filaments of different melt draw ratio, it was made clear that the elastic deformation increases with increasing apparent melt draw ratio. Finally, the optical anisotropy of the filaments was related to the deformation ratio. It was concluded that Kuhn and Gr \ddot{u} n's equation may be applicable for polystyrene but not for polyethylene.

INTRODUCTION

When polymeric substances, which are a kind of viscoelastic body, are subjected to such deformations as stretching, shearing, and compression, configurational changes take place in the polymer molecules of which they are composed, accompanied by a considerable amount of intermolecular slippage. Elastic deformation, caused by the configurational change of the polymer, results in an increase of anisotropy of optical and tensile properties of the substance. To the contrary, viscous flow does not affect the properties and merely decreases the cross-sectional area of the specimen. Therefore, it seems to be of interest to separate the elastic contribution from total deformation, from both a theoretical and practical point of view.

There are many methods for determining quantitatively the anisotropy of polymeric substances, e.g., infrared dichroism for whole polymer, x-ray diffraction for the crystalline phase, fluorescence for the amorphous phase.

Measurement of birefringence is one of the most useful technique for estimation of degree of orientation. Kuhn and Grün¹ have theoretically derived an equation concerned with the relation between deformation ratio and the birefringence for ideal rubbers. In spite of this development in the science and engineering for linear polymers, no theoretical approach to the relation has been established, because of the complicated behavior of crystalline deformation and the optical and stress relaxation during deformation.

Cleermann, Karn, and Williams² and Andrews³ have tried to divide the apparent draw ratio into the elastic deformation ratio and the viscous flow ratio components by heat treatment of polystyrene monofilaments above its glass transition temperature and obtained some interesting results.

In this paper, the procedure is applied to one amorphous polystyrene and three high-density polyethylene filaments which have been oriented by melt drawing. The objectives of this paper are to confirm the availability of the retraction technique for crystalline polymers and to elucidate the relation between the apparent draw ratio and the elastic deformation ratio.

EXPERIMENTAL

Materials and Preparation of Specimens

The polymers used in this study and the spinning conditions of their preparation are summarized in Table I.

TABLE I
Summary of Polymer Properties and Spinning Temperature

Polymer	Molecular weight	Density, g/cc	Spinning temp, °C
Polystyrene	185,000	—	240
Polyethylene 1	40,000	0.960	170
Polyethylene 2	70,000	0.955	170
Polyethylene 3	120,000	0.955	170

Filaments were spun with a research spinning machine which was made up of a 20 mm extruder, a pair of take-up devices, and a winder. Melt drawing was carried out by taking up the resultant filament at a rate faster than the velocity of extrusion of the molten polymer stream through the spinneret of the spinning machine. The polymer stream was cooled and solidified in the atmosphere.

Heat Treatment (Thermal Retraction) of Melt-Drawn Filaments

Filaments, put in a small cage made of 100-mesh stainless steel net, were immersed into a bath which was filled with PEG 400 [a poly(ethylene glycol) whose molecular weight is about 400] or silicone oil, for polystyrene or polyethylene, respectively, at various temperatures for some specified periods.

After treatment, the filaments were removed from the bath and cooled to room temperature. The retraction ratio was determined from the lengths of the specimens before and after heat treatment. The processing variables for polystyrene were temperatures of 100, 105, 110, 115, 120, 125, 130, 140, 150, 160, and 170°C for times of 1.5, 2.0, 3.0, 4.0, 6.0, 7.0, 10, 15, 20, 30, 40, or 60 min. For high-density polyethylene, the variables were 135, 150, 160, 170, 180, 190, and 195°C; 3.0, 4.25, 6.0, 6.5, 9.0, 13, 15, 20, and 30 min. At 95°C, polystyrene filaments did not show any detectable retraction. At highest temperature, i.e., 170°C, the shape of the specimen was retained. This implies that the effects of swelling by PEG and interfacial tension between the filament and PEG can be regarded as negligible. Certainly, the weight of a specimen was not changed by the treatment.

The same procedure was carried out to study the interaction of silicone with polyethylene.

Results and Discussion

Retraction of Polystyrene Monofilaments

The retraction curves for polystyrene filaments whose melt draw ratio is 180 are shown in Figure 1; they show a marked temperature dependence as expected. The ordinate of this graph is the logarithm of the length of the specimen treated for a time t relative to the initial length; the abscissa is the treatment time. Fox and Flory⁴ found that the glass transition temperature of polystyrene is a function of its degree of polymerization: $T_g = 100 - 1.8 \times 10^{-5}M^{-1}$, where M is the molecular weight of the polymer and T_g is in degrees centigrade. From this relation and the result in Figure 1, it seems that T_g of the polymer examined is a few degrees lower than 100°C.

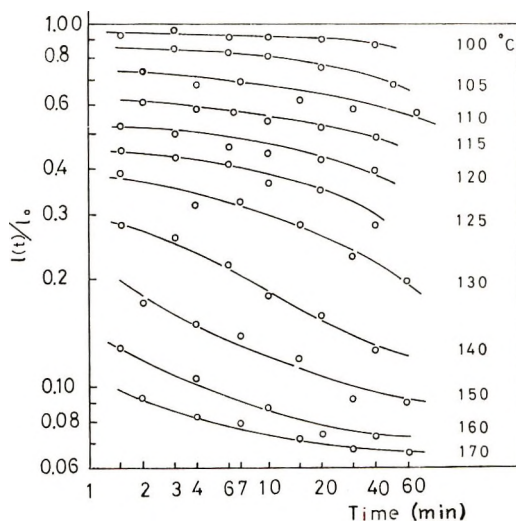


Fig. 1. Temperature dependence of retraction curves for polystyrene monofilament.

On selecting an appropriate shift factor a_T adoption of the time-temperature superposition principle leads to Figure 2. In this case, data were reduced to 170°C.

Figure 3 shows the relation between a_T and the bath temperature T . Since the apparent activation energy of viscoelastic relaxation ΔH is given by $\Delta H = 2.303 R d \log a_T / d(1/T)$, it can be calculated from the tangent of

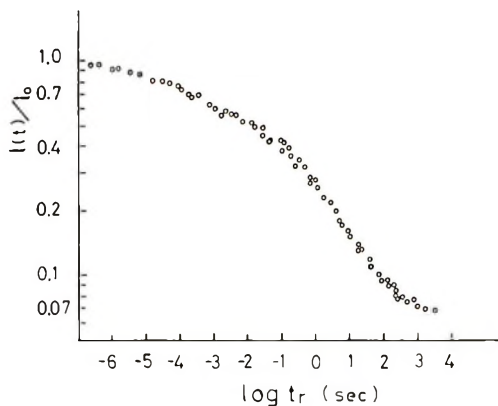


Fig. 2. Master curve for polystyrene reduced to 170°C.

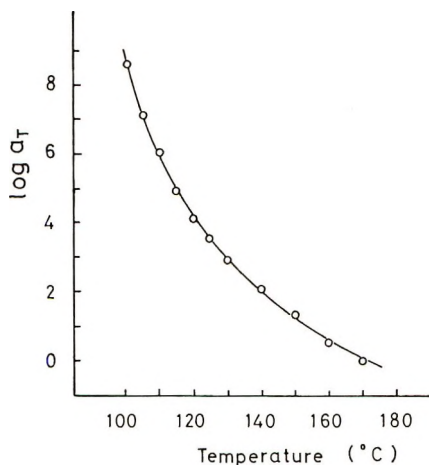


Fig. 3. Relation between logarithm of shift factor and retraction temperature.

the plot of $\log a_T$ versus reciprocal temperature. Results are shown in Figure 4. As expected, the plots do not lie on a straight line within the temperature range covered. For comparison, the data from stress relaxation for an unfractionated polystyrene, measured by Fujita and Ninomiya,⁵ were superimposed on the figure. As was pointed out by Andrews,³ the activation energies obtained by the retraction technique are rather larger than those from others. Since further discussion must be based on the

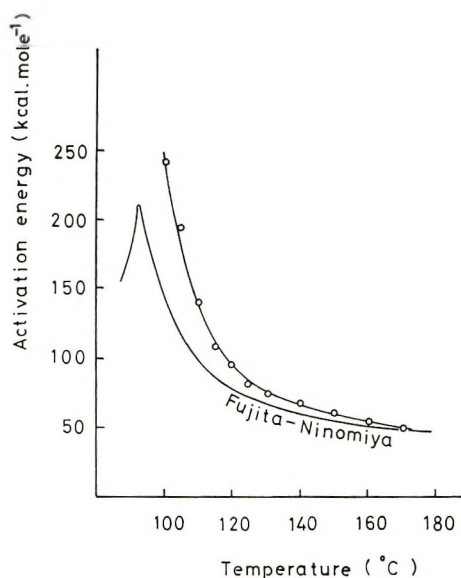


Fig. 4. Change in activation energy with temperature. Also shown are data from stress relaxation measured by Fujita and Ninomiya.

characteristic properties of the polymer, for instance molecular weight, T_g , etc., we shall not discuss the activation energies further.

It may be concluded that equilibrium retraction requires 7 min at 170°C.

Retraction of High-Density Polyethylene

The same procedure as mentioned in the preceding section was used for crystalline polymer. Though T_g of polyethylene is at -110°C , the existence of crystallites conserves the shape of the filament from retraction up to its melting point T_m , about 130°C . (However, cold-drawn filament shrinks below T_m .) The effects of melt draw ratio and molecular weight were examined concurrently.

Polyethylene of MW = 40,000. Curves of retraction with time are shown in Figure 5. The curves at 180 and 190°C overlap that at 170°C . This may suggest that the critical molecular weight of polyethylene is larger than 20,000 above 180°C . A master curve, as is shown in Figure 6, is obtained by sliding the data along the horizontal axis without the data at 180 and 190°C . A plot of $\log a_T$ versus reciprocal temperature gives the apparent activation energy of flow. Contrary to the case of polystyrene, as is shown in Figure 7, it obeys the Arrhenius law, and ΔH is calculated as 11.9 kcal/mole.

As was pointed out by Ferry and co-workers⁶ and Bueche,⁷ the WLF equation is applicable below $T_g + 120^\circ\text{C}$ and the relation between a_T and reciprocal temperature agrees with Arrhenius' formula above it. Since the rate of retraction of polyethylene filament is much faster than that of polystyrene even at the lowest temperature of treatment (135°C) the

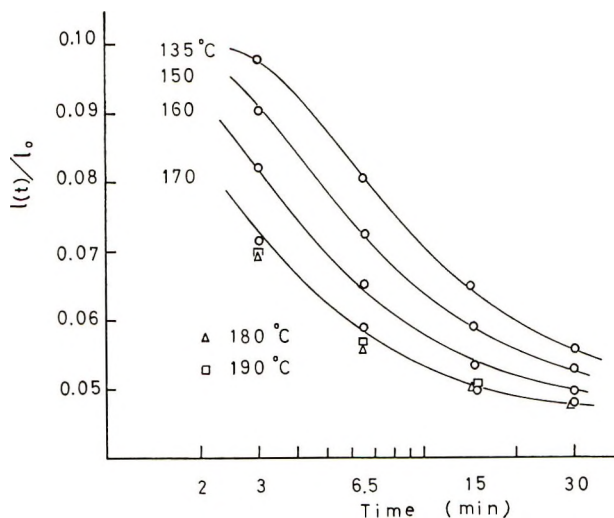


Fig. 5. Retraction curves for high-density polyethylene monofilament. (Molecular weight is 40,000; melt draw ratio is 500.)

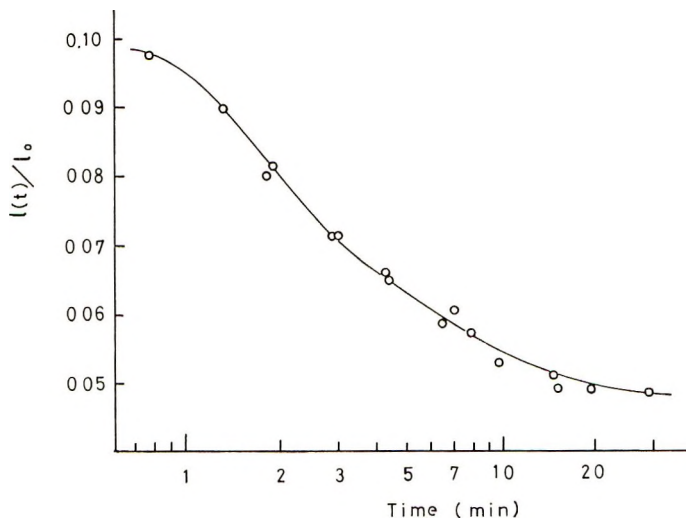


Fig. 6. Master curve for polyethylene (MW = 40,000) reduced to 170°C.

master curve can cover only a narrow region of time. It is, however, sufficient to estimate the time required for the equilibrium retraction and the elastic deformation ratio in the course of melt spinning. From these results, it is evident that 30 min or longer is required to separate the elastic contribution from that of the apparent melt draw ratio.

Polyethylene of MW = 120,000. Data on the retraction of this filament are shown in Figures 8–10. In these figures there are no irregular plots as found in Figure 5. The tangent to the curve in Figure 10 gives the ap-

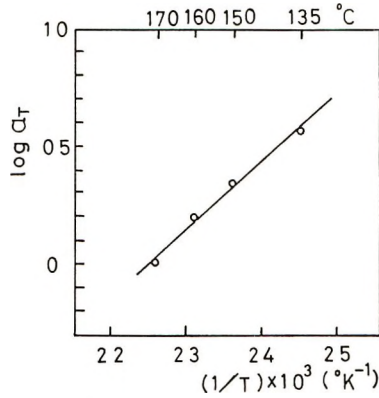


Fig. 7. Plot of logarithm of shift factor a_{τ} against reciprocal temperature. (MW = 40,000; $\Delta H = 11.9$ kcal/mole.)

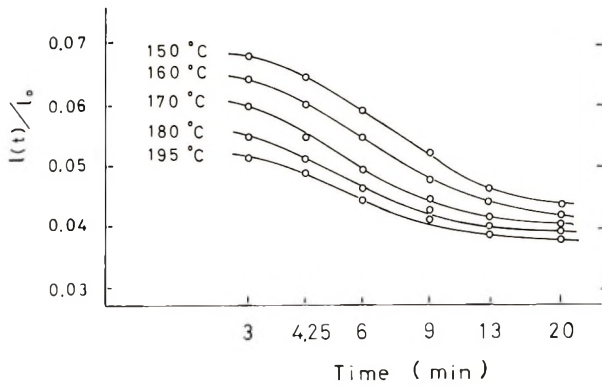


Fig. 8. Retraction curves for polyethylene monofilament. (Molecular weight is 120,000; melt draw ratio is 500.)

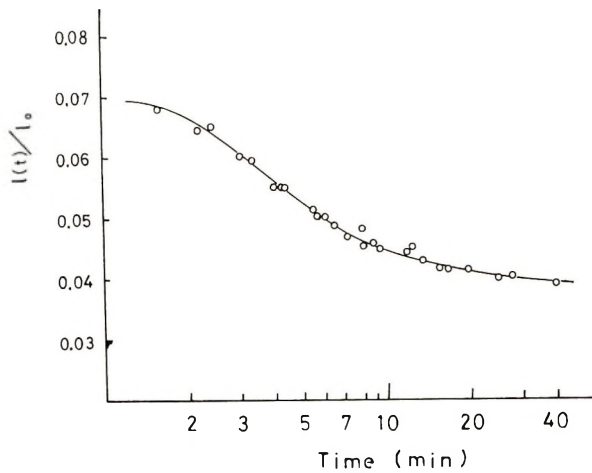


Fig. 9. Master curve for polyethylene (MW = 120,000) reduced to 170°C.

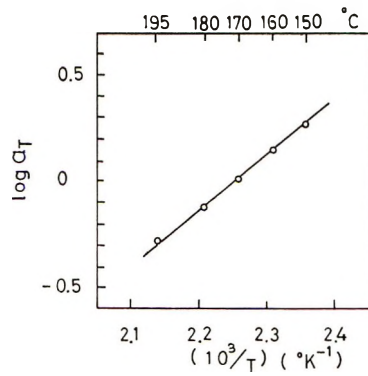


Fig. 10. Arrhenius plot of shift factor. MW = 120,000; $\Delta H = 11.5$ kcal/mole.

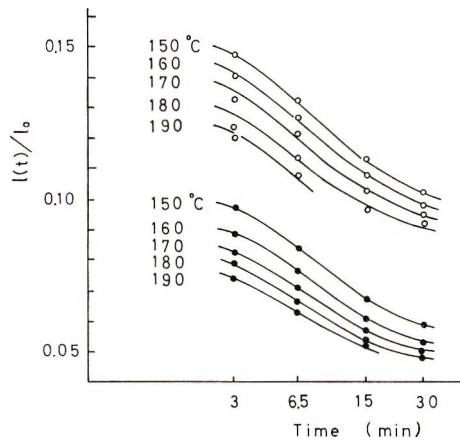


Fig. 11. Effect of melt draw ratio on retraction behavior of polyethylene (MW = 70,000) at various melt draw ratios: (O) 80; (●) 500.

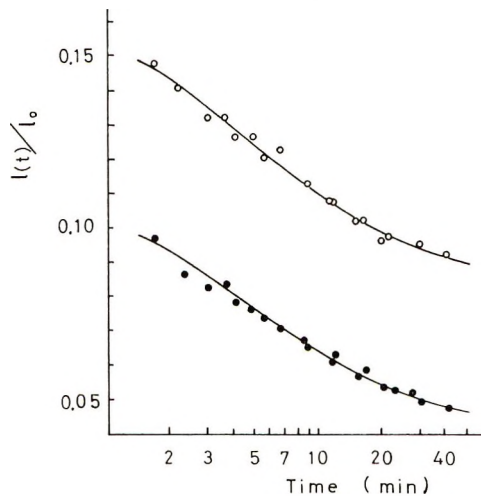


Fig. 12. Master curves of polyethylene monofilaments (MW = 70,000) reduced to 170°C: (O) melt draw ratios, 80; (●) melt draw ratio, 500.

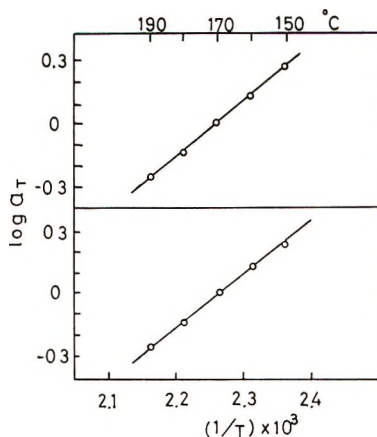


Fig. 13. Arrhenius plot of shift factor for polyethylene (MW = 70,000) at melt draw ratios of 80 (top) and 500 (bottom). $\Delta H = 11.5$ kcal/mole.

parent activation energy as 11.5 kcal/mole. The equilibrium retraction requires at least 30 min at 170°C.

Effect of Melt Draw Ratio. It may be expected that the elastic deformation ratio of polymer molecules increases monotonically with increasing melt draw ratio of the resultant filament. Two polyethylene filaments of molecular weight 70,000 and of different melt draw ratios, were subjected to retraction. In spite of the expectation, no difference was observed (Figs. 11–13) in the retraction behavior. This may be due to the narrowness of the treatment time range. If we could study the very short-time region with sufficient precision, the effect of melt draw ratio on the activation energy could be made clear.

Separation of Elastic Deformation Ratio from Total Melt Draw Ratio

The conditions for the equilibrium retraction as obtained from the above results are summarized in Table II.

Filaments of different melt draw ratio were subjected to retraction under these processing variables and their effective stretch ratios estimated. Results are shown in Figure 14. The ordinate of this figure is the logarithm of the elastic deformation ratio, abscissa being the logarithm of the apparent melt draw ratio; hence the difference between the dotted straight line and the curve obtained from experiments gives the logarithm of the

TABLE II
Temperature and Time for Reaching Equilibrium Retraction

Polymer	Temperature, °C	Time, min
Polystyrene	170	7
	160	30
Polyethylene	180	30

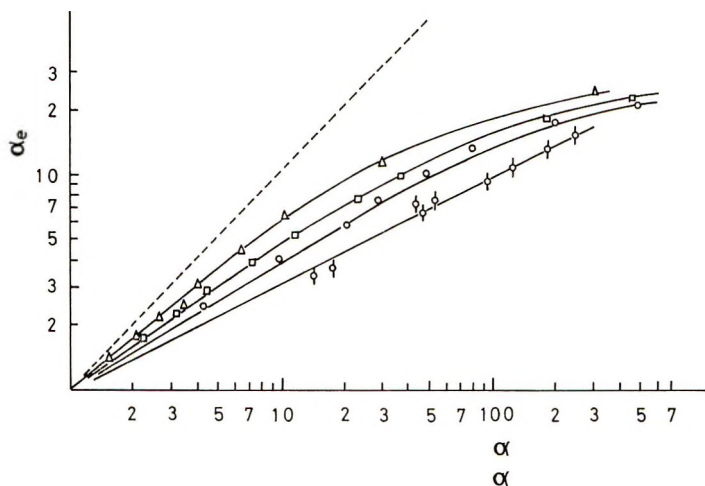


Fig. 14. Relation between melt draw ratio α and elastic deformation ratio α_e : (\odot) polystyrene; (\circ) polyethylenes, MW = 40,000; (\square) polyethylene, MW = 70,000; (\triangle) polyethylene, MW = 120,000.

viscous flow ratio. The apparent melt draw ratio is generally calculated as the ratio of the velocity of extrusion through the spinneret to that of winding. In this paper, in order to evaluate the orientation in the spinning machine, the cross-sectional area of the resultant filament was compared with that of a filament that was freely extruded, swollen, and allowed to retract.

The elastic deformation ratio increases with increasing apparent melt draw ratio. And also, it is evident that the viscous flow and/or elastic deformation are functions of molecular weight of polymer.

Change in Birefringence with Melt Draw Ratio

The birefringence Δn of as-spun filaments was measured at room temperature by using a polarizing microscope equipped with a Berek compensator. Results are shown in Figures 15 and 16 for polystyrene and polyethylene, respectively. The abscissa of Figure 15 is $(\alpha_e^2 - \alpha_e^{-1})$ for comparison with the theoretical equation of Kuhn and Grün, $\Delta n = k(\alpha_e^2 - \alpha_e^{-1})$. The birefringence of polystyrene, having a negative sign, increases monotonically with increasing elastic deformation ratio and seems to satisfy qualitatively the requirements of the theory.

On the other hand, the birefringence of polyethylene was measured for two as-spun filaments having different molecular weights, 40,000 and 120,000. Figure 16 shows that the birefringence of these filaments depends markedly upon molecular weight. Though this may be explained in terms of the density of the free end chain, more precise information is required for further discussion. It is also clear that the relation for polyethylene does not obey the theory. This may be caused by the fact that when polyethylene crystallizes from its melt the crystallizing behavior is governed not only by the extent of molecular stretching but also by cooling conditions.

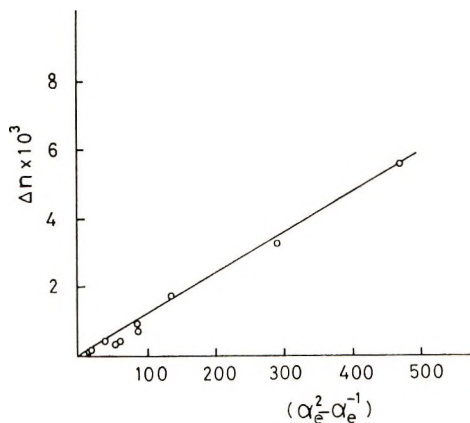


Fig. 15. Change in birefringence of polystyrene filament with elastic deformation ratio estimated by applying retraction technique.

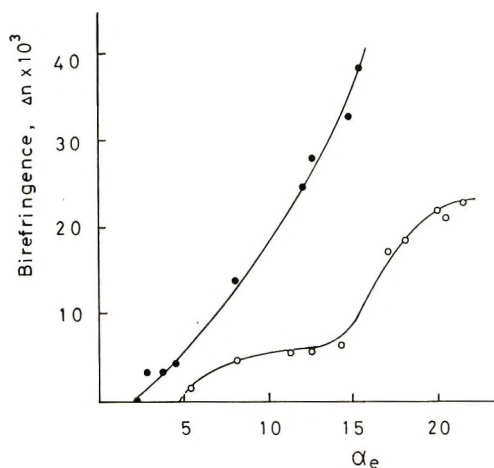


Fig. 16. Change in birefringence of polyethylene filament with elastic deformation ratio: (○) MW = 40,000; (●) MW = 120,000.

For instance, Keller⁶ has pointed out that melt-spun polyethylene filaments have an unusual orientation of crystallites, ("raw orientation"). Also, Judge and Stein⁷ have investigated the crystallization of a slightly cross-linked polyethylene and concluded that the *a*-axis orientation of folded crystals was predominant in specimens stretched 200% or less, whereas single pass type crystals were aligned along the stretching direction in specimens stretched 200% or more.

Though it is of interest to clarify the morphology of crystalline region, the change in birefringence of perfectly amorphous polyethylene must be ascertained in order to determine a quantitative expression for the relation in Figure 16. It is, however, difficult to estimate this, because of its rapid relaxation.

Retraction of Other Filaments

The retraction technique was applied to some filaments of nylon 6 and poly(ethylene terephthalate). Unfortunately, it was very difficult to estimate the equilibrium retraction because of the following reasons: (1) we could not find any suitable retraction medium, having a specific gravity similar to that of these polymers, as poly(ethylene glycol) for polystyrene and silicone for polyethylene, at elevated temperature; (2) the melt viscosity was so small that the shape of specimen was not retained during heat treatment; (3) restriction to the applicable temperature range makes the exact estimation difficult.

CONCLUSIONS

The apparent melt draw ratio may be divided by use of the retraction technique into two elemental deformation ratios, i.e., an elastic deformation ratio and a viscous flow ratio.

The rate of retraction is dependent mainly upon the treating temperature. The application of the time-temperature superposition principle to the retraction data gives a reasonable shift factor and the activation energy of flow for both amorphous and crystalline polymers.

On comparing birefringence data with retraction data for some as-spun fibers, it is clear that the degree of orientation of an amorphous polystyrene can be estimated only from its optical anisotropy, whereas the birefringence of polyethylene filament does not reflect the accurate deformation ratio of the molecules because of the complex behavior of crystallization. Hence, the extent of molecular stretching in an as-spun fiber must be determined not by an optical method but by a method such as the retraction technique.

It must be noticed that the elastic deformation ratio increases with increasing apparent melt draw ratio and that the polymer molecules in a highly stretched filament are extended along the fiber axis beyond expectation.

References

1. W. Kuhn and F. Gr \ddot{u} n, *Kolloid-Z.*, **101**, 248 (1942).
2. K. J. Cleemann, H. J. Karn, and J. L. Williams, *Mod. Plastics*, **30**, 119 (May 1953).
3. R. D. Andrews, *J. Appl. Phys.*, **26**, 1061 (1955).
4. T. G. Fox, Jr., and P. J. Flory, *J. Appl. Phys.*, **21**, 581 (1950).
5. H. Fujita and K. Ninomiya, *J. Polym. Sci.*, **24**, 233 (1957).
6. A. Keller, *J. Polym. Sci.*, **15**, 31 (1955).
7. J. T. Judge and R. S. Stein, *J. Appl. Phys.*, **32**, 2357 (1961).

Received April 14, 1970

Transient Analysis of a Viscoelastic Torsion Pendulum: Error Analysis

R. D. GLAUZ, *Department of Mathematics,
University of California, Davis, California 95616*

Synopsis

The error analysis for the transient torsion pendulum test is developed based on a linearized approximation. Tables are given for the efficient utilization of the equations in evaluating the accuracy range of the test data.

Introduction

The analysis of the transient torsion pendulum has been developed in a previous paper.¹ This continuation of that work consists of an error analysis for use in evaluating the accuracy range of test data. The physical measurements inherent in the testing process introduce small experimental errors which have varying effects on the final computed physical parameters of the material. It is assumed that under precise laboratory conditions the errors will be sufficiently small that a linearized error analysis is applicable. By using the resulting analysis either a range of error, or standard deviation of error can then be obtained.

Analysis

The method of differentials² will be used in the linearized analysis of small errors. From the previous paper¹ the following equations are obtained:

$$\alpha \cos \psi - \psi \sin \psi = 0 \tag{1}$$

$$\alpha = (\rho I_p l / I_1) [1 + (\psi^2 / I_p l^2) \int \varphi^2 dA] \tag{2}$$

$$G_1 = (\omega^2 - \lambda^2) I_1 \alpha / \psi^2 \kappa \tag{3}$$

$$G_2 = 2\omega\lambda I_1 \alpha / \psi^2 \kappa \tag{4}$$

The symbols and units are summarized in Table I.

Taking the logarithmic derivative of eqs. (1)–(4) yields

$$\frac{d\psi}{\psi} = \left(\frac{\sin \psi \cos \psi}{\psi + \sin \psi \cos \psi} \right) \frac{d\alpha}{\alpha} \tag{5}$$

TABLE I
Nomenclature

Symbol	Definition	Units
a, b	Half dimensions of rectangular cross section	in.
G_1, G_2	Complex shear modulus components	lb/in. ²
I_1	Mass moment of inertia of pendulum bob	in.-lb-sec ²
I_p	Polar moment of inertia of cross section	in. ⁴
l	Length of pendulum	in.
r	Radius of circular cross section	in.
α	Intermediate variable (inertia ratio)	
κ	Torsional constant	in. ⁴
λ	Damping factor	l./sec
ρ	Density	lb-sec ² /in. ⁴
φ	Torsion function	in. ²
ψ	Eigenvalue	—
ω	Frequency of vibration	rad/sec

$$\frac{d\alpha}{\alpha} = \frac{d\rho}{\rho} + \frac{1}{(1+f_2)} \frac{dI_p}{I_p} + \frac{(1-f_2)}{(1+f_2)} \frac{dl}{l} - \frac{dI_1}{I_1} + \frac{2f_2}{(1+f_2)} \frac{d\psi}{\psi} + \frac{f_2}{(1+f_2)} \frac{dI_2}{I_2} \quad (6)$$

$$\frac{dG_1}{G_1} = \frac{2\omega^2}{(\omega^2 - \lambda^2)} \frac{d\omega}{\omega} - \frac{2\lambda^2}{(\omega^2 - \lambda^2)} \frac{d\lambda}{\lambda} + \frac{dl}{l} + \frac{dI_1}{I_1} + \frac{d\alpha}{\alpha} - \frac{2d\psi}{\psi} - \frac{d\kappa}{\kappa} \quad (7)$$

$$\frac{dG_2}{G_2} = \frac{d\omega}{\omega} + \frac{d\lambda}{\lambda} + \frac{dl}{l} + \frac{dI_1}{I_1} + \frac{d\alpha}{\alpha} - \frac{2d\psi}{\psi} - \frac{d\kappa}{\kappa} \quad (8)$$

with

$$f_2 = \psi^2 I_\varphi / I_p l^2 \quad (9)$$

$$I_\varphi = \int \varphi^2 dA$$

Combining equations to eliminate differentials of α, ψ yields

$$\frac{dG_1}{G_1} = \frac{2\omega^2}{(\omega^2 - \lambda^2)} \frac{d\omega}{\omega} - \frac{2\lambda^2}{(\omega^2 - \lambda^2)} \frac{d\lambda}{\lambda} - \frac{d\kappa}{\kappa} + \frac{(1+f_1)}{(1+f_1 f_2)} \frac{dl}{l} + \frac{(1-f_1)}{(1+f_1 f_2)} \frac{dI_1}{I_1} + \frac{(f_1+f_1 f_2)}{(1+f_1 f_2)} \frac{d\rho}{\rho} + \frac{f_1}{(1+f_1 f_2)} \frac{dI_p}{I_p} + \frac{f_1 f_2}{(1+f_1 f_2)} \frac{dI_\varphi}{I_\varphi} \quad (10)$$

$$\frac{dG_2}{G_2} = \frac{d\omega}{\omega} + \frac{d\lambda}{\lambda} + \text{terms as in eq. (10)} \quad (11)$$

With

$$f_1 = \frac{\psi - \sin \psi \cos \psi}{\psi + \sin \psi \cos \psi} = \frac{\alpha^2 + \psi^2 - \alpha}{\alpha^2 + \psi^2 + \alpha} \quad (12)$$

$$= \frac{1}{3} \alpha - \frac{1}{15} \alpha^2 - \frac{1}{945} \alpha^3 + \frac{19}{2835} \alpha^4 - \frac{571}{42525} \alpha^5 + \dots$$

Circular Cross Section

For a circular cross-section of radius r

$$\begin{aligned}\alpha &= \frac{\rho I_p l}{I_1} \\ \kappa &= I_p = \pi r^2/2 \\ \varphi &= 0\end{aligned}\quad (13)$$

Simplification of eqs. (10) and (11) yields

$$\begin{aligned}\frac{dG_1}{G_1} &= \frac{2\omega^2}{(\omega^2 - \lambda^2)} \frac{d\omega}{\omega} - \frac{2\lambda^2}{(\omega^2 - \lambda^2)} \frac{d\lambda}{\lambda} - 4(1 - f_1) \frac{dr}{r} \\ &\quad + (1 + f_1) \frac{dl}{l} + (1 - f_1) \frac{dI_1}{I_1} + f_1 \frac{d\rho}{\rho}\end{aligned}\quad (14)$$

$$\begin{aligned}\frac{dG_2}{G_2} &= \frac{d\omega}{\omega} + \frac{d\lambda}{\lambda} - 4(1 - f_1) \frac{dr}{r} + (1 + f_1) \frac{dl}{l} \\ &\quad + (1 - f_1) \frac{dI_1}{I_1} + f_1 \frac{d\rho}{\rho}\end{aligned}\quad (15)$$

Rectangular Cross Section

For the rectangular cross section of dimensions $2a, 2b$ ($b < a$) the basic equations are:

$$\begin{aligned}I_p &= a^4 I_{p_1} \\ I_{p_1} &= 4/3(b/a)[1 + (b/a)^2]\end{aligned}\quad (16)$$

$$\kappa = a^4 \kappa_1 \quad (17)$$

$$\kappa_1 = \left[\frac{16}{3} \left(\frac{b}{a}\right)^3 - \left(\frac{b}{a}\right)^4 \left(\frac{4}{\pi}\right)^5 \sum_{n=0}^{\infty} \frac{1}{(2n+1)^5} \tanh \frac{(2n+1)\pi a}{2b} \right]$$

$$I_\varphi = \int \varphi^2 dA = a^6 I_{\varphi_1}$$

$$\begin{aligned}I_{\varphi_1} &= \left\{ \frac{4}{9} \left(\frac{b}{a}\right)^3 - \frac{16}{5} \left(\frac{b}{a}\right)^5 + \frac{1024}{\pi^6} \left(\frac{b}{a}\right)^5 \sum_{n=0}^{\infty} \frac{1}{(2n+1)^6} \right. \\ &\quad \left. \times \tanh \frac{(2n+1)\pi a}{2b} \left[\left(\frac{b}{a}\right) \frac{6}{\pi(2n+1)} + \tanh \frac{(2n+1)\pi a}{2b} \right] \right\}\end{aligned}\quad (18)$$

Hence

$$dI_p/I_p = 4(da/a) + g_1[(db/b) - (da/a)] \quad (19)$$

$$g_1 = \frac{1 + 3(b/a)^2}{1 + (b/a)^2} \quad (20)$$

$$d\kappa/\kappa = 4(da/a) + g_2[(db/b) - (da/a)] \quad (21)$$

$$\kappa_1 g_2 = \left\{ 16 \left(\frac{b}{a} \right)^3 - 4 \left(\frac{b}{a} \right)^4 \left(\frac{4}{\pi} \right)^5 \sum_{n=0}^{\infty} \frac{1}{(2n+1)^5} \tanh \frac{(2n+1)\pi a}{2b} \right. \\ \left. + 2 \left(\frac{b}{a} \right)^3 \left(\frac{4}{\pi} \right)^4 \sum_{n=0}^{\infty} \frac{1}{(2n+1)^4} \operatorname{sech}^2 \frac{(2n+1)\pi a}{2b} \right\} \quad (22)$$

$$dI_{\varphi}/I_{\varphi} = 6(da/a) + g_3[(db/b) - (da/a)] \quad (23)$$

$$I_{\varphi_1} g_3 = \frac{4}{3} \left(\frac{b}{a} \right)^3 - 16 \left(\frac{b}{a} \right)^5 + \frac{1}{4} \left(\frac{4}{\pi} \right)^6 \left[\sum_{n=0}^{\infty} \frac{36}{\pi(2n+1)^7} \left(\frac{b}{a} \right)^6 \right. \\ \times \tanh \frac{(2n+1)\pi a}{2b} + \frac{1}{(2n+1)^6} \left(\frac{b}{a} \right)^5 \\ \times \left(5 \tanh \frac{(2n+1)\pi a}{2b} - 3 \operatorname{sech}^2 \frac{(2n+1)\pi a}{2b} \right) \\ \left. - \frac{\pi}{(2n+1)^5} \left(\frac{b}{a} \right)^4 \tanh \frac{(2n+1)\pi a}{2b} \operatorname{sech}^2 \frac{(2n+1)\pi a}{2b} \right] \quad (24)$$

Combining equations yields the final differential forms for the rectangular cross section:

$$\frac{dG_1}{G_1} = \frac{2\omega^2}{(\omega^2 - \lambda^2)} \frac{d\omega}{\omega} - \frac{2\lambda^2}{(\omega^2 - \lambda^2)} \frac{d\lambda}{\lambda} + \frac{(1+f_1)}{(1+f_1 f_2)} \frac{dl}{l} + \frac{(1-f_1)}{(1+f_1 f_2)} \frac{dI_1}{I_1} \\ + \frac{(f_1 + f_1 f_2)}{(1+f_1 f_2)} \frac{d\rho}{\rho} + \frac{[(4-g_1)f_1 + g_2 - 4 + (2+g_2-g_3)f_1 f_2]}{(1+f_1 f_2)} \frac{da}{a} \\ + \frac{[f_1 g_1 - g_2 + (g_3 - g_2)f_1 f_2]}{(1+f_1 f_2)} \frac{db}{b} \quad (25)$$

$$\frac{dG_2}{G_2} = \frac{d\omega}{\omega} + \frac{d\lambda}{\lambda} + \text{terms as in eq. (25)} \quad (26)$$

To aid in the computation of eqs. (25) and (26), $g_2, g_3, I_{\varphi_1}, I_{\rho_1}$ are tabulated for various b/a ratios in Tables II and III. If upper bounds are needed, the function g_3 is bounded by $-4.0 < g_3 \leq 3.0$.

TABLE II

b/a	g_2	g_3	I_{φ_1}	I_{ρ_1}
1.00	2.000000	3.000000	0.008602	2.666667
0.99	2.009351	2.005367	0.008388	2.613732
0.98	2.018795	1.031369	0.008260	2.561589
0.97	2.028331	1.072067	0.008213	2.510231
0.96	2.037960	-0.741959	0.008240	2.459648
0.95	2.047681	-1.497078	0.008338	2.409833
0.94	2.057493	-2.146235	0.008501	2.360779
0.93	2.067396	-2.684602	0.008725	2.312476
0.92	2.077389	-3.113527	0.009004	2.264917
0.91	2.087472	-3.439134	0.009333	2.218095
0.90	2.097644	-3.670761	0.009707	2.172000

TABLE III

b/a	g_2	g_3	I_{φ_1}	I_{η_1}
1.0	2.000000	3.000000	0.008602	2.666667
0.9	2.097644	-3.670761	0.009707	2.172000
0.8	2.203989	-3.118332	0.014958	1.749333
0.7	2.317496	-1.402180	0.020140	1.390667
0.6	2.435304	-0.032956	0.022317	1.088000
0.5	2.553060	0.978712	0.020323	0.833333
0.4	2.665316	1.731283	0.014912	0.618667
0.3	2.766995	2.286468	0.008299	0.436000
0.2	2.855771	2.675480	0.003003	0.277333
0.1	2.932736	2.914004	0.000425	0.134667

Equations (10), (11) or (14), (15) or (25), (26) give the relative error of G_1 , G_2 in terms of relative errors in the measured quantities λ , ω , l , I_1 , ρ , etc. If the standard deviations of the relative errors of the measured quantities $\sigma(d\lambda/\lambda)$, $\sigma(d\omega/\omega)$, ..., are measured, then the standard deviation of the relative errors of G_1 , G_2 are readily obtained under the assumption of linearity. For example, for the circular cross section, eq. (14) becomes

$$\sigma^2 \left(\frac{dG_1}{G_1} \right) = \frac{4\omega^4}{(\omega^2 - \lambda^2)^2} \sigma^2 \left(\frac{d\omega}{\omega} \right) + \frac{4\lambda^4}{(\omega^2 - \lambda^2)^2} \sigma^2 \left(\frac{d\lambda}{\lambda} \right) + 16(1 - f_1)^2 \times \sigma^2 \left(\frac{dr}{r} \right) + (1 + f_1)^2 \sigma^2 \left(\frac{dl}{l} \right) + (1 - f_1)^2 \sigma^2 \left(\frac{dI_1}{I_1} \right) + f_1^2 \sigma^2 \left(\frac{d\rho}{\rho} \right) \quad (27)$$

Similar equations can be obtained for the other cases, on noting that for the linear case

$$\sigma^2(dz/z) = c_1^2 \sigma^2(dx/x) + c_2^2 \sigma^2(dy/y) \quad (28)$$

if

$$\frac{dz}{z} = c_1 \frac{dx}{x} + c_2 \frac{dy}{y} \quad (29)$$

References

1. R. D. Glauz, *J. Polym. Sci. A-1*, **8**, 329 (1970).
2. J. B. Scarborough, *Numerical Mathematical Analysis*, Johns Hopkins Press, Baltimore, 1962.

Received March 16, 1970

Thermal Reactions of *N,N'* Bis(*p*-nitrophenyl)sulfamide and *p*-Benzoquinone Dioxime–Acid Mixtures

S. R. RICCITIELLO, G. M. FOHLEN, and J. A. PARKER, *National Aeronautics and Space Administration, Ames Research Center, Moffett Field, California 94035*

Synopsis

N,N' Bis(*p*-nitrophenyl)sulfamide and *p*-benzoquinone dioxime–acid mixtures were found to undergo an abrupt reaction when heated to give a black polymeric material. These polymeric materials exhibited thermal stability (TGA in N₂) up to 500°C and were insoluble in all solvents including hot concentrated sulfuric acid. From analytical data, structural formulae have been assigned to the polymeric materials that are logically derivable from the starting materials.

INTRODUCTION

It is known that nitroaniline compounds when heated in the presence of concentrated sulfuric acid undergo an abrupt reaction to give voluminous amounts of a black material and gases.^{1–3}

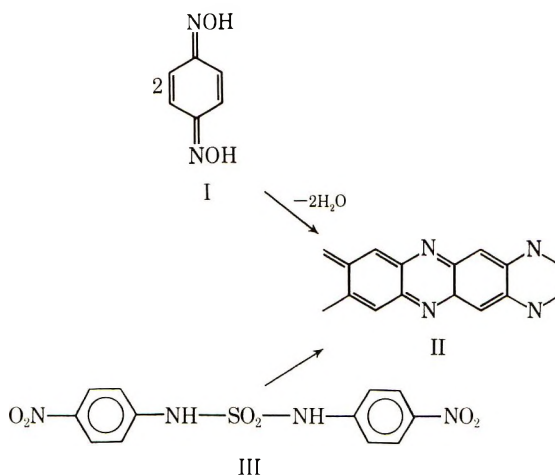
The amount of acid required to promote the reaction varies over a wide range of percentages.^{4,5} The temperature of reaction and yield of black material for this reaction, as measured by TGA at 3°C/min under nitrogen, seemed to be independent of the amount of acid used.⁵

We wish to report that *p*-benzoquinone dioxime, when heated in the presence of concentrated sulfuric or phosphoric acid, and *N,N'* bis(*p*-nitrophenyl)sulfamide, when heated without acid, react in a similar way to give low-density black material and gases.

DISCUSSION

The dehydration and self-condensation of benzoquinone dioxime (I) by acid can lead to a ladder polymer (II). The *N,N'* bis(*p*-nitrophenyl)sulfamide (III) on thermal dissociation with condensation can also lead to a similar type ladder polymer (II).

The benzoquinone dioxime–acid reaction was carried out over a range of compositions (Table I). The yield of black material and temperature of reaction, as measured by thermogravimetric analysis at 3°C/min under nitrogen, was independent of the amount of acid except when a large



excess of sulfuric acid was used (sample J-6). Here a resinous material formed without a voluminous expansion or abrupt weight change on the TGA. The reaction temperatures, listed in Table I, are taken as the temperatures at which an abrupt weight change occurs during the thermogravimetric analyses (Fig. 1). The reaction temperature for all cases was approximately 110°C except for sample J-1, which reacted at 138°C.

TABLE I
Thermogravimetric Analysis (N₂ atmosphere, 3°C/min)

Sample ^a	Mixture composition		T_{act} , °C	$Y_{C(est)}$, %
	Material	wt, g		
F-1	*		180	48
J-6	{ Dioxime	1.38	—	—
	{ Sulfuric acid	3.92		
J-1	{ Dioxime	1.38	138	72
	{ Sulfuric acid	1.96		
J-2	{ Dioxime	1.38	111	52
	{ Sulfuric acid	0.98		
J-3	{ Dioxime	1.38	108	49
	{ Sulfuric acid	0.66		
J-4	{ Dioxime	1.38	110	50
	{ Sulfuric acid	0.51		
J-5	{ Dioxime	1.38	111	50
	{ Sulfuric acid	0.392		
P-1	{ Dioxime	1.38	110	80
	{ Phosphoric acid	4.62		
P-2	{ Dioxime	1.38	105	76
	{ Phosphoric acid	2.31		
P-3	{ Dioxime	1.38	115	67
	{ Phosphoric acid	1.15		

^a F refers to *N,N'* bis(*p*-nitrophenyl)sulfamide, J to benzoquinone dioxime-sulfuric acid mixtures, P to benzoquinone dioxime-phosphoric acid mixtures.

The material yield at the end of reaction was approximately 50% in all the sulfuric acid mixtures except for sample J-1 (Table I), which yielded 72%. The phosphoric acid mixtures gave higher yields of material after reaction (Table I) than those with sulfuric acid. The reaction temperature for the *N,N'* bis(*p*-nitrophenyl)sulfamide was higher than that of the ben-

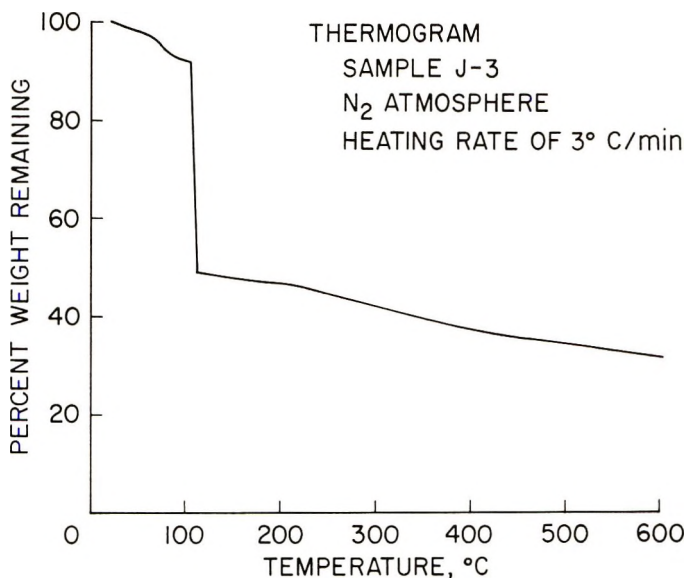


Fig. 1. Thermogram of sample J-3.

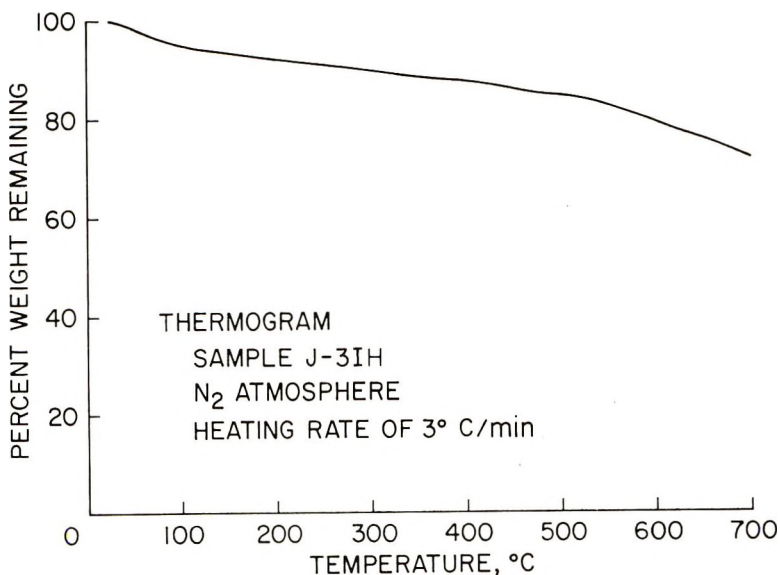


Fig. 2. Thermogram of sample J-3IH.

TABLE II
 Elemental Analyses for Self-Condensation Polymers^a

Sample	Origin ^b	C, %	H, %	O, %	N, %	S, %	P, %
F-1I	<i>N,N'</i> Bis(<i>p</i> -nitrophenyl)-sulfamide	62.49	1.94	12.50	20.95	3.07	—
J-6I	3.92 g H ₂ SO ₄ + 1.38 g QD	57.61	1.97	22.63	14.41	3.12	—
J-1I	1.96 g H ₂ SO ₄ + 1.38 g QD	54.30	2.17	21.15	16.25	5.84	—
J-2I	1.98 g H ₂ SO ₄ + 1.38 g QD	54.08	2.43	20.46	17.19	6.32	—
J-3I	0.66 g H ₂ SO ₄ + 1.38 g QD	55.89	2.60	18.92	17.86	5.57	—
J-4I	0.51 g H ₂ SO ₄ + 1.38 g QD	56.56	2.58	17.61	19.35	4.72	—
J-6I	0.39 g H ₂ SO ₄ + 1.38 g QD	58.55	2.54	15.38	19.15	4.64	—
J-3IH	J-3I, heated	61.78	1.48	9.04	25.70	0.92	—
P-1I	4.62 g H ₃ PO ₄ + 1.38 g QD	61.81	2.43	17.08 ^c	17.87	—	0.81
P-2I	2.31 g H ₃ PO ₄ + 1.38 g QD	62.52	2.51	14.57 ^c	19.65	—	0.75
P-3I	1.15 g H ₃ PO ₄ + 1.38 g QD	62.15	2.39	11.52 ^c	21.61	—	2.33

^a Analyses done by Huffman Laboratories, Wheatridge, Colorado.

^b QD denotes *p*-benzoquinone dioxime.

^c Oxygen analysis by difference.

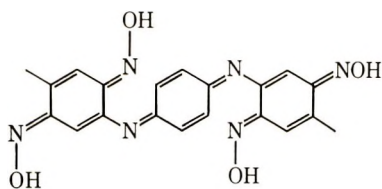
 TABLE III
 Corrected Analytical Data and Empirical Formulas for the
 Self-Condensation Polymers

Sample		Elemental analysis				Calculation for polymer unit	Type
		C, %	H, %	O, %	N, %		
F-1I	Found:	69.45	1.82	7.88	21.13	C ₆₀ H ₁₇ O ^c N ₁₆	V
	Calcd:	68.9	1.82	7.65	21.6	MW = 1045.7	
J-6I	Found:	62.65	2.14	19.5	15.69	C ₆₀ H ₂₅ O ₁₄ N ₁₃	V
	Calcd:	62.5	2.16	19.45	15.8	MW = 1151.8	
J-1I	Found:	63.8	2.55	14.6	19.1	C ₅₄ H ₂₆ O ₉ N ₁₃	V
	Calcd:	63.9	2.56	14.2	19.3	MW = 1014.7	
J-2I	Found:	64.0	2.76	13.0	20.3	C ₆₀ H ₃₀ O ₉ N ₁₆	V
	Calcd:	64.3	2.70	12.84	20.2	MW = 1120.9	
J-3I	Found:	64.2	3.00	12.15	20.50	C ₃₆ H ₂₀ O ₃ N ₁₀	V
	Calcd:	64.3	2.98	11.9	20.9	MW = 672.4	V
J-4I	Found:	63.55	2.90	11.72	21.74	C ₅₄ H ₂₁ O ₇ N ₁₆	V
	Calcd:	63.9	2.90	11.0	22.2	MW = 1015.83	
J-5I	Found:	66.0	2.86	9.39	21.6	C ₁₂ H ₉ O ₂ N ₅	V
	Calcd:	66.2	2.75	9.78	21.4	MW = 327.2	
P-1I	Found:	63.4	2.49	15.8	18.3	C ₅₄ H ₂₅ O ₁₀ N ₁₃	V
	Calcd:	63.8	2.46	15.8	17.9	MW = 1015.8	
P-2I	Found:	63.99	2.57	13.33	20.11	C ₆₀ H ₂₅ O ₉ N ₁₆	V
	Calcd:	64.3	2.61	12.86	20.19	MW = 1120.0	
P-3I	Found:	66.9	2.57	7.23	23.27	C ₆₀ H ₂₈ O ^c N ₁₈	V
	Calcd:	66.6	2.59	7.4	23.4	MW = 1080.0	
J-3IH	Found:	63.9	1.53	7.92	26.6	C ₃₆ H ₁₂ O ₃ N ₁₂	VI
	Calcd:	65.4	1.63	7.25	25.4		

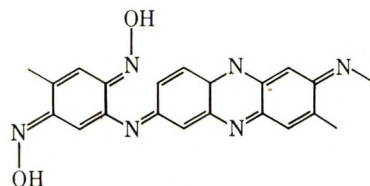
zoquinone dioxime-acid admixture (180°C). The yield for this reaction was approximately 50%, the same as for the dioxime-sulfuric acid case.

The thermal stability of these classes of residues is illustrated in Figure 2 (TGA under nitrogen at 3°C/min). The residue shows little weight loss up to a temperature of 500°C. The weight loss at 100°C was attributed to absorbed water on the material and not a thermal degradation of the material. The residues exhibit great hygroscopicity, undoubtedly due to the large surface area.

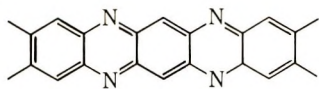
The insolubility of the residues obtained in these reactions precludes the use of all usual techniques for structural verification. Elemental analysis of the residue material was obtained and is listed in Table II. Empirical formulas were calculated for the residues after the thermal reaction the material being assumed to be polymeric in nature. The analytical data used to establish the empirical formulas were corrected for the pendant groups which were not considered a part of the repeating units in the ladder polymer (II). These pendant groups were $-\text{SO}_3^-$, $-\text{PO}_4^-$, and $\text{C}_6\text{H}_5\text{N}_2\text{O}_4\text{S}^-$, corresponding to either the sulfur or phosphorus content in the elemental analyses. The corrected analytical data, with empirical formulas and molecular weights, are listed in Table III. Molecular structures for the polymer backbones were assembled by using the corrected analytical data and empirical formulas by using the recurring units IV-VIII.



IV

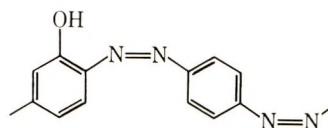


V

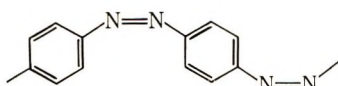


VI

Polyquinoxalines

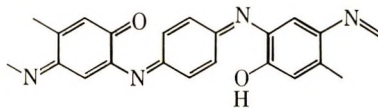


VII

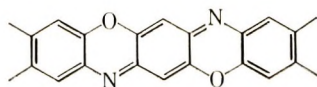


VIII

Polyazopolymer



IX



X

Polyphenoxazines

These units are derivable from the starting materials by condensation, dehydration, rearrangement, and ring closure to varying degrees. The actual structure probably is a combination of open and closed ring structures as shown in V. Assuming that complete ring closure did not occur at the relatively low activation temperatures (to 170°C), a sample, J-3I, was heated under vacuum at 400°C to obtain further ring closure. Elemental analysis of this material shows a decrease in oxygen and hydrogen and an empirical formula close to that of structure VI (sample J-3IH). However, complete ring structure did not occur. Another possibility which can occur under these conditions is that of hydrolysis of some of the oxime groups to give ladder polymers containing intermittent nitrogen-oxygen bridge structures as in IX and X (polyphenoxazines).^{6,7}

EXPERIMENTAL

Preparation of *N,N'* Bis(*p*-nitrophenyl)sulfamide

This compound was prepared by reacting *p*-nitroaniline and sulfuryl chloride in pyridine solution at -10°C to +10°C according to the method of Parnell.⁸ The melting point was 197-198°C (literature mp, 195-197°C). An infrared spectrum was obtained and supported the assigned structure.

p-Benzoquinone Dioxime-Sulfuric Acid Admixtures (J1-J6)

To 1.38 g of *p*-benzoquinone dioxime was added slowly, while stirring, concentrated sulfuric acid in the weighed amount as indicated in Table I. The admixtures ranged in physical appearance from powders, for low acid weight, to a paste as the amount of acid was increased. Care must be exercised in adding the sulfuric acid in order to prevent premature exothermic reaction.

p-Benzoquinone Dioxime-Phosphoric Acid Admixtures (P1-P3)

To 1.38 g of *p*-benzoquinone dioxime was added slowly, while stirring, 85 percent phosphoric acid in the weighed amounts as indicated in Table I. The admixtures were dark viscous pastes.

Polymers

Self-Condensation of *N,N'* Bis(*p*-nitrophenyl)sulfamide. The monomer was placed in a glass beaker and heated to a temperature of about 200°C on a hot plate. Abrupt reaction occurs with evolution of copious amounts of gases and black polymer residue. The black polymer is placed in an oven at 175-185°C for a period of 1 hr to insure complete reaction. The polymer is then removed from the beaker, ground, and dispersed in dilute sodium hydroxide. The residue is filtered, washed with approximately 500 ml of dilute sodium hydroxide, neutralized with dilute hydrochloric acid, water-washed, and finally acetone-washed. The residue is then dried for 24 hr at 120°C under vacuum prior to analysis.

Self-Condensation of *p*-Benzoquinone Dioxime-Sulfuric Acid Mixture.

The same procedure was followed as that for the *N,N'* bis(*p*-nitrophenyl)-sulfamide, except that the initial temperature on the hot plate was approximately 150°C to initiate polymerization and gaseous evolution.

Heating of Polymer with Uncyclized Units to Get Ring Closure. In a sublimation unit, 2 g of the J-3I polymer was heated under vacuum (0.5–5 mm Hg). In the first hour the temperature was raised to 250°C, in the second hour to 380–390°C, and then for the next 3 hr was maintained at 390°C (sample J-3IH).

References

1. R. E. D. Clark, *School Sci. Rev.*, **16**, 271 (1934).
2. H. N. Alyea, *J. Chem. Educ.*, **12**, 247 (1935).
3. H. N. Alyea, *J. Chem. Educ.*, **33**, No. 4, 15A (1956).
4. J. A. Parker, G. M. Fohlen, P. M. Sawko, and R. N. Griffin, *SAMPE J.*, **4**, Aug.-Sept. (1968).
5. A. C. Poshkus and J. A. Parker, *J. Appl. Polym. Sci.*, **14**, 2049 (1970).
6. J. K. Stille and M. E. Freeburger, *J. Polym. Sci. A-1*, **6**, 161 (1968).
7. J. Szita and C. S. Marvel, *J. Polym. Sci. A-1*, **7**, 3203 (1969).
8. E. W. Parnell, *J. Chem. Soc.*, **1960**, 4366.
9. I. L. Kotyarevskii et al., *Izv. Akad. Nauk. SSSR Ser. Khim.*, **1964**, 1854.
10. H. C. Bach, *Polymer Preprints*, 1966, p. 576.

Received June 10, 1970

Al(Cap)₃ as Initiator in the Anionic Polymerization of ϵ -Caprolactam at High Temperature

T. KONOMI, *Kata Research Institute, Toyo Spinning Company, Ltd., Katata, Shiga, Japan*, and
H. TANI, *Department of Polymer Science, Faculty of Science, Osaka University, Toyonaka, Osaka, Japan*

Synopsis

Mechanism for polymerization of ϵ -caprolactam in the presence of both sodium and aluminum caprolactamate was investigated at 171°C. The role of Al(Cap)₃ as an initiator was revealed. The apparent rate constant of propagation reaction decreased with the increase in the concentration of Al(Cap)₃, as the two different metal salts interact even at 171°C. The activation energy of the overall polymerization reaction with this catalyst system was estimated to be 41.18 kcal/mole.

INTRODUCTION

The peculiar catalytic behavior of MAI Et₄ and of MOAI Et₂·Al Et₃ (where M denotes alkali metal) observed in the high-temperature polymerization of ϵ -caprolactam was reported in the preceding paper.¹ Catalyst systems containing both alkali metal and aluminum caprolactamates can polymerize ϵ -caprolactam at a temperature lower than that required for the alkali metal caprolactamate catalyst and form *m*-cresol-insoluble polymers, in contrast to the latter catalyst.

In the anionic polymerization of a lower homolog, α -pyrrolidone, the role of *N*-acyl- α -pyrrolidone as an initiator has been clarified by Murahashi et al.² Independently, it was postulated by Hall³ and Sebenda et al.⁴ that the *N*-acyl-lactam moiety is the active center of the propagation reaction. It was reported also that some compounds such as *N*-(2-pyridyl)- ϵ -caprolactam enter into the initiation by tautomerization.⁵

In this paper, the positive role of Al(Cap)₃ as initiator in the interaction between these two different metal lactamates is clarified.

EXPERIMENTAL

Measurement of Temperature Change in the System

Temperature change of the polymerization system in the course of polymerization was measured in the same manner as reported in the previous paper,¹ except for the use of a chromel-alumel thermocouple instead

of a thermometer inserted in the center of the polymerizing ϵ -caprolactam. The polymerization vessel used has an inside diameter of 15 mm and a wall thickness of ca. 1 mm and contains 4.168 g of monomer.

Polymerization

Water content in ϵ -caprolactam used for polymerization was 0.007 wt-% by the Karl Fisher method.

NaAlEt_3 was synthesized following the method reported in the previous paper.¹

In the preparation of the solution of a definite concentration of $\text{Al}(\text{Cap})_3$ in a monomer, a solution of AlEt_3 in THF [$\text{AlEt}_3:\text{THF} = 1:4(\text{v/v})$], the concentration of which had been previously determined by gasometry and back-titration, was added stepwise to molten ϵ -caprolactam at 70–75°C with stirring in a stream of a dry nitrogen and removed under a reduced pressure of 5–10 mm Hg.¹ In this reaction, one mole of ethane per mole of AlEt_3 was immediately evolved, and another mole of ethane was evolved over period of 20–30 min. The reaction between AlEt_3 and ϵ -caprolactam was completed by maintaining the system at 110–120°C under 10 mm Hg for 30 min. The complete isolation and the determination of purity of the aluminum salt were not carried out.

A solution of a definite amount of $\text{NaAl}(\text{Cap})_4$ in ϵ -caprolactam was prepared by mixing the catalyst solution in the molten ϵ -caprolactam at 80°C with stirring in dry nitrogen atmosphere and treating the mixture at 120°C under 4–10 mm Hg for 30 min.

The ϵ -caprolactam solution containing various molar ratios of $\text{Al}(\text{Cap})_3$ to $\text{Na}(\text{Cap})$ was prepared by mixing the appropriate amount of the catalyst solutions [$\text{NaAl}(\text{Cap})_4$ and $\text{Al}(\text{Cap})_3$] prepared above.

The polymerization reactions were terminated with methanol in order to limit the conversion in the range of 20%. The viscosity of the polymer solution was measured in a solution prepared from 0.5 g of polymer and 100 ml of *m*-cresol at 25°C.

RESULTS

The overall polymerization rate catalyzed by sodium caprolactamate is reported to be very low in the temperature range of 140–170°C.^{6,7}

Temperatures changes in the course of the reaction of a polymerizing system immersed in a constant temperature vapor bath (butyl cellosolve, 171°C) were studied, in order to get some information concerning the mechanism of polymerization of ϵ -caprolactam by the catalyst composed of sodium and aluminum caprolactamates (Fig. 1, Table I). Two peaks of temperature were observed (Fig. 1): at the first peak (point *a*) the polymerization system containing polymer appeared transparent gellike, and at the second peak (point *b*) opaque. It is reasonable to conclude that the former peak is due to the heat of polymerization and the latter one to the heat of crystallization. The time intervals t_p (between the point 0 at

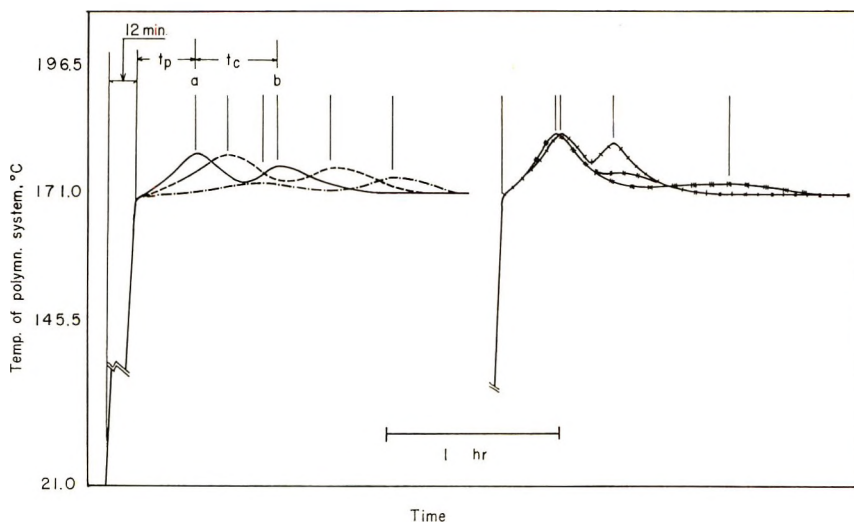


Fig. 1. Effect of catalyst concentration $[\text{NaAl}(\text{Lac})]$ on temperature change in the polymerization system during polymerization at 171°C : (---) 0.25 mole-%; (---) 0.50 mole-%; (—) 1.0 mole-%; (-+-) 2.0 mole-%; (-+-) 3.0 mole-%; (+++) 4.0 mole-%.

which the system attained 171°C and point *a*) and t_c (between points *a* and *b*) depend on the catalyst concentration. The rate of polymerization increased with the increase in the catalyst $[\text{Na}(\text{Cap})]$ concentration, while the plot of t_c versus catalyst concentration is V-shaped, t_c having a minimum at 2 mole-% of catalyst. This behavior of t_c is considered to be due to the increase of branching sites in the polymer as a result of the cooperative action of aluminum atom as an initiator: the molecular weight of polymer becomes smaller and the number of the branching sites larger

TABLE I
Temperature Changes on Polymerizing Systems due to Heats of Polymerization and of Crystallization in the Course of Polymerization at 171°C^a

Catalyst concn, mole-% ^b	t_p , min ^c	t_c , min ^d
0.25	38.5	50.4
0.50	31.2	33.6
1.00	21.6	28.8
2.00	20.9	17.8
3.00	19.2	23.1
4.00	19.2	61.0

^a Amount of monomer charged, 0.0922 mole; vapor bath, butyl cellosolve.

^b Based on $\text{NaAl}(\text{Lac})_4$.

^c t_p : time elapsed from the start of polymerization (the time at which the polymerized system reaches 170 – 171°C) to the peak of temperature by heat of polymerization.

^d t_c : time elapsed from the peak of temperature by heat of polymerization to the one by heat of crystallization.

with increasing the aluminum concentration. A balance between these two factors causes the appearance of the minimum in t_c value. This interpretation is consistent with the fact that the polymer become insoluble in *m*-cresol with increasing polymerization time and aluminum concentration.

It is important to note that at a catalyst concentration lower than 0.25 mole-% the height of the two peaks *a* and *b* become very low. This fact means that at a sufficiently low catalyst concentration the polymerizing system can be treated practically as a constant-temperature system. In this low catalyst concentration range, the time-conversion relationship was studied at various ratios of $\text{Al}(\text{Cap})_3$ to $\text{Na}(\text{Cap})$; the results obtained are shown in Table II.

TABLE II
Examination of the Action of $\text{Al}(\text{Lac})_3$ as Initiator in
the Polymerization in the Presence of $\text{Na}(\text{Lac})^a$

Na(Lac), mole-%	Al(Lac) ₃ , mole-% ^b	Polymerization time, min	$([M_0] - [M])/M_0$		
0.125	0.125	15	0.0113		
		20	0.0281		
		25	0.0482		
		30	0.0628		
		35	0.0810		
		40	0.1217		
		45	0.1413		
		0.125	0.250	15	0.0131
				20	0.0371
25	0.0550				
30	0.0705				
35	0.0920				
40	0.1401				
45	0.1641				
0.125	0.375	15	0.0181		
		20	0.0460		
		25	0.0708		
		30	0.0919		
		35	0.1250		
		40	0.1638		
		45	0.1869		

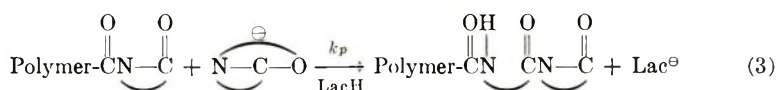
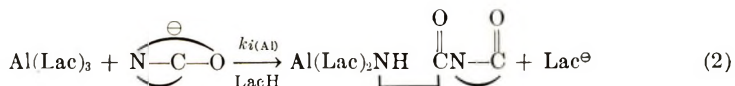
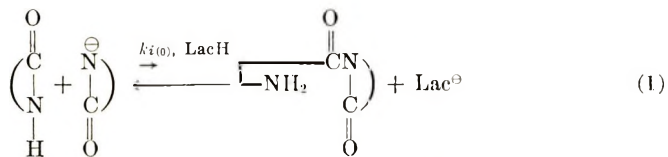
^a Polymerization temperature, 171°C.

^b The values were represented as three times the amount based on $\text{Al}(\text{Lac})_3$.

The polymerization reaction is composed of the elementary reactions, (1) and (3), in the case of Na caprolactamate. It was reported that *N*-ethylbutyramide was consumed in the reaction system containing *N*-ethylbutyramide and its sodium salt at 80°C,⁸ and the content of imide groups in the polymer was always lower than at the start of the reaction.⁹ In studying the role of $\text{Al}(\text{Cap})_3$ as an initiator, the following two assumptions were made; the catalyst concentration [$\text{Na}(\text{Cap})$ and $\text{Al}(\text{Cap})_3$] was

constant in the first stage of polymerization, and the depolymerization of polymer by lactam and polymer anion is very small at this temperature.

The latter assumption is reasonable, because the polymerization reaction was at a very low conversion and the cleavage of amide group of polymer by the attack of amide anion was small.



If $\text{Al}(\text{Cap})_3$ acts as an initiator and $k_p = k_{i(\text{Al})}$, the rate of consumption of monomer is given by eq. (4):

$$-d[\text{LacH}]/dt = k_p[\text{Lac}][\text{Al}][\text{LacH}] \quad (4)$$

where, k_p , (Lac) , (Al) , $(\text{LacH})_0$, and (LacH) indicate the rate constant of propagation reaction, the concentrations of dissociated lactam anion, $\text{Al}(\text{Cap})_3$ initiator, monomer charged, and remaining monomer at time t , respectively. A plot of $\log ([M_0]/[M])$ versus t plot was linear for an initial period less than 40 min (Fig. 2). This linearity implies that $\text{Al}(\text{Cap})_3$ acts as an initiator.

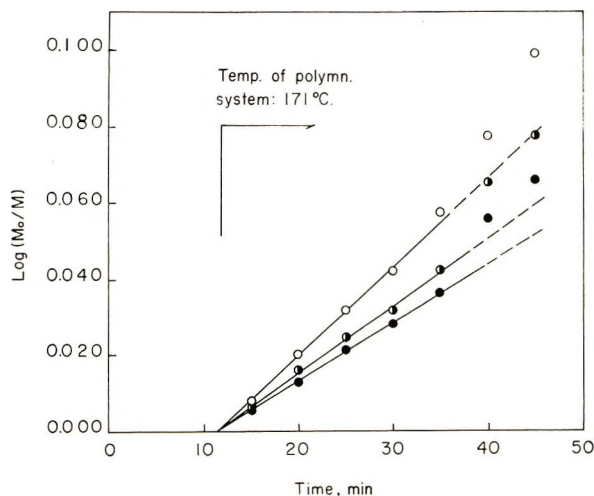
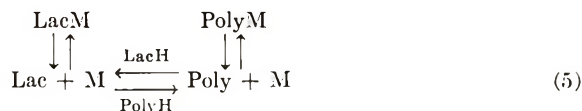


Fig. 2. Plot of $\log ([M_0]/[M])$ vs. polymerization time at various concentrations of $\text{Al}(\text{Lac})_3$ [represented as 3 $\text{Al}(\text{Lac})_3$]: (●) 0.375 mole-%; (◐) 0.750 mole-%; (○) 1.125 mole-%. Concentration of $\text{Na}(\text{Lac})$, 0.125 mole-%.

The deviation from linearity is considered to be due to the acceleration of polymerization reaction either by the increase in the degree of dissociation of Na(Cap) caused by increase in the concentration of diacylimide or by a small rise of temperature in the system as a result of the heat of polymerization.

The relative amount of amide anion of lactam and of polymer, [Lac] and [Poly], in the polymerization system depends on the relative acidity K_1 of monomer and polymer,¹⁰⁻¹² the concentration of monomer [LacH] and amide group in polymer [PolyH], and the dissociation constant K_2 between salts [LacM] and [PolyM] and anions [Lac] and [Poly] according to the scheme (5):



where:

$$[\text{Lac}]/[\text{Poly}] = K_1[\text{LacH}]/[\text{PolyH}] \quad (6)$$

$$[C_0] = [\text{Lac}] + [\text{Poly}] + [\text{LacM}] + [\text{PolyM}] \quad (7)$$

$$\frac{[\text{Lac}][\text{M}]_{\text{Lac}} \cdot [\text{Poly}][\text{M}]_{\text{Poly}}}{[\text{LacM}] \cdot [\text{PolyM}]} = K_2 \quad (8)$$

where $[C_0]$ is the initial catalyst concentration. The dissociation of Na(Lac) is extremely small.¹³

If PolyH is neglected in the first stage of polymerization,

$$[C_0] = [\text{LacM}] + [\text{PolyM}] \doteq [\text{LacM}] \quad (9)$$

$$\frac{[\text{Lac}][\text{M}]}{[\text{LacM}]} = \frac{[\text{Lac}]^2}{[C_0]} = K_2' \quad (10)$$

$$[\text{Lac}] = K_2'^{0.5}[C_0]^{0.5} \quad (11)$$

According to eqs. (4) and (11), $k_p k_2'^{0.5}$ instead of k_p was estimated against the concentration of Al(Lac)₃ (see Table III). The value of k_p was not constant and decreased with increasing concentration of Al(Lac)₃. This result is due to the decrease in contribution of Na(Lac) for the propagation reaction, because there is some interaction between Na(Lac) and Al(Lac)₃ even at 171°C. Indeed, the depression of polymerization rate and of the reactivity of MAEt₄ towards lactam caused by the interaction of the two

TABLE III
Estimation of the Apparent Propagation Reaction Constant^a

Al(Lac) ₃ , mole/kg ^b	$K_p K_2'^{0.5} [C_0]^{0.5} [\text{Al}]$, min ⁻¹	$K_p K_2'^{0.5}$, mole ^{-3/2} ·kg ^{3/2} ·min ⁻¹
0.0332	0.00155	0.980
0.0664	0.00179	0.566
0.0996	0.00233	0.491

^a Polymerization temperature, 171°C; Na(Lac) (= $[C_0]$), 0.01105 mole/kg.

^b Represented as $3 \cdot [\text{Al}(\text{Lac})_3]$, mole/kg.

metal salts has been observed by us in the polymerization of α -pyrrolidone, α -piperidone, and ϵ -caprolactam at low temperature and in the reaction of MAIET₄ with lactams.^{10,14,15}

DISCUSSION

The formation of *N*-acyl- ϵ -caprolactam by the reaction between lactam and lactam anion is reported by Sittler and Sebenda to be an prerequisite for the propagation reaction in the anionic polymerization of ϵ -caprolactam activated by alkali metal caprolactamate. The concentration of an active lactam anion which takes part effectively in the *N*-acyl- ϵ -caprolactam formation and the transamidation reaction depends on the temperature and the other conditions of the system.¹³ Indeed, for the polymerization of ϵ -caprolactam activated by Na caprolactamate, the overall activation energy 51.3 kcal/mole⁷ falls to 17.5 kcal/mole in the presence of an initiator *N,N,N',N'*-tetraacetylhexamethylenediamine.¹⁶

In the case of the catalyst system containing both Na(Cap) and Al(Cap)₃, the overall activation energy was estimated to be 41.18 kcal/mole from the dependency of polymerizability on the temperature (Fig. 3). This result implies the initiation act of Al(Cap)₃. Another phenomenon caused by the effect of the initiation by Al(Cap)₃ is observed in the crystallization behavior of the polymer specially prepared in the presence of a comparatively high concentration of Al(Cap)₃. As shown in Table IV, in systems A and C, the resulting polymer formed a crystalline opaque material

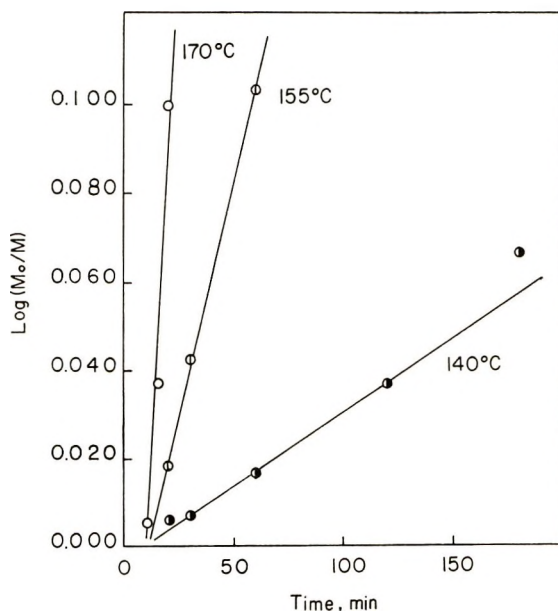


Fig. 3. Temperature dependence of polymerization activated with NaAl(Lac)₄ system. Catalyst concentration, 0.250 mole-%.

TABLE IV
Appearance and Solubility of Polymers Obtained under Various Polymerization Conditions

System	Polymerization conditions ^a		Polymerization temp, °C	Appearance of polymers ^b	η_{sp}/c		MeOH-soluble part, wt-%	Remaining Al after extraction, mole-% ^c
	Catalyst	Initiator			Before extraction	After extraction		
A	NaAl(Lac) ₄	None	250	Crystallized opaque	0.548	0.789	30.3	2.48
B	NaAl(Lac) ₄	None	200	Non-crystallized glass-like	Insoluble	Insoluble	19.2	2.74
C	NaAl(Lac) ₄	NAcCL	100	Crystallized opaque	0.440	0.541	19.3	2.69

^a Polymerization time, 1 hr; NaAl(Lac)₄, 5 mole-%; NAcCL (*N*-Acetylcaprolactam), 2.5 mole-%.

^b After 48 hr the polymerization system cooled to room temperature.

^c Extracted for 20 hr.

after cooling or in the course of polymerization, while in system B an apparently noncrystalline transparent, and glasslike polymer was obtained. The insoluble polymer formed only in system B; in this case, the cross-linking in resulting polymer occurs even at the initiation stage. These results suggest a different role for $\text{Al}(\text{Cap})_3$ in these three systems: $\text{Al}(\text{Cap})_3$ acts as a catalyst in system A, as an initiator in system B, and preferentially as a catalyst due to the presence of an initiator in system C.

On the other hand, the amounts of remaining Al were nearly the same in these systems, in spite of the difference in polymer solubility and in the role of $\text{Al}(\text{Cap})_3$. This fact suggests a difference in the bonding nature of aluminum which is dependent on the polymerization temperature.

References

1. T. Konomi and H. Tani, *J. Polym. Sci. A-1*, **7**, 2269 (1969).
2. S. Murahashi, H. Yuki, and H. Sekiguchi, *Ann. Rept. Inst. Fiber Res. (Osaka)*, **10**, 88, 93 (1957).
3. H. K. Hall, Jr., *J. Amer. Chem. Soc.*, **80**, 6404 (1958).
4. J. Sebenda and J. Kralicek, *Coll. Czech. Chem. Commun.*, **23**, 766 (1958).
5. Belg. 623,840 (1963); Japan. Pat., 9978 (1965) (Allied Chem. Corp.).
6. E. H. Mottus, R. M. Hendrick, and J. M. Butler, paper presented at American Chemical Society Meeting, San Francisco, 1968; *Preprints*, p. 390.
7. E. Sittler and J. Sebenda, *Coll. Czech. Chem. Commun.*, **33**, 3182 (1968).
8. J. Sebenda, B. Masar, and Z. Bukac, in *Macromolecular Chemistry, Prague, 1965* (*J. Polym. Sci. C*, **16**), O. Wichterle and B. Sedláček, Eds., Interscience, New York, 1967, p. 339.
9. J. Sebenda and B. Mikulova, *Coll. Czech. Chem. Commun.*, **29**, 738 (1964).
10. H. Tani and T. Konomi, *J. Polym. Sci. A-1*, **6**, 2295 (1968).
11. R. Huisgen and H. Walz, *Chem. Ber.*, **86**, 2616 (1956).
12. R. Huisgen, H. Brade, M. Walz, and I. Glogger, *Ber.*, **90**, 1437 (1957).
13. E. Sittler and J. Sebenda, in *Macromolecular Chemistry, Prague, 1965* (*J. Polym. Sci. C*, **16**), O. Wichterle and B. Sedláček, Eds., Interscience, New York, 1967, p. 67.
14. T. Konomi and H. Tani, *J. Polym. Sci. A-1*, **4**, 301 (1966).
15. T. Konomi and H. Tani, *J. Polym. Sci. A-1*, **7**, 2255 (1969).
16. E. Sittler and J. Sebenda, *Coll. Czech. Chem. Commun.*, **33**, 270 (1968).

Received July 29, 1969

Revised July 22, 1970

Syntheses and Properties of Photochromic Polymers of the Mercury Thiocarbazonate Series

HIROYOSHI KAMOGAWA, *Research Institute for Polymers and Textiles, Kanagawa, Yokohama, Japan*

Synopsis

Photochromic vinyl polymers of the mercuric thiocarbazonate series were synthesized via the three sequences: (1) synthesis of *p*-(meth)acrylamidophenyl mercuric acetate(II) by the reaction of (meth)acrylyl chloride with *p*-aminophenyl mercuric acetate, followed by polymerization to afford corresponding polymers(III) and subsequent reaction with diphenyl- or di- β -naphthyl-thiocarbazone, (2) alternative preparation of III by the reaction of (meth)acrylyl chloride polymers with *p*-aminophenyl mercuric acetate, and (3) reaction of *N*-hydroxymethyl (meth)acrylamide polymers with *p*-amidophenyl mercuric thiocarbazonates. The photochromic behavior of these polymers was investigated to provide data which might indicate the effect of steric conditions on the isomerization of the photochromic components in polymers both under illumination and in dark recovery.

In preceding papers,^{1,2} we reported the syntheses and photochromic behavior of a number of azobenzene and thionine polymers.

In the meantime, Vandewijer and Smets³ also reported the results of the examinations of the photochromic behavior of spiropyran copolymers prepared by radical copolymerization of 5-methacrylamino-3,3'-dimethyl-6'-nitrobenzthiazolinospiropyran with different vinyl monomers.

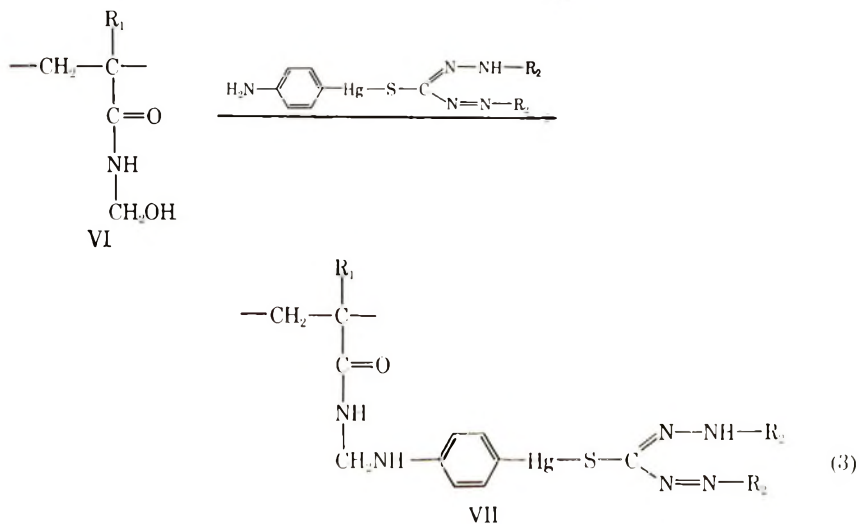
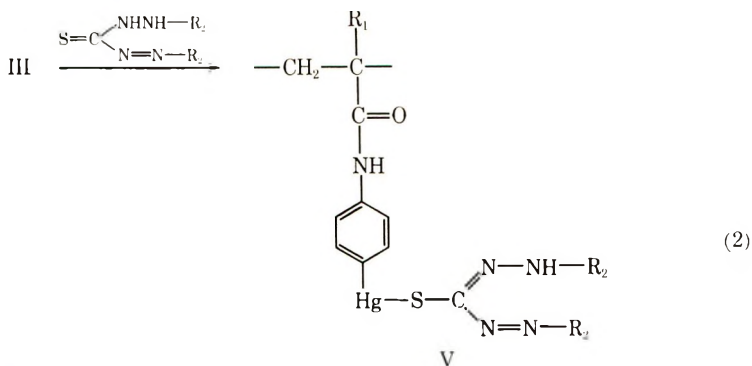
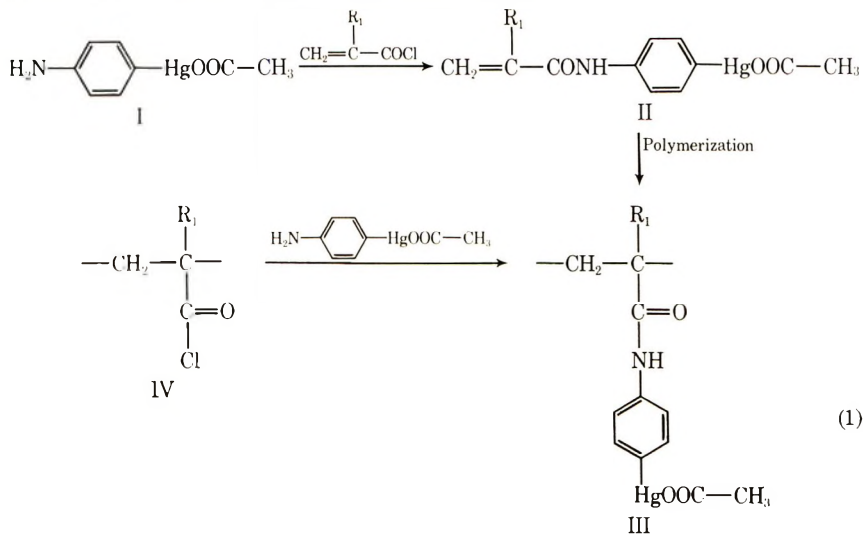
This paper reports the results of investigations of the syntheses and properties of photochromic vinyl polymers of the mercury thiocarbazonate series.

Thiocarbazonates, especially diphenylthiocarbazone (dithizone), have long been used as reagents for the colorimetric analysis of trace metals.⁴ Around 1950, Irving et al.⁵ and Webb et al.⁶ reported independently that the mercury(II) complex of diphenylthiocarbazone is photochromic. Later, Meriwether et al.^{7,8} followed up this photochromic behavior and reported a detailed study of this system, which led to the discovery of a number of photochromic metal dithizonates and a better understanding of the photochromic behavior of these complexes.

Foster and Kazan also synthesized a photochromic mercury dithizonate containing a fiber-reactive dichloro-*s*-triazynyl group and examined its application to nylon fabrics.⁹

In this report will be described three methods of preparing vinyl polymers containing a mercury thiocarbazonate group as side chain. Thus,

to prepare *p*-(meth)acrylamidophenyl mercury thiocarbazonate polymers, the reaction sequences (1) and (2) were employed.



To prepare *p*-(meth)acrylamidomethylaminophenyl mercury thiocarbazonate polymers, the reaction sequence (3) was employed, starting with *N*-hydroxymethyl(meth)acrylamide polymers, where R₁ and R₂ represent H or methyl and phenyl, β -naphthyl, or their nuclear substitution product, respectively.

EXPERIMENTAL

p-Methacrylamidophenyl Mercuric Acetate (II)

A 3.5-g portion of *p*-aminophenyl mercuric acetate (I), 0.3 g of hydroquinone, and 1.5 ml of anhydrous ethylamine were dissolved in 20 ml of anhydrous *N,N*-dimethylacetamide. To this solution was added dropwise under ice cooling 10 ml of a *N,N*-dimethylacetamide solution containing 1.5 ml of methacrylyl chloride, followed by stirring for 2 hr. Acetic acid (20 ml) was then added to the reaction mixture, and the resulting solution was poured into a large quantity of water to afford white precipitates. Recrystallization from a dimethylformamide (DMF)-water combination gave 2.8 g of white crystals of mp 224–226°C (with polymerization), which corresponds to 80% yield.

ANAL. Calcd for C₁₂H₁₃NO₃Hg: C, 34.36%; H, 3.11%; N, 3.33%; Hg, 47.72%. Found: C, 35.08%; H, 3.02%; N, 3.00%; Hg, 48.99%.

The infrared spectrum by KBr method indicated characteristic absorptions close to those of the reference compound, *p*-acetamido-phenyl mercuric acetate, including those at 1650 and 910 cm⁻¹ which are attributable to the amido group and the methacrylic double bond, respectively, thereby denoting that the compound II was obtained.

p-Acrylamidophenyl mercuric acetate (II') was also synthesized in 86% yield by the same procedure; mp 208–210°C (with polymerization).

ANAL. Calcd for C₁₁H₁₁NO₃Hg: C, 30.76%; H, 2.79%; N, 3.56%; Hg, 50.75%. Found: C, 31.85%; H, 2.65%; N, 3.62%; Hg, 48.91%.

The infrared spectrum by KBr method also indicated characteristic absorptions close to those of *p*-acetamidophenyl mercuric acetate, including those at 1650 and 990 cm⁻¹ which are attributable to the amido group and the acrylic double bond, respectively, thereby denoting that the desired compound was obtained.

p-Methacrylamidophenyl Mercuric Acetate Polymer (III)

The monomers II and II' were polymerized in sealed ampoules under vacuum with α , α' -azobisisobutyronitrile as initiator. The polymerization conditions and the intrinsic viscosities $[\eta]$ of the polymers thus obtained are summarized in Table I.

A typical example is as follows. A solution of 0.1 g of monomer II', 0.9 g of styrene, 5.7 g of dioxane, and 0.01 g of α , α' -azobisisobutyronitrile was put into a Pyrex glass ampoule, which was then evacuated and sealed

TABLE I
Polymerization Conditions for Acryl amidophenyl or
Methacrylamidophenyl Mercuric Acetate^a

Sample	Monomer	Solvent	Con- version, %	$[\eta]$, dl/g ^b
1	II	Dimethylformamide	65	0.181 ^c
2	II-styrene (1:9) ^d	Dioxane	89	0.356
3	II-methyl acrylate (1:9) ^d	"	82	0.301
4	II'-styrene (1:9) ^d	"	84	0.359

^a Polymerization was carried out in 15% total monomer concentrations for 72 hr at 80°C.

^b At 20°C in dioxane unless otherwise noted.

^c At 20°C, in DMF.

^d Weight ratio.

off. Upon standing 72 hr at 80°C, a viscous colorless solution resulted. It was poured into benzene to separate out a small amount of precipitates produced, followed by precipitation into ethanol. The polymer was redissolved in dioxane and reprecipitated into ethanol, followed by freeze-drying from dioxane to afford a white powder in 84% yield (Sample 4).

An alternate procedure for preparation of polymer III or its acryl equivalent III' consists of the use of methacrylyl or acrylyl chloride polymers, instead of the respective monomers, for the reaction with compound I. Thus, in a typical example, a solution of 0.1 ml of freshly distilled acrylyl chloride, 0.9 ml of styrene, 4 ml of anhydrous dioxane, and 0.01 g of α, α' -azobisisobutyronitrile in a sealed ampoule was polymerized with exclusion of air for 30 hr at 80°C. The viscous solution thus obtained (intrinsic viscosity at 20°C, 0.511 dl/g) was diluted with 10 ml of anhydrous dioxane, followed by dropwise addition to a solution of 0.7 g of *p*-aminophenyl mercuric acetate in 30 ml dioxane containing 0.4 g of triethylamine under water cooling. Stirring was continued further for 2 hr, 10 ml of glacial acetic acid added, and the polymer III' was isolated by adding a large amount of ethanol. Analysis for mercury indicated that 75% of the acyl portion of the polymer reacted.

***p*-Methacrylamidophenyl Mercuric Thiocarbazonate Polymer (IV)**

Polymer III and III' were converted into thiocarbazonates with diphenyl or di- β -naphthyl thiocarbazonates in the presence of sodium bicarbonate. A typical example is as follows.

To a solution of 1 g of a II'-styrene copolymer (Sample 4) in 20 ml dioxane was added 5 g of sodium bicarbonate; the mixture was stirred vigorously at ambient temperature, and 0.5 g of diphenyl thiocarbazonate (dithizone) was added in small portions, followed by 30 min stirring. The resulting red-orange solution was poured into a large amount of ethanol.

The orange precipitates thus produced were collected by filtration, rinsed thoroughly with ethanol, and freeze-dried from dioxane to afford an orange powder. Sulfur analysis gave 81.2% conversion to thiocarbazonate based on the acrylic component in the polymer.

***p*-Acrylamidomethylaminophenyl Mercuric Thiocarbazonate Polymers (VII)**

In a typical example, a solution of 0.1 g of *N*-hydroxymethylacrylamide, 0.45 g of methyl methacrylate, 0.45 g of butyl acrylate, and 0.01 g of α,α' -azobisisobutyronitrile in 4 ml of dioxane was put into a Pyrex glass ampoule, which was then evacuated and sealed off. Polymerization was carried out at 80°C for 72 hr to afford a viscous solution ($[\eta] = 0.405$ dl/g). To 1 ml of the polymer solution diluted with 10 ml of dioxane was added in small portions 0.1 g of *p*-amino-phenyl mercuric di- β -naphthylthiocarbazonate, prepared by the reaction of *p*-aminophenyl mercuric acetate with di- β -naphthylthiocarbazonate in the presence of sodium bicarbonate. Stirring was continued at 40°C for 10 hr in the dark. The red reaction mixture was then poured into water to precipitate the polymer. Dissolution in dioxane and reprecipitation into water was repeated at least three times, followed by freeze-drying from dioxane to afford a red powder. Sulfur analysis gave 45.1% conversion to thiocarbazonate.

Preparation of Sample

The polymer films were prepared by drying dioxane solutions spread over glass plates at ambient temperatures to ca. 0.05 mm thickness. At least a week elapsed before measurements of photochromism.

Measuring Instrument

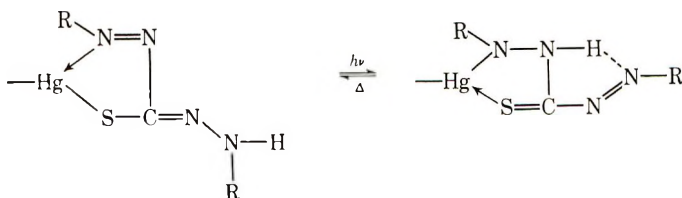
A Hitachi rapid-scan spectrophotometer (Model RSP-2) with a scanning time of ca. 0.15 sec from 220 to 700 $m\mu$ and fitted with a 150-W xenon lamp as radiation source, was employed for the investigation of photochromic behavior.

RESULTS AND DISCUSSION

Spectral Change During Irradiation

Figure 1 indicates a typical spectral change of a mercury thiocarbazonate polymer film during irradiation.

As in the case of low molecular mercuric dithizonates, an absorption peak around 500 $m\mu$ causing an orange to red color decreases its intensity with irradiation, whereas a new peak appears around 600 $m\mu$ (blue), presumably due to the photoinduced isomerization.⁸



The first-order rate constant k_1 can be determined by using $\log E_0/E$ versus t relationships, where E_0 and E , denote absorbances before and during irradiation, respectively, and t is irradiation time. Some examples are shown in Figure 2, where the effect of wavelength of irradiation is also clearly recognized. Thus, the B-filter having the maximum transmittance at $460\text{ m}\mu$, which is the closest of the three to the dark absorption peak ($485\text{ m}\mu$) of the polymer, provided the highest value of k_1 , as expected. This wavelength dependence of the rate of spectral change under illumination is in a marked contrast with that in the photochromic polymers of the thionine series having the dark absorption peak above $600\text{ m}\mu$, where the R-filter gives the highest rate, as indicated in Figure 3.

In Table II are summarized the results of the investigations of the spectral changes of the mercury thiocarbazonate polymers during irradiation.

As generally observed in photochromic polymers as well as in polymer blends with photochromics,¹⁰ the rates of spectral change both during

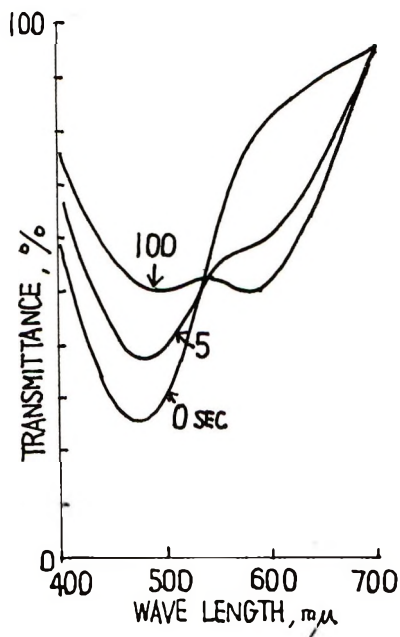


Fig. 1. Spectral change of *p*-methacrylamidophenyl mercuric diphenylthiocarbazonate-styrene (1:9 by weight) copolymer film with irradiation at 15°C . Figures in the diagram denote irradiation times in seconds.

TABLE II
 Spectral Change during Irradiation^a

No.	Polymer ^b	State	Absorption		E_{11}^L/E_{11}^{Dc}	E_{11}^L/E_{11}^{De} (time to max, sec)
			maxi- mum before irrad. (I), m μ	New peak by irrad. (II), m μ		
101	APDT	Soln ^d	480	580	0.338	3.57(5)
102	APDT	C ₂ H ₄ Cl ₂ Soln	480	575	0.060	0.175/0(10)
103	APDT	In Pst film	485	575	0.322	1.93(5)
104	PACDT-ST-1	Soln ^d	480	580	0.234	6.00(5)
105	PACDT-ST-1	Film	480	575	0.278	6.95(100)
106	PACDT-ST-2	Soln ^d	480	580	0.257	5.40(5)
107	PACDT-ST-2	Film	490	580	0.578	5.92(100)
108	PMACDT-ST-1	Soln ^d	485	575	0.189	6.90(5)
109	PMACDT-ST-1	Film	480	580	0.343	6.67(100)
110	PACDT-MA-2	Soln ^d	485	575	0.114	10.7(5)
111	PACDT-MA-2	Film	480	580	0.422	8.46(100)
112	PAMADT-ST	Soln ^d	480	580	0.376	2.42(5)
113	PAMADT-ST	Film	490	575	0.480	2.27(100)
114	PAMADT-MA	Soln ^d	480	575	0.384	1.70(5)
115	PAMADT-MA	Film	510	—	0.731	—
116	PACNT-MA	Soln ^d	500	600	0.368	5.77(100)
117	PACNT-MA	Film	500	800	0.432	11.2(100)

^a Irradiation was continued for 100 sec at 15°C.

^b APDT: *p*-acetamidophenyl mercuric diphenylthiocarbazonate; PACDT-ST-1, PACDT-ST-2: *p*-acrylamidophenyl mercuric diphenylthiocarbazonate-styrene (1:9 by weight) copolymer, prepared according to the reaction sequences (1) and (2), respectively; PMACDT-ST-1: *p*-methacrylamidophenyl mercuric diphenylthiocarbazonate-styrene (1:9 by weight) copolymer, prepared according to the reaction sequence (1); PACDT-MA-2: *p*-acrylamidophenyl mercuric diphenylthiocarbazonate-methyl acrylate (1:9 by weight) copolymer, prepared according to the reaction sequence (2); PAMADT-ST and PAMADT-MA: *p*-acrylamidomethylaminophenyl mercuric diphenyl thiocarbazonate-styrene and -methyl acrylate (each 1:9 by weight) copolymers, prepared according to the reaction sequence (3); PACNT-MA: *p*-acrylamidophenyl mercuric di- β -naphthylthiocarbazonate-methyl acrylate (1:9 by weight) copolymer prepared according to the reaction sequence (1).

^c E_{11}^L/E_{11}^{Dc} , E_{11}^L/E_{11}^{De} : ratios of the absorbance under illumination to that in dark at absorption maxima I and II, respectively.

^d Dioxane solution.

illumination and in recovery prefer the solution state. It is interesting to note here that, in the case of polymer films, the intensity of the new absorption peak (II) increases with increasing irradiation time finally to reach an equilibrium, whereas in polymer solutions and in blends of matrix polymers with mercury thiocarbazonates (e.g., No. 103, with polystyrene as matrix), the new peak appears and then essentially disappears again with the progress of irradiation. Values other than 100 in the parentheses

in the last column of Table II indicate that E_{II}^L/E_{II}^D passes a maximum value with increasing irradiation time. This might be due to the steric inhibition of further unnecessary structural changes in the photochromic component, which might strongly appear in the case of polymer films.

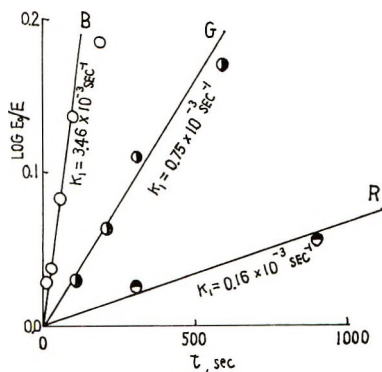


Fig. 2. Relationships between $\log E_0/E$ and t at 15°C for *p*-acrylamidophenyl mercuric diphenylthiocarbazonate-methyl acrylate (1:9 by weight) copolymer film. B, G, and R denote Toshiba blue (transmission peak, $460\text{ m}\mu$), green ($530\text{ m}\mu$), and red ($700\text{ m}\mu$) filters, respectively.

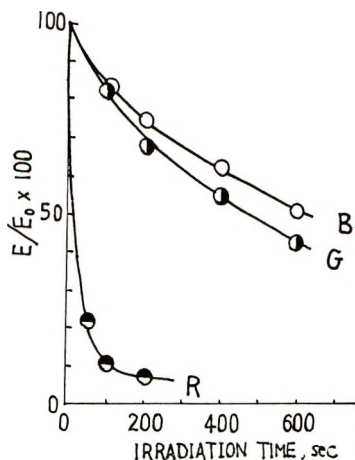


Fig. 3. Decrease of the absorbance at absorption peak ($630\text{ m}\mu$) with irradiation time for acrylamidomethyl trimethylthionine chloride polymer film prepared with poly(vinyl alcohol) and 10% of papain.

Intensity of the new peak was the highest with a corresponding progressive increase of the value in dioxane solution under the same conditions in the case of the film (No. 117) made of a *p*-acrylamidophenyl mercuric di- β -naphthyl thiocarbazonate polymer, in which the steric requirements for further structural changes might be the most severe, presumably denoting the effect of steric conditions.

Recovery in the Dark

Since the spectral recovery in the dark or under a diminished light intensity is of thermal nature, this reverse reaction takes place rather slowly in the solid state such as film at ordinary temperatures, due to steric hindrances against the isomerization of the photochromic component as described above.

Table III indicates the first-order rate constant k_2 and time for half-change $t_{1/2}$ as determined with the new absorption peak (II) caused by the photoisomerization product.

TABLE III
Spectral Recovery in the Dark^a

No.	Polymer	State	Abs. peak (II), $m\mu$	$k_2 \times 10^3$, sec^{-1}	$t_{1/2}$, sec
101	APDT	Soln ^b	580	18.8	37
102	APDT	C ₂ H ₄ Cl ₂ soln	575	18.4	38
103	APDT	In PST film	575	0.21	3300
104	PACDT-ST-1	Soln ^b	580	4.45	156
106	PACDT-ST-2	Soln ^b	580	5.09	136
108	PACDT-ST-1	Soln ^b	575	1.86	373
110	PACDT-MA-2	Soln ^b	575	77.1	9
111	PACDT-MA-2	Film	580	0.88	788
112	PAMADT-ST	Soln ^b	580	11.0	63
114	PAMADT-MA	Soln ^b	575	1.75	396
116	PACNT-MA	Soln ^b	600	5.76	120
117	PACNT-MA	Film	600	—	3600

^a After 20 sec irradiation at 15°C.

^b Dioxane solution.

It is readily recognized, in this case too, that the rates of the reverse reaction are advantageous for the solution state. Effect of temperature upon $t_{1/2}$ is given in Table IV. The rate of recovery in the solid state also appears to depend upon the kind of comonomer employed: e.g., copolymers with styrene which are more stiff and have higher glass transition

TABLE IV
Effect of Temperature upon the Time for Half-Recovery ($t_{1/2}$) in the Film

No.	Polymer	Temperature, °C	Abs. peak (II), $m\mu$	$t_{1/2}$, sec
111	PACDT-MA-2	15	580	788
	"	65	580	63
117	PACNT-MA	15	600	3600
	"	40	600	750
	"	65	600	64

temperatures provided considerably larger values of $t_{1/2}$ as compared with copolymers with methyl acrylate which are more flexible, thereby denoting the importance of steric condition here too.

References

1. H. Kamogawa, M. Kato, and H. Sugiyama, *J. Polym. Sci. A-1*, **6**, 2967 (1968).
2. H. Kamogawa, *J. Appl. Polym. Sci.*, **13**, 1883 (1969).
3. P. H. Vandewijer and G. Smets, in *Macromolecular Chemistry, Brussels-Louvain 1967 (J. Polym. Sci. C, 22)*, G. Smets, Ed., Interscience, New York, 1968, p. 231.
4. E. B. Sandell, *Colorimetric Determination of Traces of Metals*, Interscience, New York, 1959.
5. H. Irving, G. Andrews, and E. J. Risdon, *J. Chem. Soc.*, **1949**, 541.
6. J. L. A. Webb, I. S. Bhatia, A. H. Corwin, and A. G. Sharp, *J. Amer. Chem. Soc.*, **72**, 91 (1950).
7. L. S. Meriwether, E. C. Breitner, and C. L. Sloan, *J. Amer. Chem. Soc.*, **87**, 4441 (1965).
8. L. S. Meriwether, E. C. Breitner, and N. B. Colthup, *J. Amer. Chem. Soc.*, **87**, 4448 (1965).
9. W. H. Foster, Jr. and J. Kazan, *Text. Res. J.*, **37**, 376 (1967).
10. Z. G. Gardlung and J. J. Laverty, *J. Polym. Sci. B*, **7**, 719 (1969).

Received August 3, 1970

Reduction of Composite NMR Spectra by Using an Analog Computer*

V. D. MOCHEL and W. E. CLAXTON, *Central Research Laboratories,
The Firestone Tire and Rubber Company, Akron, Ohio 44317*

Synopsis

An analog computer program has been devised to resolve complex composite curves such as might be encountered in various forms of spectroscopy or chromatography. Seven Gaussian or Lorentzian curves, or any combination of seven curves, can be used and displayed simultaneously to resolve the composite curves. Various degrees of skew and truncation, as well as slanted and curved baselines, can be introduced. The peak amplitude, width and position can be determined from potentiometer settings. The integrated relative area of each of the peaks is read out on a digital voltmeter with a reproducibility of about $\pm 0.1\%$. The utility of the technique is demonstrated by resolving highly overlapped peaks in NMR spectra of butadiene-styrene copolymers. It is necessary to use as many as eight curves to resolve the styrene aromatic proton resonance. This analysis yields styrene-centered distributions and styrene sequence distributions from the NMR spectra of butadiene-styrene copolymers. In addition, it is shown that a distinction can be made between short styrene sequences, which contain two and three styrene units, and long styrene sequences, which include all sequences longer than three units.

INTRODUCTION

The separation of a complex composite curve into its components is a problem frequently encountered in various forms of spectroscopy or chromatography. In the polymer industry important details of polymer structure and composition can be revealed by the resolution of curves in nuclear magnetic resonance (NMR) spectroscopy, infrared spectroscopy, gel permeation chromatography, gas chromatography and other instruments. A commercial analog instrument for curve resolving is available (DuPont curve analyzer, Model 310), and other special instruments have been built for this purpose.^{1,2} Digital computer programs have also been written to decompose overlapping distributions,³⁻⁵ but it is believed that analog computers are better suited for this type of problem because the scientist can interact with the solution more conveniently.

High-resolution NMR has become an important tool in the study of sequence distributions in copolymers since Ferguson⁶ first demonstrated this

* Paper presented to the American Chemical Society, Division of Rubber Chemistry, Symposium on Use of Computers in the Rubber Industry, Washington, D. C., May 5-8, 1970.

application. Several investigators⁷⁻¹⁰ used NMR to study sequence distributions of styrene-methyl methacrylate copolymers. Recently Harwood and co-workers¹¹ extended the NMR study of styrene-methacrylonitrile copolymers. Data based on assignment of methine and α -methyl proton resonances to various triad and pentad distributions agreed well with calculated results.

In butadiene-styrene copolymers, monomer sequence information from NMR is practically nonexistent because of overlapping of pertinent resonances. From the aromatic proton resonance of the styrene units in butadiene-styrene copolymers, Mochel¹² obtained "block styrene" values in close agreement with those from the chemical method¹³ which uses osmium tetroxide for chain degradation. More recently, it was shown¹⁴ that monomer sequence distribution information could be derived from the overlapped aromatic proton resonance of butadiene-styrene copolymers.

This paper describes the reduction of data obtained by using an analog computer to resolve overlapped peaks of the styrene aromatic proton resonance of butadiene-styrene copolymers. It is demonstrated how this data is used to determine the styrene triad distributions and the styrene sequence distribution in these copolymers.

EXPERIMENTAL

Thirty-six emulsion copolymers and 57 *n*-BuLi-catalyzed butadiene-styrene copolymers were used in this study. All were polymerized in bottles at 50°C. A common recipe was used for the emulsion polymers, and the *n*-BuLi polymers were prepared in hexane or in heptane.

The 60 MHz NMR spectra were obtained at 28°C with a Varian Model DA-60-IL spectrometer. Copolymer compositions were determined by integrating the NMR spectra with a Varian Model V-3521A Integrator/Decoupler. The copolymer solution concentration for NMR measurements was 10% (w/v) in CCl₄, CS₂, or hexachlorobutadiene. A small amount of tetramethylsilane (TMS) was added as internal reference.

The curve analysis was accomplished with an E.A.I. TR-48 analog computer which was programmed by Claxton, Clarke, and Breeden.¹⁵ Seven Gaussian or Lorentzian, or any combination of seven peaks, can be used simultaneously to resolve the overlapped peaks. The integrated relative areas of these peaks are read out on a digital voltmeter with a reproducibility of about 0.1%, which is a small error compared to the precision of the curve analysis.

PROGRAMMING CONSIDERATIONS

One of the most important features of this analog computer program is that the *X* axis of the trace is generated by a single integrator as a linear ramp. This axis is common to all channels and is connected to the horizontal axis of an *X*-*Y* plotter. The wiring diagram of this portion is shown in Figure 1. The initial condition (IC) at this integrator determines the

starting position of the X axis. The rate at which the computer will sweep the X axis is controlled by the input rate potentiometer setting at the integrator.

Another important feature of this program is that variable diode function generators (VDFG) are used to generate the distributions. In this work, Gaussian functions and Lorentzian functions are used; however, other distributions could be set up with VDFG cards for special cases. Examples of the Gaussian and the Lorentzian distributions are shown in Figure 2 along with the appropriate equations. In the Lorentz equation, b is the width at half height (half width), but in the Gauss equation b' is a measure of the standard deviation. The Gaussian half width is $(2.61) b'$ and is thus 2.61 times as wide as the Lorentzian half width. A is the maximum amplitude of the distribution.

There are advantages in using VDFG's to generate these distributions. (1) Since both distributions involve the common term $(\Delta x/b)^2$ and since this is always positive, a single distribution requires only the plus or minus card of a VDFG. (2) The distribution function can be programmed from a tabulation of $|\Delta x/b'|$ for the Gaussian and of $|\Delta x/b|$ for the Lorentzian function, eliminating the need for a squaring circuit. This is important since it eliminates the need for an expensive multiplier to generate each function. (3) Since $|\Delta x/b'|$ and $|\Delta x/b|$ cover similar ranges, a channel can be switched from Gaussian or Lorentzian merely by inserting the ap-

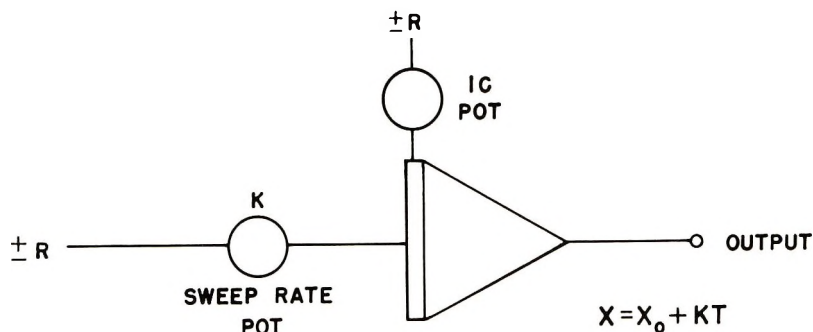


Fig. 1. Schematic for generating a common X axis.

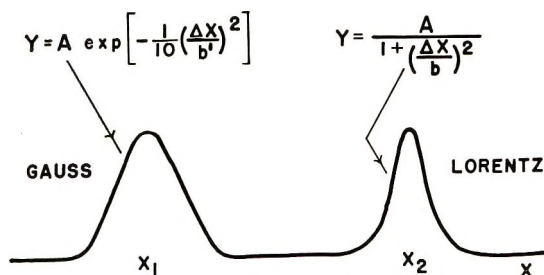


Fig. 2. Comparison of Gaussian and Lorentzian distributions.

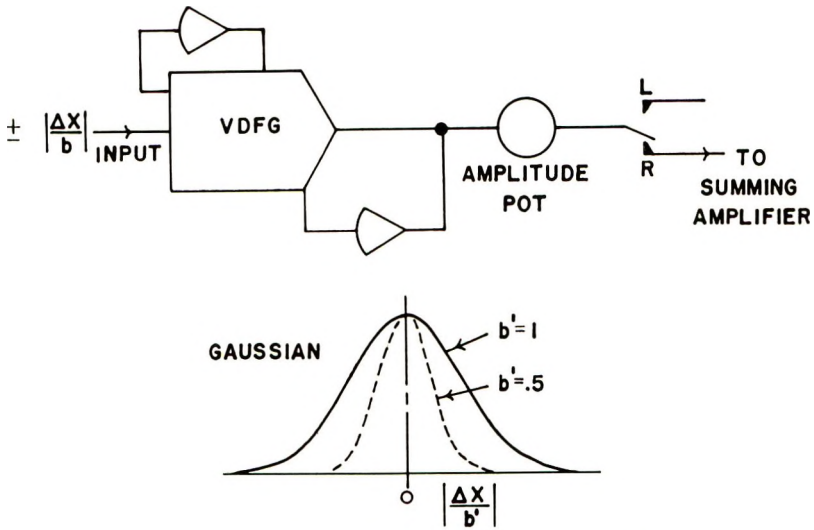


Fig. 3. Schematic showing peak generation with VDFG.

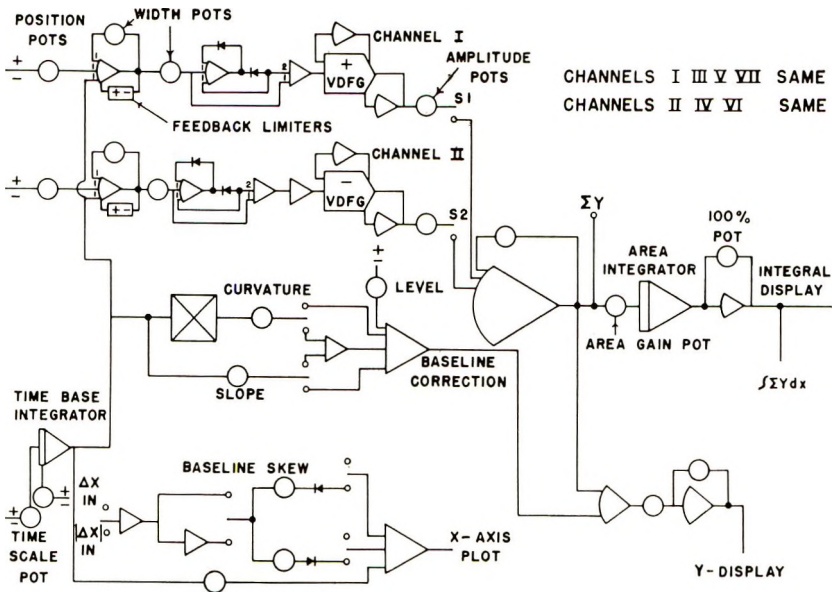


Fig. 4. Composite curve analyzer schematic.

propriate VDFG card. Any combination of functions can be obtained without changing the patch panel. Figure 3 shows the part of the wiring scheme which includes the VDFG. Amplitude potentiometers are used at the output of the VDFG's to vary the maximum amplitude of each function independently.

The complete curve analyzer schematic diagram is shown in Figure 4. Other important features of this program are that the peak amplitude, the

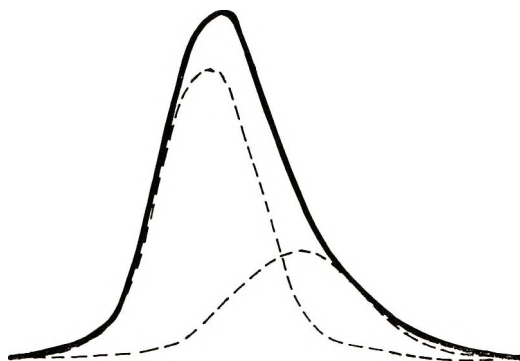


Fig. 5. Gaussian distribution with skew to the right (—). This can be fit with skewed baseline or with two symmetrical Gaussian distributions (---).

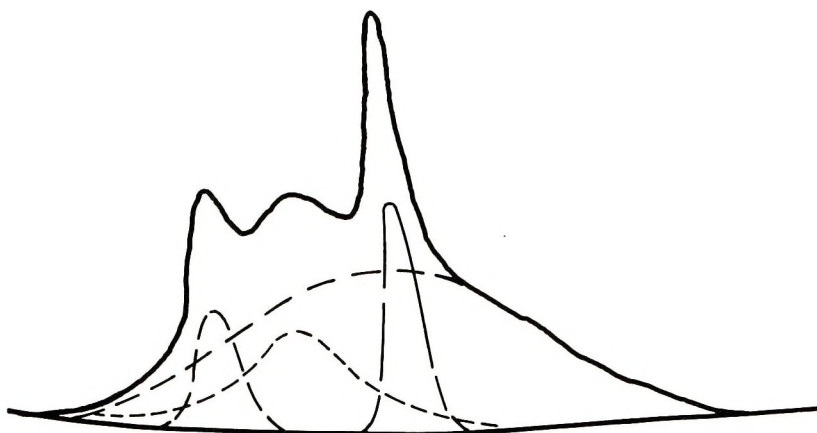


Fig. 6. Composite distribution fitted with a curved baseline.

width and the position can be independently varied and determined from potentiometer settings. The integrated relative area of each of the peaks is read out on a digital voltmeter with a reproducibility of about $\pm 0.1\%$.

Various degrees of skew and truncation, as well as slanted and curved baselines, can also be introduced. Figure 5 shows a typical skewed distribution (solid line). With the form of baseline skewing as shown in Figure 4, the Y value as a function of time has been left unchanged; hence, the area readout is the same with or without baseline skewing. The principal use of this feature would be in providing a quick match to an obviously nonsymmetrical distribution, after which, with baseline skew omitted, the symmetrical part could be separately displayed or plotted. The difference would then be obtained by setting up another peak in the problem to account for the difference. This is shown by the dashed lines in Figure 5. The result of overlapping two Gaussian and two Lorentzian distributions and superimposing these on a curved baseline can be seen in Figure 6. The ability to easily slant or curve the baseline is especially im-

portant in analyzing infrared spectra and many other analytical instrument outputs where baseline drift occurs.

CURVE ANALYSIS

The curve analysis is accomplished by first taping a Polaroid transparency of the composite curve on the face of the oscilloscope and then introducing an appropriate number and type of curves until a good match is obtained. For greatest accuracy fine adjustments of the various parameters can be made by fitting the curves directly to the original experimental curve on an X - Y plotter. Seven curves can be displayed simultaneously or individually on the oscilloscope or on an X - Y plotter. The area under the composite curve is integrated and adjusted to give a 100% reading on a digital voltmeter. Then each of the curves contributing to the composite is integrated individually. Thus, the area of each of the peaks is read out directly as the percentage of the total composite curve area.

RESULTS AND DISCUSSION

Monomer Sequence Distributions

The basis for this NMR curve analysis method lies in the fact that the aromatic proton resonance of polystyrene consists of two well-resolved peaks with an integrated intensity ratio of 3 to 2 as shown in Figure 7. Bovey, Tiers, and Filipovich¹⁶ attributed the resonance at 3.0 τ to the *para* and the two *meta* protons and that at 3.5 τ to the two *ortho* protons. Both peaks are shifted upfield (to higher τ values) from the aromatic resonance of a single styrene unit or a model compound such as toluene (2.86 τ), but the *ortho* proton peak experiences the greater shift. These chemical shifts result from a "ring current" effect and an overlapping of the phenyl rings of neighboring styrene units.

From the relative intensity of the shifted *ortho* proton resonance compared to the total styrene aromatic resonance, the NMR "block styrene" value can be determined in copolymers. Also something can be learned of the sequence distribution, especially with *n*-BuLi copolymers. If the sequence lengths are large, determining the relative area of the *ortho* proton

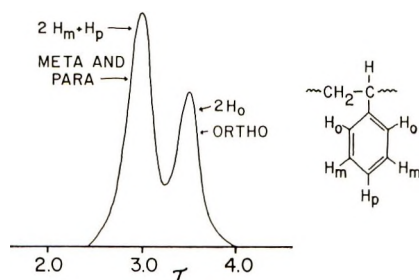


Fig. 7. Aromatic proton resonance of atactic polystyrene in CCl_4 at 28°C.

resonance is simple because the peaks are well separated. However, if the styrene sequences are short, this resonance appears merely as a broadening or a shoulder on the main aromatic resonance. Resolving these curves by eye or with an electronic integrator with any reasonable accuracy is practically impossible. Curve analysis with the analog computer accomplishes the task quite well.

Emulsion Copolymers

Bovey and co-workers¹⁶ studied emulsion butadiene styrene copolymers and estimated that the styrene sequence length must be 8–10 units before the shoulder appears in the main aromatic peak. In the 60 MHz NMR spectra of the emulsion copolymers we observed the progressive formation of a shoulder, a gradual shifting to higher field and finally the formation of a resolved peak in the aromatic resonance as \bar{m}_s , the average styrene sequence length, increased. This trend is shown in Figure 8 in which \bar{m}_s is listed for each polymer. It is not until an \bar{m}_s of 5.45 (or a copolymer composition of 90% styrene) is reached that the *ortho* proton peak becomes resolved. An NMR spectrometer with a higher field strength would effect a separation at a lower \bar{m}_s , of course. \bar{m}_s was calculated with eq. (1),

$$\bar{m}_s = 2S/R$$

where S is mole per cent styrene in the copolymer and R is the run number.¹⁷

As an approximation, there should be three peaks under the aromatic resonance envelope: two for the block styrene and one for the nonblock styrene. We used the analog computer for curve analysis to resolve these peaks. Since the two peaks in polystyrene are fitted very nicely by Gaussian curves, these functions were chosen for "block styrene" peaks. Simi-

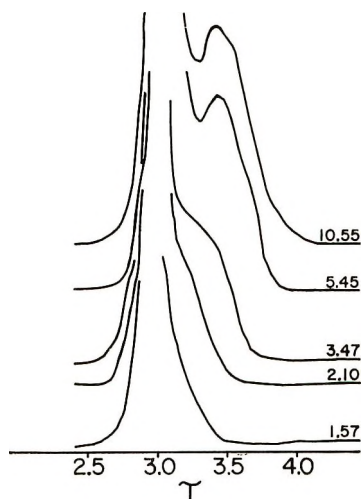


Fig. 8. Aromatic resonance of emulsion butadiene styrene copolymers. Shows formation of shoulder as \bar{m}_s increases.

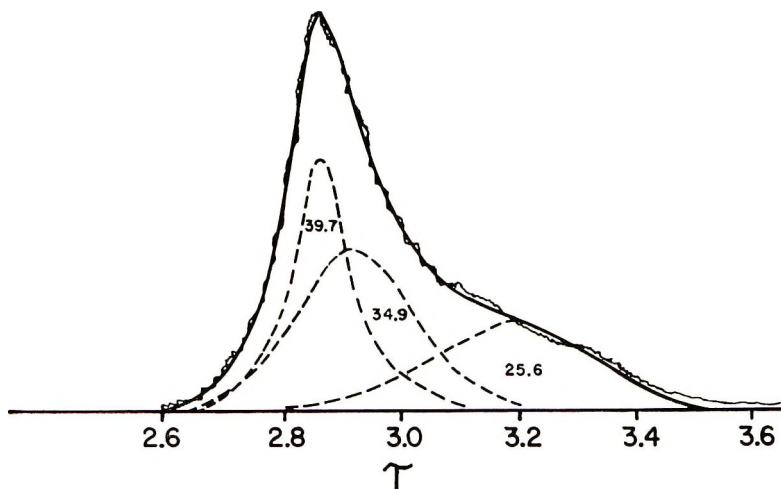


Fig. 9. Curve analysis of expanded aromatic resonance of a copolymer. Numbers under the peaks are integrated relative areas. Solid, smooth curve is calculated envelope.

larly, a Lorentzian function was chosen for the nonblock styrene portion because the low-styrene copolymer resonance best approximates it. The most physically meaningful solutions were obtained with this combination.

A typical solution is shown in Figure 9. The resolved peaks from left to right are due to nonblock styrene, block styrene *meta* and *para* protons, and block styrene *ortho* protons. The numbers corresponding to each of the curves are relative areas compared to the total area of the composite envelope. The smooth, solid line is the computed envelope, and the jagged envelope is the experimental curve.

Since the ratio of the areas of the two block styrene peaks should be 3:2, an attempt was made to impose this restriction on all solutions. With this restriction, which is sometimes difficult to achieve, the solutions are quite unique.

n-Butyllithium Copolymers

Polymerization data and copolymer compositions of 20 *n*-BuLi copolymers are shown in Table I. The styrene content in the feed ranges from about 10 to 90 mole-%.

Calculated values of copolymer styrene resulted from the set of reactivity ratios,¹⁴ $r_{BD} = 15.0 \pm 1.4$ and $r_S = 0.025 \pm 0.080$. The standard deviation between calculated and NMR copolymer styrene is 2.4%. This good agreement is important because it shows that the terminal model used in the calculation and the reactivity ratios are valid for this system. It also gives confidence in the calculated sequence distribution and the calculated values for block styrene which will be described. Copolymer styrene values in the fourth column of Table I were calculated with Harwood's sequence distribution computer program.¹⁸

TABLE I
n-BuLi Butadiene-Styrene Copolymers

Copolymer	Styrene in feed, mole-%	Conversion, wt-%	Styrene in copolymer, wt-%	
			Calcd ^a	NMR
22	9.98	39.1	1.83	1.81
23	19.2	2.46	2.97	3.09
24	33.9	8.46	6.50	7.53
25	33.9	34.0	9.30	9.36
26	49.7	37.4	20.0	21.6
27	60.0	27.4	24.7	24.1
28	60.0	35.0	30.6	30.2
29	60.0	44.3	42.0	43.9
30	70.0	10.4	25.5	23.4
31	70.0	22.8	33.6	31.5
32	70.0	46.2	60.6	53.4
33	80.2	2.4	32.4	31.8
34	80.0	6.1	34.5	33.3
35	80.0	16.8	43.9	45.2
36	80.0	20.3	48.1	48.2
37	80.0	22.4	50.9	50.3
38	80.0	42.8	73.1	72.4
39	90.0	11.6	60.5	55.5
40	90.0	20.9	74.0	69.4
41	90.0	65.3	91.6	90.9

^a Calculated assuming $r_{BD} = 15.0$, $r_S = 0.025$. Standard deviation (57 polymers) = 2.4%.

Curve analysis of the aromatic resonance of *n*-BuLi copolymers is more complicated but also more fruitful than that of emulsion copolymers. The complexity of resolving these curves is illustrated by Figure 10 which is the aromatic resonance of copolymer 23 in Table I. Again, the jagged line is the experimental curve and the smooth one is the calculated envelope which is the sum of the broken-line peaks. Eight peaks—four Lorentzian and four Gaussian—were used for this solution. This is the minimum number of peaks necessary for an adequate fit to the experimental curve, especially for copolymers with short styrene sequences. Although only seven peaks can be displayed simultaneously with the curve analyzer, more than seven can be used by first fitting the composite curve on one side and then moving two or three peaks to the other side to complete the fit. As long as the area integrator gain is not changed, the areas of the reused peaks will still be proportional to the total area. The only restriction is that the new peaks can not overlap with those in the first locations because this would change the total area. The curve in Figure 10 is characteristic of the aromatic resonance of the isolated styrene unit in a copolymer prepared by *n*-BuLi initiation.

The two low-intensity dashed peaks at about 3.0 and 3.1 τ in Figure 10 are in the positions which we assign to the *meta* and *para* and to the *ortho* proton peaks, respectively, of short sequences (blocks) of styrene. These

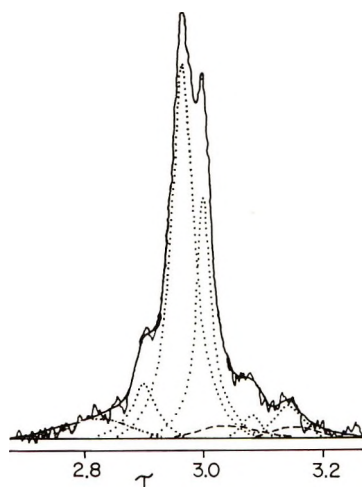


Fig. 10. Curve analysis of aromatic resonance of isolated styrene unit in *n*-BuLi copolymer; copolymer 24: (—) calculated envelope; (--) positions of short styrene sequences; (···) unassigned.

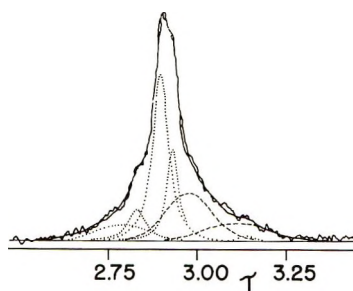


Fig. 11. Curve analysis of copolymer 34. Dashed curves at about 3.0 τ and 3.1 τ are due to short sequences. Comparison of these curves with those in Fig. 10 shows increase as number of short sequences increase.

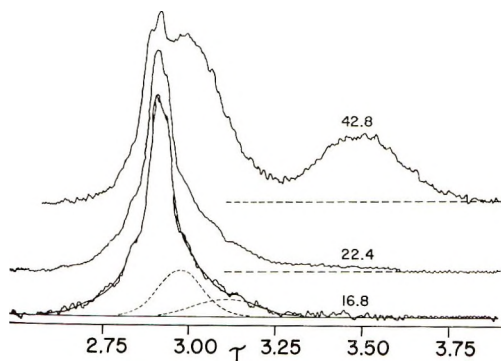


Fig. 12. Aromatic resonance of copolymers 35, 37, and 38. Illustrates formation and growth of *ortho* proton resonance at 3.5 τ due to long styrene sequences.

peaks increase as the number of short sequences increase. This is shown in Figure 11 which is copolymer 35 of Table I. Again, the two dashed curves are due to the short styrene sequences.

Figure 12 illustrates an important and striking difference between emulsion and *n*-BuLi butadiene styrene aromatic proton resonances. The spectra resulted from copolymers 35, 37, and 38. All are derived from monomer feed compositions containing 80% styrene but different conversions, which are shown above the curves. The lowest spectrum includes the dashed peaks as shown in Figure 11. At about 22.4% conversion a weak, broad resonance starts to appear at about 3.5 τ , and this (and the resonance at 3.0 τ) increases as conversion increases. The two dashed curves, due to the short sequences, remain in the same positions but also increase. Curve analysis of the aromatic resonance of *n*-BuLi copolymers permits a rather clear separation between "short" and "long" styrene sequences.

Recall from Figure 8 that the shoulder in the aromatic resonance shifts gradually to the right as the styrene sequence lengths increase. This difference in aromatic resonance between emulsion and *n*-BuLi copolymers is less apparent for the long styrene sequences because the *ortho* peak in emulsion copolymers eventually shifts to 3.5 τ also. We believe this difference arises from differences in tacticity of styrene sequences. An isotactic structure is expected to cause a greater overlapping of phenyl rings and hence a larger shift to high field than a syndiotactic structure. Thus, it is presumed the *n*-BuLi system generates more nearly isotactic styrene sequences than the emulsion system.

Table II shows the curve analysis results of most of the *n*-BuLi copolymers of Table I. NMR-curve analysis results are divided into short sequences, long sequences, and total for block styrene values. The total values are not the sums of columns 2 and 3 but are obtained by summing both *ortho* resonances and the *meta* and *para* resonances of short and long sequences. These values should be the most accurate for total sequences.

The "NMR direct" values are obtained directly from the spectrum by a method described previously.¹² This method can be used only if the *ortho* peak is at least partially resolved.

One of the outputs of the sequence distribution computer program is the weight fraction of the total polymer of A or B sequences containing 1 to 10 monomer units. Sequence lengths over 10 units are lumped into one figure. It is from the styrene sequence fractions that the calculated block styrene figures are obtained. Since the NMR-curve analysis method does not distinguish between the individual styrene sequences but includes the total of all sequences over a certain minimum length in the block styrene figure, we can sum the calculated styrene sequences from the longest to shorter ones until the accumulated total corresponds to the NMR value. This will demonstrate the lower limit of the NMR method.

The last four columns [ACWP(*n*)] of Table II list the accumulated weight percentages of all styrene sequences of length *n* and greater. For example, the sixth column [ACWP (2)] is the sum of the weight percentages of all

TABLE II
 Curve Analysis of *n*-BuLi Copolymers

Copoly- mer	Block styrene, wt-%							
	Curve anal. (NMR)			NMR Direct	Calculated			
	Short seq.	Long seq.	Total		ACWP (2)	ACWP (3)	ACWP (4)	ACWP (5)
22	0.05		0.05		0.01	0.00	0.00	0.00
24	0.45		0.45		0.18	0.00	0.00	0.00
26	3.4		3.4		2.5	0.29	0.04	0.01
27	3.1		3.1		3.6	0.48	0.06	0.01
28	8.5	3.5	10.4	1.2	7.5	2.1	0.63	0.21
29			20.4	17.2	21.8	15.5	12.7	11.1
31	7.6		7.6		7.6	1.6	0.33	0.07
32	8.3	33.0	41.3		43.5	37.0	34.0	32.2
33	8.0		8.0		6.0	0.86	0.11	0.01
34	7.5		7.5		7.1	1.1	0.17	0.02
35	13.6		13.6		14.5	4.3	1.3	0.40
36	16.0		16.0		19.8	8.1	3.5	1.6
37	16.9	5.4	25.5		24.0	12.0	6.5	3.8
38		54.3	61.7	49.1	58.6	51.7	48.2	46.0
39	27.5		27.5		33.5	16.9	8.5	4.4
40		26.7	52.0	27.0	57.2	45.5	38.3	33.5
41		77.7	85.5	77.0	82.7	76.5	72.7	70.2

styrene sequences two units in length and longer, i.e., it includes all but the isolated styrene units. Similarly, the seventh column includes all styrene sequences longer than two units, etc.

From these columns it is seen that copolymers 22 and 24 (Fig. 10) essentially contain only isolated styrene units. For the copolymers which have only short sequences, the short sequence values agree very closely to ACWP (2), indicating a sequence length of two units is the lower limit for the curve analysis method. Copolymers 28, 32, and 37 have values for both short and long sequences. The long sequence values correlate closely with ACWP (3) and ACWP (4), as do the "direct" NMR results. In these copolymers there is also good agreement between the short sequence values and [ACWP (2)-ACWP (4)]. There are short and long styrene sequences in copolymers 29, 38, 40, and 41 also, but unique curve fitting is difficult for the short sequences because of overlap.

From these data we conclude the "short" sequences consist of two and three styrene units, and the "long" sequences include all sequences longer than three units. Also, the NMR "direct" method measures the long sequences in both *n*-BuLi and emulsion copolymers.

The *ortho* proton resonance for the short styrene sequences correspond to the *ortho* protons of styrene units centered in the triads (BSS + SSB), and the *ortho* proton resonance of the long styrene sequences correspond to those of the styrene units centered in SSS triads. In support of this, Kinstle and Harwood¹⁹ have shown by a study of 3,4,5-trideuteriostyrene homopolymers

TABLE III
Triad Distributions of *n*-BuLi Copolymers

Copolymer	f_{SSS}		$(f_{SSB} + f_{SSS})$		f_{BSB}		$(f_{SSS} + f_{SSB} + f_{BSB})$		$f_{SSS} + f_{BSB}$	
	Calcd	Obs	Calcd	Obs	Calcd	Obs	Calcd	Obs	Calcd	Obs
22	0.000	0.00	0.007	0.028	0.993	0.97				
24	0.000	0.00	0.027	0.065	0.973	0.93				
26	0.005	0.00	0.118	0.16	0.877	0.84				
27	0.007	0.00	0.140	0.13	0.853	0.87				
28	0.027	0.12	0.219	0.28	0.754	0.60	0.246	0.34		
29	0.261		0.259		0.480	0.53	0.520	0.47		
31	0.0175		0.209	0.24	0.774	0.76	0.717	0.77	0.792	0.76
32	0.527	0.62	0.190		0.283	0.23				
33	0.010	0.00	0.176	0.25	0.815	0.75				
34	0.012	0.00	0.193	0.23	0.796	0.78				
35	0.039		0.291	0.28	0.670				0.709	0.72
36	0.073		0.338	0.33	0.589				0.662	0.67
37	0.113		0.359	0.34	0.529	0.55				
38	0.625	0.11	0.177		0.198	0.15	0.802	0.85		
39	0.128		0.425		0.447	0.50	0.553	0.50		
40	0.443	0.39	0.330	0.36	0.227	0.25	0.773	0.75		
41	0.745		0.152		0.103	0.14	0.897	0.86		

and copolymers with methyl methacrylate that the resonance of *ortho* protons centered in (MSS + SSM) and SSS triads occur at 3.2 and 3.5 τ , in agreement with our assumptions. From these resonances the corresponding styrene-centered triad fractions can be calculated. The fraction, f_{BSB} , is determined by difference since the sum of the three fractions equals unity.

Table III compares calculated and observed styrene-centered distributions for *n*-BuLi copolymers. The agreement is excellent between calculated and observed values for f_{BSB} . In general it is not quite as good for the other fractions. However, copolymers 33-38 show especially good agreement for the other fractions as well. In some cases the sum of two fractions, but not the individual fractions, could be observed. These are listed in the last four columns. Agreement between calculated and observed is again good.

Calculated styrene sequence weight distributions, $\text{WD}(n)$, are listed in Table IV for copolymers having only short sequences ($n = 2, 3$). These are

TABLE IV
Styrene Sequence Weight Distributions in *n*-BuLi Copolymers

Copolymer	Calcd $\text{WD}(n)$		[$\text{WD}(2) + \text{WD}(3)$]	
	$\text{WD}(2)$	$\text{WD}(3)$	Calcd	Obs
22	0.007	0.000	0.007	0.03
24	0.026	0.001	0.027	0.07
26	0.109	0.013	0.122	0.16
27	0.128	0.017	0.145	0.13
28	0.179	0.046	0.225	0.28
31	0.180	0.037	0.217	0.24
33	0.158	0.023	0.181	0.25
34	0.172	0.028	0.200	0.23
35	0.232	0.069	0.301	0.28
36	0.243	0.095	0.338	0.33
37	0.237	0.106	0.343	0.34
39	0.273	0.139	0.412	0.50

the fractions of styrene units which are in sequences of length 2 and 3. In this case, $\text{WD}(2) + \text{WD}(3)$ should equal the observed fraction of styrene in short sequences. The last two columns show close agreement between calculated and experimental results for this quantity.

The data of Tables III and IV demonstrate that styrene-centered triad fractions and some sequence weight distribution information can be determined experimentally for *n*-BuLi butadiene styrene copolymers. Each of these quantities (or a combination) can be related to a run number,¹⁷ R , from which all other sequence-related quantities can be calculated since penultimate effects are apparently not important for this system. For example,

$$\text{WD}(1) = f_{\text{BSB}} = R^2/4S^2 \quad (2)$$

where R is the run number and S is the mole percentage of copolymer styrene. Such quantities are quite accurate for low conversion copolymers. Complications can be encountered for high conversion copolymers because of nonhomogeneity of the composition; however, calculations show that this is still a good approximation for these copolymers.

Comparison with Perfectly Random Copolymers

A convenient and useful way to display the results of the NMR curve analysis is shown in Figures 13 and 14. The smooth curves in both figures show how the styrene sequences of length n vary with the copolymer composition for "perfectly random" butadiene styrene copolymers. A perfectly random copolymer as defined by Wall²⁰ ($r_1 = r_2 = 1$) is an "ideal" copolymer in which the composition and the sequence distribution are

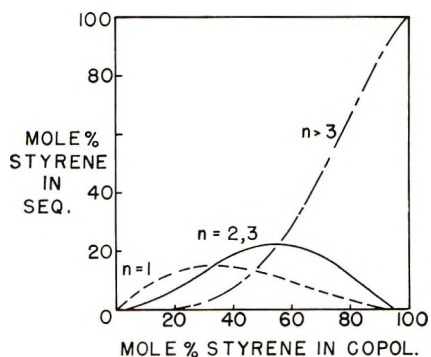


Fig. 13. Styrene sequence distribution for perfectly random butadiene-styrene copolymers.

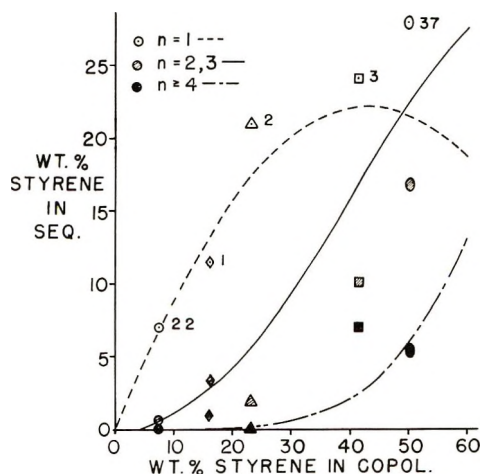


Fig. 14. Comparison of styrene sequence distributions of experimental and perfectly random butadiene-styrene copolymers.

uniform over the entire length of the polymer chain, i.e., they are independent of the conversion. The curves in Figures 13 and 14 also are valid for all other cases of "ideal" copolymers ($r_1 r_2 = 1$) at any given copolymer composition; however, the sequence distribution does vary along the chain for all other cases. The perfectly random copolymer represents a standard by which all other real copolymers can be compared. Since much effort is expended in trying to "randomize" copolymers, these curves provide a convenient visual comparison to show the effectiveness of the randomization process.

The three curves in Figure 13 correspond to the mole percent styrene in the copolymer in sequence lengths of 1 unit, 2 and 3 units, and greater than 3 units, respectively. These curves correspond to the "boxes" or categories into which the NMR-curve analysis results fall.

Figure 14 is essentially the same plot, except the sequence distribution is reported on a weight-per cent basis and the scale is expanded to allow a more detailed inspection of the most useful range of copolymer composition. This form of reporting the data might be more useful to polymer chemists, since they tend to think in terms of weight per cent. The styrene-centered triad distributions could also be plotted and compared with that of ideal copolymers, but sequence distributions are probably more easily visualized than triad distributions.

Experimental points resulting from the NMR curve analysis of some butadiene styrene copolymers are plotted in Figure 14 for easy comparison with perfectly random copolymers. There are three points for each experimental polymer. The open symbols represent the isolated styrene units ($n = 1$), the cross-hatched symbols represent sequences of two and three units, and the solid symbols correspond to the sum of all styrene sequences longer than 3 units ($n \geq 4$). It is easily seen that samples 22 and 1 have measured sequence distributions which are very close to "perfectly random." Samples 2, 3, and 37 have more of the isolated styrene units than perfectly random copolymers of the same composition. This is shown by the open symbols lying above the $n = 1$ curve (dashed line). Sample 3 has more of the longer sequences and less of the short sequences than expected from a perfectly random copolymer. It should be pointed out that the sum of the values represented by the three symbols for each polymer equals the total styrene in the copolymer. The long sequences and the short sequences are measured, but the isolated styrene units are obtained by difference. Therefore, if one symbol lies off the appropriate curve, there must be a compensating deviation by at least one other symbol.

It is important to note that this method of measuring and displaying styrene sequence distributions does not depend upon how the copolymer was made nor its history. Conversely, the method of NMR curve analysis will not reveal the history of the polymer but measures the end result. If the polymer contains long styrene sequences, these would be detected, but it would not be possible to determine when during the polymerization they entered the chain. It is a useful means of measuring the sequence distribu-

tion of a copolymer and comparing it with that expected for a perfectly random copolymer.

CONCLUSIONS

A method is described for determining styrene sequence distribution in butadiene-styrene copolymers. An analog computer is used to resolve overlapped peaks in the styrene aromatic proton NMR spectrum. Two important features of this analog computer program are: (1) the X -axis is common to all channels and is generated by a single integrator and (2) variable diode function generators are used to generate the distributions.

Seven Gaussian or seven Lorentzian, or any combination of seven curves, can be displayed simultaneously or individually on the oscilloscope or on an X - Y plotter. Various degrees of skew and truncation, as well as slanted and curved baselines, can be introduced. The amplitude, width and position of each peak can be varied independently. The relative area of each peak can be read out on a digital voltmeter with a reproducibility of about $\pm 0.1\%$.

In n -BuLi copolymers a quite quantitative distinction can be made between short blocks, which contain two and three styrene units, and long blocks, which include styrene sequences four units and longer. The resonance attributed to long blocks appears as a separate peak at 3.5τ at the start of formation of styrene sequences longer than three units. However, the *ortho* proton resonance of emulsion copolymers gradually shifts to higher fields as styrene sequence length increases until it, too, reaches 3.5τ . This difference might be due to a greater isotactic character of n -BuLi copolymers. The direct NMR method for block styrene includes all sequences greater than three units in length.

Styrene-centered triad distributions in butadiene-styrene copolymers can be determined experimentally from the aromatic proton resonance. Agreement between calculated and NMR curve analysis results is good, especially for n -BuLi copolymers. For copolymers with only short styrene sequences, styrene sequence weight distribution information can also be obtained from the spectrum. From either of these experimental quantities one can calculate all other sequence-related properties for any copolymer. Thus it is now possible to determine approximate styrene-centered distributions and styrene sequence distributions from butadiene-styrene copolymers.

A useful way to display the results of the NMR curve analysis is to plot them on a graph which shows the variation of styrene sequence distribution as a function of copolymer composition for perfectly random copolymers. The deviations in sequence distribution between the experimental and the perfectly random copolymers are quickly and easily seen.

We wish to thank Mr. R. E. Clarke and Mr. L. E. Breeden for their help in programming the analog computer for curve analysis. We also gratefully acknowledge the many helpful suggestions of Prof. H. J. Harwood and Dr. B. L. Johnson. The permission of The Firestone Tire and Rubber Co. to publish this paper is appreciated.

References

1. F. W. Noble, J. E. Hayes, Jr., and M. Eden, *Proc. Inst. Radio Engrs.*, **47**, 1952 (1959).
2. C. S. French, G. H. Townes, D. R. Bellis, R. M. Cook, W. R. Fair, and W. W. Holt, *Rev. Sci. Instr.*, **25**, 765 (1954).
3. W. D. Keller, T. R. Lusebrink, and C. H. Sederholm, *J. Chem. Phys.*, **44**, 782 (1966).
4. H. Stone, *J. Opt. Soc. Amer.*, **52**, 998 (1962).
5. L. E. Vesceius, Firestone Central Research Laboratories, unpublished results.
6. R. C. Ferguson, *J. Amer. Chem. Soc.*, **82**, 2416 (1960).
7. F. A. Bovey, *J. Polym. Sci.*, **62**, 197 (1962).
8. A. Nishioka, Y. Kato, and N. Ashikari, *J. Polym. Sci.*, **62**, S10 (1962).
9. Y. Yamashita, K. Ito, S. Ikuma, and H. Kada, *J. Polym. Sci. B*, **6**, 219 (1968).
10. H. J. Harwood and W. M. Ritchey, *J. Polym. Sci. B*, **3**, 419 (1965).
11. M. Murano, K. Shimizu, and H. J. Harwood, paper presented at American Chemical Society Meeting, 1969; *Polym. Preprints*, **10**, No. 193 (1969).
12. V. D. Mochel, *Rubber Chem. Technol.*, **40**, 1200 (1967).
13. I. M. Kolthoff, T. S. Lee, and C. W. Carr, *J. Polym. Sci.*, **1**, 429 (1946).
14. V. D. Mochel and B. L. Johnson, *Proc. 4th Intern. Synthetic Rubber Symp., London SRS4*, **3**, 74 (1969); *Rubber Chem. Technol.*, **43**, 1138 (1970).
15. W. E. Claxton, R. E. Clarke, and L. E. Breeden, paper presented at Midwestern Simulation Councils, Inc. Meeting, Akron University, Akron, Nov. 1969.
16. F. A. Bovey, G. V. D. Tiers, and G. Filipovich, *J. Polym. Sci.*, **38**, 73 (1959).
17. H. J. Harwood and W. M. Ritchey, *J. Polym. Sci. B*, **2**, 601 (1964).
18. H. J. Harwood, in *The Computer in Polymer Science (J. Polym. Sci. C, 25)*, J. B. Kinsinger, Ed.), Interscience, New York, 1968, p. 37.
19. J. F. Kinstle and H. J. Harwood, paper presented at American Chemical Society Meeting, 1969; *Polym. Preprints*, **10**, No. 2, 1389 (1969).
20. F. T. Wall, *J. Amer. Chem. Soc.*, **66**, 2050 (1944).

Received June 22, 1970

Revised August 10, 1970

Irradiation-Grafted Polymeric Films.

I. Preparation and Properties of Acrylic Acid-Grafted Polyethylene Films

H. F. HAMIL, L. M. ADAMS, W. W. HARLOWE, JR., and E. C. MARTIN, *Southwest Research Institute, San Antonio, Texas 78228*

Synopsis

Graft copolymers of low-density polyethylene film and acrylic acid have been prepared by the direct grafting technique. The properties of 27.4, 33.9, 41.2, and 46.4 wt-% poly(acrylic acid) graft copolymer films have been compared. Measurements include degree and uniformity of grafting, gel water content, degree of swelling on wetting, tensile strength, elongation, ion-exchange capacity, water-vapor transmission, and water flux and solute rejection under reverse osmosis conditions. These properties were found to vary as the composition of the graft copolymer changed; most properties were found to be a linear function of the degree of grafting.

INTRODUCTION

The radiation-induced graft polymerization of monomers to solid polymer films has been studied with a wide variety of monomers and polymers.¹⁻³ Two general techniques for radiation-induced grafting can be employed; the preirradiation method, where a polymer is "activated" by irradiation, either in the presence or absence of oxygen, and subsequently allowed to react with a monomer,^{4,5} and the direct method, where a polymer is dissolved or immersed in a monomer and the mixture irradiated.⁶

The direct grafting method was utilized in this study to prepare a graded series of polyethylene-poly(acrylic acid) graft copolymers. The ease with which reaction parameters such as grafting solution composition, irradiation dose rate, and total dose can be varied to give specific copolymers makes the direct grafting method particularly suitable for such a study. After preparation of the copolymer films, some physical and chemical properties of the films were measured in order to determine the effect of the added poly(acrylic acid).

EXPERIMENTAL

Materials

Glacial acrylic acid (Rohm and Haas Company) stabilized with 200 ppm MEHQ was used without further purification.

Benzene (Texas Solvents and Chemical Company) was nitration grade material and was used as received.

Carbon tetrachloride (ACS grade, Matheson Scientific Company) was used as a chain transfer agent in the grafting reaction.

Polyethylene (Dow Chemical Company) was a nominal 1-mil thickness film, designated Dow 400 film. This film was fabricated from low-density polyethylene (0.921 g/cc) and was additive-free except for 1000 ppm CaCO_3 .

Cheesecloth used as interleaving material in the rolls of polyethylene film during grafting was designated Chicopee 28 \times 24 and was obtained from Chicopee Mills, Inc., New York, N. Y.

Equipment

Radiation Facility. The irradiation grafting was conducted in Southwest Research Institute's Radiation Effects Facility. The source used consisted of approximately 10,000 Ci of high specific activity ^{60}Co . The individual ^{60}Co sources are individually encapsulated in stainless steel tapes, $\frac{1}{2} \times \frac{1}{8}$ in. To provide a uniform radiation field, wide enough for eight samples and high enough to cover the large rolls used in the grafting step, the individual ^{60}Co tapes are evenly spaced on the centerline of a vertical semi-parabolic holder which is mounted on a remotely controlled dolly.

Detailed dosimetry by use of Bausch and Lomb cobalt glass chip technique was performed on the irradiation tables and irradiation vessels. The entire assembly was adjusted, in position or source strength, until it was determined that the incident dose rates were those desired for each of the eight turntable positions, within the error of the dosimetry system. The target incident dose rate was 12,000 Rads/hr. Higher or lower dose rates could then be obtained by decreasing or increasing the target to source distance. Dosimetry at one or two points in the target array would then be sufficient, since the irradiation field was symmetrical and uniform.

Reverse Osmosis Test Module. Reverse osmosis data on the graft copolymer films was obtained by using 2-in. diam stainless steel reverse osmosis cells similar in design to that described by Manjikian.⁷

The reverse osmosis test loops were pressurized to the desired pressure using compressed air. Feed solution was circulated from a surge tank through the reverse osmosis cells by a peristaltic type pump installed in a pressure housing. Feed flow in the test cells was 25 cm/sec at the periphery of the cell and increased to ca. 200 cm/sec at the central exit port of the cell.

Analysis of the feed and product water was by electrical conductivity, by use of Leeds and Northrup Company Model No. 4866 bridge.

Procedures

Grafting Procedure. Polyethylene film, in 25-ft lengths, was backed with cheesecloth as an interleaving material and rolled onto $\frac{1}{4}$ -in. aluminum pipes, which were capped at one end. During the process of preparing the

film rolls, small sections were cut from the polyethylene film at 5-ft intervals, weighed and the weight recorded, and replaced in the rolls. The rolls of film and backing material were placed in hydrometer jars (75 mm \times 550 mm), and the jars sealed with rubber stoppers fitted with inlet and outlet tubes. The aluminum pipes protruded through the stoppers and served as thermocouple wells, allowing temperatures to be monitored during grafting.

The sealed hydrometer jars were connected to a vacuum system and evacuated to ca. 2 mm Hg. After backflushing with nitrogen, the jars were again evacuated and the grafting solution drawn into the jars. The filled jars were alternatively evacuated and backflushed with nitrogen several times before sealing the inlet and outlet tubes. The filled tubes were allowed to stand at least 24 hr to provide time for the film to equilibrate with the grafting solution. Grafting solution compositions for the four films reported here were benzene solutions containing 10, 15, 20, and 25 wt-% glacial acrylic acid. Carbon tetrachloride, which functions as a chain transfer agent was added in a weight ratio of one part carbon tetrachloride to five parts acrylic acid.

The hydrometer jars were placed on motor-driven turntables in the irradiation facility and irradiated at a dose rate of 0.012 Mrad/hr until a total dose of 0.815 Mrad had been applied. The hydrometer jars were rotated during the irradiation period in order to apply a uniform radiation dose to the film.

After completion of the irradiation period, the jars were removed from the irradiation facility and allowed to stand for 24 hr in order to permit reaction of any remaining active sites.

The films were removed from the jars, separated from the backing material, and washed in 5 wt-% potassium hydroxide at 95–98°C for 1 hr. The film was washed further with water at 95–98°C to remove soluble homopolymer and excess potassium hydroxide. The small samples were removed from each roll, washed as above, and then treated with hot 5 wt-% HCl to convert them to the free acid form. These samples were vacuum-dried to constant weight and the weight recorded. From the weight gain of the samples, the uniformity and degree of grafting along each roll was calculated.

Gel Water Content. The gel water content of the copolymer films was determined by taking samples of the films as their potassium salts and soaking them overnight in deionized water. The samples were blotted dry, then placed in weighing vials, and their wet weight recorded. After drying to constant weight at 105°C, their weight was redetermined. Gel water content was calculated from the dry weight of film and the water content as determined by weight loss on drying.

Degree of Swelling on Wetting. Samples of film in the potassium salt form were cut by using a 1 \times 2 in. die. Film thicknesses were determined by using a Starrett No. 657-617 thickness gauge. Length and width measurements were made with a steel rule graduated in 0.01-in. increments. After the dry dimensions were determined, the film samples were soaked

overnight in deionized water, blotted dry of surface water on absorbent paper, and the dimensions remeasured.

Tensile Strength and Elongation at Yield. Tensile strength and elongation at yield were determined by means of a Gardner tensile apparatus. Films were as the potassium salts, and determinations were made on both wet and dry samples. Tensile strips (0.38 × 6.0 in.) were cut by use of a die, care being taken to avoid nicks or tears on the edges of the strips.

Water Vapor Transmission. Water vapor transmission measurements were made in accordance with the appropriate A.S.T.M. method.⁸

Ion-Exchange Capacity. Samples were prepared, and total cation exchange capacities of the copolymer films were determined in accordance with Method 502.1 in the Office of Saline Water *Test Manual (Tentative) or Permselective Membranes*.⁹

RESULTS AND DISCUSSION

Composition of the Graft Copolymers

It was found that the composition of the graft copolymer produced was a function of the acrylic acid concentration in the grafting solution, over an acrylic acid concentration range of 10–25 wt-%. The data obtained on analysis of the four copolymers from this study are presented in Table I. Under the reaction conditions used, the direct grafting technique produces quite uniform copolymer films. The variation in the weight percent poly(acrylic acid) in the copolymers over the 25-ft length of the films was less than 1%, compared with the average value, with the exception of film S-82, which showed a maximum variation of 2.1% compared with the average value. Similarly, the grafting efficiency was uniform along the film length and was essentially the same for all four films, indicating that the efficiency of monomer utilization is independent of the monomer concentration in the grafting solution.

In Figure 1, the degree of grafting, defined as the grams of poly(acrylic acid) formed in the copolymer per gram of starting polyethylene, is depicted as a function of the acrylic acid concentration in the grafting solution. It was found that the degree of grafting was a linear function of the acrylic acid concentration.

In a previous study,¹⁰ 1-mil polyethylene film was grafted with a 25 wt-% acrylic acid, 5 wt-% carbon tetrachloride, 70 wt-% benzene solution. The irradiation dose rates were varied from 0.0125 to 0.021 Mrad/hr, and the total dose was varied from 0.671 to 1.700 Mrad. Over this range of dose rates and total doses, composition of the copolymer produced did not vary significantly.

According to Odian,¹¹ the rate of graft polymerization is given by the equation

$$R_p = \frac{[M]R_i^{1/2}k_p}{(2k_t)^{1/2}}$$

TABLE I
Effect of Acrylic Acid Concentration in the Grafting Solution on the Graft Copolymer Composition

Film no.	Grafting solution composition, wt-%			Sample distance, ft from end of roll	Degree of grafting (avg) ^a	Grafting efficiency (avg) ^b	Poly(acrylic acid) in product wt-% (avg)
	Acrylic acid	CCl ₄	C ₆ H ₆				
S-81	25	5	70	5	0.85	10.8	45.9
				10	0.86	10.9	46.2
S-82	20	4	76	15	0.89	11.3	47.2
				20	0.86	10.9	46.2
S-83	15	3	82	5	0.75	11.9	42.9
				10	0.69	10.9	40.9
S-84	10	2	88	15	0.64	10.2	39.1
				20	0.71	11.3	41.7
S-83	15	3	82	5	0.51	10.8	33.9
				10	0.50	10.6	33.1
S-84	10	2	88	15	0.51	10.8	33.7
				20	0.54	11.4	34.9
S-84	10	2	88	5	0.40	12.7	28.6
				10	0.37	11.7	27.0
S-84	10	2	88	15	0.37	11.7	27.1
				20	0.38	12.1	27.4

^a Weight of poly(acrylic acid) in the graft copolymer/weight of starting polyethylene.

^b Weight of poly(acrylic acid) in the graft copolymer/weight of acrylic acid consumed.

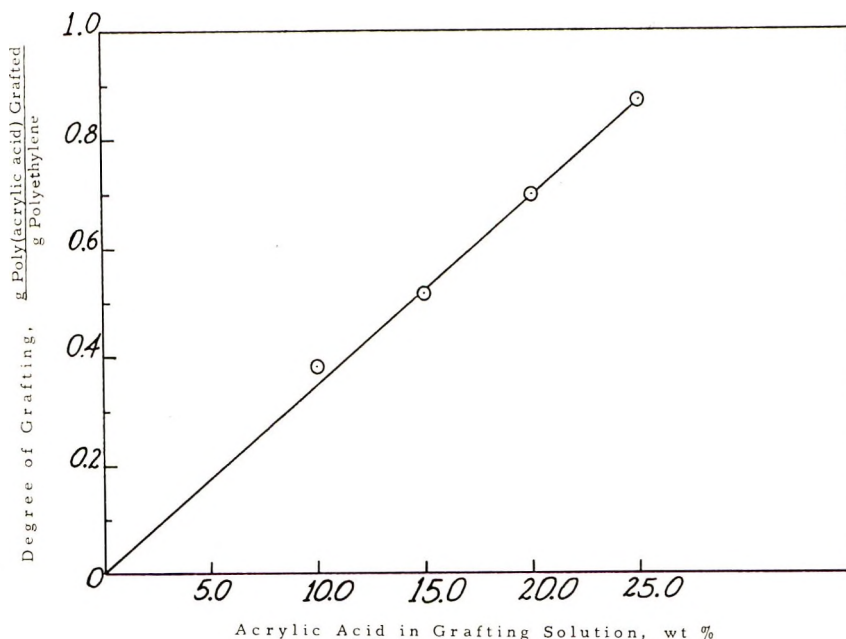


Fig. 1. Effect of acrylic acid concentration in the grafting solution on the degree of grafting of the copolymer films.

where R_p is the rate of grafting, in moles of monomer grafted per liter of monomer-solvent-amorphous polyethylene, per second; $[M]$ is the monomer concentration, in moles of monomer per liter of monomer-solvent-amorphous polyethylene; R_i is the initiation rate, in moles of amorphous polyethylene free radicals per liter of monomer-solvent-amorphous polyethylene per second; k_p , k_t are the propagation and bimolecular termination rate constants, respectively. Since the ratio $k_p/(2k_t)^{1/2}$ is a constant for a given monomer-polymer-solvent system, the rate of graft polymerization R_p should be controlled by the concentration of the monomer and the concentration of free radicals in the polymer. For the acrylic acid-polyethylene-benzene system, we found that the total amount of poly(acrylic acid) in the copolymer was independent of radiation intensity at uniform irradiation periods and independent of total dose.¹⁰ Since dose rate and total dose control the rate of production of radicals and the total number of radicals produced, this implies that R_i is not a controlling factor in the rate of graft polymerization with this system within the limits of dose rates and total dose described above. Conversely, maintaining a constant rate of production of polyethylene radicals, as in the present study, and varying the monomer concentration in the grafting solution gives a series of copolymers in which the poly(acrylic acid) content is a linear function of acrylic acid concentration.

In the present study, it would appear that at the irradiation dose rates used, sufficient polyethylene radicals are produced to utilize all available

monomer in the film. Since the acrylic acid concentration in the polyethylene film will be controlled by the external concentration of acrylic acid and by the diffusion coefficient of acrylic acid in polyethylene, for this system one has a diffusion-controlled process, and the composition of the copolymer can be controlled by control of the acrylic acid concentration in the grafting solution.

From the data in Table I, it can be seen that copolymer films containing relatively large amounts (46.4 wt-%) of poly(acrylic acid) can be prepared by the direct grafting technique, at ambient temperatures. By contrast, polyethylene-poly(acrylic acid) graft copolymers prepared by the preirradiation technique¹² contained a maximum of 20.3 wt-% poly(acrylic acid), with the graft polymerization step run at 120–140°C. Radiation doses were nominally the same in both cases.

Effect of Copolymer Composition on Film Properties

Gel Water Content. The graft copolymers in the potassium salt form are hydrophilic and readily imbibe water on wetting. From the data presented in Table II, it can be seen that the gel water content of the films increases from S-84, which has the lowest poly(potassium acrylate) content, to S-81, which has the highest poly(potassium acrylate) content. These data are depicted graphically in Figure 2, where it can be seen that a linear relationship exists between poly(potassium acrylate) content and the gel water content of the saturated films.

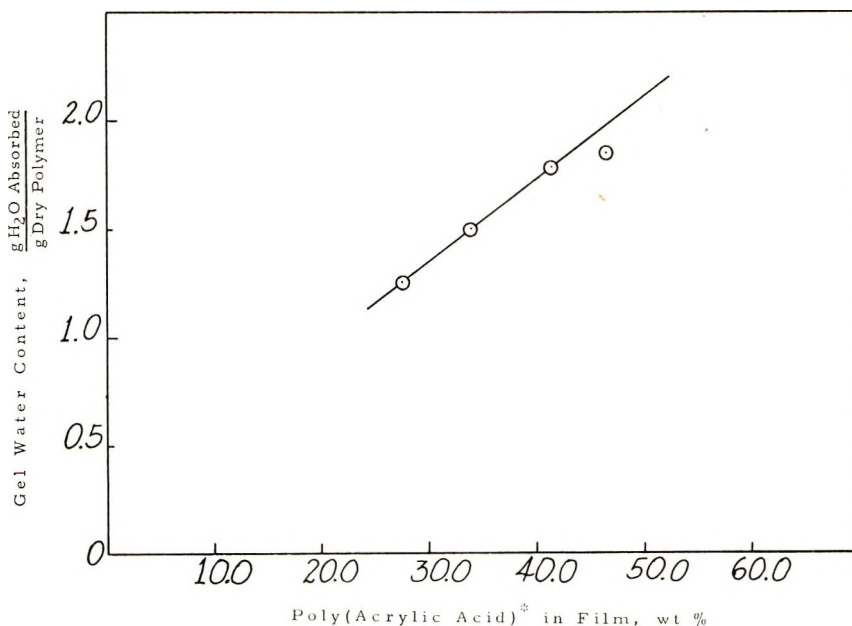


Fig. 2. Effect of poly(acrylic acid) content (potassium salt form) of the graft copolymer on water absorption. (* Films as potassium salts.)

TABLE II
Effect of Copolymer Composition on Film Properties

Film no.	Gel water content, g H ₂ O imbibed/ g dry copolymer	Degree of swelling on wetting						Length, in.		Tensile strength, psi		Elongation %		
		Thickness, mils		Width, in.		% Change		Dry	Wet	Dry ^a	Wet	Dry ^a	Wet	
		Dry	Wet	Dry	Wet	Dry	Wet	Dry	Wet	Dry ^a	Wet	Dry ^a	Wet	
S-81	1.85	1.45	2.00	37.9	1.00	1.36	36.0	2.00	2.74	37.0	1655	510	>100	70
S-82	1.79	1.34	1.75	30.6	0.99	1.30	31.3	2.00	2.64	32.0	1985	378	>100	45
S-83	1.50	1.33	1.80	35.3	1.00	1.25	25.0	2.02	2.57	27.2	2665	735	>100	55
S-84	1.26	1.21	1.55	28.1	1.00	1.20	20.0	2.00	2.43	21.5	2495	903	>100	84

^a Dry films were equilibrated with air at 77°F and 50% RH.

Degree of Swelling. Upon wetting, the films, in the salt form, all undergo dimensional changes. For the two more highly grafted films (S-81 and S-82), the dimensional changes are essentially uniform in all three dimensions (Table II), while for the remaining two films (S-83 and S-84) there was a greater relative change in thickness than in width or length. Comparison of the four films shows that the degree of swelling is a function of the degree of grafting, with the largest dimensional changes occurring in the most highly grafted film, and decreasing as the degree of grafting decreases.

Tensile Strength. The tensile strength at the yield point was determined for the copolymer films in the salt form. Measurements were made on both wet and dry tensile strips. Tensile strengths for the dry specimens were higher than for the original ungrafted polyethylene, which had a tensile strength of 1850 psi, except for the most highly grafted film, S-81 (Table II). When the films were saturated with water, there was a considerable loss of tensile strength. The tensile strength decreased by a factor of about 3 to 5, depending on the film being measured. There was no linear correlation between either wet or dry tensile strength and copolymer composition, but the general trend in both cases was a decrease in tensile strength with increasing poly(potassium acrylate) content of the copolymer.

Elongation. The elongation at the yieldpoint was determined for wet and dry films in the potassium salt form (Table II). For all four films, elongations of greater than 100% were obtained on the dry samples. For the wet samples, elongations in the range of 45–84% were observed, but again no correlation with copolymer composition could be made.

Ion-Exchange Capacity. Since the polyethylene–poly(acrylic acid) graft copolymers contain relatively high concentrations of carboxylic acid groups, they should function as weak cation exchange materials. Based on the poly(acrylic acid) content of the copolymers, ion-exchange capacities for the four materials were calculated. Experimental values for the ion exchange capacities were determined and compared with the calculated values (Table III). Excellent agreement between the calculated and experimental values for all four films was obtained. Presumably due to the relatively large amounts of water imbibed by the grafted films, an open struc-

TABLE III
Ion-Exchange Capacity of Acrylic Acid-Grafted Polyethylene Films

Film no.	Degree of grafting	Ion-exchange capacity, meq/dry g	
		Calculated from degree of grafting	Experimental
S-81	0.87 ± 0.02	6.35 ± 0.06	6.40
S-82	0.70 ± 0.03	5.64 ± 0.14	5.67
S-83	0.52 ± 0.01	4.64 ± 0.07	4.71
S-84	0.38 ± 0.01	3.77 ± 0.06	3.83

TABLE IV
Water Vapor Transmission of Acrylic Acid-Grafted Polyethylene Films^a

Film no.	Water vapor transmission, g-cm/m ² -24 hr	Equilibrium, water content, wt-%	Film thickness (wet), mils
S-81	9.10	37.2	1.6
S-82	7.10	38.1	1.5
S-83	5.46	35.2	1.2
S-84	5.11	35.0	1.1

^a Films as potassium salts.

ture is obtained in the swollen polymer, and essentially all the carboxyl groups are available for ion exchange.

Water Vapor Transmission. Water vapor transmission through the graft copolymer films, in the potassium salt form, was measured in conformance with the appropriate A.S.T.M. method.⁸

It is found that the water vapor transmission increased as the degree of grafting increased (Table IV). When the water vapor transmission was plotted as a function of the degree of grafting, the linear plot shown in

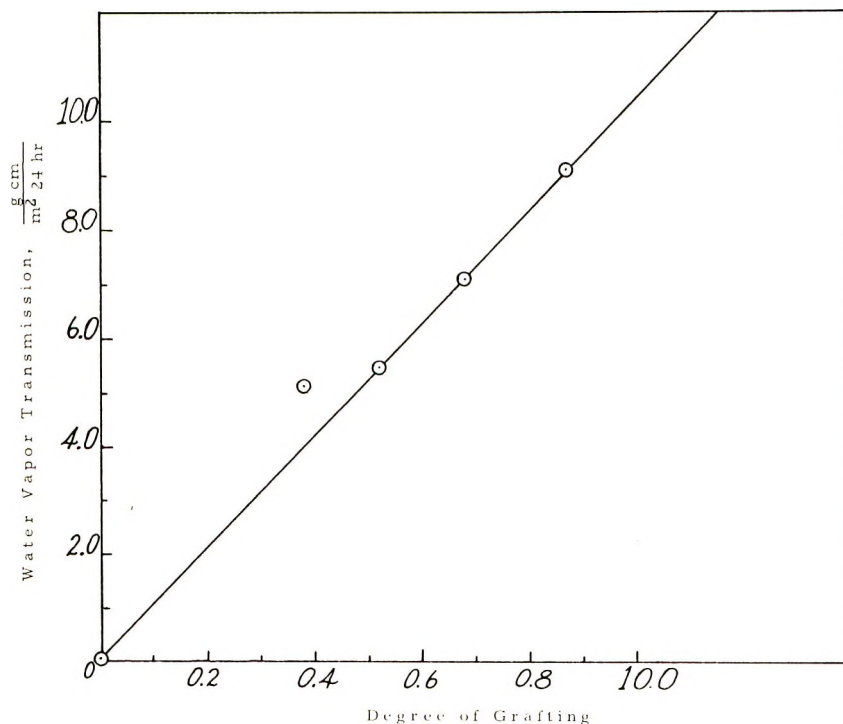


Fig. 3. Effect of poly(acrylic acid) content in the copolymer film on water vapor transmission.

Figure 3 was obtained. The value for the water vapor transmission for low-density polyethylene was obtained from published data.¹³

The equilibrium water concentration of the films under the test conditions (100% RH, 50% RH) was also determined, and was found to increase as the degree of grafting increased, except that the value for film S-81 was lower than expected.

Reverse Osmosis Studies. The water flux and salt rejection for these membranes were determined at 400 psig with 0.25-wt% saline feed. As the amount of poly(potassium acrylate) in the film decreased, the water flux decreased, and the salt rejection increased. Examination of the data presented in Table V suggested that the decreasing flux observed with decreasing poly(potassium acrylate) content might be explained by the decreasing gel water content in the graft copolymer shown in Table II. If it is accepted that water transport through poly(potassium acrylate)-grafted membranes is a direct function of the amount of imbibed water in the membrane, and the demonstrated facts of strongly coupled water-salt flows along with very high equilibrium water contents are considered, then the following mechanism of transport through these membranes can be proposed.

In the wet state the films contain large amounts of imbibed water and are in a swollen gellike state. The water in interstitial spaces between the polymer chains provides a medium for ionization of the potassium polyacrylate, which results in mobile potassium ions in the interstitial spaces and fixed carboxyl ions on the polymer chains. Water transport through the membrane under hydraulic pressure would occur by viscous flow through the interstitial spaces and would increase with increasing degree of hydration, since the cross-sectional area between the polymer chains would increase as the polymer chains were forced farther apart by the larger volume of imbibed water. Salt rejection in the solution moving through the interstitial space would be due to simple ion exclusion and would decrease as the degree of hydration increases, since the average charge density in the interstitial spaces due to the fixed carboxyl ions on the polymer chains would decrease as the polymer chains occupy a decreasing percent of the hydrated volume of the swollen film.

Where the salt rejection is due to ion exclusion, divalent cations should be more selectively rejected than monovalent cations due to their larger diameter and greater charge density.

Reverse osmosis runs with 0.028 *M* sodium sulfate and 0.028 *M* dibasic sodium phosphate were conducted. It was assumed that, with larger polyvalent anions, the effective repulsion due to the fixed negative charge on the polymer carboxyl groups would be greater, and higher rejections of these salts would be obtained. As can be seen from the data shown in Table V, rejections of 90% or better were obtained in both cases for four different films with varying amounts of poly(acrylic acid) in the film. With sodium sulfate, the rejection was essentially constant at 91%, while water flux appeared to decrease with decreasing degree of grafting except for sample

TABLE V
Rejection of Various Solutes by Acrylic Acid-Grafted Polyethylene Membranes^a

Film no.	NaCl, 0.046M			Na ₂ SO ₄ , 0.028M			Na ₂ HPO ₄ , 0.028M			Poly(acrylic acid) content, wt-% in copolymer
	Flux, Gfd	S.R., %	Membrane constant A, cm ³ /cm ² -sec-atm × 10 ⁶	Flux, Gfd	S.R., %	Membrane constant A, cm ³ /cm ² -sec-atm × 10 ⁶	Flux, Gfd	S.R., %	Membrane constant A, cm ³ /cm ² -sec-atm × 10 ⁶	
S-81	2.84	67.7	0.49	2.98	91.5	0.52	2.86	91.2	0.50	46.4
S-82	2.78	68.9	0.48	3.02	90.9	0.53	2.54	91.9	0.45	41.2
S-83	2.48	69.0	0.43	2.72	90.8	0.47	3.24	90.0	0.57	33.9
S-84	2.27	72.2	0.39	2.53	91.0	0.42	1.54	93.0	0.27	27.5

^a All data obtained at 400 psig, all films as potassium salts.

S-82, which has a slightly higher flux than S-81. This decrease in water flux parallels that observed in reverse osmosis experiments on this series of films with sodium chloride. However, the water fluxes were slightly higher with the sodium sulfate feed, than with the sodium chloride feed.

When dibasic sodium phosphate was utilized as feed, salt rejections were 90% or better, and water fluxes were comparable to those obtained with the other solutes. With the phosphate feed, a trend of decreasing flux and increasing rejection with decreasing degree of grafting is seen, except for sample S-83, which shows a higher than expected flux with a lower rejection.

These results bear out the postulate that salt rejection is due to simple ion exclusion, as would be expected for ion-exchange membranes.

CONCLUSIONS

We have prepared a series of acrylic acid grafted polyethylene films by the direct grafting technique. Under the reaction conditions employed, we found the grafting step to be diffusion-controlled, which allows ready control of the final copolymer composition by controlling the concentration of acrylic acid in the grafting solution.

Determination of some physical properties and transport coefficients for the graft copolymer films indicated that these properties of the copolymer films change with the graft copolymer composition. Further, it was found that the properties of these films were a linear function of the amount of poly(acrylic acid) in the graft copolymer.

We believe that this work indicates that the direct grafting technique is a convenient route to graft copolymers, and that the ease with which copolymers of desired composition can be obtained makes this method valuable in that polymers can be readily tailored to give specified properties.

We wish to thank the Office of Saline Water, United States Department of the Interior, for support of a portion of this work under Contract No. 14-01-0001-2129.

References

1. A. Chapiro, *Radiation Chemistry of Polymeric Systems*, Interscience, New York, 1962, Chap. 12.
2. G. Odian and H. W. Chandler, in *Advances in Nuclear Science and Technology*, Vol. 1, E. J. Henley and P. Greebles, Eds., Academic Press, New York, 1962, p. 85.
3. H. A. J. Battaerd and G. W. Tregear, *Graft Copolymers (Polymer Reviews, Vol. 16)*, Interscience, New York, 1967.
4. A. Chapiro, M. Magat, and J. Sebban, French Pat. 1,125,537 (1956).
5. A. Chapiro, M. Magat, and J. Sebban, Brit. Pat. 809,838 (1959).
6. A. Chapiro, M. Magat, and J. Sebban, French Pat. 1,111,725 (1955).
7. S. Manjikian, *Ind. Eng. Chem., Prod. Res. Devel.*, **6**, 23 (1967).
8. A.S.T.M. Method of Test E96-63T, Water Vapor Transmission of Materials in Sheet Form.
9. *Test Manual (Tentative) for Permselective Membranes*, Office of Saline Water Research and Development Report No. 77, U. S. Department of the Interior, Washington, D. C., 1964.

10. L. M. Adams, W. W. Harlowe, Jr., and G. C. Lawrason, *Development of Battery Separator Material Process*, Southwest Research Institute, Interim Report (August, 1967), Jet Propulsion Laboratory, California Institute of Technology Contract No. 951718.

11. G. Odian, M. Sobel, A. Rossi, and R. Klein, *J. Polym. Sci.*, **55**, 663 (1961).

12. J. K. Rieke, G. M. Hart, and F. L. Saunders, in *Macromolecular Chemistry, Paris 1963* (*J. Polym. Sci. C*, **4**), M. Magat, Ed., Interscience, New York, 1963, p. 589.

13. J. Frados, Ed., *Modern Plastics Encyclopedia, 1968*, **45**, No. 1A, McGraw-Hill, New York, 1967, p. 525.

Received June 30, 1970

Structure of Polymers Obtained from Sulfur Monochloride and Olefins Containing Sulfonium Salt Structures

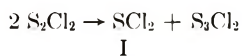
F. LAUTENSCHLAEGER, *Dunlop Research Centre, Sheridan Park, Ontario, Canada*

Synopsis

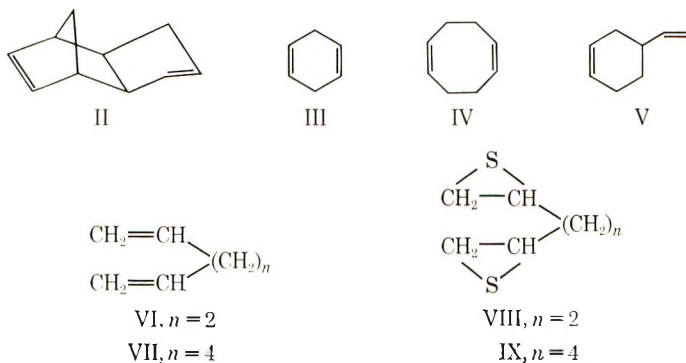
Reactions of sulfur monochloride with diolefins lead to polymeric products which can be reduced to diepisulfides in low yield. In reactions with cyclic triolefins, polymers containing tricyclic sulfonium structures are obtained as a result of transannular additions and subsequent transannular displacements. Due to the insolubility and reactivity of these ionic structures, only incomplete structural assignments could be made, but the reactions are studied on similar cyclic structures which provide model systems.

RESULTS AND DISCUSSION

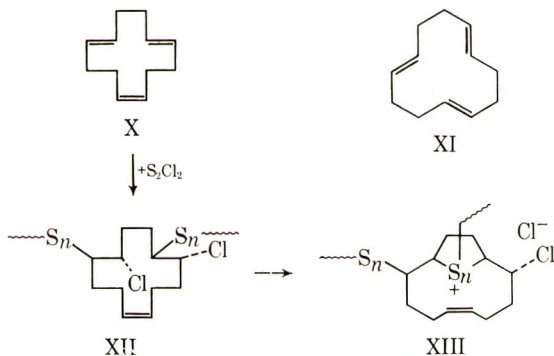
During investigations of the reactions of sulfur monochloride with olefins¹⁻³ it was observed that reactions with diolefins lead to oligomeric or polymeric products. In several instances, these products were reduced to unsaturated episulfides.³ The generality of this addition reaction has been demonstrated^{1,4} However, contrary to earlier reports concerning the nature of such reactions,^{5,6} it was assumed that the addition of sulfur monochloride leads to disulfide polymers^{1,2} exclusively. More recent results support the complexity of that addition reaction^{3,7} which is essentially a result of a disproportionation of I into sulfur dichloride and



trisulfur dichloride. We consider the recently reported polymerization of sulfur chlorides with diolefins not as novel^{1,2} since the major product (>98%) of a reaction of I with 2,3-dimethylbutadiene-1,3 had been reported to be polymeric in an earlier investigation.⁸ We have independently investigated the addition of I to diolefins and obtained polymeric products from the diolefins II-VII. The presence of the disulfide linkage in these addition products can be demonstrated by their reduction to the diepisulfides VIII and IX in low yields (~10%) by means of aluminum amalgam according to a recently disclosed procedure.³



An attempted extension of this reaction to the cyclic triolefins X and XI has led to the formation of products which are insoluble in aprotic solvents. Therefore, an investigation of their structure was initiated. In

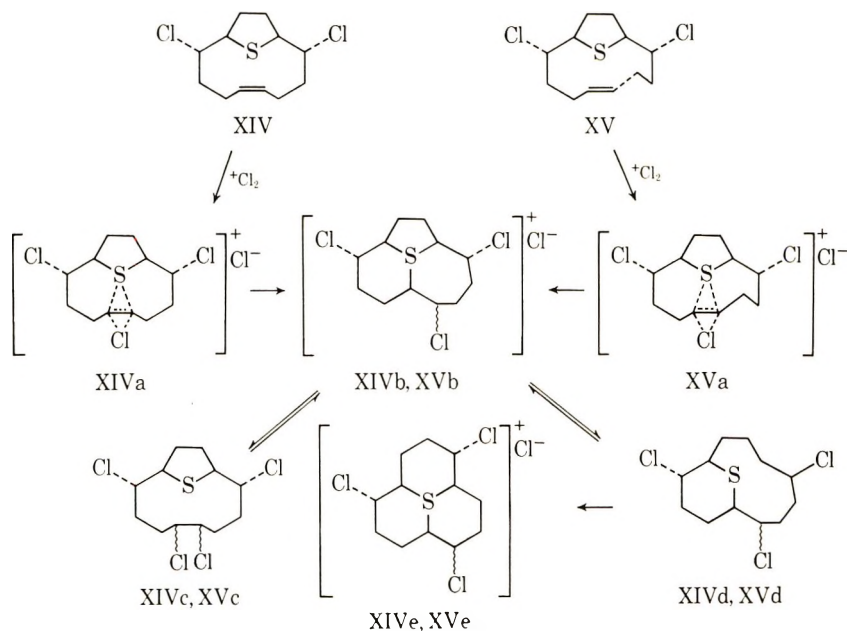


general, the presence of an additional double bond and the use of a medium-size ring system in this addition reaction may lead to several secondary reactions. For example, it is conceivable that after the formation of the initial addition product XII, displacement of a chloride ion in this sterically crowded ring system might lead to a bicyclic sulfonium salt such as structure XIII. The transannular addition of alkylsulfenyl chlorides to cyclooctadiene-1,5 provides a recent example for this type of sulfonium salt formation.⁹ However, a uniform structure would not be anticipated because of the tendency of disproportionation of I, which would result in the formation of mono-, di- and trisulfide links in the addition product XII. Furthermore, geometric isomers might result since addition of I to two olefinic sites in X or XI may occur by a random approach, placing carbon-sulfur and carbon-chlorine bonds in various nonequivalent positions. An added complication could arise from the possibility that the formation of XIII might involve the displacement of a chloride ion by mono-, di- or even trisulfide groups. Since it was uncertain whether both di- and trisulfide links can participate in the formation of sulfonium salts, transan-

nular interactions in these bicyclic ring systems were investigated and various additions were studied.

We have observed that from the reaction of X with equimolar amounts of I in methylene chloride as reaction medium, 12% of the product separates as insoluble powder, another 37% separates on dilution with diethyl ether whereas 51% remains as a soluble polymer. When this reaction was carried out in hexane, an insoluble product was obtained in nearly quantitative yield. For the identification of these structures, spectroscopic data were inconclusive except for either the presence or absence of both *cis* and *trans* unsaturation in the infrared and nuclear magnetic resonance spectra. The nuclear magnetic resonance spectra of all products showed extremely poor resolution and permit no structural assignments. However, the structures of the transannular addition product of sulfur dichloride to both X and XI, which were shown to be XIV and XV,¹⁰ were considered to be closely related systems and were chosen for studying transannular reactions.

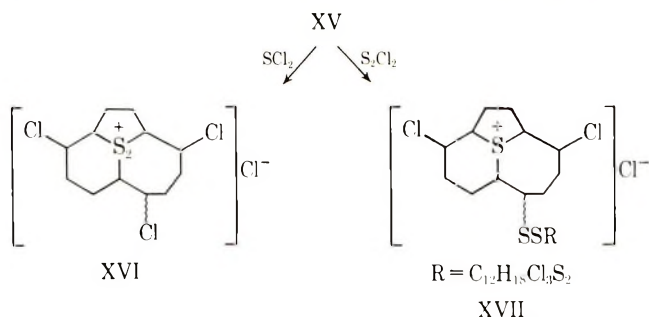
We have observed that transannular reactions proceed readily. The addition of chlorine to XIV and XV leads to nonidentical sulfonium salts,



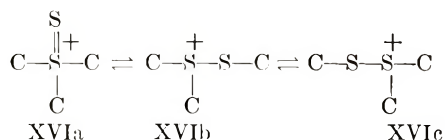
for which structures XIVb and XVb are assigned. The nonidentity of XIVb and XVb is evident from nuclear magnetic resonance and infrared spectra, as well as differences in their thermal stability. The saltlike character is evident from their solubility in water and insolubility in aprotic solvents. It is suggested that the formation of XIVb and XVb proceeds

via the sulfonium intermediates XIVa and XVa. Although these structures could be defined on the basis of an assumption that a direct transannular reaction occurs, rearrangement of the carbon-sulfur skeleton in that tricyclic structure is conceivable. Such a rearrangement could proceed via an equilibrium between sulfonium salt and the tetrachlorosulfides XIVc and XVc or XIVd and XVd.

It was observed that transannular addition was not restricted to the addition of chlorine. In a surprising novel reaction, addition of sulfur dichloride to XV leads to an intramolecular 1:1 addition product in a yield of 75%. Nuclear magnetic resonance and infrared spectra indicate the absence of olefinic unsaturation, and the insolubility of the product in aprotic solvents again suggests the formation of a sulfonium salt. Structure XVI is assigned for that product, which would represent a sulfonium



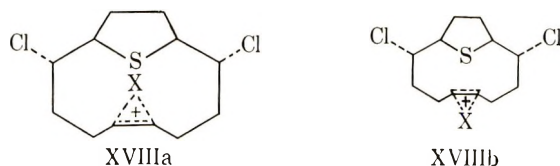
ion where the positive charge is located on a disulfide linkage. It is of interest to speculate on the nature of the sulfur-sulfur bond, which could be represented by the tautomeric structures XVIa-XVIc. Tautomerism between XVIIb and XVIc would provide a mechanism for the rearrangement of



the tricyclic structure into a thermodynamically more preferred ring structure. Such a rearrangement could also proceed via the nonionic tetrachlorides analogous to the monosulfide XVd.

In contrast to the formation of an intramolecular 1:1 addition product from sulfur dichloride and XV, addition of sulfur monochloride to XV leads to a 1:2 intermolecular addition product in a yield of 86%. The infrared spectrum of this sulfonium salt indicates the absence of unsaturation and the structure XVII is postulated for that addition product.

In summary, the reaction of the bicyclic olefinic sulfide XV with chlorine, sulfur dichloride or sulfur monochloride may lead to intramolecular or intermolecular additions, depending on the nature of the electrophile.



It may be assumed, that addition of the electrophile proceeds to give the intermediate XVIIIa or XVIIIb, whereby the steric requirements of X determine whether insertion into the ring system by an endocyclic approach, XVIIIa, or by an exocyclic approach (XVIIIb) occurs. It appears as if the bicyclic ring system XV readily accommodates the $-\overset{+}{\text{S}}_2-$ group, but that $-\overset{+}{\text{S}}_3-$ is not incorporated into that ring system since a predominantly 2:1 addition of XV and I is observed.

It can therefore be concluded that polymers obtained from I and the cyclododecatrienes X and XI consist at least partially of structural units containing sulfonium salt structures. Crosslinking would proceed via addition of I to the remaining olefinic site in initial addition products. The possibility for the formation of polymer XIII with both mono- and disulfide linkages participating in the formation of sulfonium structures is conceivable on the basis of the synthesis of the model compound XVI. The reactivity of these polymeric systems deserve further attention, particularly with respect to the anticipated case of displacement of the chlorine atom in β -position to the sulfur atom.

EXPERIMENTAL

Satisfactory analyses were obtained from the addition products of I to the diolefins II-VII.

Aluminum amalgam was prepared according to the procedure of Vogel.¹¹ Sulfur monochloride was obtained from the Hooker Chemical Co. Both isomers of 1,5,9-cyclododecatriene were purified by fractional distillation.

The reaction of sulfur monochloride with exo-dicyclopentadiene(II), cyclohexadiene-1,4(III), cyclooctadiene-1,5(IV), vinylcyclohexene-4(V), hexadiene-1,5(VI), and octadiene-1,7 (VII) were carried out by gradual addition of sulfur monochloride to equimolar amounts of the diolefin in the absence of solvent between 25°C and 60°C. Highly viscous to semisolid products are obtained. In case of the olefins IV-VII, cyclic or bicyclic chlorosulfides, corresponding to the sulfur dichloride addition product to these diolefins, could be isolated.

Reduction of Sulfur Monochloride Addition Product of VI and VII with Aluminum Amalgam

To solutions of the polymers obtained from sulfur monochloride and diolefin in tetrahydrofuran was added aluminum amalgam in the amount of

100 g for that amount of addition product which was obtained from 135 g (1 mole) of sulfur monochloride and 1 mole of diolefin. Water (100 ml) was added over a period of 1 hr with rapid mechanical stirring. After completion of that addition, the slurry was vacuum filtered, the residue washed with tetrahydrofuran and the combined filtrates were partially evaporated on a rotary evaporator. After dilution with three times its volume of diethyl ether, the organic layer was washed repeatedly with water, dried with magnesium sulfate and distilled to give the diepisulfides VIII and IX, respectively, in yields from 8 to 15%.

The diepisulfide VIII is characterized by its bp 116°C/16 mm; $n_D^{20} = 1.5420$.

ANAL. Calcd for $C_8H_{10}S_2$: C, 49.32%; H, 6.85%; S, 43.85%. Found: C, 49.59%; H, 6.89%; S, 43.80%.

The diepisulfide of octadiene-1,7 (9) is characterized by its bp 74°C/0.3 mm Hg and mp 41.5–43°C after recrystallization at –20°C from pentane and subsequent sublimation.

ANAL. Calcd for $C_8H_{14}S_2$: C, 55.17%; H, 8.05%; S, 36.78%. Found: C, 55.26%; H, 8.03%; S, 36.80%.

The products are further identified by their desulfurization with triphenylphosphine to the corresponding diolefins in carbon disulfide and their infrared absorption spectra by comparison with authentic samples.

Reaction of Sulfur Monochloride with *trans,trans,cis*-Cyclododecatriene-1,5,9 to Give XII and XIII

To a solution of 35.64 g (0.22 mole) of cyclododecatriene X in 150 ml of hexane was added 27 g (0.2 mole) of sulfur monochloride over a period of 24 hr. A white precipitate formed during that period. A negative test with potassium iodide was obtained after stirring the suspension for another 12 hr at ambient temperature. After filtration and washing the product with hot hexane, 59 g (99%) of crude product was obtained.

ANAL. Calcd for $C_{12}H_{18}Cl_2S_2$: C, 48.62%; H, 6.09%; Cl, 23.87%; S, 21.56%. Found: C, 48.41%; H, 6.25%; Cl, 23.70%; S, 21.70%.

The product is insoluble in carbon tetrachloride, chlorobenzene, ethyl acetate but soluble in hot nitromethane. The infrared spectrum shows generally poor resolution but major absorption peaks in the region of 2000–650 cm^{-1} are observed at 1440, 1220 (wide), 980, and 773 cm^{-1} .

To a solution of 3.245 g (0.02 mole) of cyclododecatriene-1,5,9 (*trans,trans,cis*) in 50 ml of methylene chloride was added 2.700 g (0.02 mole) of freshly distilled sulfur monochloride in 50 ml of methylene chloride. The solution was stirred at 30°C for 8 hr, after which a negative test with potassium iodide was obtained. The clear solution was decanted from 0.72 g (12%) of a polymeric product, A, which was deposited on the wall of the

reaction vessel. On dilution with 100 ml of anhydrous diethyl ether, 2.233 g (37%) of material, B, was filtered off. On standing of the solution for 64 hr only traces of insoluble product separated. Evaporation of the solution on a rotary evaporator gave 3.0 g (51%) of resinous material, C, which was soluble in chloroform and benzene.

ANAL. Calcd for $C_{12}H_{18}Cl_2S_2$: C, 48.62%; H, 6.09%; Cl, 23.87%; S, 21.56%. Found: (A) C, 40.43%; H, 5.55%; Cl, 32.43%; S, 19.44%. (B) C, 45.15%; H, 6.17%; Cl, 25.48%; S, 21.26%. (C) C, 52.14%; H, 6.93%; Cl, 20.56%; S, 20.98%.

The infrared spectrum of A is poorly resolved, it shows major absorption bands (KBr) at 3410, 2920, 1615, and 1440 cm^{-1} but only very weak indication for the presence of *trans* unsaturation at 980 cm^{-1} . The spectrum of B shows increased absorption for *trans* unsaturation, whereas product C shows both *trans* and *cis* unsaturation at 980 and 710 cm^{-1} , respectively.

The reaction of sulfur monochloride with *trans,trans,trans*-cyclododecatriene-1,5,9 (XI) was carried out in methylene chloride as solvent as described for its isomer X. Three fractions which were distinguished by their solubilities show the following elemental analyses.

ANAL. Calcd for $C_{12}H_{18}Cl_2S_2$: C, 48.62%; H, 6.09%; Cl, 23.87%; S, 21.56%. Found: A, 0.7 g (11% yield): C, 50.19%; H, 5.50%; Cl, 33.60%; S, 18.86%. B, 1.75 g (29% yield): C, 43.39%; H, 5.54%; Cl, 26.55%; S, 20.48%. C, 3.56 g (60% yield): C, 48.92%; H, 6.53%; Cl, 18.02%; S, 20.72%.

Formation of Cyclic β,β' -Dichlorosulfides

From the reactions of the diolefins IV, V, VI, and VII with sulfur monochloride up to 15% of the products were found to be cyclic sulfides identical with the sulfur dichloride addition products of these diolefins.

Reaction of Chlorine with XV

To a solution of 6.0 g (0.023 mole) of XV in 100 ml of methylene chloride was added chlorine at $-20^\circ C$ with stirring until a positive test with potassium iodide was obtained. The crystalline precipitate was suction filtered and air-dried to give 7.28 g (96%) of XVb, mp $170.5-171^\circ C$ (dec). The product is soluble in water and methanol, but insoluble in carbon tetrachloride, acetonitrile, and dimethylformamide. Recrystallization from water provided an analytical sample.

ANAL. Calcd for $C_{12}H_{16}Cl_2S$: C, 42.19%; H, 5.39%; S, 9.53%; Cl, 42.17%. Found: C, 42.41%; H, 5.44%; S, 9.56%; Cl, 42.69%.

The infrared spectrum of XVb shows the following absorption bands which are not observed in the isomeric structure XIVb: 1372, 1295, 1284, 1237, 1222, 1195, 1146, 1046, 1009, and 734 cm^{-1} .

The sulfonium salt can be recovered unchanged from a solution in acetic acid/dioxane (1:3) as evidenced by the infrared spectrum of the recovered sample.

Reaction of Chlorine with XIV

Under conditions identical as described in the formation of XVb, the product XIVb was obtained in a yield of 79%, mp 227–235°C (dec). Recrystallization from water (40°C) left the product unaffected.

ANAL. Calcd for $C_{12}H_{18}Cl_2S$: C, 42.19%; H, 5.39%; S, 9.53%; Cl, 42.17%. Found: C, 42.20%; H, 5.24%; S, 9.38%; Cl, 42.69%.

The nonidentity of XIVb and XVb is shown by the infrared spectrum of XIVb, which shows the following absorption peaks (potassium bromide pellet) which are not observed in XVb: 1180, 1027, 876, 745, 625, 579, 453, 399 cm^{-1} .

Reaction of 2,9-Dichloro-13-thiabicyclo[8.2.1]-5-tridecene (*trans*) (XV) with Sulfur Dichloride to Give XVI

Into a solution of 5.3 g (0.02 mole) of XV in 100 ml of methylene chloride was added 2.06 g (0.02 mole) of sulfur dichloride at an internal temperature of $-20^{\circ}C$. Discoloration of the solution was complete after 30 min, when a negative test with potassium iodide was obtained. The precipitated product was filtered off and washed with methylene chloride to give 5.5 g (75%) of XVI, mp 80–120°C (dec).

ANAL. Calcd for $C_{12}H_{18}Cl_2S_2$: C, 39.14%; H, 4.93%. Found: C, 39.79%; H, 5.43%.

The product is infinitely soluble in methanol, partially soluble in cold acetic acid and water, but insoluble in common aprotic organic solvents. The infrared spectrum (KBr pellet) shows major absorption bands at 1289 and 1206 cm^{-1} which are not present in the sulfonium salt XVb. Furthermore, absorption bands in XVI at 1295, 1284, 1211, 916, 908, 906, and 783 are not observed in XVb. The infrared spectrum in Nujol is essentially identical with that in potassium bromide.

A nuclear magnetic resonance spectrum of a solution of XVIb in deuterated methanol (prepared and recorded at $-30^{\circ}C$) shows a wide peak for CH_2 -protons at 2.0 ppm and an unresolved wide peak for the remaining CHX-protons between 3.5 and 5.0 ppm. If this solution is prepared and recorded at $-70^{\circ}C$, only further widening of these bands is observed. A solution of XVI in deuterated water, prepared and recorded at $5^{\circ}C$, shows essentially the same spectrum as in deuterated methanol.

Reaction of 2,9-Dichloro-1,3-thiabicyclo[8.2.1]-5-tridecene (*trans*) with Sulfur Monochloride to Give XVII

Into a solution of 5.3 g (0.02 mole) of XV in 50 ml of methylene chloride was added 2.7 g (0.02 mole) of freshly distilled sulfur monochloride dropwise with stirring at an internal temperature of $-20^{\circ}C$. Immediate precipitation occurred but a positive test for sulfur chloride was obtained with potassium iodide. The addition of another 5.3 g (0.02 mole) of XVI was

required to completely consume all sulfenyl halide. Filtration and washing of the colorless powder with methylene chloride gave 11.7 g (86.7%) of product, mp 146–149°C (dec). Further purification of this sample could not be achieved and the presence of XVI must be assumed as the result of the decomposition of sulfur monochloride in sulfur dichloride and dichloro-trisulfane.

ANAL. Calcd for $C_{23}H_{36}Cl_6S_4$: C, 43.31%; H, 5.45%; S, 19.27%; Cl, 31.96%. Found: C, 41.05%; H, 5.42%; S, 19.96%; Cl, 33.43%.

The infrared spectrum is characterized by strong absorption peaks at 684 and 1438 cm^{-1} .

The author is grateful to Mr. Derek Johnson for technical assistance, to the National Research Council of Canada for financial support and to Prof. J. K. Stille for supplying the low-temperature nuclear magnetic resonance spectra.

References

1. R. A. Meyers and E. R. Wilson, *J. Polym. Sci. B*, **6**, 587 (1968).
2. R. A. Meyers and E. R. Wilson, *J. Macromol. Sci. A*, **3**, 169 (1969).
3. F. Lautenschlaeger and N. V. Schwartz, *J. Org. Chem.*, **34**, 3991 (1969).
4. F. Lautenschlaeger, Can. Pat. 790,599 (1968).
5. R. C. Fison, D. M. Burness, R. E. Foster, and R. D. Lipscomb, *J. Org. Chem.*, **11**, 499 (1946).
6. R. C. Fison, C. C. Price, and D. M. Burness, *J. Org. Chem.*, **11**, 475 (1946).
7. I. L. Knunyants and A. V. Fokin, *Bull. Acad. Sci. U.S.S.R. Div. Chem. Sci.*, **4**, 627 (1955).
8. H. J. Backer and J. Strating, *Rec. Trav. Chim.*, **54**, 52 (1935).
9. W. H. Mueller, *J. Amer. Chem. Soc.*, **91**, 1223 (1969).
10. F. Lautenschlaeger, *J. Org. Chem.*, **3**, 2627 (1968).
11. A. I. Vogel, *Practical Organic Chemistry*, Longmans, Green, London, 1957.

Received June 24, 1970

Revised September 3, 1970

Sequence Distribution of Poly(ether)urethane Elastomer

HAJIME SUZUKI, *Katata Research Institute, Toyobo Company Ltd.,
Otsu, Shiga, Japan*

Synopsis

Poly(ether)urethane elastomers (PEUE) having different sequence distributions can be synthesized by the reaction of *p*-phenylene diisocyanate, poly(oxytetramethylene glycol), and hydrazine by four different routes. The degree of the sequence distribution of PEUE was determined by high-resolution NMR spectroscopy. The sequence distribution of PEUE synthesized by the prepolymer method in solvent (method 1) was found to coincide with the sequence distribution calculated from the reactivity ratio of two isocyanate groups in *p*-phenylene diisocyanate. On the other hand, the sequence distribution of PEUE obtained by the prepolymer method without solvent (method 2) was found to deviate from that expected from the reactivity ratio. The degree of the distribution of monomers in PEUE having the same composition ratio corresponded to the infrared absorbance ratio at 1720 and 1700 cm^{-1} .

INTRODUCTION

Poly(ether)urethane elastomers (PEUE) prepared from *p*-phenylene diisocyanate (PDI), poly(oxytetramethylene glycol) (PTG), and hydrazine (HD) can be obtained by many methods. PEUE having the same or different composition ratio and different degree of sequence distribution were synthesized by four different methods. The determination of the sequence distribution of PEUE by NMR has been described in a preliminary report.¹ The present paper is a detailed report of the sequence distribution of PEUE prepared by the following four methods.

Method 1 is a prepolymer method or two-step polymerization method. In this method PTG was treated with PDI in solvent in order to prepare a prepolymer with terminal isocyanate groups. The prepolymer thus obtained was then dissolved in dimethylacetamide (DMAC) and extended to PEUE by the reaction with a molar equivalent of HD.

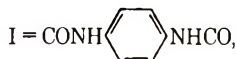
In method 2, PTG was treated with PDI without solvent in order to prepare the prepolymer with terminal isocyanate groups, and after the prepolymer reaction PEUE was obtained by the same method as method 1.

Method 3 is a so-called semipolymer or three-step polymerization method. In this method PTG was treated with PDI without solvent in order to prepare semipolymer with terminal hydroxyl groups. This semipolymer was then treated with PDI without solvent or in solvents in order to

prepare the prepolymer with terminal isocyanate groups, and the prepolymer with terminal isocyanate groups was extended to PEUE by the reaction with a molar equivalent of HD.

In method 4, PTG was treated with PDI without solvent in order to prepare prepolymer with terminal isocyanate groups. After the prepolymer reaction, PDI was added to the prepolymer with terminal isocyanate groups, and the mixture of the prepolymer and PDI was extended to PEUE by the reaction with a molar equivalent amount of HD.

The structures of the PEUE obtained by the above methods can be expressed by the following equation:



In the above formula $-(I-E)_n$ is the so-called "soft" segment or poly(ether)-urethane segment, and $-(I-A)_m$ is the so-called "hard" segment or urea segment. The number-average sequence lengths of the $-(I-E)_n$ unit ($n = L_{nIE}$) and the $-(I-A)_m$ unit ($m = L_{nIA}$) are given by eqs. (2) and (3):

$$\overline{L_{nIE}} = \frac{(P_{E-I-A}/2) + P_{E-I-E}}{(P_{E-I-A}/2)} \quad (2)$$

$$\overline{L_{nIA}} = \frac{(P_{E-I-A}/2) + P_{A-I-A}}{(P_{E-I-A}/2)} \quad (3)$$

where P_{E-I-E} , P_{A-I-A} , and P_{E-I-A} represent the proportion of the integrated intensities of E-I-E, A-I-A, and E-I-A signals, respectively, to the total intensities of the diisocyanate residues. These three kinds of PDI residues, E-I-E, A-I-A, and E-I-A, were identified at 7.42, 7.28 and 7.35 ppm as a benzene signal,¹ respectively, in DMAC containing 5% lithium chloride. Furthermore the degree of sequence distribution of PEUE may be defined by the above terms:²

$$B = (1/\overline{L_{nIE}}) + (1/\overline{L_{nIA}}) \quad (4)$$

If $B < 1$, these units tend to cluster in blocks of each unit, and finally $B = 0$ in a homopolymer mixture, whereas if $B > 1$, the sequence length becomes shorter, and $B = 2$ in an alternating copolymer.

For the PEUE polymers obtained in this experiment of a given composition,

$$\frac{m}{n} = \frac{\overline{L_{nIA}}}{\overline{L_{nIE}}} = \text{constant} \quad (5)$$

and consequently as L_{nIE} increases, L_{nIA} must increase to satisfy the above expression. In other words, while m/n remains constant, the repeating sequences of I-E units and I-A units in the chain of PEUE are each becoming longer.

EXPERIMENTAL

Reagents

Benzene, toluene, cyclohexane and DMAC were purified by the usual method. PDI was purified by sublimation. Commercial PTG with an average molecular weight of 807 was used without further purification.

Polymers

Methods 1 and 2. In method 1 the prepolymer was prepared by reacting 0.02 mole of PTG with 0.04 mole of PDI in 100 ml of solvent at 30°C for 3 hr. The completeness of the prepolymer reaction was ascertained by the *n*-dibutylamine titration method reported by Stagg.³ The PEUE polymers were prepared from the prepolymers and 0.02 mole of HD as a chain extender.

In the case of method 2 the prepolymer was prepared by reacting PTG with PDI without solvent at 75°C for 3 hr. The molar ratios of the monomers and other procedure were the same as in method 1 after the prepolymer reaction.

Method 3. Semipolymer with terminal hydroxy groups was prepared by reacting PTG with PDI without solvent at 75°C for 1.5 hr. The various molar ratios of PTG and PDI are listed in Table I. The prepolymer was prepared by reacting the semipolymer and 1 mole of PDI without solvent. The prepolymer with terminal isocyanate groups was reacted with 0.5 mole of HD as a chain extender in DMAC.

Method 4. In this method PEUE polymers having the same composition ratio and different degree of sequence distribution were synthesized by the following procedure. The prepolymers were prepared by

TABLE I
Molar Ratios of Semipolymers

No.	PTG, mole	PDI, mole
1	1.5	1.0
2	1.3	0.8
3	1.1	0.6
4	1.0	0.5

TABLE II
Preparation of PEUE

No.	PDI, mole	
	Prepolymer	After the prepolymer
1	0.040	0.000
2	0.035	0.005
3	0.030	0.010
4	0.025	0.015

reacting 0.020 mole of PTG and PDI (0.040–0.025 mole as seen in Table II) without solvent at 75°C for 2 hr. After the prepolymer reaction, PDI (0.00–0.015 mole as seen in Table II) was added to the prepolymer, and the mixtures of the prepolymer and PDI were reacted with 0.020 mole of HD as a chain extender in DMAC at 7°C for 1 hr.

Measurement of NMR Spectra

NMR spectra were obtained with a Varian A-60 Spectrometer operating at 60 McPs. The solutions containing 15% (w/v) PEUE and tetramethylsilane as an internal reference in DMAC containing 5% lithium chloride were run at 70°C.

Measurement of Infrared Spectra

Infrared spectra of PEUE were obtained with a Hitachi EPI-S2 type infrared spectrophotometer and with the use of thin films cast on a glass plate from the DMAC solution. The samples were heat-treated at 100°C for 10 min for evaporation of solvent.

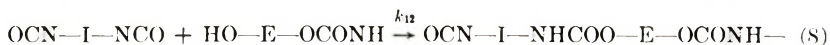
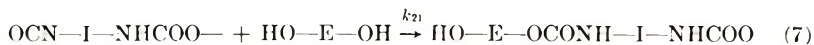
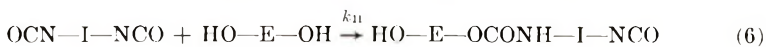
RESULTS AND DISCUSSION

As shown in the experimental section, PEUE can be synthesized by four different methods.

Method 1 and Method 2

In these methods the distribution of monomers in PEUE may be decided by the apparent reactivity ratio of the two isocyanate groups in PDI.

In the prepolymerization, the following reaction scheme may hold:



where OCN-I-NCO and HO-E-OH denote PDI and PTG, respectively, and where k denotes a rate constant. Assuming that $k_{11} = k_{12} = k_1$ and that $k_{21} = k_{22} = k_2$, the reactivity ratio of the two isocyanate groups in PDI is given by:

$$A = k_2/k_1$$

Thus, the rate of the reaction may be expressed by eqs. (10)–(12):

$$d[\text{I}_1]/dt = -2k_1[\text{I}_1][\text{E}] \quad (10)$$

$$d[\text{I}_2]/dt = k_1[\text{I}_1][\text{E}] - k_2[\text{I}_2][\text{E}] \quad (11)$$

$$d[\text{E}]/dt = -k_1[\text{I}_1][\text{E}] - k_2[\text{I}_2][\text{E}] \quad (12)$$

where $[I_1]$, $[I_2]$, and $[E]$ are the concentrations of isocyanate group in PDI and in OCN-I-NHCOO- and PTG, respectively. From eqs. (10) and (11),

$$d[I_2]/d[I_1] = (k_2/2k_1)([I_2]/[I_1]) - 1/2 \quad (13)$$

In the case of $A \neq 2$, the integration of eq. (13) from time 0 to T , which is the time for prepolymer reaction, gives the following result:⁴

$$\frac{2}{(2-A)} \log \left\{ 1 - \left(1 - \frac{A}{2} \right) \frac{P_{A-I-E}}{P_{A-I-A}} \right\} = \log \left(\frac{1}{P_{A-I-A}} \right) \quad (14)$$

Similarly, for $A = 2$:

$$\frac{P_{A-I-E}}{P_{A-I-A}} = \ln \frac{1}{P_{A-I-A}} \quad (15)$$

The intensities of the three kinds of linkages or sequences (A-I-A, A-I-E, and E-I-E) were measured by NMR. The measured results of molar fractions of three structural units of PEUE obtained by method 1 and 2 are listed in Table III. By inserting the values of P_{A-I-A} and P_{A-I-E} into eq. (14), the reactivity ratio A can be calculated. The results are shown in Table III. The degree of block character B is listed in the last column. Bailey et al.⁵ reported that the reactivity ratio of PDI was about 0.28. This result is nearly equal to the results of method 1. Therefore the sequence distribution of PEUE synthesized by method 1 can be assumed from the reactivity ratio ($A = k_2/k_1$) of the two isocyanate groups. The sequence length of the hard segment of PEUE synthesized by method 2 was longer than that assumed by the reactivity ratio. The difference between methods 1 and 2 may be due to the difference in extent of homogeneous and heterogeneous reaction in the prepolymer reaction. When there is solvent in the prepolymer reaction, the reaction may be a homogeneous reaction. When there is no solvent in the prepolymer reaction, the reaction between PTG and PDI occurs through the solvation of PDI into PTG. Therefore the reaction rate of PDI with PTG may be affected by viscosity and agitation. The greater block character of sample 5 (method 2) in comparison with samples 1-4 (method 1) may be due to the heterogeneous reaction.

TABLE III
Molar Fraction of Three Structural Units, Block Character, and
Reactivity Ratio of PEUE Synthesized by Methods 1 and 2

No.	Solvent in prepolymer reaction	P_{A-I-A}	P_{E-I-E}	P_{A-I-E}	A	B
1	Toluene	0.155	0.155	0.690	0.339	1.38
2	Benzene	0.160	0.160	0.680	0.359	1.36
3	DMAC	0.163	0.163	0.674	0.376	1.35
4	Cyclohexane	0.174	0.174	0.652	0.435	1.30
5	None (method 2)	0.197	0.197	0.606	0.562	1.21

Method 3

Table IV shows the sequence distributions of PEUE samples obtained by method 3. In this method PEUE with the almost equal sequence lengths of hard segment and different sequence lengths of soft segment could be obtained.

TABLE IV
Molar Fraction of Three Structural Units, Block Character, and
Sequence Lengths of Soft Segments and Hard Segments

No.	[urethane]/ [urea]	P_{A-1-A}	P_{E-1-E}	P_{A-1-E}	B	$\overline{L_{n1A}}$	$\overline{L_{n1E}}$
1	3/1	0.086	0.586	0.328	0.87	1.52	4.57
2	2.6/1	0.086	0.531	0.383	0.95	1.45	3.77
3	2.2/1	0.087	0.462	0.451	1.05	1.39	3.05
4	2/1	0.089	0.422	0.489	1.10	1.36	2.73

Method 4

PEUEs, which had the same composition ratio but a different degree of block character, were synthesized by this method. Table V shows the results. Although the PEUE samples in Table V have the same composi-

TABLE V
Molar Fraction of Three Structural Units, Block Character, and
Sequence Lengths of Soft Segments and Hard Segments

No.	P_{A-1-A}	P_{E-1-E}	P_{A-1-E}	B	$\overline{L_{n1A}}$	$\overline{L_{n1E}}$
1	0.197	0.197	0.606	1.21	1.65	1.65
2	0.256	0.256	0.489	0.98	2.04	2.04
3	0.329	0.329	0.342	0.68	2.92	2.92
4	0.387	0.387	0.225	0.45	4.44	4.44

tion ratio, the sequence lengths of soft and hard segments are different. The sequence length of hard segment corresponds to the amount of PDI used between the prepolymer reaction and the chain extender reaction in Table II, therefore a sample 4 had the longest sequence length of hard segment in Table V. The ratio of PTG and HD in Table V is unity, therefore the sequence length of hard segment was the same as that of soft segment.

Figure 1 shows the relationship between the absorbance ratio at 1720 and 1700 cm^{-1} and the block character parameter B . From Figure 1, it is evident there is a relation between the block character and the absorbance ratio at 1720 and 1700 cm^{-1} . Therefore these peaks are assumed to be assignable to the urethane linkage for two different states, such as the paracrystalline part⁶ of a hard segment and a liquidlike state of a soft segment. The absorbance at 1720 cm^{-1} is assumed to be assigned to the C=O stretching vibration of the urethane linkage (E-I-E) in a soft segment and the

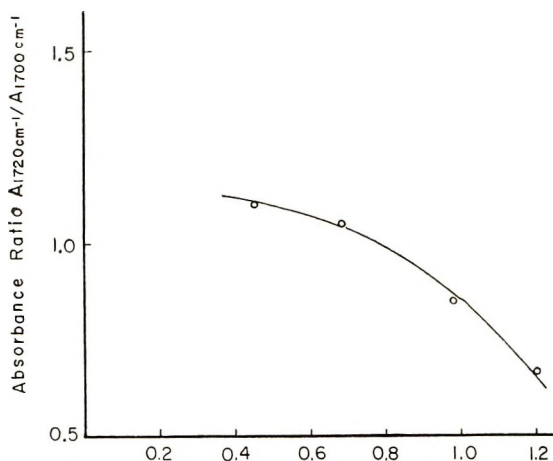


Fig. 1. Relation between the absorbance ratio at 1720 and 1700 cm^{-1} and the degree of block character.

1700 cm^{-1} absorbance may be assigned to the C=O stretching vibration of the urethane linkage (E-I-H) at the end of the hard segment with a hydrogen bond for the paracrystalline state.⁶

These studies will be very useful for the elucidation of the relationship between the structure and the physical properties of the elastomers. Some of these relationships have been reported in another paper.⁷

References

1. H. Suzuki, *J. Polym. Sci. B*, **8**, 767 (1970).
2. H. Suzuki and H. Ono, *Bull. Chem. Soc. Japan*, **43**, 687 (1970).
3. H. E. Stagg, *Analyst*, **71**, 557 (1946).
4. H. Suzuki and H. Ono, *Bull. Chem. Soc. Japan*, **43**, 682 (1970).
5. M. E. Bailey, V. Kriss, and R. G. Spaunburgh, *Ind. Eng. Chem.*, **48**, 794 (1956).
6. R. Bonart, *J. Macromol. Sci.-Phys.*, **B2**, 115 (1968).
7. I. Kimura, H. Suzuki, K. Saito, K. Watanabe, and H. Ono, *Kogyo Kagaku Zasshi*, **73**, 1541 (1970).

Received April 9, 1970

Some Studies on a Polymer from Urea

PRANAB C. BANDYOPADHYAY and ASOKE K. DAS,
*Department of Chemistry, Indian Institute of Technology,
Kharagpur, West Bengal, India*

Synopsis

A polymer having the structure of guanidinopolyhydroxynitrile has been produced by heating an equimolar mixture of urea and anhydrous $ZnCl_2$ in nitrogen at $300^\circ C$ and 27 atm. The structure has been established from elemental analysis, percentage of nitrogen as primary amine, and ultraviolet and infrared spectra of the polymer and its derivatives. A mechanism of the polymerization based on some experimental evidence has been suggested. Its physical properties have been attributed to its skeletal structure and ring closure by hydrogen bonding. Thermograms reveal that it is stable to $150^\circ C$, after which it decomposes slowly till a 75% weight residue is obtained at $575^\circ C$ with a constant weight plateau extended to $680^\circ C$. In acid solvents, protonation occurs at the $-NH_2$ group or the azomethine nitrogen atoms, producing polycations. The polyelectrolytic character in acids has been confirmed by viscometric and osmotic studies and the molecules tend to be both coiled up and associated in solutions. $[\eta]$ in anhydrous formic acid is 0.3636 dl/g. The molecular weights of the polymer and its various fractions range between 39,500 and 25,900. Dielectric constants, dielectric losses, and conductivities of the polymer have also been measured as functions of frequency and temperature and it has been proved that the dispersion is due to dipole polarization. The average energy of the dipole is 1.73×10^{-2} eV/ $^\circ K$, the intrinsic activation energy for conduction is 0.186 eV, the conductivities being of the order of 2×10^{-6} to 7×10^{-7} mho-cm $^{-1}$. The polymer is therefore a semiconductor. The number of charge carriers is 2.12×10^{16} /cm 3 , which agrees reasonably well with the value, 6.66×10^{16} , obtained from spin-density calculations from ESR signals.

INTRODUCTION

Synthesis of some linear polymers consisting of recurring conjugated azomethine ($-C=N-$) bonds has recently been reported.¹⁻³ Polymeric systems containing conjugated double bonds behave usually as semiconductors and are also quite thermoresistant. As only a very small amount of information is so far available regarding the physicochemical properties of these new materials, preparation of a related polymer under higher pressures has been attempted, and a systematic study of the physicochemical properties of the substance has been carried out to characterize it. The present paper reports the results of these investigations.

EXPERIMENTAL

Preparation and Fractionation of the Polymer

Urea (C.P. grade) was finely powdered, dried at 40–45°C under vacuum (30 mm Hg) and mixed intimately with an equimolar quantity of pure anhydrous zinc chloride (dried at 180°C for 5–6 hr under vacuum). The mixture was then heated for 3–6 hr in a high-pressure stainless steel reactor at 300–450°C in an atmosphere of nitrogen under 11–42 atm. The solid product, along with much ammonia gas, was taken out, washed with 25% NH_4OH and then water to remove all soluble matter, and dissolved in an excess of warm 85% formic acid. The product was reprecipitated by adding water, centrifuged, dialyzed against water, and dried at 40–45°C under vacuum to a constant weight. It was found free from zinc by the usual tests.

The color of the substance varies from cream to light brown, depending on the temperature, pressure, and the duration of heating at the time of its formation. It neither melts nor softens and is insoluble in all common organic solvents, but dissolves partly in an excess of warm, concentrated acids. Although the material does not swell in water even on standing, it may be separated from the acid solution on gradual dilution with water or ammonium hydroxide as a highly swollen, gellike mass with an enormous rise in the viscosity of the solution. Fractionation of the polymer into a number of fractions is thus possible.

A 2.0-g portion of the polymer (A) (produced at 300°C and 27 atm from an equimolar mixture of urea and anhydrous zinc chloride by heating for 6 hr) was dissolved in 100 ml of warm 98–100% formic acid, filtered from a small amount of residue, and cooled; 4*N* NH_4OH was added portionwise with centrifugation and frequent shaking to yield a precipitate each time. All fractions obtained were washed with water, dried, and stored in vacuum.

Preparation of Derivatives of A

Methylation (Quaternization). To a suspension of 1.0 g of A in 10 ml of dimethylformamide, heating to 90°C, was added dropwise over a period of 20 min 5 g of dimethyl sulfate with constant stirring. The temperature rose to 140–145°C. Refluxing and stirring were continued at 145°C for an additional 100 min. The resulting clear solution was cooled and poured into 20 ml of methanol. Addition of concentrated NH_4OH till the pH of the solution rose to 8 yielded heavy yellow-colored solid. This solid (B), suspected to be the methylated product, was filtered, washed several times with hot methanol and dried at 50°C under vacuum for 6 hr. The yield was 0.8 g.

Acetylation. A mixture of 0.5 g of A, 25 ml of acetic anhydride, and 5 drops of concentrated H_2SO_4 was refluxed for 5 min. The brown solution was cooled and neutralized with solid Na_2CO_3 when a dark brown solid separated. The acetylated derivative (C) was washed with water to remove traces of sulfates and dried. The yield was 0.10 g.

Estimation of Nitrogen Present as $-\text{NH}_2$ in A. The normal microchemical methods of estimating nitrogen including the one applied by Bircumshaw, Taylor and Whiffen⁴ for analysis of paracyanogen proved unsatisfactory for all three compounds A, B, and C. The percentage of nitrogen only in A, present as $-\text{NH}_2$, was determined by the method and apparatus described by Pregl.⁵ The polymer A was diazotized in 50% acetic acid and in 4*N* HCl and the diazo compound formed was subsequently decomposed by heating to give off nitrogen, which was measured over alkaline potassium permanganate solution in a microaudiometer.

Viscosity Measurements

All viscosity measurements were done on the unfractionated polymer A at $35 \pm 0.01^\circ\text{C}$ by use of two Ostwald capillary viscometers, one having flow times of 173.2 and 259.2 sec for water and anhydrous formic acid, respectively, and the other having flow times of 84.35 and 126.2 sec for water and 84.2% formic acid, respectively. The difference in the pycnometric densities at 35°C between the solution and the solvent, though slight in the concentration range chosen for study (0.06–0.95 g/100 ml), was not ignored, but kinetic energy correction, which was small for such flow time, was not done. Solvents used were anhydrous formic acid, 84.2% formic acid, and 0.164*M*, 0.224*M*, and 0.589*M* sodium formate solutions in anhydrous formic acid.

Anhydrous formic acid (bp 100.5°C and mp 8.2°C) was prepared from crystallizable A.R. 98–100% formic acid by repeated distillation over phthalic anhydride at $34\text{--}35^\circ\text{C}/60$ mm Hg. Titration with a standard base showed that the distillate contained 99.98% formic acid. The sodium formate was of reagent grade. Concentration of the polymer, in the most concentrated solution in each series of the solvents, was determined from the difference between the constant weight of the residue, after evaporating a known volume of the solution and that from the solvent. Other solutions were prepared by dilution with the corresponding solvent so that the polymer concentrations in them could be directly known.

Osmometry

Osmotic pressures of dilute solutions of the untreated polymer A as well as its different fractions were measured at $35 \pm 0.01^\circ\text{C}$ by a Zimm-Meyer-son osmometer with the use of Ultracella Filter membranes (obtained by courtesy of M/s Sartorius Membranfilter, Gottingen, West Germany) after proper conditioning. Solvents used were 4*N* formic acid and various sodium formate solutions ($3.912 \times 10^{-2}M$, $4.809 \times 10^{-2}M$, $6.792 \times 10^{-2}M$, $2.573 \times 10^{-1}M$, and $3.518 \times 10^{-1}M$) in 4*N* formic acid. The blocks, packing nuts, and the screws of the osmometer were made of stainless steel. Blank experiments were performed to ensure that the material of the osmometer was resistant to acids. Polymer concentrations in the solutions and their densities were determined as described in the viscosity section.

Thermogravimetry

Thermogravimetric analysis of A was done as usual in nitrogen and in air. Temperature was increased at a constant rate of 12.5°C/min.

Dielectric Measurements

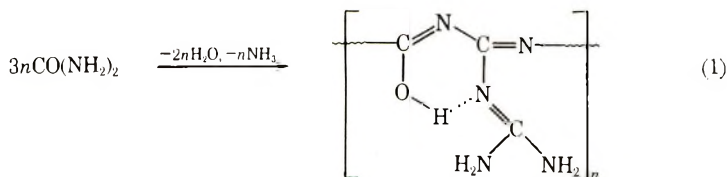
Dielectric constants, dielectric losses, and dielectric conductivities were measured as functions of frequency and temperature.

The substance A was finely powdered and compressed into a thin circular pellet (diameter 1.32 cm and thickness 0.303 cm) by means of an oil press. Colloidal silver paint was applied on both surfaces of the pellet to ensure good electrical contact with the condenser plates. The dielectric measurements on the pellet were then taken by a Marconi circuit magnification meter type, TF 329G in the frequency range 10^5 – 5×10^6 Hz at room temperature and for a definite frequency of 10^6 Hz at temperatures between 34 and 154°C by using the resonance curve principle.⁶ Measurements at temperatures higher than that of the room were done by placing the test pellet in a sample holder of known capacitance fitted with a heating coil and a thermocouple.

RESULTS AND DISCUSSION

Characterization of the Polymer

Table I shows the relative yields of the polymer A in weight per cent on the basis of the equation (1):

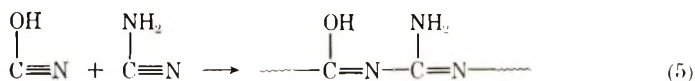
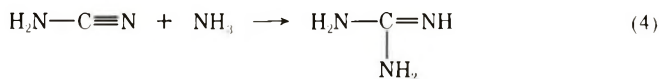
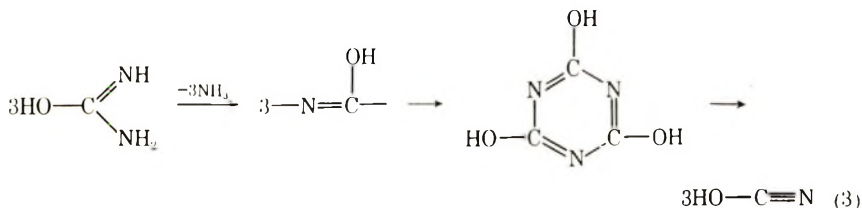
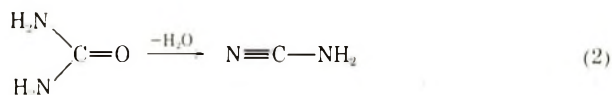


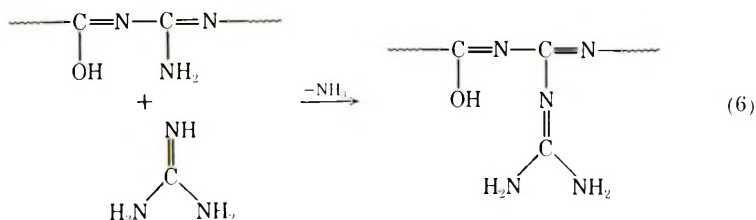
It is not possible to establish any optimum condition for maximum yield of the polymer from these data. It is, however, clear that as the reactor is heated until a desired constant temperature is reached, the extent of dissociation and of dehydration of urea, under the superincumbent pressure and the subsequent reactions between the simpler gaseous and solid products definitely increase, causing a gradual rise in the pressure of the system. The maximum pressure that develops within the reactor at the equilibrium temperature depends not only on the temperature and the initial nitrogen pressure at the time of setting, but also on the quantity of urea (at a constant urea: ZnCl_2 molar ratio). This pressure does not change further during the period of heating. A higher temperature and a greater pressure increase the yield, the effect of reaction time being maximum at 5 hr.

TABLE I
Effect of Temperature, Pressure, and Duration of Heating
on Yield at Urea: ZnCl₂ Molar Ratio of 1:1

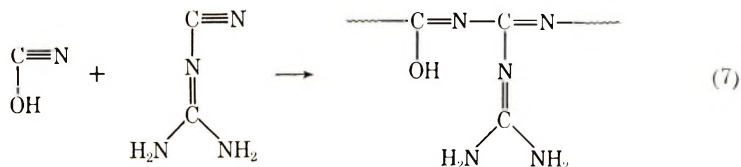
Temperature, °C	Duration, of heating, hr	Pressure, psi	Yield, wt-%
300	6	620	34.7
300	6	400	29.5
320	6	400	34.9
350	6	400	60.2
400	6	400	62.4
450	6	400	65.3
300	5	160	31.5
300	5	400	49.6
350	5	400	66.0
400	5	400	68.0
450	5	400	72.0
450	4	400	68.4
450	3	400	60.2

The mechanism shown in eqs. (2)–(6) may be suggested for the polymerization. Urea, on dry distillation in presence of anhydrous zinc chloride, yields ammonia and cyanuric acid, which subsequently decomposes into cyanic acid vapor. Urea is partly dehydrated to cyanamide. The cyanamide and cyanic acid then copolymerize in the presence of zinc chloride to give an addition polymer as an intermediate product. This ultimately undergoes a condensation reaction with guanidine produced from cyanic acid and ammonia to form the final polymer, which is a guanidino derivative of polyhydroxynitrile.



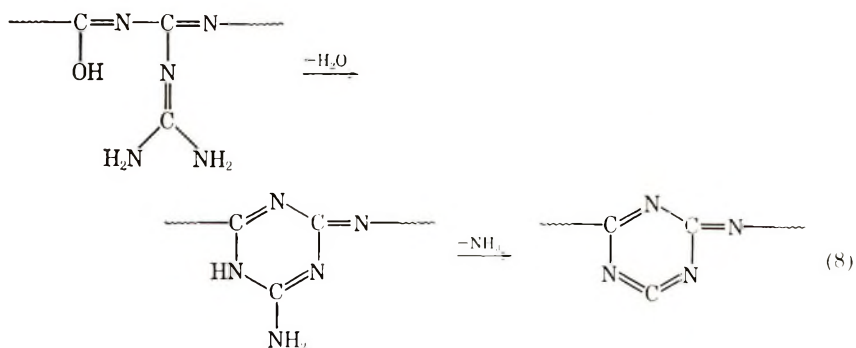


Alternatively, cyanamide may melt and dimerize to dicyanodiamide, which then copolymerizes with cyanic acid to give the polymer [eq. (7)].



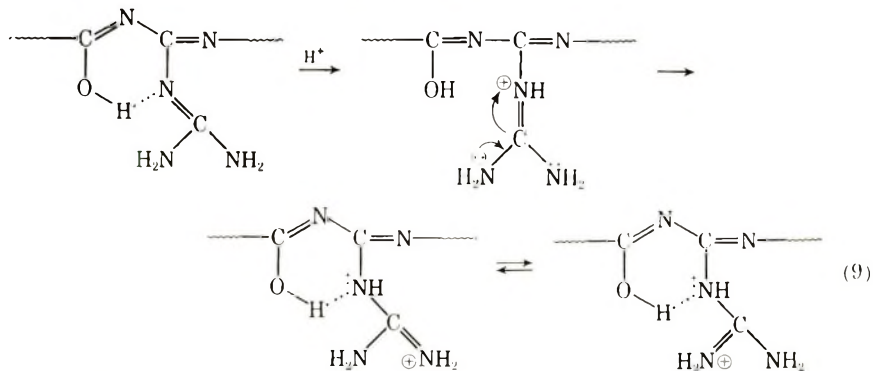
These mechanisms are supported by positive evidences that the same polymer could be effectively formed by heating mixtures of the stable intermediates in requisite proportions under identical conditions.

The thermogram of the polymer (Fig. 1) in nitrogen shows that it is stable up to about 150°C, after which it slowly decomposes till 75% weight residue is obtained at 575°C. It remains stable to 680°C, above which thermal degradation occurs comparatively fast. The thermogram in air is also similar in appearance except beyond 580°C, where there is no such constant residue plateau and it probably undergoes oxidative degradation rapidly. The 50% weight residue is obtained at 750°C. However, the thermograms corroborate the fact that the substance loses both water and ammonia perceptibly when heated above 200°C in air to form probably a more thermostable compound having ring-structured segments [eq. (8)].

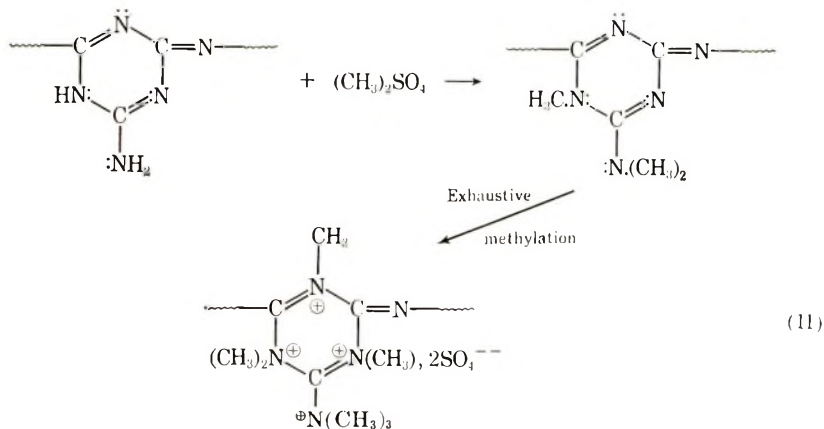
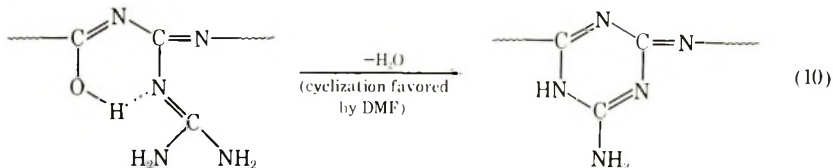


The resistance of the polymer to solvents and its infusibility may be attributed to the ---C=N--- skeleton and ring closure due to hydrogen bonding.

In acid media, protonation at the strongly basic guanidinium group to give a conjugate acid followed by attainment of a stabler structure due to resonance occurs according to the scheme of eq. (9).



Methylation of the polymer may proceed as in eqs. (10) and (11).



Acetylation occurs according to eq. (12)

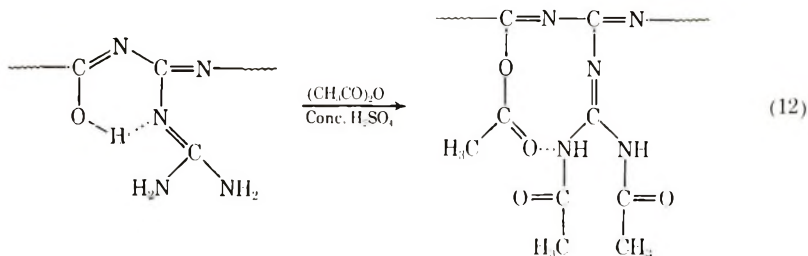


Table II shows the results of elemental analysis and estimation of nitrogen as primary amine.

The ultraviolet spectrum of solid A taken in KBr (Fig. 2) shows a medium absorption peak at 210 m μ attributable to $\pi \rightarrow \pi^*$ transitions in the

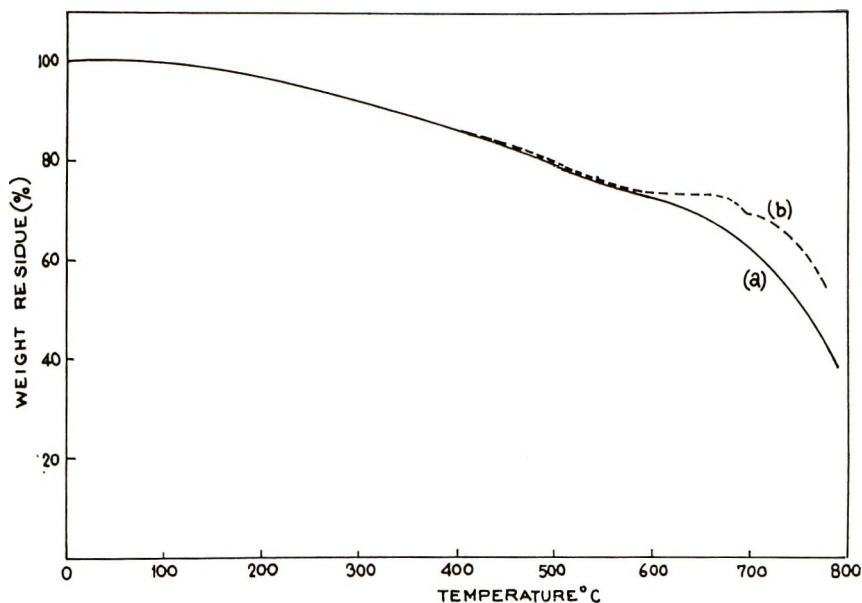


Fig. 1. Thermogravimetric analysis of the polymer: (a) in air; (b) in nitrogen.

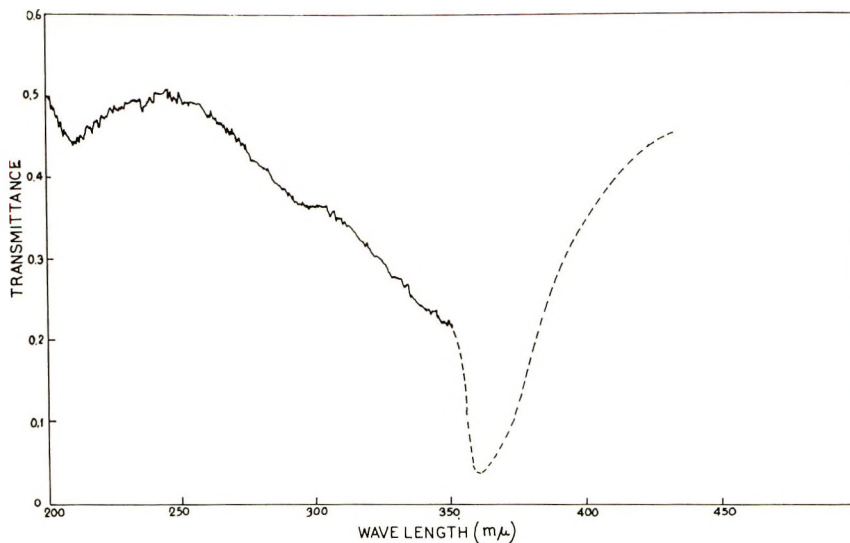
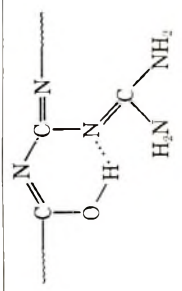
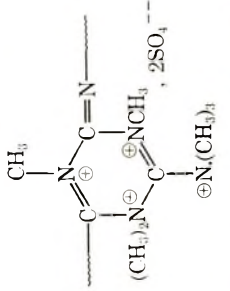
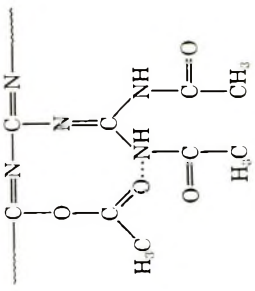


Fig. 2. Ultraviolet spectrum of the polymer: (—) solid polymer in KBr; (--) polymer in 0.1N HCl.

TABLE II
Elemental Analysis and Estimation of Nitrogen Present as Primary Amine

Compd.	Formula	C, %		H, %		N, %		N, % (as NH ₂)		S, %	
		Calcd.	Found	Calcd.	Found	Calcd.	Found	Calcd.	Found	Calcd.	Found
A		28.34	27.80	3.93	3.67	55.12	54.63	22.05	23.20	—	—
B		29.78	30.10	5.21	4.48	17.37	—	—	—	15.88	14.21
C		42.68	41.75	4.35	4.59	27.67	26.43	—	—	—	—

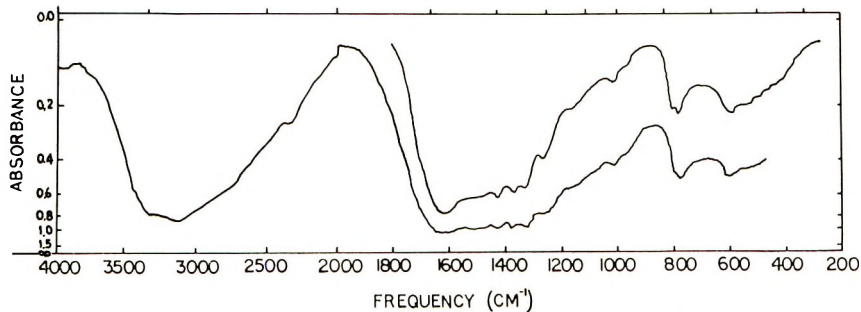
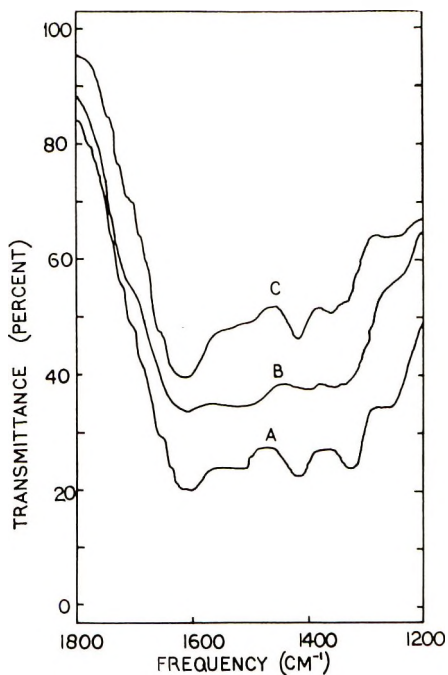


Fig. 3. Infrared spectra of polymer A.

Fig. 4. Infrared spectra of polymer A, its methyl derivative B, and its acetyl derivative C in KBr in the region 1200–1800 cm^{-1} .

—C=N— systems of the polymer. This band which should lie ordinarily in the far ultraviolet around $190 \text{ m}\mu$ for simple imines reveals a bathochromic shift due to polyconjugation.

The ultraviolet spectrum of A in 0.1*N* HCl solution taken in the region 320–430 $\text{m}\mu$ and presented along with the solid-state spectrum in the same figure shows a strong absorption at 360 $\text{m}\mu$. This may be accounted for by the superimposition of the $\pi \rightarrow \pi^*$ and the two possible $n \rightarrow \pi^*$ transitions.

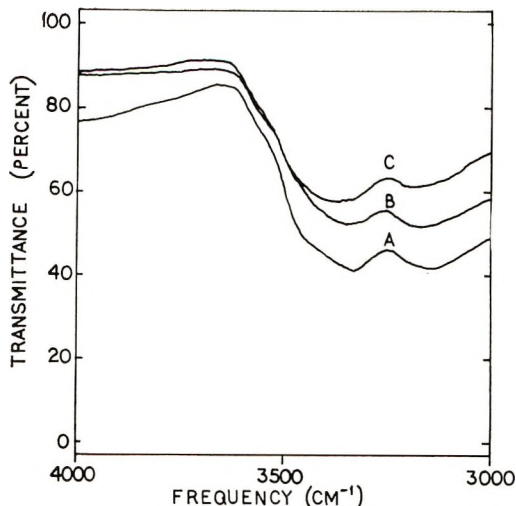


Fig. 5. Infrared spectra of polymer A, its methyl derivative B, and its acetyl derivative C in KBr in the region 3000–3500 cm^{-1} .

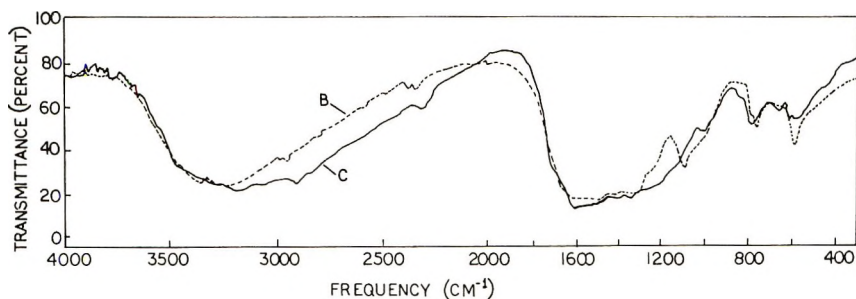


Fig. 6. Infrared spectra of the methyl derivative B and the acetyl derivative C of the polymer.

The infrared spectrum of A in KBr pellet (Figs. 3–5) shows an intense absorption band in the 1620 cm^{-1} region, corresponding to the $\text{C}=\text{N}$ stretching vibrations of the conjugated azomethines and the guanidine residues. The band at 1420 cm^{-1} is due to the bending frequency of the hydrogen bonded $\text{C}-\text{OH}$ group. The bands at 1325 , 1365 , and 1260 cm^{-1} are characteristic of the $\text{C}-\text{N}$ stretching, and the weak absorption at 1025 cm^{-1} is due to some restricted $\text{C}-\text{O}$ stretching. The bands at 800 , 780 , and 600 cm^{-1} correspond to the different $\text{N}-\text{H}$ deformation vibrations. The two wide bands in the 3150 and 3340 cm^{-1} regions are due to overlapping of the $\text{N}-\text{H}$ stretching vibrations and the $\text{O}-\text{H}$ stretching vibrations somewhat modified by intramolecular hydrogen bonding.

The infrared spectrum of B in KBr (Figs. 4–6) exhibits similar features with the $\text{O}-\text{H}$ bands totally absent. The band in the region $1300-1600 \text{ cm}^{-1}$ is slightly broader, probably due to the hetero-ring structure besides the conjugated $\text{C}=\text{N}$ skeleton. In addition there is a sharp peak at 1105

cm^{-1} due to C—N stretching in the substituted guanidine group (alkylamines).

The infrared spectrum of C in KBr (Figs. 4–6) reveals a small suppressed peak at 1025 cm^{-1} due to C—O stretching and an intensely sharp peak at 1425 cm^{-1} due to coupling of C—O—C bending frequency with an amide band. Polyconjugation in the chain and hydrogen bonding between oxygen of the esteric carbonyl and the N-substituted-amido hydrogen are probably responsible for a shift in the carbonyl stretching assignment towards smaller frequencies and overlapping with the main broad band.

Viscosity Characteristics

From Figure 7, it is evident that the reduced viscosity (η_{sp}/c) in pure anhydrous formic acid rises very sharply with diminishing concentration c and at fairly low c rapidly drops, imparting to the curve a hump-like appearance. The rates of rise and of subsequent fall of η_{sp}/c with diminishing c in anhydrous formic acid containing a small proportion of sodium formate are slow, and the hump consequently flattens out. As the amount of sodium formate is increased, the η_{sp}/c of the polymer A not only linearly

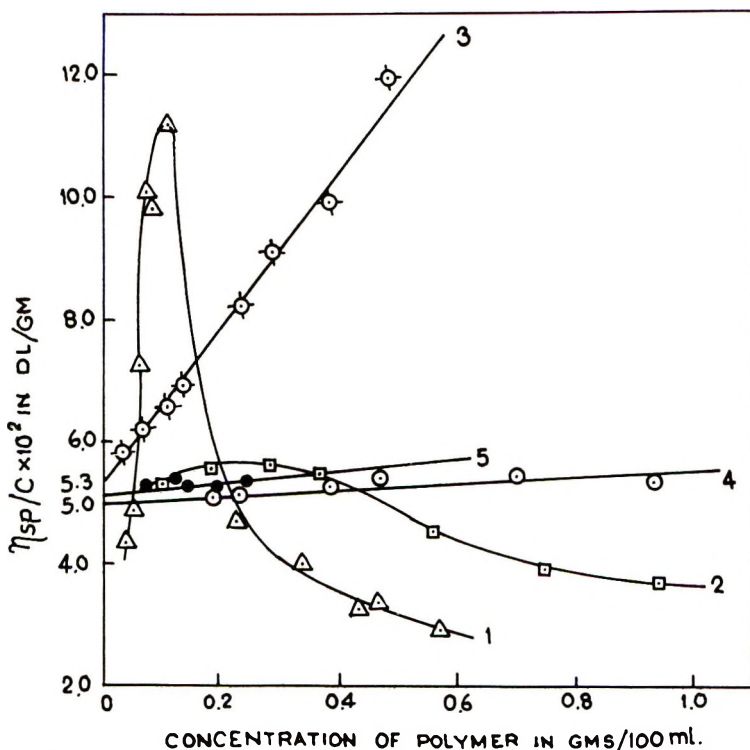
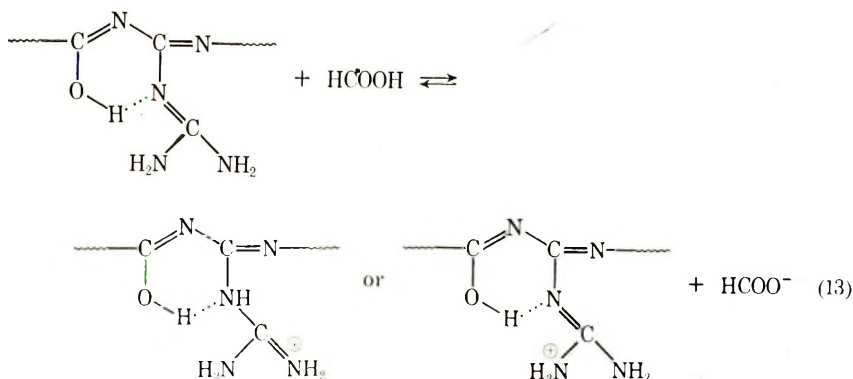


Fig. 7. Reduced viscosity η_{sp}/c of the polymer in formic acid solutions: (1) in anhydrous formic acid only; (2) in $0.164M$ Na formate in anhydrous formic acid; (3) in $0.22M$ Na formate in anhydrous formic acid; (4) in $0.589M$ Na formate in anhydrous formic acid; (5) in 84.2% formic acid.

increases with increasing c , but also diminishes with increase of the concentration of sodium formate. A similar effect is also produced by addition of water. Such a behavior of the polymer may be explained by the polyelectrolytic concept of Fuoss.

When the polymer A is dissolved in anhydrous formic acid, it is protonated on the strongly basic $-\text{NH}_2$ groups or the azomethine nitrogen atoms belonging to the guanidino groups, producing polycations and formate ions.



The polyion with a large number of positive charges along its dimension attracts the formate ions. As a result, the formate ions cluster around the positive centers forming ion-aggregates, deprotonate the polyion in some segments, or just move about in the solvent phase. This decreases the effective charge density of the polyion. However, such polyions carrying different amounts of charges are in reversible equilibrium with one another in the solution. Hence when such a solution is gradually diluted with anhydrous formic acid, the extent of protonation is enhanced and the ion-clusters also disintegrate. η_{sp}/c , therefore, increases due to increase in the intermolecular and intramolecular coulombic repulsion and the consequent increase in the degree of uncoiling of the flexible polyion chains. The drop in η_{sp}/c at low polymer concentrations may be attributed partly to an effect of dilution on the highly stretched polyion chains which are practically nonextensible and partly to a possible absorption of a small quantity of moisture by the solution leading to increased formate ion concentration and partial neutralization of charges.

The addition of sodium formate helps to shield the polyion-charges, by formation of opposite ion-atmospheres or by counterion association, thereby reducing the electrostatic repulsion between the polyion charges.

When the concentration of sodium formate is sufficient to suppress the polyelectrolytic character through ion association, η_{sp}/c plot becomes linear with positive slope. Any further increase in the concentration of sodium formate reduces η_{sp}/c . This is corroborated from the values of intrinsic viscosities of the polymer in anhydrous formic acid at different concentrations of added sodium formate, as given in Table III. Intrinsic

TABLE III
Intrinsic Viscosities in Formic Acid at Various
Concentrations of Sodium Formate

Sodium formate concn, <i>M</i>	Intrinsic viscosity [η], dl/g
0	0.3636
0.164	0.1818
0.224	0.0530
0.589	0.0500

viscosities [η] were found by extrapolating the linear η_{sp}/c versus c plots (Fig. 7) to infinite dilution, or from the linear plots of reciprocal η_{sp}/c against $c^{1/2}$, on assuming the Fuoss relation⁷ to hold.

The effect of water on viscosity may be interpreted in terms of a reversal of the equilibrium between the polyions of varying charge densities.⁸ Although the polymer is a stronger base than water in formic acid, a substantial part of the protons associated with the polyion is made available to water for formation of oxonium ions, because the concentration of the polymer in the solution is much smaller than that of water. Hence, due to a shift of the equilibrium towards deprotonation, the polymer loses its polyelectrolytic character and η_{sp}/c decreases. The intrinsic viscosity of the polymer in aqueous 84.2% formic acid is 0.051.

Osmotic Behavior

Table IV is a summary of the results of osmotic pressure (π) measurements on the untreated polymer and its various fractions. The solvent used for osmotic pressure measurement was 4*N* formic acid in presence of 3.912×10^{-2} *M* sodium formate.

Figure 8 shows a plot of π/c versus c plot of the untreated polymer in 4*N* formic acid. The sharp rise of π/c with diminishing c is due to escape of

TABLE IV
Osmotic Molecular Weight of the Polymer Fractions

Fraction no. ^a	Weight fraction, %	Osmotic molecular weight (\bar{M}_n)
1	13.3	39,500
2	7.7	36,370
3	11.6	33,260
4	38.4	31,010
5	15.2	29,580
6	2.4	27,630
7	6.7	25,920
Unfractionated	—	33,700

^a Insoluble part = 4.7 wt-%.

counterions from the polymer coil so that the reduction in the number of particles responsible for osmotic pressure upon dilution is more than compensated for by the liberation of counterions from the polymer coil. By adding a large quantity of sodium formate in equal concentrations to the solvent and the solution chambers, the association of counterions with the polyions is so great that the polyelectrolyte remains practically undissoci-

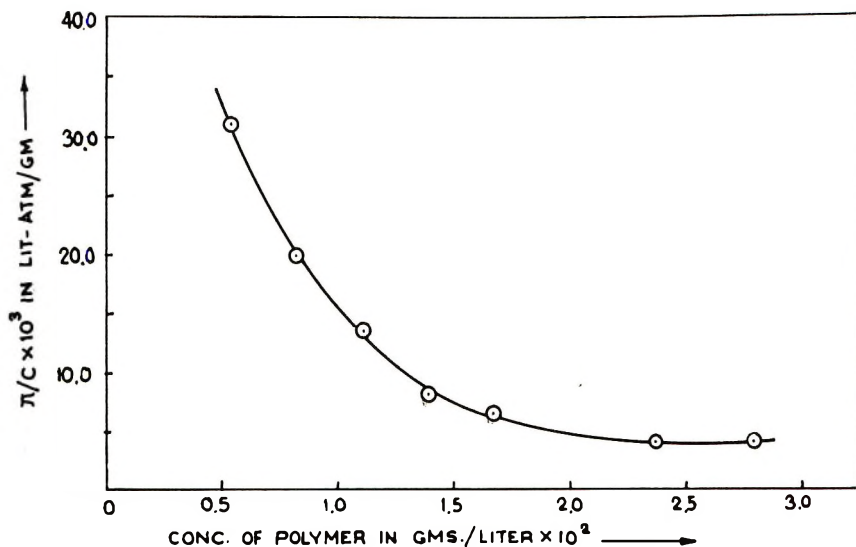


Fig. 8. Plot of π/c vs. c of unfractionated polymer in 4*N* formic acid.

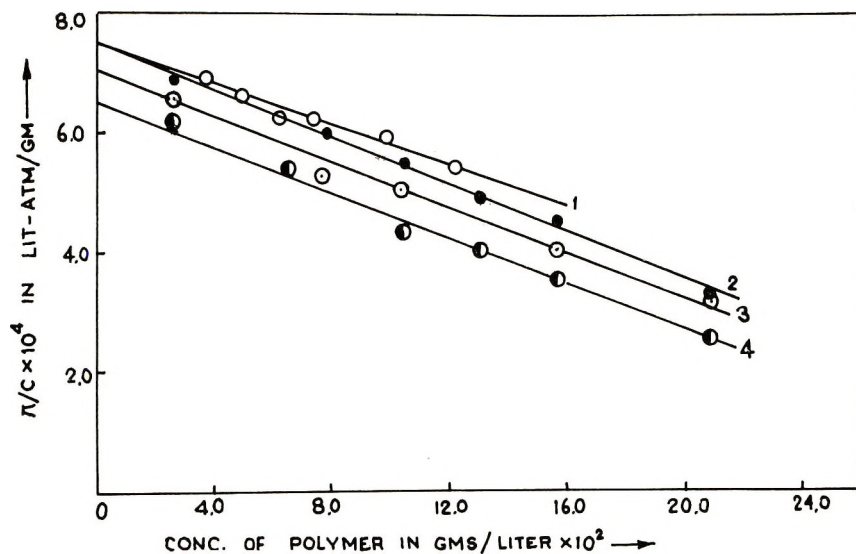


Fig. 9. Plot of π/c vs. c of unfractionated polymer in 4*N* formic acid solutions in presence of electrolytes: (1) $3.912 \times 10^{-2}M$ Na formate; (2) $6.792 \times 10^{-2}M$ Na formate; (3) $2.573 \times 10^{-1}M$ Na formate; (4) $3.518 \times 10^{-1}M$ Na formate.

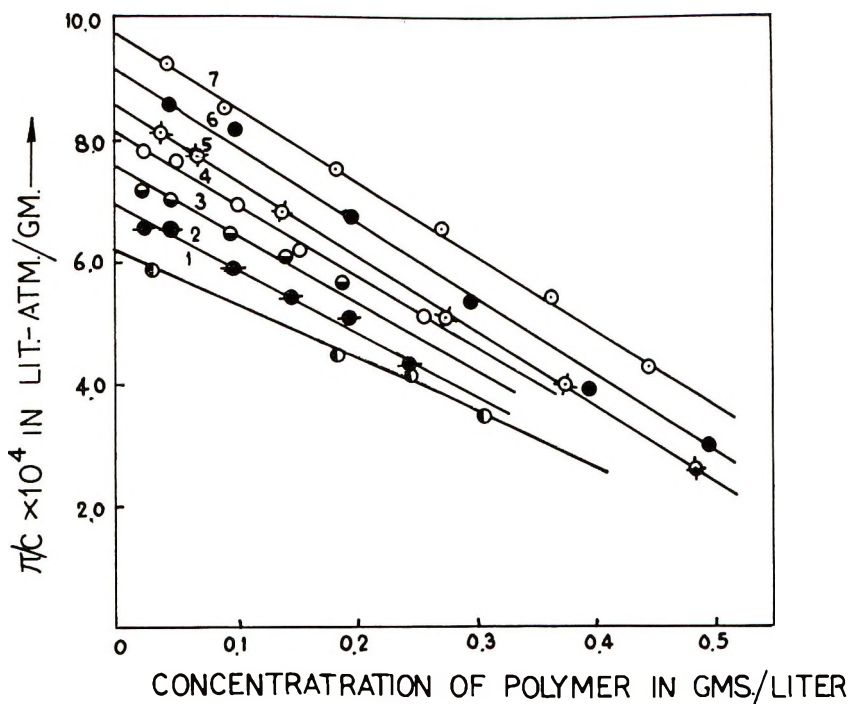


Fig. 10. Plot of π/c vs. c for the different fractions of the polymer in 4*N* formic acid solutions in the presence of $3.912 \times 10^{-2}M$ Na formate.

ated. Hence the plots (Figs. 9–11) of π/c versus c of the polymer and its fractions are linear, and an extrapolation of the plots provides molecular weights. It should be noted that the slope of the plot is negative, which may be explained as follows.⁹

The intermolecular polymer–polymer attraction probably exceeds the polymer–solvent interaction, so that the heat of dilution is positive and fairly large. Therefore the polymer molecules tend to be coiled up or associated. If the effect is due to only coiling of the linear chains, the intercept on the π/c axis of the plots should be the same, although the slope will increase with increase of concentration of sodium formate. On the contrary, if the effect is due to association of the molecules only, the values of the intercepts will be less; i.e., the molecular weight should increase with increasing concentration of sodium formate.

It should be noted that the plots of π/c versus c of any two randomly chosen fractions of the polymer (fractions 1 and 4) converge to the same points on the π/c axis for two different concentrations of sodium formate (0.03912*M* and 0.04809*M*), and the same is also true for the untreated polymer at sodium formate concentrations of 0.03912 and 0.06792*M*. But at a still larger ionic strength, when the degree of association becomes more prominent, the plots for the untreated polymer do not give the same intercept and hence the molecular weight varies.

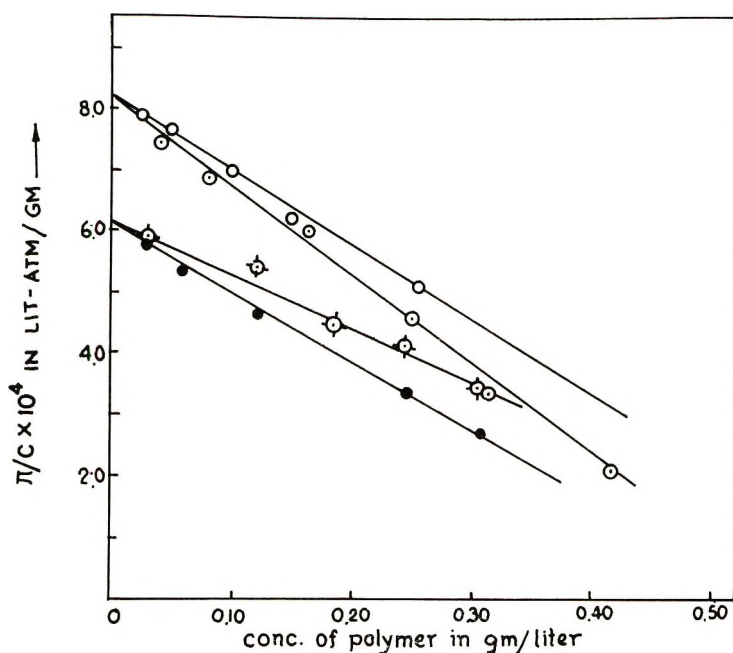


Fig. 11. Plot of π/c vs. c for different polymer fractions in 4*N* formic acid: (●) fraction 1 in presence of $4.809 \times 10^{-2}M$ Na formate; (⊖) fraction 1 in presence of $3.912 \times 10^{-2}M$ Na formate; (○) fraction 4 in presence of $3.912 \times 10^{-2}M$ formate Na; (⊙) fraction 4 in presence of $4.809 \times 10^{-2}M$ Na formate.

It is clear, therefore, that both random coiling and association occur in the solutions of the neutral undissociated polymer.

Dielectric Properties

The dielectric constant K' , dielectric loss K'' and the dielectric specific conductivity (σ) of the polymer, the latter of which is actually $\omega K'' K'_0$, where ω is the frequency and K'_0 the dielectric constant of the substance in vacuum, are shown as functions of frequency at room temperature in Figure 12.

The variation of K' and K'' with temperature at a frequency of 10^6 Hz is presented in Figure 13 and the plot of $\log \sigma$ versus the reciprocal absolute temperature $1/T$ is given in Figure 14.

It is known that K' depends on electronic, ionic, dipole-orientational, and interfacial polarizations. The latter arises out of heterogeneity of the sample due to conducting impurities, molecular weight distribution, or crystal defects, and exerts its influence only at low frequencies. In the frequency region studied, the contribution of the last factor is nonoperative. However, the manner in which K' decreases beyond 10^6 Hz and then assumes a value almost independent of frequency is suggestive of the presence of dipoles in the solid polymer, the orientability of which lags the applied ac voltage resulting in energy loss. The maximum loss factor K''_{max} at

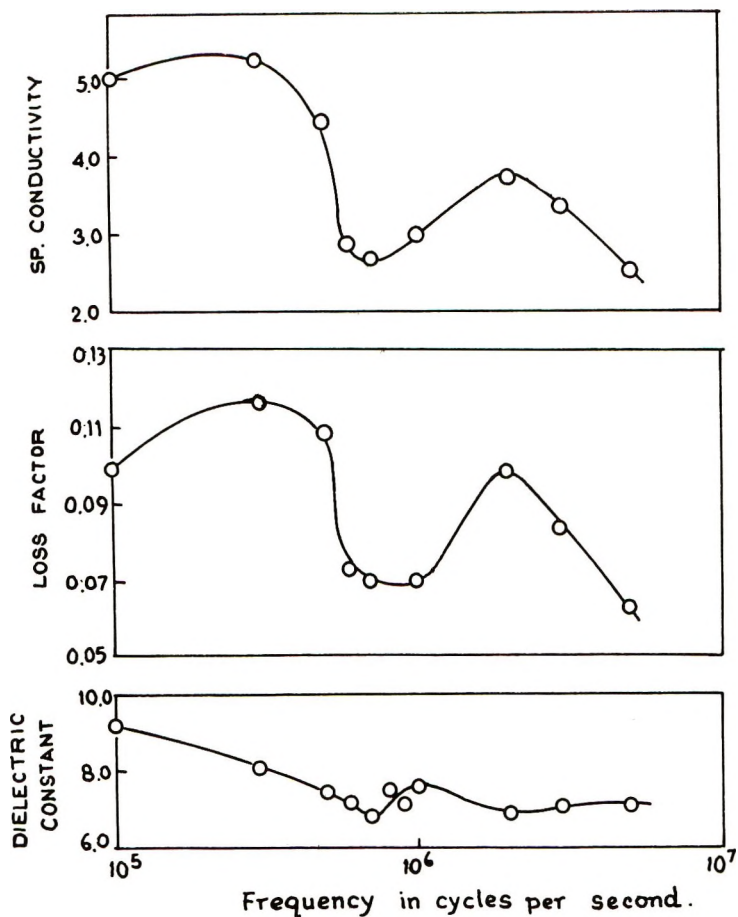


Fig. 12. Effect of frequency on dielectric constant, loss factor, and specific conductance. Frequency is plotted on log scale.

room temperature is given by $K''_{\max} = 0.14(K'_s - K'_\alpha)$, where K'_s is the highest K' and K'_α the lowest K' equal to K' at a hypothetical infinite frequency in the region of dielectric absorption. This shows that there is a band of relaxation times τ of the dipoles distributed about a most probable value, τ_0 , which is responsible for a slight broadening of the loss factor peak without changing the magnitude of the dispersion.

That the anomalous dispersion is due to dipole polarization is also evident from the influence of temperature on K' , K'' , and σ , and from the slight decrease in the factor from 0.14 to 0.11 with the rise of temperature. On assuming that K'_α remains unaffected by change of temperature, because it consists of electronic and ionic polarizations only, K''_{\max} at $82^\circ\text{C} = 0.11(K'_s - K'_\alpha)$. The initial increase in K'' with increase of T may be due to the space-charge contribution becoming more prominent at higher temperatures and becoming a maximum at 82°C . K' at room temperature

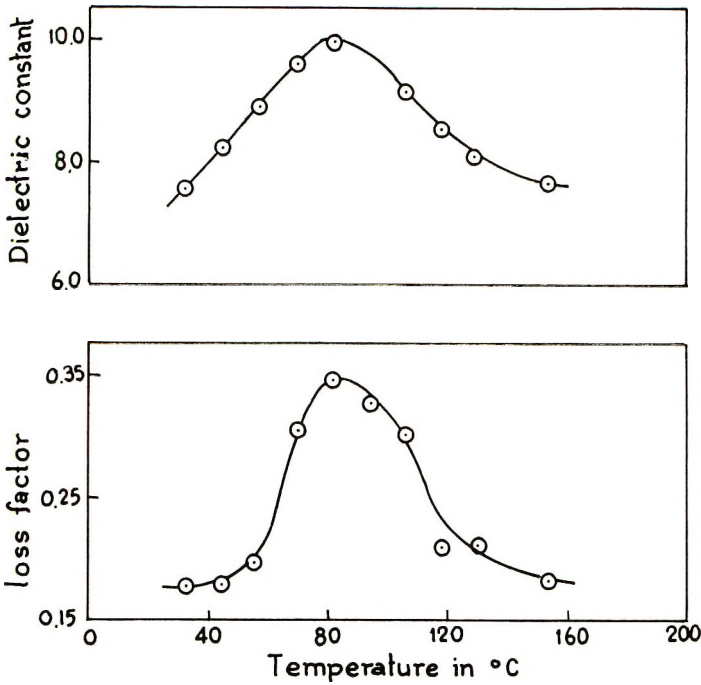


Fig. 13. Effect of temperature on dielectric constant and loss factor.

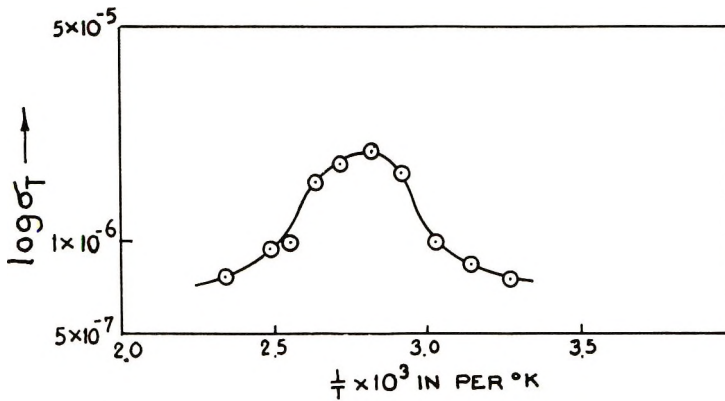


Fig. 14. Effect of temperature on specific conductivity.

attains a maximum at a frequency of 8×10^{-5} Hz, and K' at 10^6 Hz attains a maximum at 82°C . Hence, the average energy E associated with the dipole, calculated from the relation, $\tau = \tau_0 e^{E/kt}$, where k is Boltzmann constant, is 1.73×10^{-2} eV/°K.

The intrinsic activation energy ΔE for conduction calculated by the extrapolation method from the descending portion of the $\log \sigma$ versus $1/T$ plot, assuming from quasilinearity the validity of the relation, $\sigma = \sigma_0 e^{\Delta E/kT}$, is 0.186 eV, and the frequency-dependent conductivities in the temperature

region 34–154°C are of the order of 2×10^{-6} – 7×10^{-7} mho-cm⁻¹. The relative ease with which the conduction can be thermally excited may, therefore, be regarded as a justification for classifying the substance as a semiconducting polymer.

The number of charge carriers, n_i , per cubic centimeter of the substance calculated from the formula $n_i = n_0 e^{-\Delta E/kT}$, is found to be 2.12×10^{16} , whereas the result of spin density measurement on the sample from its ESR signal shows that the value of n_i is 6.66×10^{16} /cm³. This is a fair agreement, on considering the higher molecular weight of the associated polymer used for calculation of n_0 .

The average dipole moment $\bar{\mu}$ of the polymer molecule calculated from the positive slope of the plot of $(K' - 1)/(K' + 2)$ versus $1/T$, which is equal to $4\pi\bar{\mu}^2\eta/9k$, where k is Boltzmann constant and $n = Nd/M$, d being the density of the polymer with respect to water, based on the assumption that the Debye equation holds good, is 24.16 D, which is admittedly too high for a stable simple molecule to possess. But it is interesting to note that the resultant dipole moment μ_0 of each repeating unit calculated¹⁰ from $\bar{\mu} = \mu_0 Z^{1/2}$, where Z is the number of such units in a molecule, is just 1.5 D, the moment of a single —NH₂ group. This relation is valid only when the polymer molecule is flexible and its dipoles are free to rotate in all directions with respect to one another.

The authors desire to express their sincere gratitude to Dr. B. K. Banerji of the Planning and Development Division, Fertilizer Corporation of India Limited, Sindri and Dr. K. V. Rao, of the Department of Physics, I.I.T., Kharagpur, for some of the experimental work contained herein and also to the Council of Scientific and Industrial Research, for granting financial aid to one of the authors (A. K. D.).

References

1. Ya. M. Paushkin and A. F. Lunin, *Vysokomol. Soedin.*, **6**, 1467 (1964); *Dokl. Akad. Nauk. SSSR*, **150**, 823 (1963); *ibid.*, **167**, 1346 (1966).
2. Ya. M. Paushkin, A. F. Lunin, and O. Yu. Omarov, *Vysokomol. Soedin.*, **6**, 734 (1964).
3. Ya. M. Paushkin, A. F. Lunin, and A. A. Karpov, *Tr. Mosk. Inst. Neftekhim. Gaz Prom.*, **51**, 43 (1964).
4. L. L. Bircumshaw, F. M. Taylor, and D. H. Whiffen, *J. Chem. Soc.*, **1954**, 931.
5. F. Pregl, *Quantitative Organic Microanalysis*, J. A. Churchill, Ltd., London, 1951, p. 177.
6. K. V. Rao, *J. Phys. Chem. Solids*, **20**, 193 (1961).
7. R. M. Fuoss and U. P. Strauss, *Ann. N. Y. Acad. Sci.*, **51**, 836 (1949); *J. Polym. Sci.*, **3**, 246 (1948).
8. J. R. Schaefgen and C. F. Trivisonno, *J. Amer. Chem. Soc.*, **73**, 4580 (1951).
9. M. L. Huggins, *Ind. Eng. Chem.*, **35**, 216, 980 (1943).
10. P. Debye and F. Bueche, *J. Chem. Phys.*, **19**, 589 (1951).

Received April 23, 1970

Revised July 22, 1970

Partial Ladder Polymers with Anthraquinone Units. Reaction of 1,2,5,6-Tetraaminoanthraquinone with *p*-Benzoquinone Derivatives

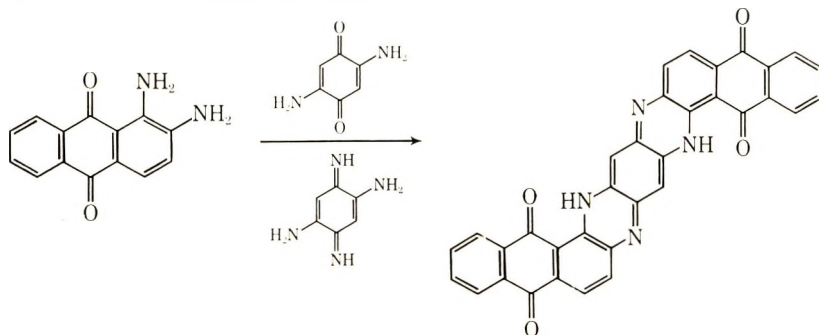
J. SZITA* and C. S. MARVEL, *Department of Chemistry,
The University of Arizona, Tucson, Arizona 85721*

Synopsis

1,2,5,6-Tetraaminoanthraquinone has been condensed with 2,5-diaminobenzoquinone, 2,5-diaminobenzoquinone diimide, and 2,5-diaminohydroquinone to give partial ladder polymers which are only slightly soluble in sulfuric acid and do not produce soluble products on reduction with sodium dithionite in alkaline media.

Previous work has shown that tetraamines condense with 2,5-diaminobenzoquinone, 2,5-diaminobenzoquinonediimide, and 2,5-diaminohydroquinone to give partial ladder structures which are quite thermally stable and very intractable.¹ Since it has been found that certain polymers with anthraquinone recurring units are soluble in aqueous-organic solvent mixtures on reduction with sodium dithionite,² it was thought worthwhile to treat 1,2,5,6-tetraaminoanthraquinone with these hydroquinone derivatives.

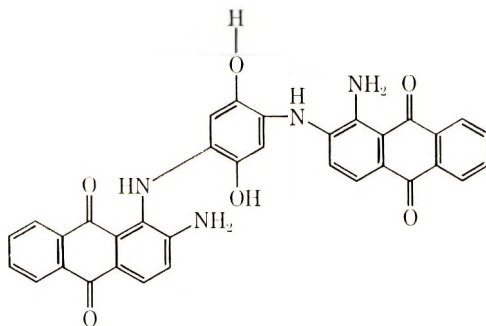
Preliminary experiments with model compounds and polymerization reaction indicated that the anthraquinone derivatives could be condensed in polyphosphoric acid to give good yields of products. Thus, 1,2-diaminoanthraquinone and either 2,5-diaminobenzoquinone or 2,5-diaminobenzoquinonediimide in polyphosphoric acid at 150–200°C gave a 75–90% yield of the expected model compound I.



I

* Present address: Fibers Division, American Cyanamid Company, Stamford, Conn. 06904.

When 2,5-diaminohydroquinone was treated with this tetraamine in polyphosphoric acid at 150°C, the product was not the expected completely cyclized product but appeared to be the open-chain product (II).



II

In polymerization experiments with 1,2,5,6-tetraaminoanthraquinone, the same general results were obtained. Polymers were obtained in polyphosphoric acid at 170°C but all were of low molecular weight, soluble in

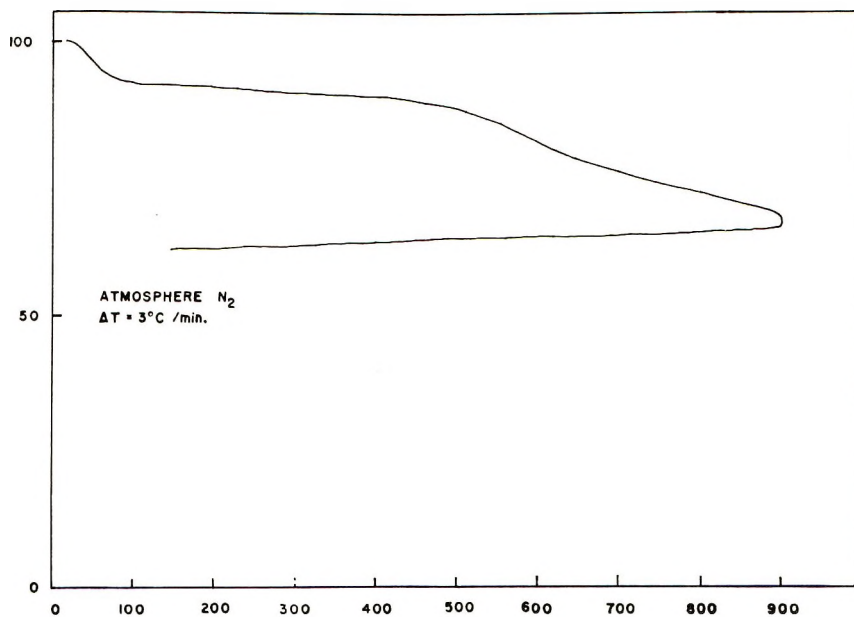
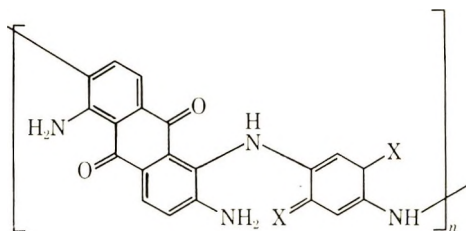
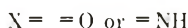


Fig. 1. TGA curve for HP-28 (Table I).

sulfuric acid, and had inherent viscosities in the range of 0.04–0.19. Analyses and infrared data indicated they were primarily uncyclized condensation products (III).



III



Heating these products further at 390°C gave products which indicated partial ring closure (or crosslinking) but all were extremely insoluble in sulfuric acid and in base after they were reduced with sodium dithionite.

A typical TGA curve (HP-28, Table I) is shown in Figure 1. The first drop in weight is obviously due to elimination of water; decomposition subsequently sets in at about 518°C.

EXPERIMENTAL

Monomers

1,2-Diaminoanthraquinone (DAA) was purchased from Aldrich Chemical Company and purified by recrystallization from nitrobenzene.

ANAL. Calcd for $C_{10}H_{10}N_2O_2$: C, 70.59%; H, 4.23%; N, 11.76%; O, 13.42%. Found: C, 70.03%; H, 3.88%; N, 12.05%; O, 14.17%.

1,2,5,6-Tetraaminoanthraquinone (TAA) and the benzoquinone derivatives (DAB, DBI and DAH) were prepared as described earlier.^{1,2}

Model Compounds

Condensation of 1,2-Diaminoanthraquinone (DAA) with 2,5-Diamino-p-benzoquinone (DAB)

A mixture of 1.192 g (0.005 mole) of DAA (recrystallized from nitrobenzene) and 0.346 g (0.0025 mole) of DAB was dissolved in 24 g of PPA (82.5%) (Matheson Coleman and Bell) and heated to 160°C under vacuum for 30 min and held a further 30 min at this temperature. In the next 60 min, the temperature was raised to 200°C under nitrogen atmosphere and maintained for 60 min. The cooled black solution was precipitated by pouring it into 1.5 liter of distilled water and then kept over night. After filtration the black precipitate was neutralized with diluted ammonium carbonate, washed with water until neutral and extracted with water for 4 days. Drying in vacuum oven at 70°C gave a yield of 1.263 g (93%).

The infrared spectrum of the product shows three weak broad bands in the range of 1600–1200 cm^{-1} (1580, 1430, and 1250 cm^{-1} , and very weak shoulders at 1620 and 1630 cm^{-1} ($C_6H_5-NH_2$).

ANAL. Calcd for $C_{33}H_{16}N_4O_4$: C, 75.00%; H, 2.96%; N, 10.30%. Found: C, 74.45%; H, 2.98%; N, 11.36%.

Condensation of 1,2-Diaminoanthraquinone (DAA) with 2,5-Diamino-p-benzoquinonediimide (DBI)

Method 1. In 24 g of PPA were dissolved 1.192 g (0.005 mole) of DAA (recrystallized) and 0.3404 g (0.0025 mole) of DBI (recrystallized from DMAc) and the solution heated at 150–170°C under vacuum for 60 min. In the next 30 min the temperature was raised to 200°C and kept for 60 min (N₂ atmosphere). The black highly viscous solution was treated as described in the previous experiment. The yield was 1.155 g (85%).

The infrared spectrum (KBr pellet) showed broad bands (m) at 1580, 1450 and 1260 cm⁻¹ and shoulders at 1620 and 1640 cm⁻¹.

ANAL. Calcd for C₃₄H₁₆N₄O₄: C, 75.00%; H, 2.96%; N, 10.30%. Found: C, 74.13%; H, 3.18%; N, 12.88%.

Method 2. A mixture of 1.1920 g (0.005 mole) of DAA and 0.3404 g (0.0025 mole) of DBI were suspended in 30 g of PPA (82.5%) and heated to 150°C slowly during 3 hr under a nitrogen atmosphere and maintained for 2 hr. After cooling the dark solution was precipitated in 800 ml of distilled water and the product collected by filtration, neutralized with ammonium carbonate, washed, and extracted with water for 4 days. After drying in a vacuum oven at 80–90°C, the yield was 0.985 g (74%).

ANAL. Calcd for C₃₄H₂₂N₆O₄: C, 70.59%; H, 3.83%; N, 14.53%. Found: C, 70.82%; H, 3.62%; N, 13.19%.

In a glass tube 400 mg of the above product was heated under reduced pressure. The temperature was raised slowly to 240°C in 4 hr and kept for 1 hr.

Infrared bands appeared at 1580(m), 1550(m), 1540(m), 1485(s), 1320(m), 1260–1290(m) cm⁻¹; broad shoulder: 1620–1660 cm⁻¹.

ANAL. Calcd for C₃₀H₁₉N₅O₄: C, 72.74%; H, 3.41%; N, 12.46%. Found: C, 72.72%; H, 3.24%; N, 12.97%.

Condensation of 1,2-Diaminoanthraquinone (DAA) with 2,5-Diamino-p-hydroquinone dihydrochloride (DAH)

DAA (2.383 g, 0.01 mole) and DAH (1.066 g, 0.005 mole) were dissolved at room temperature in 50 g of PPA (82.5%). The brown solution was heated under vacuum to 170°C in 40 min (intensive gas evolution, HCl) and kept at that temperature for 50 min. In the next 30 min the temperature was raised to 200°C under N₂ atmosphere and maintained for 1.5 hr. After cooling the black viscous solution was treated as described before. The yield was 2.461 g (90%).

ANAL. Calcd for C₃₄H₁₈N₄O₄: C, 74.73%; H, 3.32%; N, 10.25%. Found: C, 74.79%; H, 2.99%; N, 12.34%.

Polymers

Condensation of 1,2,5,6-Tetraaminoanthraquinone (TAA) and 2,5-Diamino-p-benzoquinone (DAB)

Method 1. In 30 g of PPA (82.5%) was dissolved 0.691 g (0.005 mole) of DAB and 1.341 g (0.005 mole) of TAA and the solution heated to 160°C in 20 min under vacuum and kept for 30 min. In the next 10 min the temperature was raised to 200°C and maintained (nitrogen atmosphere) for 90 min, when the highly viscous solution turned to a black rubbery mass. After cooling it was put into 1 liter of distilled water and kept over night. The black polymer thus obtained was filtered, neutralized with ammonium carbonate solution, washed and extracted with water for 5 days. The yield was 1.682 g. The part soluble in concentrated sulfuric acid comprised 23%, η_{inh} 0.04 (determined in concentrated sulfuric acid at 30°C).

The infrared spectrum showed two broad weak absorptions at 1490–1410 cm^{-1} and 1370–1300 cm^{-1} and a broad weak shoulder at 1640–1500 cm^{-1} .

In a glass tube 600 mg of the above polymer was heated under reduced pressure. The temperature was raised in the first hour to 300°C, then to 330°C in the second hour, and for the next 3 hr was kept at 360–370°C. After heating, the polymer became insoluble.

Elemental analysis of the above and of the following polymers are shown in Table I. In the infrared spectrum after heating no considerable change was observed (the shoulder at 1640 cm^{-1} became less).

Method 2. In 25 g of PPA were placed 0.671 g (0.0025 mole) of TAA and 0.3455 g (0.0025 mole) of DAB and the mixture heated under reduced pressure (50–70 mm Hg) to 80°C in 60 min, to 110°C in the next 60 min, and in the next 5 hr slowly to 170°C. After cooling, the dark viscous solution was precipitated in 1 liter of distilled water. The precipitate was collected by filtration, neutralized with ammonium carbonate, washed and extracted with water for 4 days and dried in vacuum at 80–90°C. The yield was 0.684 g. The black polymer thus obtained was completely soluble in concentrated H_2SO_4 . The infrared spectrum showed two strong bands at 1530 and 1250 cm^{-1} and two broad shoulders at 1640–1550 cm^{-1} and 1500–1420 cm^{-1} .

Method 3. The reaction was carried out with the same amount of starting materials as the above but under different conditions. Instead of 25 g, 21 g of PPA was used as solvent. The temperature was raised during the reaction as follows: from room temperature to 110°C in 2 hr; from 110°C to 140°C in further 2 hr; to 170°C in the next 3 hr; in the last 4.5 hr to 195°C. The yield was 0.959 g and 25% of the polymer was soluble in concentrated H_2SO_4 after 24 hr at 110°C. The infrared spectrum showed a weak broad band at 1460–1400 cm^{-1} and weak broad shoulders at 1640–1500 and 1380–1200 cm^{-1} .

Both of the above products were heated in the solid state under reduced pressure (1–2 mm Hg) as follows: the temperature was raised in 1.5 hr

TABLE I
 Condensation of 1,2,5,6-Tetraaminoanthraquinone (TAA) with *p*-Benzoquinone Derivatives

Expt no.	Starting materials ^a	Experimental conditions			Solubility in conc. H ₂ SO ₄ (%)	η_{inh}^b	Elemental analysis (Found) ^c			
		Medium	Temp, °C	Time, hr			C, %	H, %	N, %	Residue, %
P-28	TAA + DAB	PPA	25-200 200	1 1.5 ^d	23	0.04	67.58	2.69	15.76	0.99
HP-28	P-28	Solid state	140-360 360-370	2 3	<1	—	68.08	1.99	16.12	1.93
P-38	TAA + DAB	PPA	25-170 170-195	6 4.5	25	0.11	64.91	2.80	15.17	2.28
HP-38	P-38	Solid state	140-350 350-360	1.5 4	<1	—	67.74	2.08	16.29	—
P-34	TAA + DAB	PPA	25-110 110-170	2	100	0.07	63.37	3.04	15.02	2.56
HP-34	P-34	Solid state	140-350 350-360	1.5 4	<1	—	65.13	2.56	16.21	0.94
P-33	TAA + DBI	PPA	25-100 100-170	1	100	0.07	66.51	3.28	18.01	1.03
HP-33	P-33	Solid state	140-350 350-360	1.5 4	10	<0.01	67.34	2.82	17.26	0.98
P-37	TAA + DAH	PPA	25-160 160-190	6 5.5	8	0.19	68.00	3.02	15.10	1.58
HP-37	P-37	Solid state	140-350 350-360	1.5 4	<1	—	70.12	2.75	16.36	—
P-32	TAA + DAH	PPA	25-170 170	2.5	100	0.11	67.57	3.24	16.26	0.65
HP-32	P-32	Solid state	140-350 350-360	1.5	<1	—	69.63	2.80	16.21	0.92

^a DAB = 1,2-diamino-*p*-benzoquinone; DBI = 1,2-diamino-*p*-benzoquinonediimide; DAH = 1,2-diamino-*p*-hydroquinone dithydrochloride.

^b Determined in concentrated H₂SO₄ at 30°C.

^c Calcd for III, X = O: C, 67.41%; H, 3.34%; N, 15.87%; Calcd for III, X = NH: C, 67.60%; H, 3.66%; N, 19.71%. Calcd for closed ring structure: C, 71.42%; H, 2.38%; N, 16.72%.

^d Reaction mixture turned to a rubbery mass.

to 350°C and kept 350–360°C for 4 hr. After heating, the products were only slightly soluble (<1%) in concentrated sulfuric acid.

After heating, the infrared spectrum of the second polymer showed a decrease of the band at 1530 cm⁻¹ and of the shoulder at 1640 cm⁻¹.

Condensation of TAA and 2,5-Diamino-p-benzoquinonediimide (DBI)

In 25 g of PPA were suspended 0.671 g (0.0025 mole) of TAA and 0.3404 g (0.0025 mole) of DBI and the mixture was heated under reduced pressure (60–70 mm Hg) to 100°C in 1 hr and in the next 6 hr slowly to 170°C. The dark viscous solution thus obtained was treated as described before. The yield was 0.59 g. The dark brown product was completely soluble in concentrated sulfuric acid, $\eta_{inh} = 0.07$ (determined in concentrated H₂SO₄ at 30°C; $c = 0.5$ g/100 ml). Infrared bands were at 1640–1570(m), 1540(m), 1510–1420(m), 1250(s) cm⁻¹.

The product was heated in the solid state as described for P-34. After heating, 10% of HP-33 was soluble in concentrated sulfuric acid.

After heating, all of the above bands in the infrared spectrum decreased in intensity.

Condensation of TAA and 2,5-Diamino-p-hydroquinone dihydrochloride (DAH)

Method 1. A mixture of 0.671 g (0.0025 mole) of TAA and 0.533 g (0.0025 mole) of DAH was heated in 30 g of PPA under vacuum (70–80 mm Hg) to 100°C in 30 min then slowly to 170°C in 2 hr and kept at this temperature for the next 4 hr. The reaction mixture was treated as described before. The yield was 0.587 g. The black polymer thus obtained was completely soluble in concentrated sulfuric acid, $\eta_{inh} = 0.11$ (determined in concentrated H₂SO₄ at 30°C, $c = 0.5$ g/100 ml). The infrared spectrum showed a weak shoulder at 1635 cm⁻¹, a broad one at 1280–1200 cm⁻¹, and weak bands at 1580 and 1480–1380 cm⁻¹.

Method 2. The same amount of the starting materials as above were reacted in 25 g of PPA. After heating under N₂ atmosphere for 11.5 hr (from 25°C to 110°C in 2 hr, from 110°C to 160°C in 4 hr, and to 190°C in the last 5.5 hr) the yield was 0.824 g of a black polymer. The part soluble in concentrated H₂SO₄ was only 8% with an inherent viscosity of 0.19 (30°C).

We are indebted to Dr. G. F. L. Ehlers, Air Force Materials Laboratory, Wright-Patterson Air Force Base, for the thermogravimetric curve.

This work was supported by the Air Force Materials Laboratory, Air Force Systems Command, Wright-Patterson Air Force Base, Ohio.

References

1. J. Szita and C. S. Marvel, *J. Polym. Sci. A-1*, **7**, 3203 (1969).
2. W. Bracke and C. S. Marvel, *J. Polym. Sci. A-1*, **8**, 3177 (1970).
3. R. Pense and C. S. Marvel, *J. Polym. Sci. A-1*, **8**, 3189 (1970).

Received July 27, 1970

Revised September 4, 1970

Chemorheological Treatment of Crosslinked EPT

KENKICHI MURAKAMI and SABURO TAMURA, *Chemical Research Institute of Non-aqueous Solutions, Tohoku University, Sendai, Japan*

Synopsis

Stress relaxation mechanisms were investigated on three types of (EPT) ethylene-propylene terpolymers in air at 109°C. These polymers differ only by the structure of the crosslinkage in which there is a carbon-carbon bond, a polysulfide linkage ($-\text{S}_x-$) or a monosulfide linkage ($-\text{S}-$). All the stress relaxation of peroxide-cured EPT polymer was not due to the oxygen-induced cleavage of the main chain but to a physical flow. In the case of sulfur-cured EPT polymer, the relaxation curve is divided into three straight lines when the procedure X is used and $\log f(t)/f(0)$ is plotted linearly with time. It was concluded that this graph was in agreement with an interchange reaction of the polysulfide linkage by an oxidative cleavage of the monosulfide linkage. On the other hand, a TT-cured EPT polymer gave a plot with a straight line. This stress relaxation could be explained by an oxidative cleavage of the monosulfide linkage.

Introduction

Tobolsky et al.¹ previously investigated the mechanism dealing with the reactivities of cross linkages in ethylene-propylene rubber (EPDM) containing nonconjugated diene compounds as the third component. The main chain of EPDM was more stable to oxygen-induced cleavage compared with that of the polyisoprene rubber.

In this paper, we wish to report some additional results obtained under similar experiments in recent studies.

Materials and Experiments

Ethylene-propylene terpolymer (EPT, Royalene 301, Sumitomo Chemical Industry Ltd.) was used as material in this experiment. The crosslinked polymer was prepared by using the crosslinking agents and the methods of cross-linking described in Table I.

Three kinds of EPT polymer (Nos. 1, 2, and 3), differing only in the structure of the crosslinkage, were prepared. It is evident that the crosslinking site, in these samples, consists of a carbon-carbon bond, a polysulfide linkage ($-\text{S}_x-$) and a monosulfide linkage ($-\text{S}-$) for types 1, 2, and 3, respectively. The samples were all extracted with acetone for 72 hr and dried *in vacuo*.

TABLE I
Preparation of Cured EPT Polymers

	Sample 1	Sample 2	Sample 3
Rubber	100	100	100
Sulfur		2	
Zinc oxide		5	5
Stearic acid		2	1
Tetramethylthiuram disulfide (TT)		1	3.5
Mercaptobenzothiazole (MBT)		0.5	
Dicumyl peroxide (DCP)	2		
Curing time, min. ^a	30	20	40

^a Curing temperature, 150°C.

Results and Discussion

The stress relaxation of dicumyl peroxide-cured EPT (sample 1) was measured at 109°C in air, in nitrogen, and in air containing a proper amount of antioxidant. These stress relaxation curves [relative stress $f(t)/f(0)$ versus time $\log t$] are shown in Figure 1. From this figure, we can see that the descending curves show almost the same slope in the three samples.

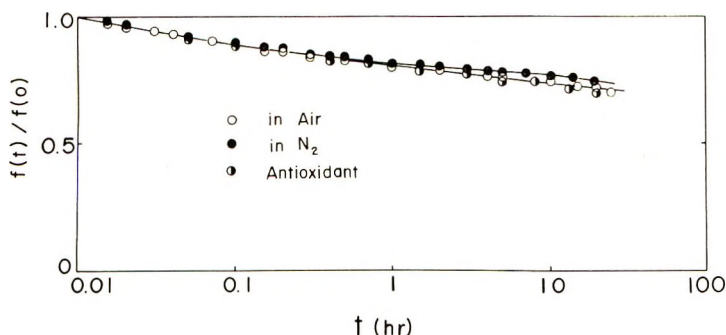


Fig. 1. Stress relaxation of dicumyl peroxide-cured EPT (sample 1) in air, under nitrogen, and in air containing a proper amount of antioxidant at 109°C.

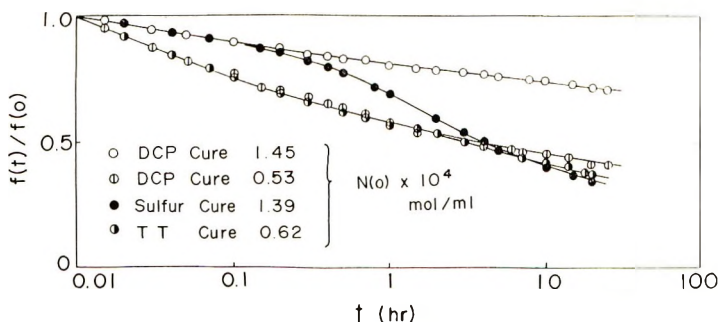


Fig. 2. Stress relaxation of samples 1, 2 (sulfur-cured EPT), and 3 (TT-cured EPT) in air at 109°C.

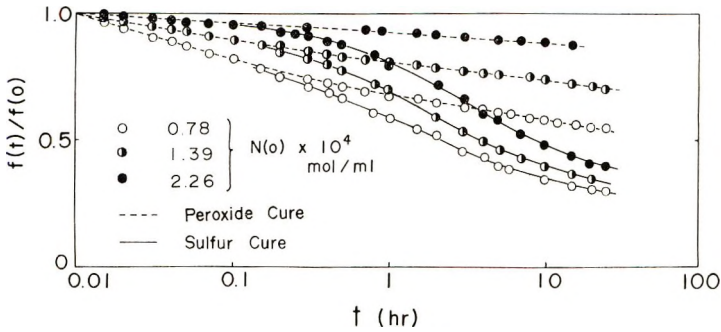


Fig. 3. Stress relaxation of three groups of samples 1 and 2 having the same value of $n(0)$ in air at 109°C .

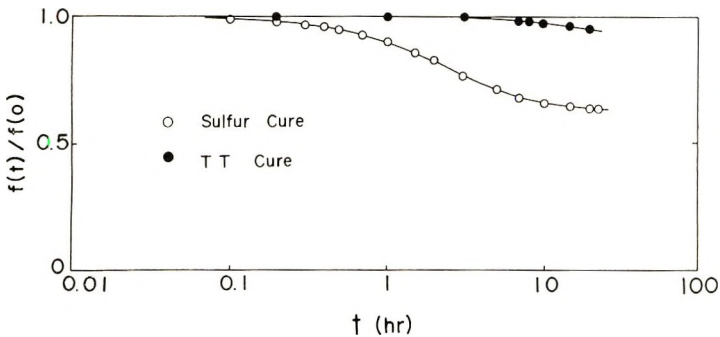


Fig. 4. Pure chemical stress relaxation of samples 2 and 3 obtained from Fig. 2.

When we consider both the chemical structure of sample 1 and the experimental conditions, it seems very reasonable to assume that the relaxation mechanism of the sample is due to a physical relaxation, that is, a physical flow of the polymer chains.

Also, the stress relaxation of type 1 samples having an initial chain density $n(0)$ of 0.53×10^{-4} and 1.45×10^{-4} mole/ml, samples 2 and 3 having $n(0)$ of 1.39×10^{-4} and 0.62 mole/ml, respectively, were measured in air at 109°C . The relation of relative stress versus time is shown in Figure 2. Because Figures 1 and 2 were obtained under the same conditions, the superposed portions of the curves for samples 2 and 3 with that of sample 1 are considered to be due to a physical relaxation. From Figure 2 it was found that the stress decay due to a physical relaxation at the initial stages is independent of the kind of crosslink if the crosslinking density of these polymers is equivalent. For further identification, we have carried out the following experiments. Materials with different kinds of crosslinks and with identical initial densities $n(0)$ were prepared. In these materials, the crosslinks are C-C bond and polysulfide linkage ($-\text{S}\hat{x}-$), and $n(0)$ of the samples have the same density, 0.78×10^{-4} , 1.39×10^{-4} , and 2.26×10^{-4} mole/ml. The stress relaxation curves obtained from these samples are shown in Figure 3. From Figure 3 it is clear that with

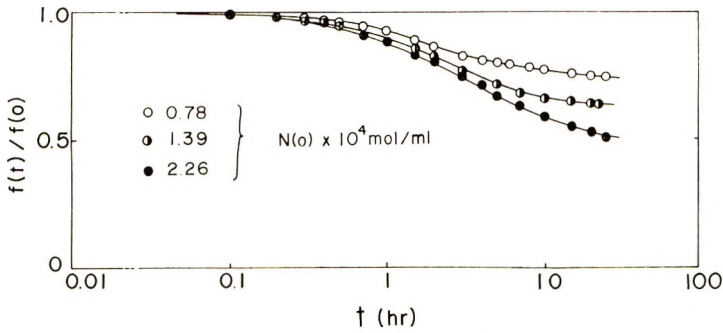


Fig. 5. Pure chemical stress relaxation of sample 2 obtained from Fig. 3.

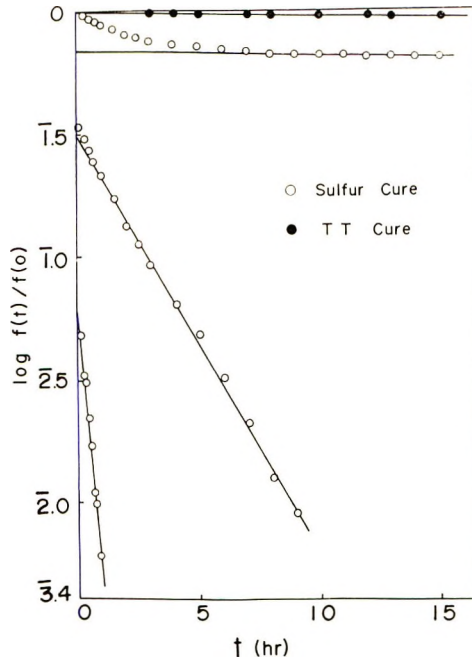


Fig. 6. Replot as $\log f(t)/f(0)$ versus time of two chemical stress relaxation curves in Fig. 4.

a nearly equal value of $n(0)$, the physical relaxations in the initial stage are the same and they overlap, regardless of the kind of crosslink.

In order to discuss the mechanisms of the chemical relaxation in detail, the portions of the stress decay based upon physical flow were reduced from the original stress relaxation curves of EPT polymers; for samples cured with TT (sample 3, Figure 2) and with sulfur (sample 2, Figs. 2 and 3) and their pure chemical stress relaxation curves were replotted (Figs. 4 and 5). It can be easily assumed from Figures 4 and 5 that few cleavages occur at the crosslink in sample 3 and the interchange reactions mostly occur at the crosslinking sites in sample 2.

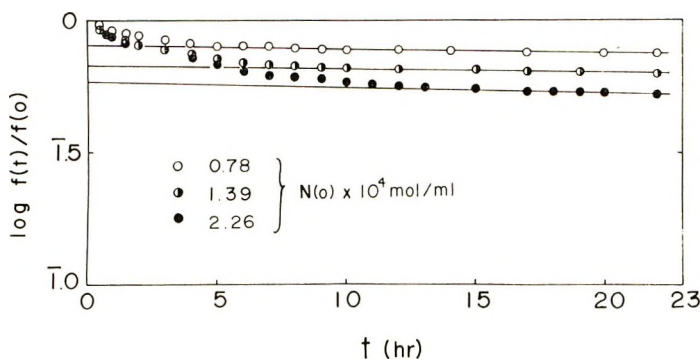


Fig. 7. Replot as $\log f(t)/f(0)$ versus time of three chemical stress relaxation curves in Fig. 5.

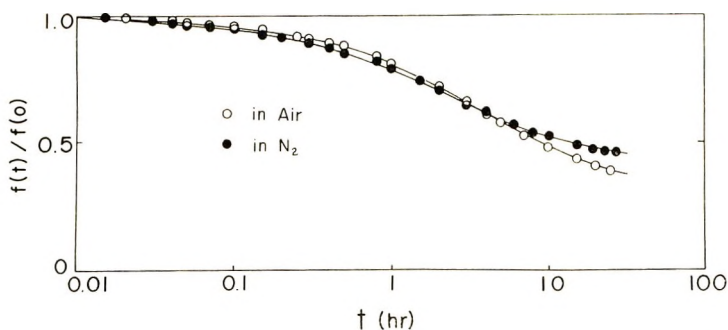


Fig. 8. Stress relaxation curves of sample 2 in air and under nitrogen at 109°C.

Then when the two chemical stress relaxation curves in Figure 4 were replotted as $\log f(t)/f(0)$ versus time, Figure 6 was obtained. From such a plot, a fine straight line was obtained for sample 3. Because there still remained a curved portion of the plot in the short-time region for sample 2 as shown in the figure, we used our suggested procedure^{2,3a} and repeated it until we obtained a straight line in the whole time scale region.

When the three curves of Figure 5 were replotted as $\log f(t)/f(0)$ versus time, as in Figure 6, three straight lines having the same slope in the long-time side region were obtained as shown in Figure 7.

The stress relaxation curve for sample 2 is divided into three fine straight lines by using procedure X as shown in Figure 6. Moreover, in Figure 6, both slopes of a straight line for sample 3 and the uppermost straight line of the three for sample 2 are identical. Further, in Figure 7, all the slopes of three straight lines for sample 2 are independent of chain density, $n(0)$.

The chemical stress relaxation curves of sample 2 under previously described conditions, that is, at 109°C in both air and nitrogen are shown in Figure 8. If these stress decays were based only on the interchange reaction of polysulfide crosslinks, it would be independent of the surroundings; however on the long-time side, it decreases somewhat more sharply in air

than in nitrogen. We may consider that in sample 2, in addition to the interchange reaction of the polysulfide linkages, an oxygen-induced cleavage of mono- and disulfide linkages in the air could explain this behavior.

Generally, scission occurs only at a crosslink in chains of the polymer network. If we represent the number of initial crosslinkages by $C(0)$, the number of scissions after time t by $q(t)$ and the proportionality constant by k , the following equation will be established.

$$dq(t)/dt = k[C(0) - q(t)] \quad (1)$$

On solving eq. (1), eq. (2) is obtained:

$$q(t) = C(0)(1 - e^{-kt}) \quad (2)$$

If $f(t)/f(0)$ is the relative stress and $n(0)$ the initial chain density if scission occurs only at the crosslinks, then eq. (3) is valid:

$$f(t)/f(0) = 1 - [2q(t)/n(0)] \quad (3)$$

In an ideal network of chains, eq. (4) is obtained:

$$2C(0) = n(0) \quad (4)$$

Therefore eq. (5) is deduced:

$$f(t)/f(0) = e^{-kt} \quad (5)$$

When scission occurs only at the crosslink in crosslinked polymer, it is obvious from eq. (5) that the stress relaxation curve is expressed by a Maxwellian decay.

On the other hand, from recent studies,^{4,5} it has been ascertained that the stress relaxation mechanism of crosslinked polymers which undergo an interchange reaction can be expressed by the sum of two exponential terms.

Now, in the case of the sulfur-cured EPT polymer (sample 2), it is assumed from the various experimental results described above that the crosslinking sites of this sample consist of polysulfide, monosulfide, and disulfide linkages. We can deduce for sample 2, that two reactions occur simultaneously at the crosslinkage: typical interchange and cleavage. Therefore it is considered from the above reactions that the relationship between relative stress and time be expressed by eq. (6):

$$\frac{f(t)}{f(0)} = Ae^{-k_1t} + Be^{-k_2t} + Ce^{-k_3t} \quad (6)$$

The first two terms in the right-hand side of eq. (6) are due to the mechanisms of typical interchange reaction and the third term refers to cleavage at the crosslinkage.

For question of why all the slopes of the first straight line in the sample 2 and the ones in the sample 3 equal independent of $n(0)$ may now be answered on the basis of eq. (5) or the third term in eq. (6). According to Tobolsky et al.^{3b,6} in the case when scission occurs only at crosslinkage in the crosslinked polymer, it is recognized that the decay curves of $f(t)/f(0)$

versus time are identical and independent of the chain density $n(0)$. Therefore the value of k of eq. (5) or the third term in eq. (6) is usually a universal constant and is independent of $n(0)$.

As for the question of why for sample 2 there are three straight lines, it is easy to understand that for one straight line there is one term in eq. (6). So, because there are three terms in eq. (6) for sample 2, there are three straight lines.

We are pleased to acknowledge the partial support of Chang Yun-Ho in our laboratory.

References

1. P. F. Lyons, T. C. P. Lee, and A. V. Tobolsky, *Rubber Chem. Technol.*, **39**, 1634 (1966).
2. A. V. Tobolsky and K. Murakami, *J. Polym. Sci.*, **40**, 443 (1959).
3. A. V. Tobolsky, *Properties and Structure of Polymers*, Wiley, New York, 1960, (a) p. 188; (b) p. 235.
4. A. V. Tobolsky, *J. Polym. Sci. B*, **2**, 823 (1964).
5. R. B. Beevers, *J. Colloid Sci.*, **19**, 40 (1964).
6. A. V. Tobolsky, *J. Appl. Phys.*, **27**, 673 (1956).

Received April 8, 1970

Revised June 6, 1970

Hydrogen-Transfer Polymerization of *cis*- and *trans*-Crotonamides

YOSHIAKI KOBUKE, KATSUMI HANJI, and
JUNJI FURUKAWA, *Department of Synthetic Chemistry,*
Kyoto University, Yoshida Kyoto, Japan, and TAKAYUKI FUENO, *Faculty*
of Engineering Science, Osaka University, Toyonaka, Osaka, Japan

Synopsis

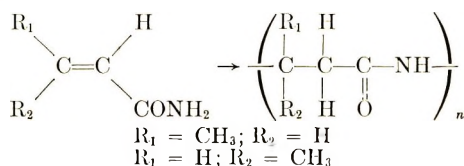
cis- and *trans*-Crotonamides were polymerized in the presence of sodium *tert*-butoxide in pyridine. It was found that both monomers undergo concurrent geometrical isomerization as well as polymerization. Polymers resulting from these isomeric monomers had identical microstructures. The rates of both polymerization and isomerization were evaluated from kinetic measurements. Kinetic investigations have also shown that the specific first-order rate coefficient was independent of the isomer compositions and was identical for *cis* and *trans* monomers. The activation enthalpy was evaluated to be 15.0 kcal/mole.

INTRODUCTION

In a previous paper,¹ we investigated the relative polymerizabilities of the *cis* and *trans* isomer pairs in the vinyl polymerization of alkyl crotonate and crotononitrile in the presence of anionic and coordinated anionic type catalysts. It was proposed that specific interactions of catalyst with polymer end and/or monomer govern the relative reactivities of these α,β -disubstituted olefins.

Much work has been conducted on the hydrogen-transfer polymerization since Breslow et al.² obtained poly(β -amino acid) from acrylamide and related compounds. However, there has been reported no systematic investigation concerning the effect of geometrical isomerism on the relative polymerizability as well as on the resulting polymer structure.

In the present study, we will report the results of the hydrogen-transfer polymerization of *cis*- and *trans*-crotonamides. Specific aims of this work are to gain insights into the relative polymerizabilities of these isomeric monomers and to examine structures of the polymers resulting from the respective isomers.



EXPERIMENTAL

Materials

Commercial *trans*-crotonamide was recrystallized twice from benzene, mp 159–160°C (lit.³ mp 159–160°C). According to the gas-chromatographic analysis, this was free from *cis* isomer and other impurities. The *cis* isomer of crotonamide was obtained by the hydration of *cis*-crotonitrile catalyzed by concentrated sulfuric acid. The *cis*-crotonitrile was obtained by the fractional distillation of the commercial *cis-trans* mixture through a Taika Kogyo spinning band column model TS-SB₁, *cis*, bp 108°C (lit.⁴ bp 108°C). This was 99–100% pure, contaminated with 0–1% of *trans* isomer. The resulting *cis*-crotonamide was recrystallized twice from benzene; mp 101°C (lit.³ mp 100–101°C). This was only 85% pure; 15% of *trans* isomer was inevitably formed by the *cis-trans* isomerization during the hydration.

Pyridine was distilled over potassium hydroxide and redistilled once more over calcium hydride under nitrogen. A middle fraction was collected. Xylene was distilled in the presence of sodium benzophenone ketyl under nitrogen.

Analysis of the Polymer Structure

The infrared spectra of the polymer were measured on KBr pellets. A Nihon Bunko infrared spectrometer model 402G was used. The NMR spectra (a 10% solution in formic acid) were recorded on a Japanese Electron Optics spectrometer model C-60H. The x-ray diffraction of powder samples of the polymer was analyzed by Cu $K\alpha$ by use of a Shimadzu Seisakusho x-ray diffractometer.

Kinetic Measurements

In a glass-stoppered flask of ca. 50 ml capacity with a side arm for nitrogen inlet was placed a 10-ml portion of monomer solution in pyridine containing Tetralin as internal standard for VPC analysis. The initial concentration of monomer was 0.20 mole/l., and the amount of Tetralin used was 60 vol% with respect to monomer. After the mixture was thermostatted at the specified temperature, an 0.125-ml portion of sodium *tert*-butoxide or *n*-butyllithium in pyridine was introduced under magnetic stirring. The concentration of catalyst was 3% (relative to the initial monomer concentration).

At specified intervals of time, aliquots of the reaction mixture were taken with a syringe, and a small amount of methanolic hydrochloric acid was added in order to stop the reaction. The residual monomers, both *cis* and *trans*, were determined by VPC. A Yanagimoto gas chromatograph, model GCG 550T, was used. A 2.25 m \times 3 mm column packed with 30% poly(ethylene glycol) 20M on Celite 545 (80–100 mesh) was operated at 180°C with helium as carrier gas. The peak integration was carried out by

using a Kimura Denshi electronic integrator model E-2A. It was found by calibration that the internal standard method fully sufficed for linearly correlating the obtained peak areas to the isomer concentrations.

RESULTS

Polymer Structure

The homopolymerization of each of the *cis* and *trans* isomers of crotonamide was conducted in pyridine or xylene, sodium *tert*-butoxide or *n*-butyllithium being used as catalyst. The results are shown in Table I.

TABLE I
Polymerization of Each *cis*- and *trans*-Crotonamide^a

Run no.	Catalyst	Monomer	Solvent	Temp, °C	Yield, %
1	<i>tert</i> -BuONa	<i>cis</i>	Pyridine	100	30.4
2	<i>tert</i> -BuONa	<i>trans</i>	Pyridine	100	32.0
3	<i>n</i> -BuLi	<i>cis</i>	Xylene	100	30.4
4 ^b	<i>n</i> -BuLi	<i>trans</i>	Xylene	100	23.3
5	<i>n</i> -BuLi	<i>cis</i>	Xylene	130	33.4
6	<i>n</i> -BuLi	<i>trans</i>	Xylene	130	44.0

^a [Monomer]₀ = 5.0×10^{-3} mole; [*tert*-BuONa] = 8.3×10^{-5} mole; [*n*-BuLi] = 7.5×10^{-5} mole; time, 24 hr.

^b Monomer was only partially soluble in this run.

The infrared spectra of the resulting polymers are shown in Figure 1.

In a given catalyst-solvent system almost identical polymers resulted from the *cis* and *trans* isomers, while the structural differences are distinct on comparing the polymers obtained by the two different types of catalyst-solvent systems.

Analogous trends were observed in both the NMR spectra and the x-ray diffraction patterns of the same samples. Figures 2 and 3 show representative NMR spectra and x-ray diffraction patterns of the polymers resulting from the *trans* isomer.

These results imply that the polymer structures resulting from the *cis* and *trans* monomers be identical with regard to the stereoregularity of the β -carbon.

Kinetic Measurements

Illustrated in Figure 4 is the reaction course of the *trans*-crotonamide in pyridine at 100°C in the presence of sodium *tert*-butoxide as catalyst. It was found that both geometrical isomerization and polymerization occurred concurrently with comparable rates. Despite the complex nature of the reaction, the polymerization reaction was found to fit the first-order kinetic law with respect to the total isomer concentration, [*cis* + *trans*].

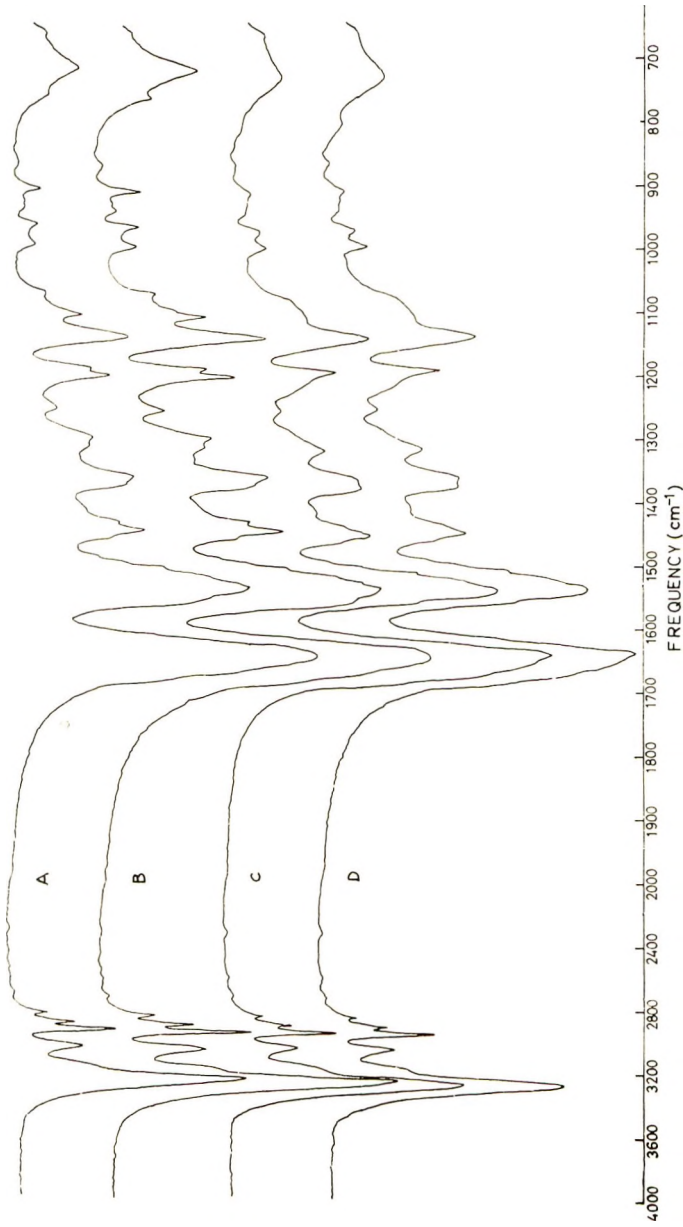


Fig. 1. Infrared spectra of polyacrylonamide prepared from each *cis* and *trans* isomer by *tert*-BuONa and *n*-BuLi: (A) *cis* isomer, *tert*-BuONa, pyridine, 100°C; (B) *trans* isomer, *tert*-BuONa, pyridine, 100°C; (C) *cis* isomer, *n*-BuLi, xylene, 130°C; (D) *trans* isomer, *n*-BuLi, xylene, 130°C.

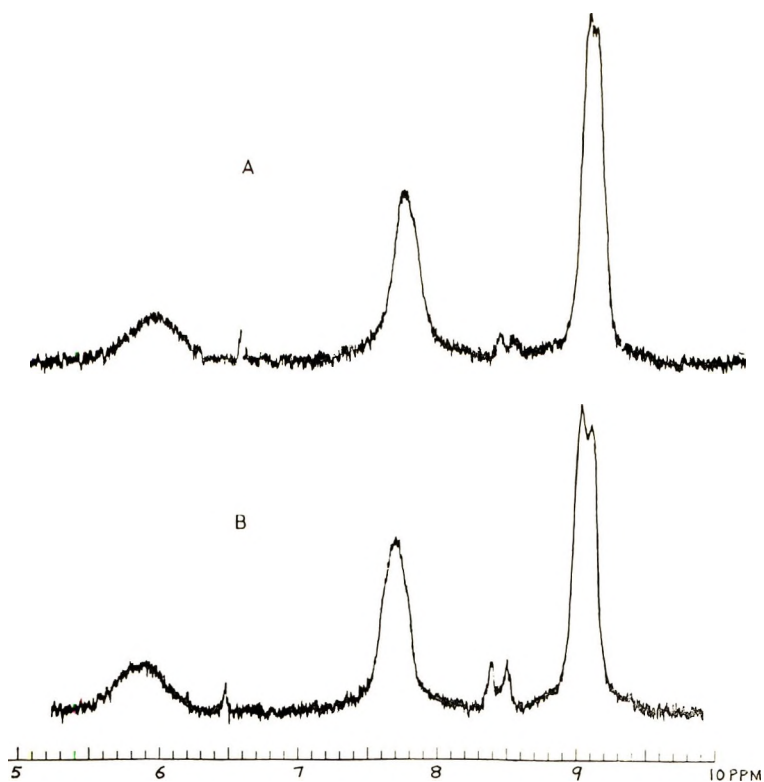


Fig. 2. NMR spectra of poly(*trans*-crotonamide). (A) *tert*-BuONa, pyridine, 100°C; (B) *n*-BuLi, xylene, 130°C.

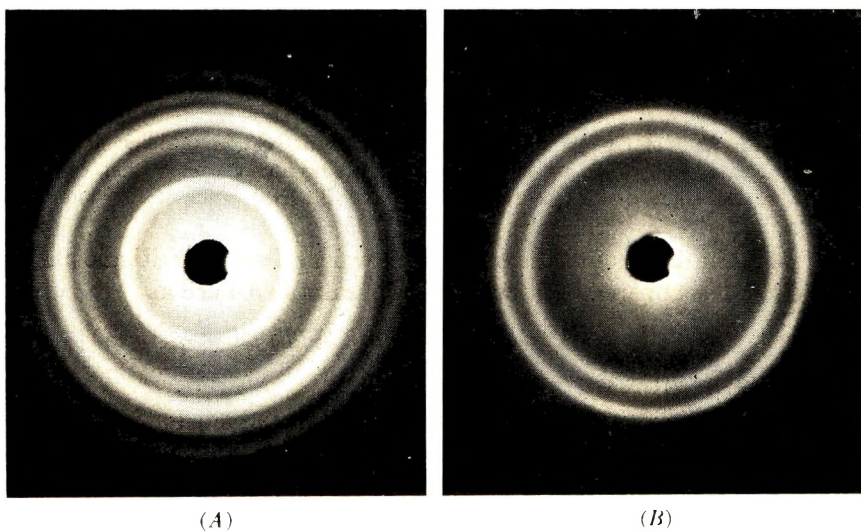


Fig. 3. X-Ray diffraction patterns of poly(*trans*-crotonamide): (A) *tert*-BuONa, pyridine, 100°C; (B) *n*-BuLi, xylene, 130°C.

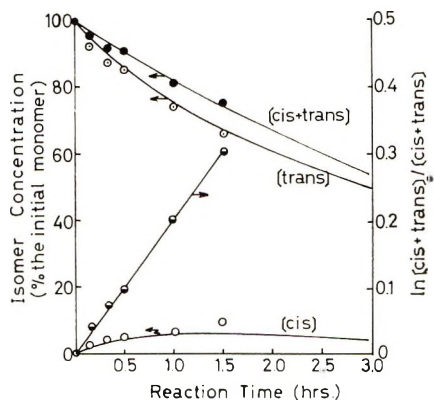


Fig. 4. Reaction of *trans*-crotonamide with *tert*-BuONa in pyridine at 100°C: (—) calculated; (O, ○, ●, ●) experimental. $[\text{Monomer}]_0 = 2.0 \times 10^{-1}$ mole/l.; $[\text{tert-BuONa}] = 6.0 \times 10^{-3}$ mole/l.

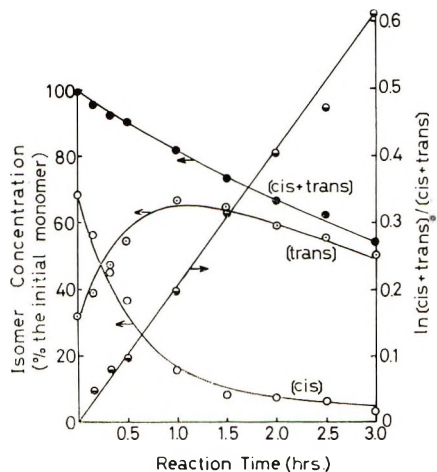


Fig. 5. Reaction of *cis*-rich crotonamide with *tert*-BuONa in pyridine at 100°C: (—) calculated; (O, ○, ●, ●) experimental. Starting isomer composition, 68% *cis*, 32% *trans*; $[\text{Monomer}]_0 = 2.0 \times 10^{-1}$ mole/l.; $[\text{tert-BuONa}] = 6.0 \times 10^{-3}$ mole/l.

The first-order decay of the monomer is shown by a semilogarithmic plot in Figure 4. The apparent first-order rate constant k , defined as

$$-d(C + T)/dt = k(C + T) \quad (1)$$

was evaluated to be $3.4 \times 10^{-3} \text{ min.}^{-1}$

A similar situation was noticed in another run conducted at 100°C with the use of a starting isomer mixture of 70% *cis* and 30% *trans*, as is depicted in Figure 5. The isomerization of the *cis* to *trans* isomer was much faster than the reverse, so that the isomer composition changed to *trans*-rich at later stages of the reaction. The first-order rate constant for the disappearance of monomer was evaluated to be $3.4 \times 10^{-3} \text{ min}^{-1}$, in per-

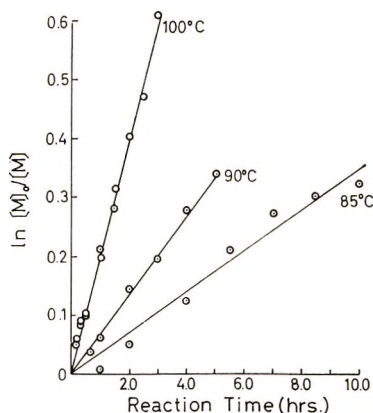


Fig. 6. First-order plots of the system, crotonamide, *tert*-BuONa, pyridine. Starting isomer: (◐) *trans*; (◑) *cis*.

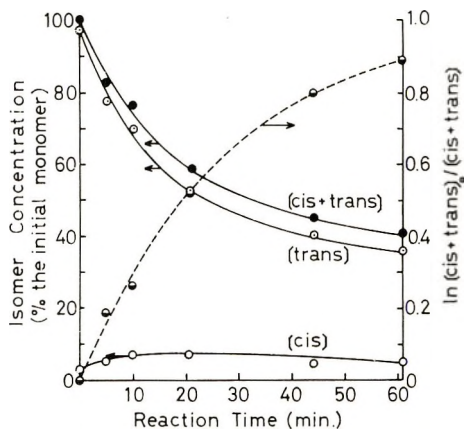


Fig. 7. Reaction of *trans*-rich crotonamide with *n*-BuLi in pyridine at 90°C. Starting isomer composition, 3% *cis*, 97% *trans*; $[Monomer]_0 = 2.0 \times 10^{-1}$ mole/l.; $[n\text{-BuLi}] = 6.0 \times 10^{-3}$ mole/l.

fect agreement with the value obtained with the use of pure *trans* isomer as the starting feed monomer.

The findings that the first-order law of the form of eq. (1) holds and that the observed first-order rate constants are independent of the isomer composition strongly suggest that the specific rate constants for polymerization of the *cis* and *trans* monomers are the same under identical reaction conditions.

The first-order plots at different temperatures in Figure 6 were found to be satisfactorily good within certain experimental errors involved. The activation enthalpy was evaluated to be 15.0 kcal/mole for this polymerization system. This value is to be compared with 9.2 kcal/mole reported for the polymerization of acrylamide by the same catalyst-solvent system.⁵

A further kinetic approach was attempted by use of *n*-butyllithium as catalyst. Unfortunately, however, the deactivation of catalyst seems to be serious in this case, as may be seen in Figure 7. The situation has prevented us from gaining additional insights into the effects of the catalyst on the relative polymerizabilities.

DISCUSSION

To elucidate a possible mechanism pertinent to the kinetic results, we assume the following scheme of elementary processes:



The rate expressions pertinent to the scheme (2)–(4) are as follows:

$$-d[C]/dt = (k_1 + k_3)[C] - k_2[T] \quad (5)$$

$$-d[T]/dt = (k_2 + k_4)[T] - k_1[C] \quad (6)$$

Solutions of the rate eqs. (5) and (6) are expressed as follows:

$$\begin{aligned} \frac{[C]}{[C_0] + [T_0]} = & \frac{1}{\lambda_1 - \lambda_2} \left(- \left\{ (k_2 + k_4 - \lambda_1) \frac{[C_0]}{[T_0] + [C_0]} \right. \right. \\ & \left. \left. + k_3 \frac{[T_0]}{[C_0] + [T_0]} \right\} e^{-\lambda_1 t} + \left\{ (k_2 + k_4 - \lambda_2) \frac{[C_0]}{[C_0] + [T_0]} \right. \right. \\ & \left. \left. + k_3 \frac{[T_0]}{[C_0] + [T_0]} \right\} e^{-\lambda_2 t} \right) \quad (7) \end{aligned}$$

$$\begin{aligned} \frac{[T]}{[C_0] + [T_0]} = & \frac{1}{\lambda_1 - \lambda_2} \left(- \left\{ (k_1 + k_3 - \lambda_1) \frac{[T_0]}{[C_0] + [T_0]} \right. \right. \\ & \left. \left. + k_4 \frac{[C_0]}{[C_0] + [T_0]} \right\} e^{-\lambda_1 t} + \left\{ (k_1 + k_3 - \lambda_2) \frac{[T_0]}{[C_0] + [T_0]} \right. \right. \\ & \left. \left. + k_4 \frac{[C_0]}{[C_0] + [T_0]} \right\} e^{-\lambda_2 t} \right) \quad (8) \end{aligned}$$

where

$$\lambda_1 = \alpha + \sqrt{\alpha^2 - \beta} \quad (9)$$

$$\lambda_2 = \alpha - \sqrt{\alpha^2 - \beta} \quad (10)$$

with

$$\alpha = (k_1 + k_2 + k_3 + k_4)/2 \quad (11)$$

$$\beta = k_2 k_3 + k_3 k_4 + k_4 k_1 \quad (12)$$

Before examining the reaction courses by the aid of eqs. (7) and (8), we sum up the eqs. (5) and (6) to obtain:

$$-\frac{d[C] + [T]}{dt} = k_3[C] + k_4[T] \quad (13)$$

The condition necessary to assure the first-order decay of the total monomer concentration, eq. (1) is as follows:

$$k_3 = k_4 = k \quad (14)$$

The rate constant k (and hence the values of k_3 and k_4) at 100°C has been obtained from the plots of $\log ([C] + [T])$ versus t , as has already been shown in Figures 4 and 5. With the values of k_3 and k_4 at hand, we may obtain the best set of k_1 and k_2 values at the same temperature by fitting eqs. (7) and (8) to the experimental points in Figures 4 and 5. The best fit resulted when the following set of rate constants were used:

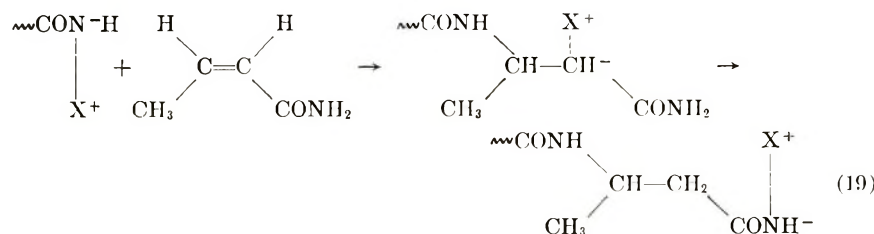
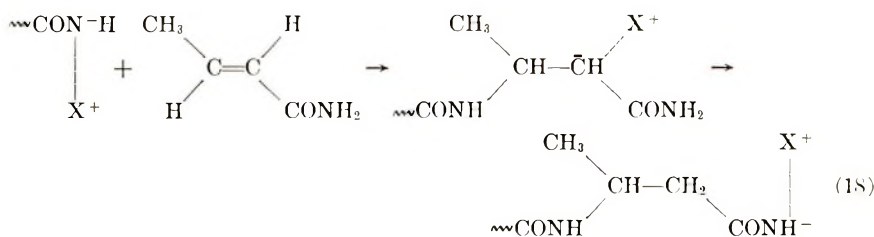
$$k_1 = 25.0 \times 10^{-3} \text{ min}^{-1} \quad (15)$$

$$k_2 = 2.5 \times 10^{-3} \text{ min}^{-1} \quad (16)$$

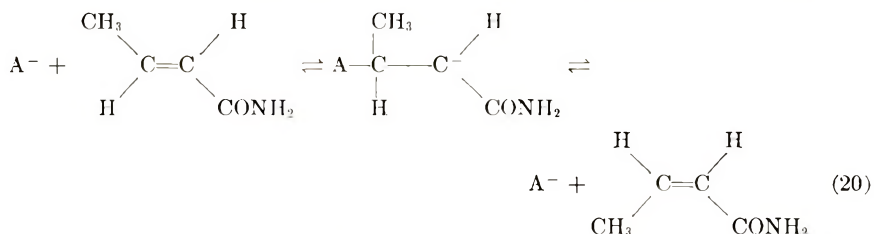
$$k_3 = k_4 = 3.4 \times 10^{-3} \text{ min}^{-1} \quad (17)$$

Those curves shown in Figures 4 and 5 are the isomer compositions calculated from eqs. (7) and (8) with the above set of rate constants. The experimental data of the isomer compositions accommodated in these figures are in fair agreement with calculated curves. This agreement seems to ensure the validity of the kinetic scheme here proposed. The isomerization equilibrium constant is thus roughly evaluated as $k_1/k_2 = 10.0$, indicating the prevalence in concentration of the *trans* isomer over the other at equilibrium at 100°C .

Hydrogen-transfer polymerization of *cis*- and *trans*-crotonamides may proceed as shown in eqs. (18) and (19).



As has already been described, the spectral data imply that the polymer structures resulting from *cis* and *trans* monomers are identical with regard to the stereoregularity of the β -carbon. This interpretation is based on the fact that no difference is observable between the spectra of polymers formed from *cis* and *trans* isomers, while distinct difference can be observed when comparisons are made between the spectra of the polymers obtained by use of the two different types of catalyst-solvent systems. However, these are of no concern whether the opening mode of the α,β -disubstituted olefin is regular or not, because the hydrogen transfer to the α -carbon makes it impossible to elucidate the opening mode of the α,β -disubstituted olefins. The concurrent isomerization reaction may be expressed as in eq. (20).



It is, however, an open question whether A^- is an ion derived from catalyst employed or polymer end itself, or other totally different mechanisms are involved.

The kinetic investigations described above strongly suggest that the *cis*- and *trans*-crotonamides have identical polymerizabilities for the *tert*-Bu-ONa-pyridine system. This result is quite characteristic of the present polymerization. This might give a denial to the hypothetical higher polymerizability of the transient *cis*-crotonamide which was assumed to be formed in the polymerization of vinylacetamide by similar catalyst-solvent systems.⁶ The nearly equal polymerizabilities of *cis*- and *trans*-crotonamides under the present conditions are compatible with the statement¹ that the *cis* and *trans* isomers of nitriles show approximately the same reactivities in the anionic polymerizations by the nonstereospecific catalyst-solvent systems.

References

1. Y. Kobuke, J. Furukawa, and T. Fueno, *J. Polym. Sci. A-1*, **5**, 2701 (1967).
2. D. S. Breslow, G. E. Hulse, and A. S. Matlack, *J. Amer. Chem. Soc.*, **79**, 3760 (1957).
3. P. Bruylants and A. Castille, *Bull. Sci. Acad. Roy. Belg.*, **13**, 767 (1928).
4. P. Bruylants and A. Christiaen, *Bull. Soc. Chim. Belges*, **34**, 144 (1925).
5. N. Ogata, *Makromol. Chem.*, **40**, 55 (1960).
6. H. Nakayama, T. Higashimura, and S. Okamura, *J. Macromol. Sci.*, **A2**, **53** (1968).

Received June 24, 1970

γ -Radiation-Induced Ionic Polymerization of Pure Liquid Styrene. III. Effect of Temperature

R. C. POTTER* and D. J. METZ, *Brookhaven National Laboratory,
Upton, New York 11973*

Synopsis

We have extended our previously reported studies on the radiation-induced ionic polymerization of styrene to higher dose rates and have covered a temperature range between 0 and 50°C. The data at 0°C are in striking agreement (up to 10⁶ rad/hr) with the mechanism proposed by Williams, Okamura, et al.; on the other hand, styrene of the highest purity exhibits a very complex behavior with temperature variations, which does not agree with this mechanism. These apparent anomalies are presented and discussed. Data are also presented on the effects of adding dry oxygen or degassed water to pure styrene.

INTRODUCTION

The initial communication¹ in this series pointed out that exhaustively purified styrene exhibits novel kinetic behavior under the influence of ⁶⁰Co γ -radiation. Very high rates of polymerization (e.g., $R_p = 400\%$ /hr at 0°C, 1 Mrad/hr), a linear dependence of R_p on dose rate, and molecular weights independent of dose rate led to the conclusion that ionic propagating species had, in some manner, been stabilized as a consequence of ultra-purification. This somewhat precipitous departure from classical radical kinetics was marred, however, by a high degree of irreproducibility of the rates of polymerization. The second paper² of the series removed this difficulty by describing a modified purification technique which so sufficiently enhanced sample purity that reproducible kinetic results were obtained. Rates of polymerization reached a limiting level far above the values previously observed (e.g., $R_p = 940\%$ /hr at 0°C, 1 Mrad/hr), while the dose rate dependence decreased to 0.70.

Preliminary results from temperature studies² exhibited bewildering complexity. It is the purpose of the present communication to report further on these temperature phenomena. Also, studies have been made on the effect of deliberately added impurities and the dependence of molecular weight upon temperature and dose rate.

* Present address: Shell Development Co., Modesto, California 95352.

EXPERIMENTAL PROCEDURE

The inherently clean nature of a vacuum is relied upon throughout the course of monomer purification and, consequently, the monomer sample is constantly maintained in a vacuum environment. In essence, the scheme for monomer purification comprises four fundamental operations: vacuum distillation, vacuum bake-out of glassware, degassing, and contacting of monomer with activated silica gel (the second and fourth steps being particularly effective in eliminating traces of water). The details of this preparative procedure have already been described.²

Temperature studies relied upon the same type of dilatometer as that used previously.² However, the deliberate addition of impurities required a new dilatometer design (Fig. 1). The preparation of a sample in such a

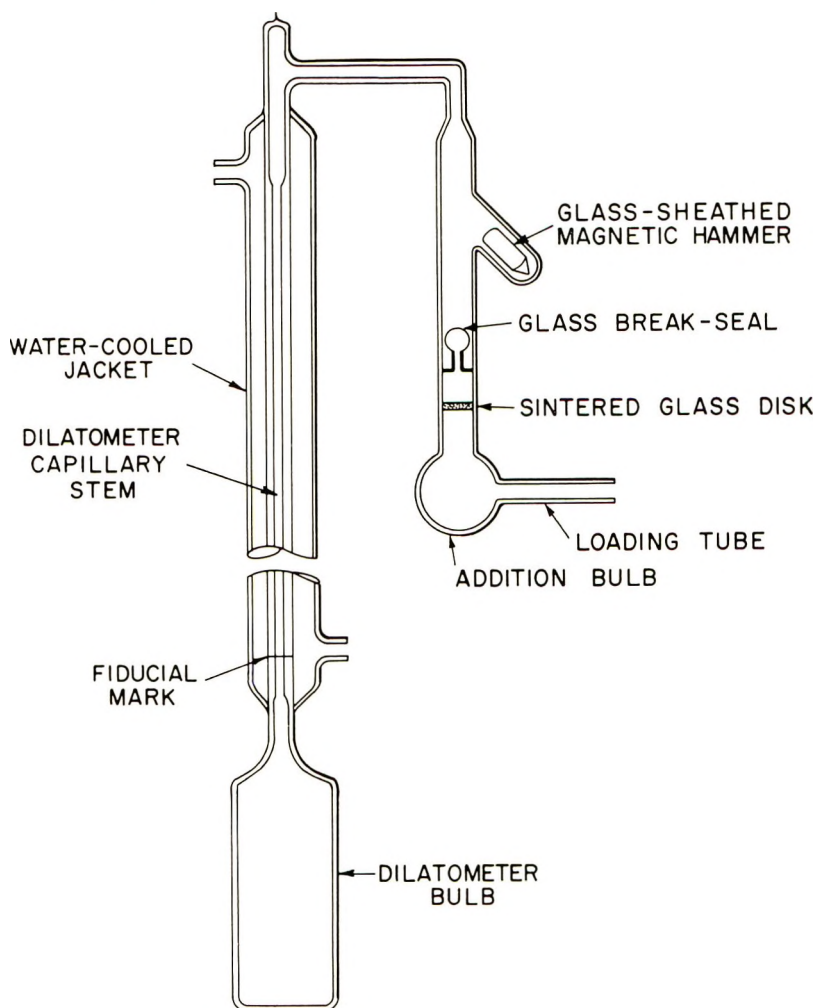


Fig. 1. Diagram of dilatometer modified to allow addition of impurity.

dilatometer requires a slight departure from the purification scheme. For the addition of oxygen, a small amount of silica gel is placed in the side-arm bulb. (Note that the sintered glass disk in Figure 1 acts as a retaining plug. Thus, when the break-seal is opened for an experiment, the silica gel is confined to the addition bulb.) By means of a length of glass tubing, the loading tube is connected directly to the high vacuum manifold. After bake-out and sealing at a point past the attachment of the loading tube, oxygen (99.6% purity) is bled into the manifold through a venting port in the vacuum system. The side-arm bulb, containing oxygen and the drying agent, is then isolated by flame-sealing the loading tube. Finally, the manifold is evacuated and rebaked with heater tape. The normal sequence in the preparative scheme is then resumed. (See Part II² for complete details on manifold, baking procedures, etc.)

In the case of water addition, it is not necessary to modify the standard procedure. The empty side-arm bulb is left exposed to the atmosphere during bake-out. After filling and sealing off the dilatometer, the loading tube of the side-arm is connected to the manifold. An ampoule of distilled water is attached to the manifold through a side-arm containing a break-seal. Upon the conclusion of a manifold bake-out, the break-seal is opened and the water is degassed. Water is then distilled into the addition bulb and the apparatus is sealed off.

Molecular weight data were obtained from eleven batch-irradiation samples. These ampoules, each shaped like a dilatometer bulb, were prepared simultaneously by the normal procedure.

Determination of molecular weight, calculation of rates of polymerization (gravimetric and dilatometric), method of irradiation, and dosimetry have all been described elsewhere.¹ Total conversions were generally kept below 10%.

RESULTS

Figure 2 shows data obtained from five dilatometers and two ampoules irradiated at 0°C. It is readily evident that over three orders of magnitude of dose rate and within fairly narrow limits of reproducibility, the relationship between the polymerization rate R_p and dose rate I can be expressed as

$$R_p \propto I^{0.65}$$

The behavior of these same samples at several temperatures is shown in Figure 3. The dilatometer on which the three highest dose rates were investigated at 0°C was not investigated at the higher temperatures. Figure 3d is a composite of the observed temperature behavior, in which each line is drawn between the dose rates over which the data were actually obtained. Instead of the parallel Arrhenius arrangement which one might expect, there is a definite skewed pattern. The 0°C and 50°C isotherms are approximately parallel, as are the 25°C and 40°C isotherms.

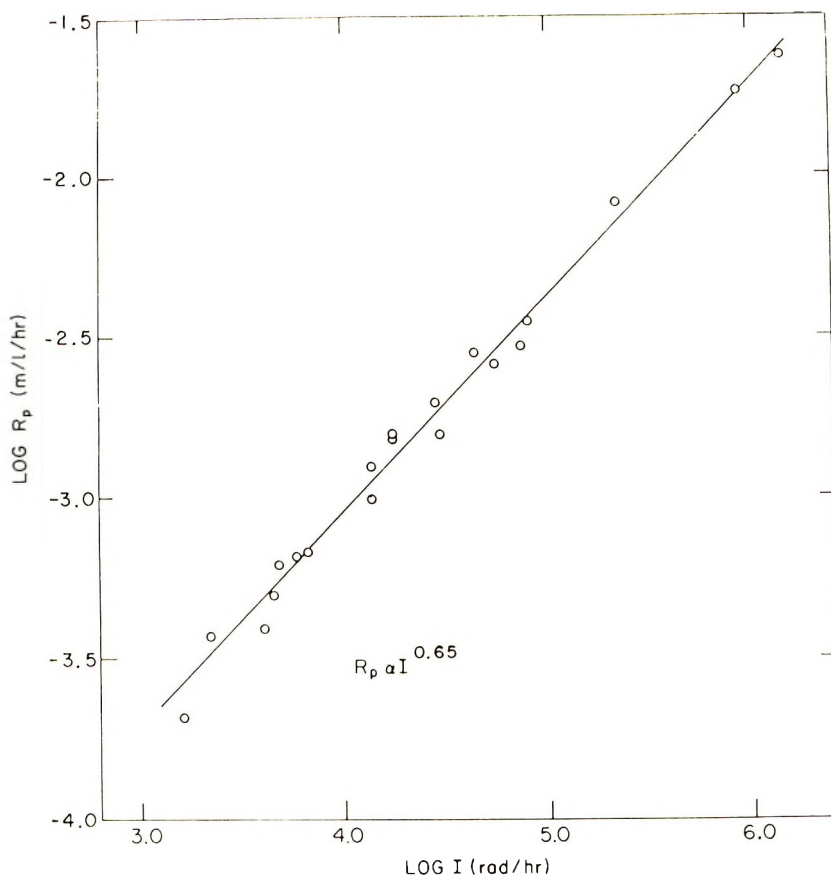


Fig. 2. Rate of polymerization of highest purity styrene at 0°C as a function of dose rate.

We have already indicated² that the preparation scheme does not always yield the maximum rates of polymerization. Presumably this occurs when a trace contaminant (such as water) is present which, ideally, should be reduced to the same level of concentration in each preparation. Thus, the rates shown in Figures 2 and 3 should be regarded as the "ceiling" rates attainable with our present method of monomer purification.

When the observed rates of polymerization do fall below the ceiling values, quite another picture of the temperature behavior develops. Figure 4 shows the results obtained from two slightly impure, independently prepared samples. It is immediately obvious that in each case the isotherms conform more closely to an Arrhenius temperature behavior and that the polymerization rate varies inversely with temperature. In addition, it can be observed that the greater the deviation from the ceiling rates, the more closely the isotherms are spaced and, further, that there is a corresponding increase in dose rate dependence.

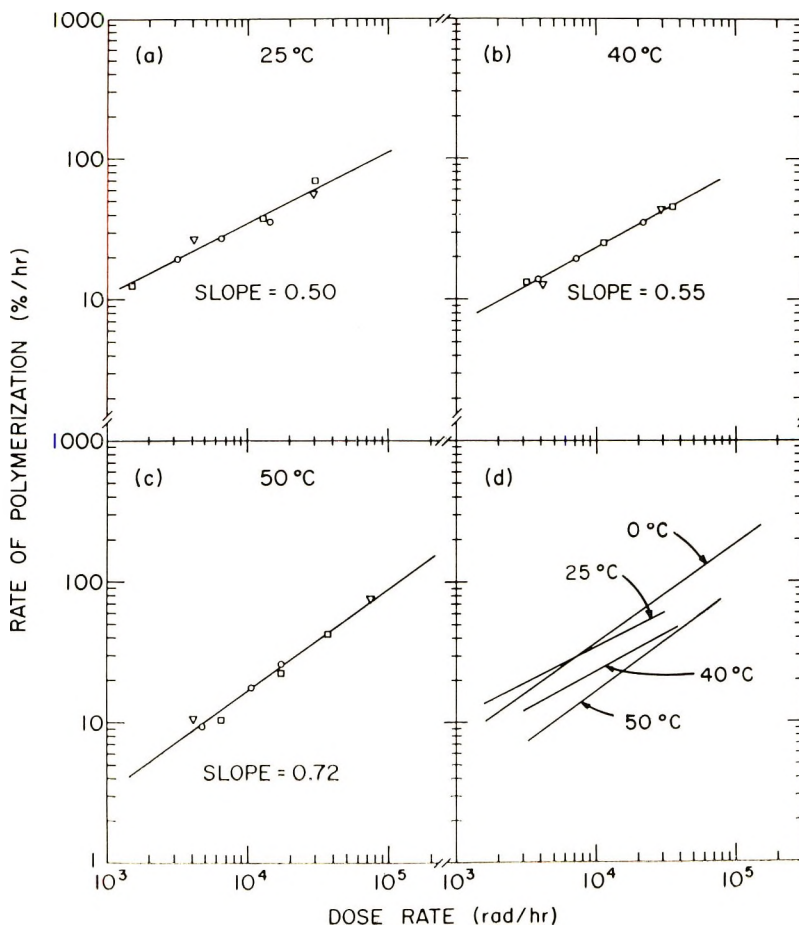


Fig. 3. Rate of polymerization of highest purity styrene as a function of dose rate at: (a) 25°C, (b) 40°C, (c) 50°C, and (d) composite of data at four temperatures.

The series of experiments involving deliberately added impurities were carried out to determine the effect of adding saturation quantities of either dry oxygen or degassed water to ultrapure styrene. The oxygen addition dilatometer contained 0.4 atm of oxygen in the side-arm bulb. This amounts to a threefold excess, based on the solubility of oxygen in styrene at room temperature.⁴ Prior to the addition of oxygen, the dilatometer was irradiated at 0°C and a dose rate of 3800 rad/hr. As illustrated in Figure 5, the resultant rate of polymerization was close to the ceiling rate.

Having established a base rate, the break-seal on the addition dilatometer was opened. The gas was distributed throughout the monomer by alternately freezing and thawing the dilatometer bulb. Upon irradiation at 0°C, the oxygen-saturated styrene exhibited a continuous decrease in rate of polymerization. Thus, at a dose rate of 3800 rad/hr, R_p decreased from 3%/hr to 0.7%/hr in 45 min. On changing to a higher dose rate (67,500

rad/hr), R_p decreased from 7.7 to 5.2%/hr in 35 min. On returning to a dose rate of 3800 rad/hr, the rate of reaction was 0.3%/hr.

At this point, the rate of decrease of R_p was low enough so that a dose rate dependence could be obtained. Figure 5 shows that this dependence (0.87) has increased above the ceiling value (0.65). Finally, the styrene was

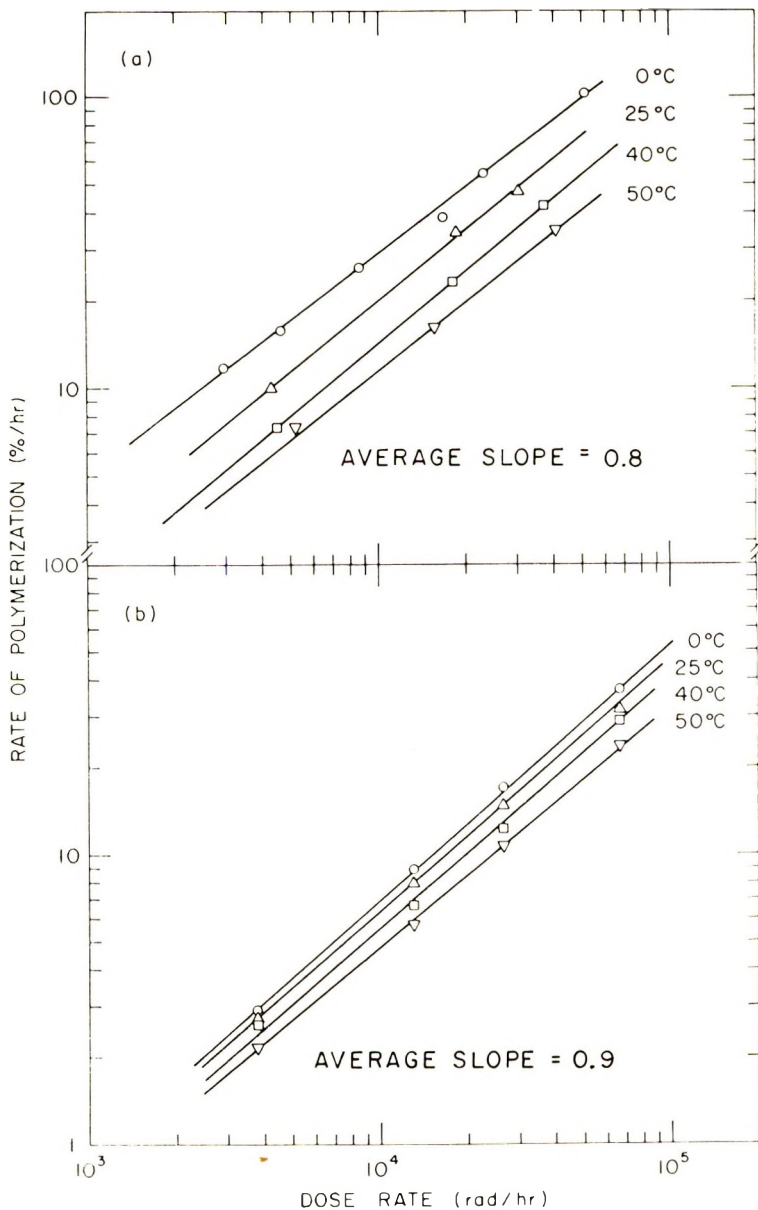


Fig. 4. Rate of polymerization of two slightly impure samples of styrene as a function of dose rate at several temperatures.

mixed further with the remaining oxygen which, at 67,500 rad/hr, resulted in a rate of polymerization which was about three times the classical value.

The effect of deliberately adding water to the reaction system was investigated with another, independently prepared impurity-addition

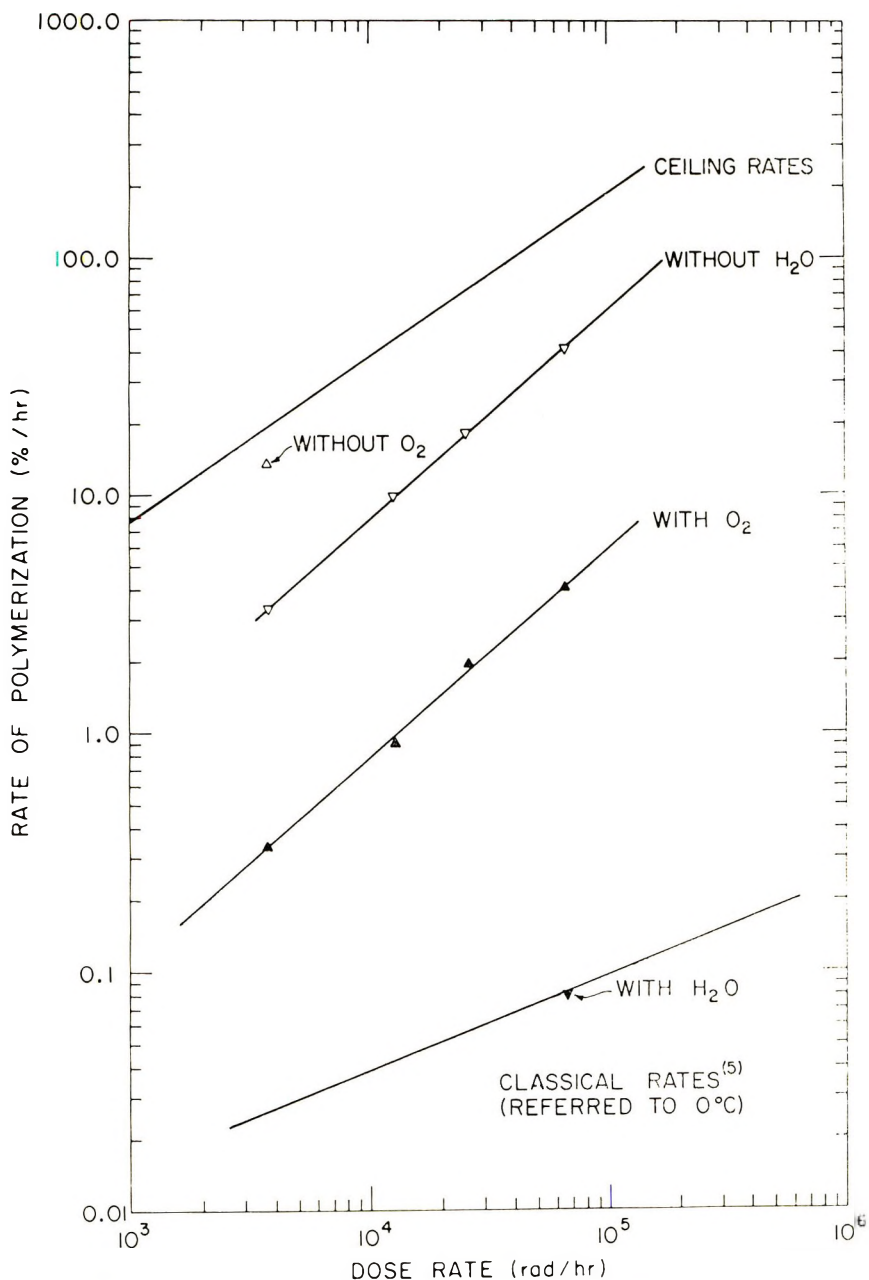


Fig. 5. Effect of adding either dry oxygen or degassed water to styrene which exhibits ionic kinetics before addition of impurity.

dilatometer. Again, base rates were established before the addition of the impurity. In Figure 5 it is seen that the rates of the original sample are considerably below the maximum rates, yet clearly within the range where the principal propagating species must be ions. After opening the glass break-seal, a small amount of water was distilled into the dilatometer capillary by the condensing effect of water flowing through the dilatometer cooling jacket. The dilatometer bulb was frozen; then the side-arm bulb was frozen and sealed. The amount of water transferred was estimated by the difference in meniscus height of the thermally equilibrated (0°C) dilatometer before and after addition. Thus, the sample contained 0.2% water (by weight), which is ten times the saturation value at 0°C.⁴ The water was thoroughly mixed with the styrene by several freeze-thaw cycles. The excess water, in the form of a small immiscible bead, was easily visible. When the sample was reirradiated at 67,500 rad/hr, the experimental rate of reaction coincided with the classical free-radical rate as shown in Figure 5.

The molecular weight data for the eleven ampoules are presented in Table I. The rates of polymerization of these samples, calculated as the ratio of

TABLE I
 \bar{M} Values of Polystyrene at Several Dose Rates and Temperatures

T , °C	M at various I			
	4100 rad/hr	13,700 rad/hr	29,200 rad/hr	73,800 rad/hr
0	85,000	86,000	91,000	90,000
25	88,000	—	82,000	—
40	80,000	—	71,000	—
50	71,000	—	68,000	67,000

total conversion to time, fall on the ceiling rate curves displayed in Figures 2 and 3 at the four different temperatures.

DISCUSSION

Comparison with Theory

Sufficient evidence has been presented^{1,2,7-12} to demonstrate conclusively that the radiation-induced polymerization of pure liquid styrene proceeds by an ionic mechanism at temperatures below, at, and above room temperature. The condition which must be met is the reduction of impurities (in most cases water) to levels far below direct analytical detection. Under these conditions the normal free radical polymerization, which may or may not be interfered with by the ionic processes, constitutes an almost negligible contribution to the net results. Thus the process can be described as an ionic polymerization.

Williams et al.¹³ have provided a rather successful quantitative description of the process for styrene, isobutyl vinyl ether, and α -methylstyrene,

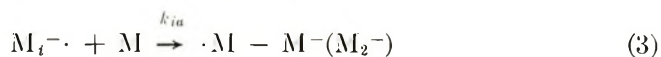
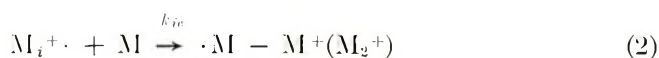
which, in principle, should also be applicable to other monomers which show similar behavior. The assumed kinetic mechanism and the several physical assumptions are reproduced here, with the use of their nomenclature,¹³ for the reader's convenience.

For a pure monomer (M) which is absorbing energy from a radiation field at the rate of I (eV/cm³-sec) and producing free (separated) ions with a yield of G_i ions per 100 eV energy absorbed, the mechanism of eqs. (1)-(11) is written.

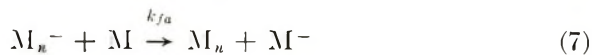
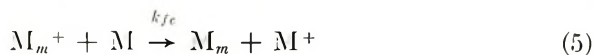
Initiation:



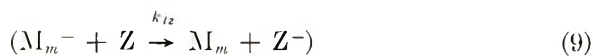
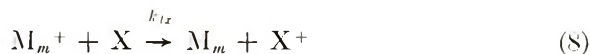
$$R_i = IG_i/100$$



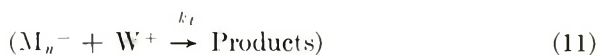
Propagation and transfer:



Termination by impurity:



Termination by recombination:



In this scheme the nature of M and M_m^+ or M_n^- is obvious, X (and Z) represent impurities, and $[\text{Y}^-]$ represents the total concentration of all negative species (while $[\text{W}^+]$ represents the total concentration of all positive species). Reactions (9) and (10) are absent from the original scheme and are included here only for generality. They, and several other reactions, are neglected on the basis of assumptions incorporated in the original scheme.¹³

Reaction (5) and its counterpart reaction (7) are included because, unless there is a great amount of chain transfer to monomer, abnormally high values of G_i are calculated. For instance, in styrene at 0°C and at a dose rate $I = 3 \times 10^{13}$ eV/cm³-sec, the measured rate of polymerization is 14.5%/hr.² This yields a value of G_i (monomer molecules disappearing per 100 eV absorbed) of 610,000. Since the average \overline{DP} is of the order of 10^3 (see Table I), in the absence of chain transfer a value of $G_i = 10^3$ would result. Such values cannot be reconciled with any known ion yields in either the gaseous state or condensed phases, requiring that the origin of most molecular chains is regenerative chain transfer rather than direct initiation by radiation.

On accepting the frequent occurrence of chain transfer to monomer in styrene and the demonstrated inhibitory effects of water,^{1,2,10-12} ammonia,¹⁴ and amines,¹⁴ and the apparent relationship between proton affinity and efficiency of retardation,¹⁴ it is postulated¹³ that the mechanism can be further simplified by assuming that reactions (6), (7), (9), and (11) represent processes of negligible importance, i.e., the principal propagating species is the carbonium ion, M_m^+ . Invoking steady-state kinetics, assuming that rate constants are not a function of the size of the reacting species and imposing the condition of electrical charge neutrality on the system, Williams et al.¹³ show, in a simple and elegant fashion, that the rate of polymerization R_p can be expressed as a function of several kinetic parameters, viz.,

$$R_p = \frac{R_i k_p [M]}{(R_i k_t)^{1/2} + k_{tx} [X]} \quad (12)$$

where k_p has replaced k_{pc} .

It is interesting to investigate briefly the asymptotic behavior predicted by eq. (12). Under those conditions where the impurity level is quite high but still allows for predominating ionic propagation,

$$k_{tx} [X] \gg (R_i k_t)^{1/2}$$

and

$$R_p \propto R_i \propto I$$

At the other end of the range of behavior, where the impurity level is insignificant

$$(R_i k_t)^{1/2} \gg k_{tx} [X]$$

$$R_p \propto R_i^{1/2} \propto I^{1/2}$$

In general, then, it is to be expected that

$$R_p \propto I^n \quad 0.5 \leq n \leq 1$$

depending on the importance of impurity termination (and hence impurity concentration) relative to ion-ion recombination. This range of behavior as a function of purity has been reported by us previously.^{1,2}

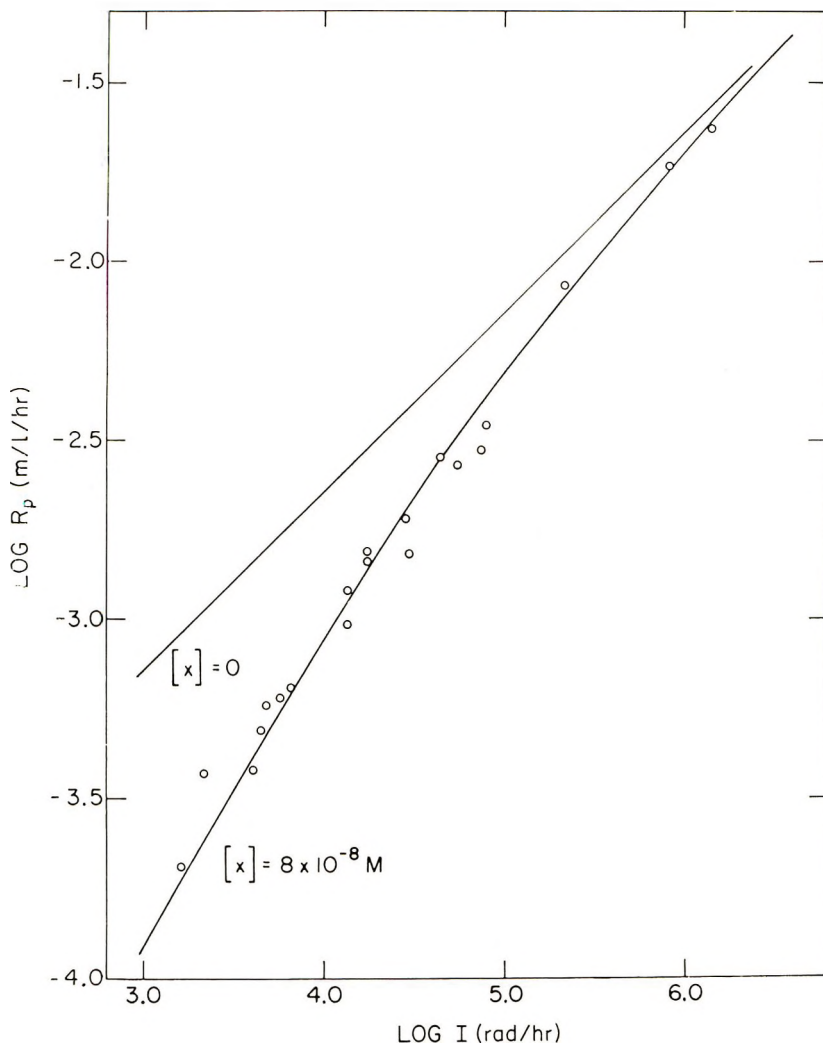


Fig. 6. Plots of calculated [eq. (12)] values of $\log R_p$ vs. $\log I$ at two values of impurity concentration $[X]$. Points are experimental values shown in Figure 2.

On returning to the quantitative use of eq. (12), Williams et al.¹³ have shown that, assuming the following values of rate constants

$$k_t = 2 \times 10^{11} \text{ l./mole-sec} \quad (\text{conductivity measurements})^{11}$$

$$k_{tz} = 1 \times 10^{10} \text{ l./mole-sec} \quad (\text{diffusion controlled})$$

and assuming $G_i = 0.10$, measured rates of polymerization at 15°C ¹⁴ and 0°C ² yield values of the rate constant for propagation of the order

$$k_p \approx (2.5-3.5) \times 10^6 \text{ l./mole-sec}$$

Since this value is low because of a small contribution from impurity termination, these authors¹³ suggest a slightly larger approximate value:

$$k_p \approx 5 \times 10^6 \text{ l./mole-sec}$$

The data presented in Figure 2 have been replotted in Figure 6. In the former instance, a straight line of slope 0.65 had been drawn through the data points; in Figure 6, a smooth curve has been drawn through these same data points calculated from eq. (12) and by using the following values of the rate constants, G_i , impurity concentration, and the known density of styrene at 0°C:⁴

$$G_i = 0.10$$

$$\rho = 0.924 \text{ at } 0^\circ\text{C}$$

$$k_t = 1.0 \times 10^{11} \text{ l./mole-sec}$$

$$k_{tx} = 1.0 \times 10^{10} \text{ l./mole-sec}$$

$$k_p = 5.0 \times 10^6 \text{ l./mole-sec}$$

$$[X] = 8 \times 10^{-10} \text{ mole/l.}$$

In addition, the limiting square-root dependence line ($[X] = 0$) is also indicated in Figure 6.

It is immediately apparent that, over three orders of magnitude of dose rate, the experimental data are remarkably well represented by the curve calculated from eq. (12) if a slight downward adjustment of k_t from the suggested¹³ value of 2×10^{11} /mole-sec to 1×10^{11} l./mole-sec is made. (Although, it is really not justified to imply that any of these rate constants are known to within the accuracy implied by this adjustment, manipulation of the values was necessary so that the three experimental points at the highest dose rates would not fall above the calculated limiting square root line. Trial and error indicated that this adjustment of k_t would give the best fit over the entire range of the measured variables.) This agreement is striking confirmation of the qualitative and quantitative predictions of Williams et al.¹³

A question which may properly be asked is "Do all the data on styrene fit the proposed mechanism?" Unfortunately, the answer is in the negative. The two sets of data that do not fit into the scheme involve the following set of observations: (a) the inability, so far, for any workers to obtain a square-root dependence of R_p on I for styrene, under any conditions of purity achieved, and (b) the apparent anomalous temperature behavior of styrene when it is very pure.

Dose Rate Dependence of R_p

Let us look at the first question. Although at least one monomer¹⁵ has been observed to attain a square-root behavior ($R_p \propto I^{1/2}$) under conditions of very rigorous purification, the most careful work by Ueno et al.¹⁴ and

ourselves,² including the present data, have failed to achieve this condition for styrene. Williams et al.¹³ have ascribed their dose rate dependence of 0.62 (at 15°C) to the fact that, even at the highest dose rates of approximately 1×10^5 rad/hr, the impurity termination reaction is not negligible. On a straight-line plot (see Fig. 2), we have extended the range of dose rate by an additional order of magnitude, and have still failed to observe the expected diminution of the impurity termination reaction.

In addition, we have also measured¹⁶ a "rate of polymerization" dilatometrically in a very high instantaneous dose rate situation, i.e., under pulsed radiolysis. A sample of styrene was manually given several sets of 10 pulses (1 μ sec/pulse, interpulse interval ≈ 0.1 sec) and thermally equilibrated after each set of 10 pulses. The instantaneous dose rate (dose per pulse) was 8.5×10^{12} rad/hr.⁹ Since the ionic lifetimes should be of the order of only a few microseconds, based on either Hayashi's calculation¹¹ or our own observations,⁹ we believe it to be justified to assume that the reaction initiated in each single pulse was essentially terminated before the next pulse arrived at the sample. On this basis we calculate a rate of polymerization, R_p , of approximately 3×10^3 mole/l.-sec at 8.5×10^{12} rad/hr.

If one uses eq. (12) with the assumed values of the rate constants, one would calculate $R_p \approx 7 \times 10^1$ mole/l.-sec, or approximately 40 times lower than the observed value. On the other hand, if one extrapolates the straight-line correlation of the experimental data (see Fig. 2), a value of $R_p \approx 2 \times 10^3$ mole/l.-sec at the same dose rate results. Any adjustment of the specific rate constants in eq. (12) to bring that expression into closer agreement with the observed value at this very highest dose rate would adversely affect the good agreement achieved at the lower dose rates.

An alternative is to assume that an unidentified terminating agent, W, is produced during irradiation in such a fashion that its steady-state concentration is proportional to the dose rate, and that it acts in much the same fashion as X, e.g.



Equation (12) would then become

$$R_p = \frac{R_i k_p [M]}{(R_i k_t)^{1/2} + k_{tx}[X] + k_{tw}[W]} \quad (15)$$

or, assuming, in the steady state,

$$[W] = aI \quad (16)$$

$$R_p = \frac{R_i k_p [M]}{(R_i k_t)^{1/2} + k_{tx}[X] + ak_{tw}I} \quad (17)$$

The speculative nature of this suggestion is obvious, especially since no identification of this inhibiting species has been made or attempted. De-

pending on the values of the parameters a and k_{tr} , however, it would supply a phenomenological explanation of the data.

Temperature Dependence of R_p

With respect to the other question, by far the more serious one, eq. (12) would not predict the anomalous temperature behavior reported in our previous communication,² reported also by Ueno et al.¹⁴ and further confirmed by data presented here. Ueno et al.¹⁴ report observing a maximum polymerization rate in the vicinity of 35°C at a dose rate of 1.4×10^4 rad/hr. Our data indicate that a maximum value of R_p occurs at approximately the same temperature but at a dose rate of about 4×10^3 rad/hr. This slight quantitative discrepancy does not detract from the documentation of the existence of the phenomenon and may be traced to the slightly higher rates of polymerization which we have observed at a given dose rate and temperature.

In commenting on their observation of this phenomenon, Ueno et al.¹⁴ have suggested that it may be related to a temperature-dependent association of water in the hydrocarbon medium. For any given total water content, the effective concentration of water available for terminating growing chains would increase with temperature, leading to a decrease in the overall polymerization rate. We will reserve further comment on this until after a crude examination of the combined dose rate-temperature- R_p behavior shown in Figure 3.

Although it is difficult to extract an exact expression for the overall temperature coefficient for the polymerization rate from eq. (12), an approximate expression can be considered. Thus

$$E_{\text{total}} \approx E_i + E_p - bE_t' \quad (18)$$

where E_i and E_p are the temperature coefficients for initiation and propagation, respectively, and E_t' is meant to express the temperature coefficient for the combined processes of chain termination by impurity and by charge neutralization. In either extreme circumstance, E_t' would be unambiguously defined. Moreover, the value of b could be assigned the value of 1 or $1/2$ for termination by impurity or by charge neutralization, respectively.

Although the free ion yields of several irradiated hydrocarbons have been found by Schmidt and Allen¹⁷ to be slightly temperature-dependent, the effect is small, and it will be assumed here that E_i is essentially zero. Regarding E_p , the temperature coefficient for a styryl carbanion has been determined¹⁸ to be 5–6 kcal/mole in several solvents, and the coefficient for the styryl carbonium ion has been estimated¹⁹ to be 3–4 kcal/mole. Thus, to a reasonable approximation, the temperature coefficient for the ionic propagation of styrene under irradiation can be given by

$$E_{\text{total}} \approx 3 - bE_t' \quad (19)$$

the lower estimate for E_p being chosen arbitrarily.

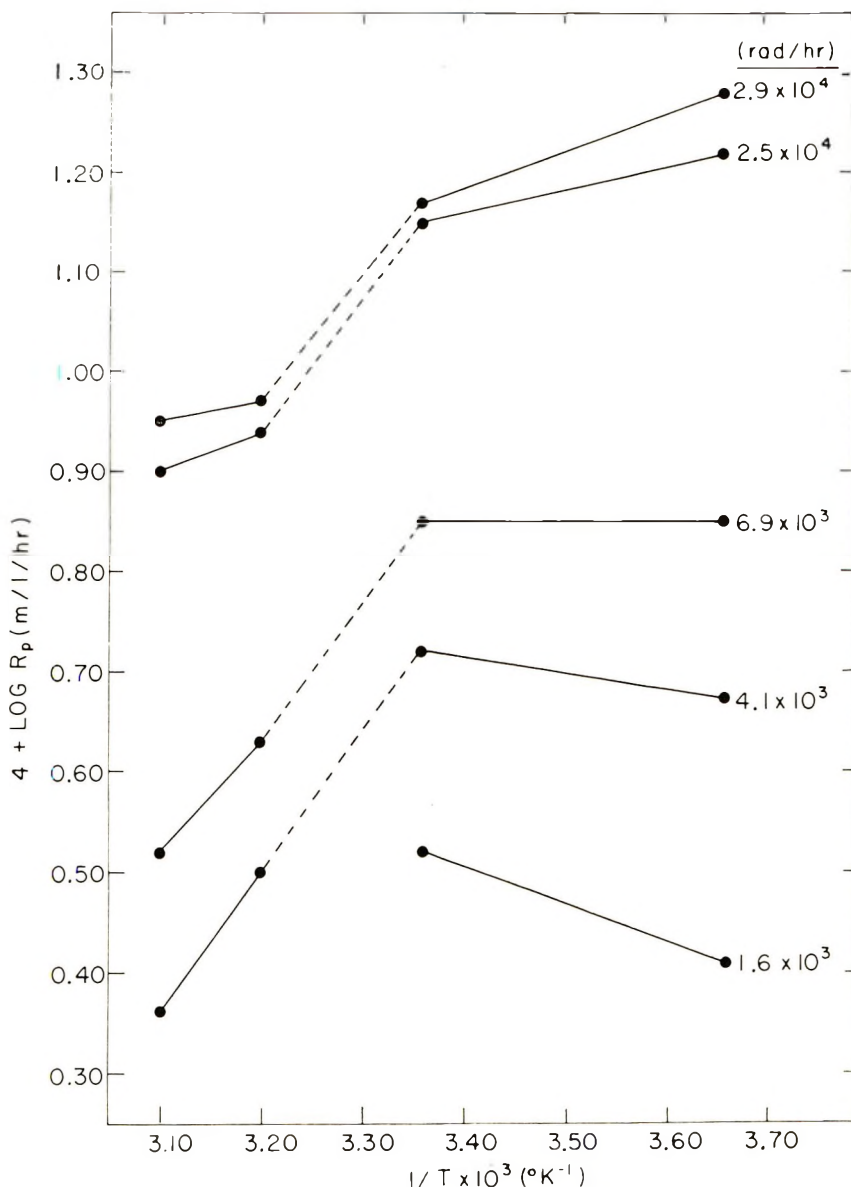


Fig. 7. Plots of $\log R_p$ vs. $1/T$ for highest purity styrene at several dose rates.

Figure 7 is based on the experimental data shown in Figure 3 and represents a plot of R_p versus $1/T$ at several chosen dose rates, within the range of the experimental data. From these plots, two-point approximations of the overall temperature coefficients can be made. These approximations, along with values of bE_i' calculated with eq. (19), are tabulated in Table II. The values in this table are to be viewed merely as indicative of general trends, and not firmly established values of temperature coefficients. With

this in mind, it appears that the contribution of the chain termination processes varies between 1 and 9 kcal/mole, depending on both the temperature range and the dose rate.

Both of the chain termination processes considered so far—charge recombination and reaction with impurity—have been considered to be diffusion controlled processes with rate constants $k_t \approx 10^{11}$ l./mole-sec and $k_{tz} \approx 10^{10}$ l./mole-sec, respectively. If k_t and k_{tz} are both diffusion-controlled, it would be expected that their temperature coefficients, in the absence of any specific ion-ion or ion-dipole effects, would be of the order of magnitude of the temperature coefficient of the viscosity of the medium.

TABLE II
Approximate Overall Temperature Coefficients

Dose rate, rad/hr	Temperature coefficients, kcal/mole					
	0-25°C		25-40°C		40-50°C	
	E_{total}	bE_t'	E_{total}	bE_t'	E_{total}	bE_t'
1.6×10^3	+2	+1	—	—	—	—
4.1×10^3	+1	+2	-6	+9	-6	+9
6.9×10^3	0	+3	-6	+9	-5	+8
2.5×10^4	-1	+4	-6	+9	-2	+5
2.9×10^4	-1.5	+4.5	-6	+9	-1	+4

For styrene, the activation energy of viscosity, between 10 and 50°C, is 2.1 kcal/mole.⁴ Thus the activation energies of both chain termination processes are expected to be approximately 2 kcal/mole.

The question then arises whether the large values of the temperature dependence of the chain-terminating processes can be ascribed to the temperature dependence of the degree of association of water in this system. An empirical investigation of this may be made on the basis of the data presented in Figure 8b. This sample displayed a dose rate dependence of approximately 0.9, indicating termination principally by reaction with impurity. For this sample, eq. (12) can be simplified to,

$$R_p = R_i k_p [M] / k_{tz} [X] \quad (20)$$

and

$$E_{\text{total}} = E_p - E_{tz} \quad (21)$$

Since the observed overall temperature coefficient for this sample is approximately -1.5 kcal/mole, $E_{tz} \approx 4.5$ kcal/mole, which value will include not only the temperature dependence of the actual reaction with impurity, but also the temperature dependence of the assumed degree of association of water in styrene. Comparison of this value with some of the entries in Table II leads to the conclusion that there must be a more temperature-

dependent termination process to account for bE_t' values in excess of 4–5 kcal/mole.

Moreover, in Figure 3, the data at 25°C and 40°C both correspond to a square-root dependence of rate on dose rate. The mechanism under consideration would predict

$$R_p = R_i^{1/2}[M](k_p/k_t)^{1/2}$$

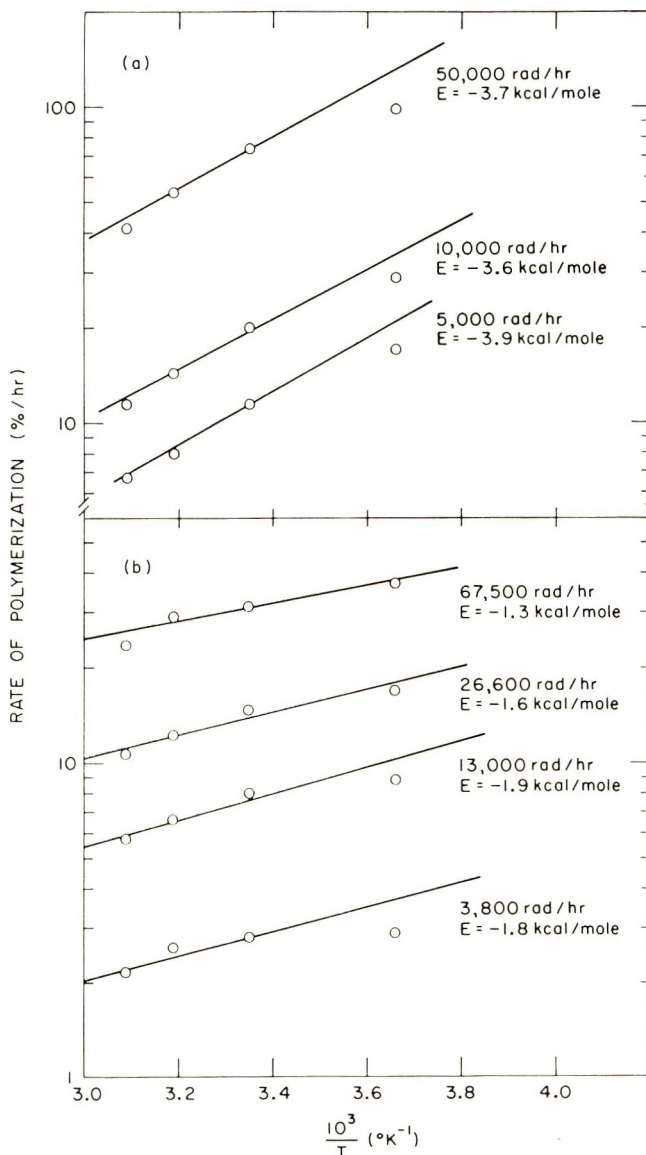


Fig. 8. Plots of $\log R_p$ vs. $1/T$ for two slightly impure styrene samples at several dose rates.

and

$$\begin{aligned} E_{\text{total}} &= E_p - 1/2 E_t \\ &= 3 - 1/2 E_t \end{aligned}$$

The value of E_{total} between 25 and 40°C given in Table II would then lead to the startling result that $E_t \approx 18$ kcal/mole for ion-ion recombination. Thus, although the square-root dependence of R_p on I would appear to demonstrate termination solely by ion-ion recombination, these data seem to indicate the presence of some other termination process with a higher temperature coefficient.

Although we are not in a position to offer a mechanistic interpretation of the temperature-dose rate behavior as a function of impurity, we would like to make the following phenomenological observations. At the very highest rates of polymerization, and hence lowest impurity levels, the temperature behavior is quite anomalous^{1,14} and indicates overall temperature coefficients as low as -6 kcal/mole. As the impurity level increases, the dose rate dependence increases, and the temperature coefficient (more well defined here than at the maximum rates) increases through values of -4 and -1.5 kcal/mole, as indicated in Figure 8. Ueno et al.¹⁰ indicate that for even lower absolute rates of polymerization (and hence higher impurity concentration) the temperature coefficient is essentially zero.

More recently, Huang and Westlake²⁰ have reported an overall temperature coefficient of $+3.1$ kcal/mole for higher impurity concentrations, where the contributions of ionic and free-radical propagation are comparable. Finally, when the styrene is water-saturated and the propagation is exclusively by free radicals, the temperature coefficient rises to $+7.15$ kcal/mole.⁵

Nature of the Propagating Species

As will be recalled, there is a preponderance of evidence to suggest that the principal propagating species in the system under discussion is a carbonium ion, either normal or radical. What, then is the nature and the role of the negatively charged species?

It appears reasonable to assume that some fraction of the ejected electrons will become captured (solvated) by styrene when they become thermalized. Moreover, carbanions can be formed by heterolytic scission of an excited molecule, yielding a carbanion radical in the process. Thus, the occurrence of carbanion radicals seems assured. Do these contribute significantly to the overall polymerization process other than as chain-terminating agents?

Hayashi et al.¹¹ have assumed that the contribution of a styryl anion, in the presence of styryl cation, is negligible. This is based on two lines of evidence. Firstly, Hayashi et al.¹¹ have indicated that the upper limit of k_p for the bare styryl cation is of the order of 8×10^8 l./mole-sec based on scavenger studies, and the lower limit is approximately 5×10^6 l./mole-sec

based on conductivity measurements. Since the value of k_p for the styryl anion has been measured as 6.5×10^4 l./mole-sec²¹ and 1.3×10^5 l./mole-sec,²² it would appear to follow that the above assumption is correct by several orders of magnitude. However, the values of k_p for the styryl anion adding to styrene monomer were measured in THF solution.^{21,22} Since the ion-induced dipole force between the styryl anion and the styrene molecule should be about four times higher in bulk styrene (dielectric constant ≈ 2) than it is in THF (dielectric constant ≈ 8), it might be expected that the values of k_p "corrected" for the dielectric constant would lie between 2×10^5 and 5×10^5 l./mole-sec. The upper value of this "corrected" k_p for the styryl anion is approximately $1/10$ of the lower limit of k_p for the styryl cation as given by Hayashi et al.¹¹

The second line of evidence considered by Hayashi et al.¹¹ is based on a comparison of the experimentally determined average value of the sum of the ionic mobilities in irradiated styrene compared to the equivalent average mobility in irradiated cyclohexane. For styrene, the average value of the total ionic mobilities is estimated to be at the order of 4×10^{-4} cm²/V-sec. This is to be compared with the same authors'¹¹ computed average mobility of a growing styryl cation, estimated to be of the order of 4×10^{-5} cm²/V-sec, on the basis of the published value of the diffusion coefficient for a "living" polystyrene dianion ($D\bar{P} = 25$) in THF.²³ This would seem to imply that the average growing anion is of the order of $1/10$ the size of the average growing cation.

Thus, on the basis of both the relative values of the propagation rate constants and ionic mobilities, it appears that the propagation of anionic species may account for approximately 10% of the conversion of monomer to polymer in this system.

In a related study, Katayama et al.²⁴ have recently reported that the anionic and cationic mobilities in irradiated α -methylstyrene are, respectively, 1.5×10^{-4} and 5.0×10^{-4} cm²/V-sec. It is not surprising that the two mobilities should be closer in value in this system than in styrene since the average degree of polymerization in α -methylstyrene is known to be at least an order of magnitude less than in styrene. The principal determining factor of this parameter, for the carbonium ions, is chain transfer to monomer.

At the present, the theory of ion-ion and ion-molecule reactions in condensed systems is not sufficiently advanced to explain the apparent inconsistencies between the experimental data and the kinetic scheme proposed by Williams et al.¹³ At first thought, it might be argued that the inclusion of propagating carbanions might introduce sufficient parameters to account for the anomalous temperature behavior, much of which appears to reside in the termination process(es).

Amis and Jaffe,²⁵ in considering the reaction between an ion and a dipolar molecule, derived an expression for the variation of the specific rate constant with dielectric constant. According to their predictions, the rate constant for a reaction involving a positive ion would decrease with increasing di-

electric constant, whereas the opposite behavior was predicted for a negative ion. A modified form of their equation was later given by Quinlan and Amis,²⁶ for solutions of zero ionic strength, and is

$$\ln k = k_{x=0} \Big|_{D=\infty} + (z\epsilon\mu_0/DkTr_0^2) \quad (22)$$

where $k_{x=0} \Big|_{D=\infty}$ is the specific rate constant for the reaction at zero ionic strength in a medium of infinite dielectric constant (a reference state), z is the algebraic value of the valence of the attacking ion, ϵ the electronic charge, μ_0 the dipole moment of the molecule, D the dielectric constant of the medium and r_0 the distance of closest approach of the ion to the molecule in the activated complex. The important feature of this treatment is that the valence of the ion appears to the first power, and the equation predicts a dependency on the independent variable D (or T) according to the valence sign of the ion. This behavior has been observed in a number of systems.²⁷

It should be pointed out, however, that Laidler and Eyring²⁸ have offered an alternative treatment of the same general process. The difference in the resulting equation which is most pertinent to this discussion is that the latter workers develop a correction similar to that of Amis et al.^{25,26} but containing the square of the ionic valence. Interestingly enough, there are data that fit the Quinlan-Amis equation, and there are data on other systems that fit the Laidler-Eyring equation. This confusing state of affairs is a reflection of the paucity of sound experimental and theoretical work in this branch of physical chemistry.

Taking the Quinlan-Amis equation, and considering the quantity

$$z\epsilon\mu_0 N_{av}/Dr_0^2$$

as the contribution of electrostatic interactions to the overall temperature coefficient of the rate constant, a value of 8 kcal/mole results from assuming $\mu_0 = 2 \times 10^{-18}$ esu (for a water molecule), $D = 2$ (for styrene), and $r_0 = 3 \text{ \AA}$. This "electrostatic" activation energy will be added to the activation energy corresponding to $k_{x=0} \Big|_{D=\infty}$ in the case of a negative ion, and subtracted from the analogous quantity in the case of a positive ion-dipole reaction. Moreover, μ_0 should really be replaced by the "external" dipole moment, which depends on the dielectric constant of the medium and its polarizability, as given by Onsager,²⁹ and the entire term should be multiplied by $\cos \theta$ to account for the directionality of the reaction coordinate with respect to the dipole axis. Obviously the numerical value of this correction will vary with so many parameters whose numerical values are unknown that it is not possible to actually compute it from first principles.

The important thing, however, is that the temperature coefficient for an ion-dipole reaction in solution, even at zero ionic strength, may be a composite quantity. According to the above arguments, the temperature coefficient for a positive ion-dipole reaction might even be negative. In the system presently under discussion, ion-dipole (or ion-induced dipole) reac-

tions are involved in the propagation, transfer to monomer, and impurity termination steps, and the entire temperature behavior may be expected to be quite complex.

Summarizing our thinking on the matter of which ion or ions are responsible for the propagation, we feel that, although the mechanism of Williams et al.¹³ provides a remarkably good quantitative description of the data at a fixed temperature, it fails to explain the temperature variations of the rate of polymerization as reported by Ueno et al.¹⁴ and Potter et al.² and further extended in this study. We do not feel that the data presently available warrant the omission of anionic propagation in the treatment of Williams et al.¹³ A more detailed set of data is necessary to settle this question quantitatively.

Effect of Water and Oxygen

In all of our previous work on styrene^{1,2,7-9} we have attributed to water the major, if not exclusive, role in obscuring ionic propagation in the radiation polymerization of the pure degassed monomer. The reasoning was of a negative nature, in that increasingly higher rates of polymerization were obtained as the drying technique used in sample preparation was improved. In the present study, it has been clearly demonstrated that the addition of degassed water, sufficient to saturate the sample, will cause the complete elimination of the ionic propagation previously observed in the same sample when dry.

The effect of adding dry oxygen to a previously dry, degassed sample of styrene is apparently quite complex. A number of years ago, Collinson et al.,³⁰ observed oxygen inhibition in the radiation-induced ionic polymerization of isobutene. Their explanation of this effect was that homogeneously distributed oxygen could capture near-thermal electrons and prevent their stabilization on the vessel walls or an adventitiously present dirt. This would lead to a more rapid neutralization of positively charged, growing ions and thus inhibit the reaction.

In the present study with styrene, we observed a large initial decrease in the rate of polymerization upon addition of oxygen. The reaction rate continued to decrease with increased total dose (and, presumably consumption of oxygen). Further addition of oxygen suppressed the rate even further. Our observations were terminated at the point where the final rate of polymerization, in the presence of oxygen, was about threefold that which would be expected of the pure, free-radical process and two orders of magnitude lower than that for the ionic process, before oxygen addition.

Since oxygen alone did not appear to have any marked effect on the formation of the styryl radical ion in our previously reported pulse radiolysis investigation,⁹ we suspect that the observed inhibition by oxygen in the steady-state irradiation is due to the rather rapid formation of oxygenated inhibitors (alcohols, aldehydes, etc.) in the oxygen-saturated irradiated styrene.

Molecular Weights

Although it is quite tempting to point out several apparent parallels between molecular weight trends with temperature and rates of polymerization at the two dose rates more extensively studied, we recognize that a detailed analysis of the tabulated molecular weights would imply a higher degree of confidence in their absolute values than is warranted.

All of the values in Table I point to an average degree of polymerization of between 700 and 900. On taking 800 as an overall average and considering that it is likely that chain transfer to monomer by the growing carbonium ion is the major contributing factor to this value, it appears that

$$k_p/k_{fc} \approx 800$$

as a first approximation.

A more detailed study of molecular weight distributions is presently in progress and will be reported in a future communication.

CONCLUSIONS

The rate of polymerization of styrene is a complex function of the temperature, dose rate and purity of the sample. The behavior is consistent with an ionic mechanism. Independent studies by others¹⁴ have indicated that the ions responsible for the propagation are predominantly carbonium ions. A kinetic scheme has been proposed by Williams et al.¹³ based on a single propagating species and assuming reasonable values of rate constants for several diffusion controlled steps in the process. Our data at 0°C show a remarkably good fit to the calculated rate of polymerization versus dose rate curve, and to that extent, tend to confirm the validity of the approach, as well as the assumed and derived rate constant values.

On the other hand, the scheme does not account for the observed maximum in the rate of polymerization with temperature, in certain dose rate regions. Nor does it account for the apparent failure of the rate of polymerization to achieve a square-root dependence on dose rate at very high dose rates, in the temperature range where the data fit the theoretical curve at lower dose rates.

We believe that the process is much more complicated, and that further studies are needed to more clearly establish the role played by all the reactive intermediates present. Several areas of investigation suggest themselves, namely, pulse radiolysis, electrical conductivity (mobility), molecular weight distributions, and careful kinetic studies in several solvents. In such studies, however, one must not be satisfied with data obtained at only one or perhaps two temperatures.

This work was supported by the Division of Research of the U. S. Atomic Energy Commission.

One of us (R. C. P.) wishes to express his appreciation to Yale University and the DuPont Company for financial assistance during the tenure of this investigation. We are also indebted to Profs. M. Szwarc and F. Williams for several enlightening dis-

cussions. Finally, we would like to acknowledge the excellent technical assistance of C. L. Johnson in helping to develop the experimental techniques in this investigation.

This work is taken in part from the doctoral dissertation of R. C. Potter submitted to the Graduate School of Yale University in partial fulfillment of the requirements for degree of Doctor of Philosophy in Chemical Engineering.

References

1. R. C. Potter, C. L. Johnson, R. H. Bretton, and D. J. Metz, *J. Polym. Sci. A-1*, **4**, 419 (1966).
2. R. C. Potter, R. H. Bretton, and D. J. Metz, *J. Polymer. Sci. A-1*, **4**, 2295 (1966).
3. K. O'Driscoll, N. Y. State Univ. at Buffalo, private communication.
4. R. H. Boundy and R. F. Boyer, *Styrene, Its Polymers, Copolymers and Derivatives*, Reinhold, New York, 1952.
5. A. Chapiro, *Radiation Chemistry of Polymeric Systems*, Interscience, New York, 1962.
6. F. L. Dalton and R. L. Vale, Wantage Radiation Laboratory, unpublished results.
7. C. L. Johnson and D. J. Metz, paper presented at American Chemical Society Meeting, New York, September 1963; *Polym. Preprints*, **4**, 440 (1963).
8. D. J. Metz, *Trans. Amer. Nucl. Soc.*, **7**, 313 (1964).
9. D. J. Metz, R. C. Potter, and J. K. Thomas, *J. Polym. Sci. A-1*, **5**, 877 (1967).
10. K. Ueno, K. Hayashi, and S. Okamura, *Polymer*, **7**, 431 (1966).
11. K. Hayashi, H. Yamazawa, T. Takagaki, F. Williams, K. Hayashi, and S. Okamura, *Trans. Faraday Soc.*, **63**, 1489 (1967).
12. K. Hayashi, H. Yamazawa, K. Ueno, K. Hayashi, H. Kamiyama, F. Williams, and S. Okamura, Abstracts of Symposium on Macromolecular Chemistry, Tokyo-Kyoto, Sept. 1966.
13. F. Williams, K. Hayashi, K. Ueno, K. Hayashi, and S. Okamura, *Trans. Faraday Soc.*, **63**, 1501 (1967).
14. K. Ueno, F. Williams, K. Hayashi, and S. Okamura, *Trans. Faraday Soc.*, **63**, 1478 (1967).
15. D. J. Metz, *Advan. Chem.*, **66**, 170 (1967).
16. D. J. Metz, R. C. Potter, and J. K. Thomas, unpublished data.
17. W. F. Schmidt and A. O. Allen, *J. Chem. Phys.*, in press.
18. T. Shimomura, K. J. Tölle, J. Smid, and M. Szwarc, *J. Amer. Chem. Soc.*, **89**, 766 (1967).
19. M. Szwarc, State College of Forestry at Syracuse, private communication.
20. R. Y. M. Huang and J. F. Westlake, *J. Polym. Sci. B*, **7**, 713 (1969).
21. D. N. Bhattacharyya, C. L. Lee, J. Smid, and M. Szwarc, *J. Phys. Chem.*, **69**, 612 (1965).
22. H. Hostalka and G. V. Schulz, *J. Polym. Sci. B*, **3**, 175, 1043 (1965).
23. K. J. Tölle, J. Smid, and M. Szwarc, *J. Polym. Sci. B*, **3**, 1037 (1965).
24. M. Katayama, H. Yamazaki, and Y. Ozawa, *Bull. Chem. Soc.*, Japan, in press.
25. E. S. Amis and G. Jaffé, *J. Chem. Phys.*, **10**, 598 (1942).
26. J. E. Quinlan and E. S. Amis, *J. Amer. Chem. Soc.*, **77**, 4187 (1955).
27. E. S. Amis, *Solvent Effects on Reaction Rates and Mechanisms*, Academic Press, New York, 1966, Chapter 2.
28. K. J. Laidler and H. Eyring, *Ann. N. Y. Acad. Sci.*, **39**, 303 (1940).
29. L. Onsager, *J. Amer. Chem. Soc.*, **58**, 1486 (1936).
30. E. Collinson, F. S. Dainton, and H. A. Gillis, *J. Phys. Chem.*, **63**, 909 (1959).

Received March 20, 1970

Revised August 13, 1970

Radiation-Induced Polymerization of Tetraoxane in the Solid State*

YOSHIAKI NAKASE, MASARU YOSHIDA, AKIHIKO ITO,
and KOICHIRO HAYASHI, *Takasaki Radiation Chemistry Research
Establishment, Japan Atomic Energy Research Institute,
Takasaki, Gumma, Japan*

Synopsis

The radiation-induced polymerization of tetraoxane in the solid state has been investigated in air and *in vacuo*. The polymerization rate was higher in air than *in vacuo*, whereas the molecular weight of the polymer obtained at high conversion in air was considerably lower than that *in vacuo*. A large decrease in the molecular weight with increasing polymer yield observed in air may be explained mainly by degradation during polymerization.

Two papers on the radiation-induced polymerization of tetraoxane, the cyclic tetramer of formaldehyde, have been published. Hayashi et al.¹ first reported the radiation-induced polymerization, and Cannavo et al.² reported the electron microscopic observation of the polymerization. On the other hand, many papers on the radiation-induced polymerization of trioxane, the cyclic trimer of formaldehyde, have appeared. It was reported that the post-polymerization rate is higher in air than *in vacuo* and that peroxides are formed by the pre-irradiation in air.³ The molecular weight of the polymer increases with the polymer yield both in air^{4,5} and *in vacuo*.⁶

Similarly, in the case of tetraoxane, we observed a higher post-polymerization rate in air than *in vacuo*. In the present study, however, we found a distinct effect of oxygen on the molecular weight of polyoxymethylene obtained, i.e., the molecular weight of the polymer was reduced remarkably when the polymerization of tetraoxane was carried out in air.⁷

A 1-g sample of tetraoxane purified by sublimation was placed in a glass ampoule of 8 mm inside diameter and irradiated with γ -rays from a 126,000 Ci⁶⁰Co source after the ampoule was sealed at a given pressure of air.

Figure 1 shows the relationship between the pressure of air and the reduced viscosity of polymers obtained in both in-source and post-polymerization of tetraoxane. The reduced viscosity was taken as a measure

* Paper presented at the 23rd Annual Meeting of the Chemical Society of Japan, Tokyo, April 1970.

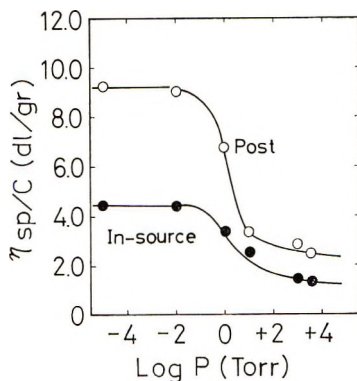


Fig. 1. Relationship between pressure of air and η_{sp}/c of polymers obtained in the radiation-induced polymerization of tetraoxane: (O) post-polymerization, irradiation 1×10^6 rad, -78°C , polymerization at 105°C , 2 hr (polymer yields were 33% and not affected by the pressure within this polymerization time); (●) in-source polymerization, 3×10^4 rad/hr, 105°C , 3 hr (polymer yields were 77% and not affected by the pressure).

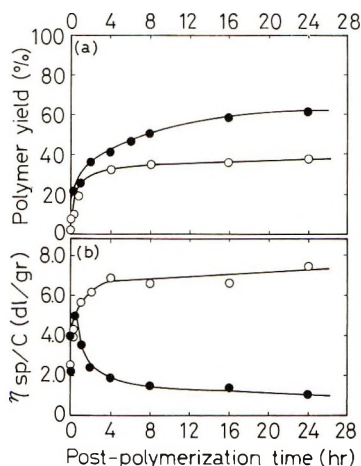


Fig. 2. Post-polymerization of tetraoxane: (a) polymerization time–yield curve and (b) polymerization time–reduced viscosity curve for polymerization (O) *in vacuo* and (●) in air. Pre-irradiation, 1×10^6 rad, -78°C ; polymerization, 105°C .

of the molecular weights of the polymers. The solution viscosity was measured as a 0.3% solution of p-chlorophenol containing 2% α -pinene.

The molecular weight of polymers seems to be reduced when the pressure exceeds 10^{-2} mm Hg. Figure 2 shows results of the post-polymerization of tetraoxane in detail.

On polymerization *in vacuo*, the molecular weight of the polymers increased monotonically with the increase in the polymer yield, and both curves of polymer yield and η_{sp}/c , indicated as open circles in Figure 2, are similar to those for trioxane. On the other hand, the molecular weight of the polymers obtained in air is sharply reduced after attaining a maximum

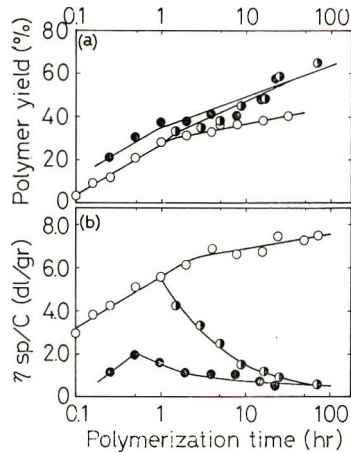


Fig. 3. Effect of air introduced in the course of post-polymerization of tetraoxane (I): pre-irradiation, 1×10^6 rad, -78°C *in vacuo*; polymerization, 105°C , (O) *in vacuo*; (●) in air; (◐) air introduced 1 hr after the start of polymerization so that the pressure attained atmospheric pressure.

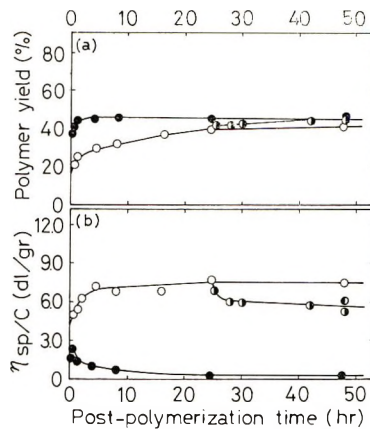


Fig. 4. Effect of air introduced in the course of the post-polymerization of tetraoxane (II): pre-irradiation, 1×10^6 rad, -78°C *in vacuo*; polymerization (O) 105°C *in vacuo*; (●) 110°C in air; (◐) air introduced 24 hr after the start of polymerization so that the pressure attained 1 atm and polymerization was continued at 110°C for 24 hr; (◑) polymer isolated before the introduction of air was maintained at 110°C for 24 hr.

value as the polymer yield increased. This tendency was not observed previously in the post-polymerization of trioxane. In the post-polymerization under a nitrogen atmosphere, results similar to those *in vacuo* were obtained. A decrease in the molecular weight of the polymer was observed after a long polymerization period, even at a polymerization temperature of 55°C , when a large pre-irradiation dose was applied. A similar tendency was found when trioxane was post-polymerized at 55°C .

It was also observed that tendencies relating to the polymer yield and the molecular weight, when tetraoxane was irradiated in air and post-polymerized *in vacuo*, were similar to those obtained when both irradiation and post-polymerization were conducted *in vacuo*, and that the tendencies observed when tetraoxane was irradiated *in vacuo* and post-polymerized in air were similar to those obtained when both irradiation and post-polymerization were conducted in air. Therefore, the atmosphere during the polymerization seems to affect the molecular weight of the polymer.

Furthermore, when air was introduced in the course of the post-polymerization *in vacuo*, a decrease in the molecular weight of the polymers was observed just after the introduction of air, while the polymer yield increased to a value similar to that attained when the polymerization was carried out in air for the whole period, as shown in Figure 3.

Figure 4 shows that only a small increase in polymer yield was obtained when air was introduced and the polymerization was continued at 110°C after the polymerization was conducted at 105°C *in vacuo* and the polymer yield almost reached its limiting value. In this case, the decrease in the molecular weight of the polymer was as small as that which occurred when the polymer isolated before the introduction of air was maintained at 110°C in air. The above facts indicate that a marked decrease in the molecular weight takes place only when an appreciable polymerization of tetraoxane takes place in the presence of oxygen.

It is not clear at present whether the decrease in the molecular weight is due to the degradation of the polymer formed before the introduction of air into the polymerization system to low molecular weight polymer or due to the formation of low molecular weight polymer after the introduction of air. However, as seen in Figure 3, the drastic decrease in the reduced viscosity may be explained mainly by the occurrence of degradation of polymers formed before the introduction of air, since, at the polymerization time of 9 hr, the reduced viscosity was decreased to about one fifth, whereas the polymer yield increased twofold compared with that just before the introduction of air. Fractionation of the polymers which would clarify this point is in progress.

It was suggested that there coexist two different mechanisms in the post-polymerization of trioxane in air.³ It is likely that there is an active species which participates in both the polymerization and the degradation of the polymer only in the presence of oxygen, and another kind of active species which participates in the polymerization either in the presence or absence of oxygen.

We believe that further studies on the effect of oxygen will elucidate the mechanism of the radiation-induced polymerization of cyclic oligomers of formaldehyde.

The authors wish to express thanks to Professor S. Okamura, Kyoto University, and Dr. T. Iwai and Dr. I. Kuriyama, JAERI, Takasaki, for their encouragement throughout this work.

References

1. K. Hayashi, H. Ochi, M. Nishii, Y. Miyake, and S. Okamura, *J. Polymer Sci. B*, **1**, 427 (1963).
2. C. Cannavo, J. Deschamps, K. Hayashi, and C. Sella, *C. R. Acad. Sci. (Paris)*, **C266**, 777 (1968).
3. K. Hayashi, H. Ochi, and S. Okamura, *J. Polym. Sci. A*, **2**, 2929 (1964).
4. N. S. Marans and F. A. Wessells, *J. Appl. Polym. Sci.*, **9**, 3681 (1964).
5. M. Sakamoto, I. Ishigaki, M. Kumakura, H. Yamashina, T. Iwai, A. Ito, and K. Hayashi, *J. Macromol. Chem.*, **1**, 639 (1966).
6. I. Ishigaki, A. Ito, T. Iwai, and K. Hayashi, *J. Polym. Sci. A-1*, **8**, 3061 (1970).
7. C. Cannavo and K. Hayashi, unpublished results.

Received July 6, 1970

Revised September 8, 1970

Copolymerization of Propylene with Acrylate by a Ziegler-Natta Type Catalyst

KIICHIRO MATSUMURA and OSAMU FUKUMOTO,*
*Kawasaki Plant, Toray Industries Inc.,
Ukishima Kawasaki, Japan*

Synopsis

Propylene was polymerized by using a Ziegler-Natta type catalyst in the presence of ethylchloroaluminum acrylate, which was formed by the reaction of diethylaluminum chloride with acrylic acid. The polymer obtained contained acrylic units which were proved to be copolymerized with propylene units by solvent extraction, infrared spectrum, and NMR spectrum. The copolymer showed much improved properties compared with the polypropylene homopolymer.

INTRODUCTION

Polypropylene has several shortcomings, most of which are due to lack of a polar group in its molecule. The most fundamental method of many to improve the shortcomings is copolymerization of propylene with a polar monomer. Polar monomers, however, are generally known to deactivate Ziegler-Natta type catalysts commonly used for the polymerization of olefinic hydrocarbons,¹ although there are some exceptions.²⁻⁶ This may be due to the deactivation of the active center or catalyst components by the polar group.

One of the ideas to suppress the deactivation reaction is to mask the polar group of the comonomers. *tert*-Butyl acrylate with a bulky *tert*-butyl group effective to mask the polar group is reported to be homopolymerized² and even to be copolymerized³ with ethylene by a Ziegler-type catalyst comprising *n*-butyllithium and titanium tetrachloride. Copolymerization of propylene with acrylate, however, has not been reported so far. This is because that the polymerization of propylene is much more difficult compared with the polymerization of ethylene.

In this paper, the copolymerization of propylene with an acrylate, ethylchloroaluminum acrylate, by a Ziegler-Natta type catalyst is reported. The copolymer thus obtained shows much improved properties.

* Present address: Head Office, Toray Industries Inc., Nihonbashi, Muromachi, Tokyo, Japan.

RESULTS AND DISCUSSION

Effect of Some Polar Monomers on $\text{TiCl}_3-(\text{C}_2\text{H}_5)_3\text{Al}_2\text{SO}_4$ System

The effect of methyl acrylate (MAC), 2-methyl-5-vinylpyridine (MVP), acrylic acid (AA), and methacrylic acid (MAA) on the polymerization activity of propylene with the $\text{TiCl}_3-(\text{C}_2\text{H}_5)_3\text{Al}_2\text{SO}_4$ system was investigated, and the results are shown in Figure 1. Even a small amount of MVP or MAC deactivates the catalyst completely, while MAA or AA deactivates catalyst only gradually, and 40 mmole of AA is necessary to deactivate the catalyst completely. This 40 mmole of AA coincides with the amount of ethyl group of $(\text{C}_2\text{H}_5)_3\text{Al}_2\text{SO}_4$ in the polymerization system.

The experimental findings that only small amount of MVP or MAC is sufficient to deactivate the catalyst completely indicates that these polar monomers react directly with the active center and deactivate it. On the contrary, the mechanism of the deactivation by MAA or AA seems to be somewhat different from that by MVP or MAC, judging from the gradual decrease of the activity with increasing addition of MAA or AA. Since AA and MAA have active hydrogens in the molecule, the most probable reaction between them and catalyst is that as shown in eq. (1), which will be discussed in the next section.

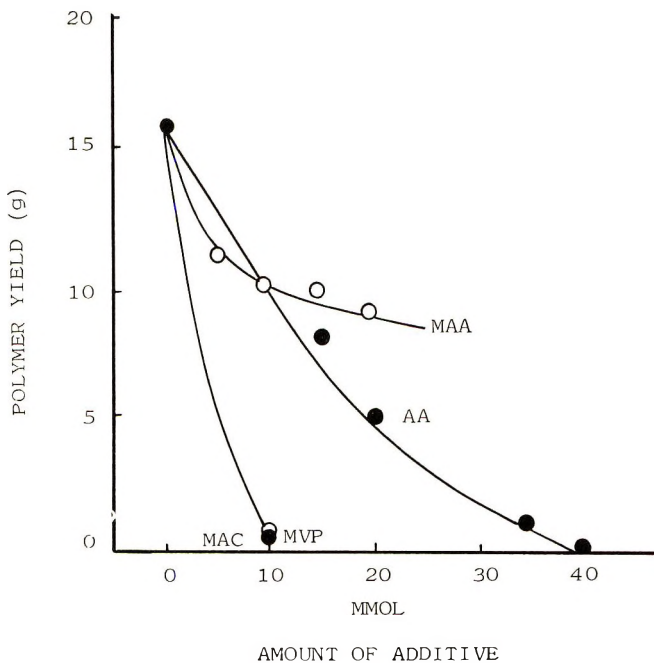


Fig. 1. Effect of acrylic acid (AA), methacrylic acid (MAA), methyl acrylate (MAC), and 2-methyl-5-vinylpyridine (MVP) on polymerization activity of propylene. Polymerization conditions: TiCl_3 , 2 mmole; $(\text{C}_2\text{H}_5)_3\text{Al}_2\text{SO}_4$, 10 mmole; *n*-heptane, 50 ml; 60°C; time, 3.5 hr; initial propylene pressure, 3 atm.

Bis(diethylaluminum) sulfate reacts with AA or MAA successively as long as the ethyl group is present in the molecule. Hence 1 mole of bis(diethylaluminum) sulfate can react with 4 moles of AA or MAA. The final reaction product may not be effective as a catalyst component since it does not contain an ethyl group in the molecule. This is the reason why the addition of a fourfold quantity of AA to bis(diethylaluminum) sulfate deactivates the catalyst completely. Although the reaction product of bis(diethylaluminum) sulfate with AA or MAA may also be a catalyst poison, this seems to have a less powerful influence than MAC or MVP on the catalyst activity. The best explanation for this difference is that the reaction product of bis(diethylaluminum) sulfate with AA or MAA has an alkylaluminum residue with larger masking effect than that of methyl group.

These experimental findings induced authors to carry out the copolymerization of propylene with acrylic acid by a Ziegler-Natta type catalyst, using the reaction product between acrylic acid and an alkylaluminum compound as comonomers.

Reaction of Diethylaluminum Chloride with Acrylic Acid

Various kinds of alkylaluminum compounds can be used to synthesize alkylaluminum acrylates which will be used as comonomers. After preliminary experiments, diethylaluminum chloride was selected, since the reaction product between diethylaluminum chloride and acrylic acid was the most simple.

An equimolar amount of acrylic acid was added gradually to a benzene solution of diethylaluminum chloride under nitrogen with cooling and stirring. The reaction proceeded with evolution of heat and a gas which proved to be ethane. The reaction product was a clear solution without any precipitate. It was subjected to analysis, and the results are shown in Table I. The infrared spectrum of the product was also obtained and is shown in Figure 2.

Chemical analysis in Table I shows that the ratios C_2H_5/Al , Cl/Al , and $CH_2=CHCOO/Al$ are all unity. Absorption bands of the infrared spectrum at around 920, 990, 1280, and 1420 cm^{-1} indicate the presence of a vinyl group, while bands at around 620 and 1580 cm^{-1} can be assigned to the carboxyl group of a salt.

TABLE I
Analysis of the Reaction Product of Diethylaluminum Chloride with Acrylic Acid^a

No.	Al, wt-%	C_2H_5 , wt-%	Cl, wt-%	$CH_2=$ $CHCOO$, wt-%	$\frac{C_2H_5}{Al}$	$\frac{Cl}{Al}$	$\frac{CH_2=}{CHCOO}$ Al	Molec- ular weight
1	4.32	4.37	5.68	10.7	0.94	1.00	0.94	306
2	4.30	4.31	5.61	11.2	0.93	0.99	0.98	314

^a Reaction conditions: nitrogen atmosphere; 16.66 g (0.138 mole) of diethylaluminum chloride was dissolved in 63.9 g of benzene, and 10.75 g (0.149 mole) of acrylic acid was added dropwise to this solution with stirring at room temperature.

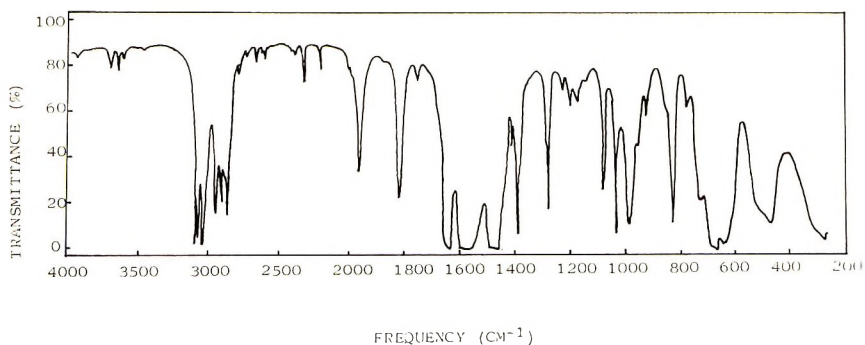


Fig. 2. Infrared spectrum of the reaction product of diethylaluminum chloride with acrylic acid (benzene solution).

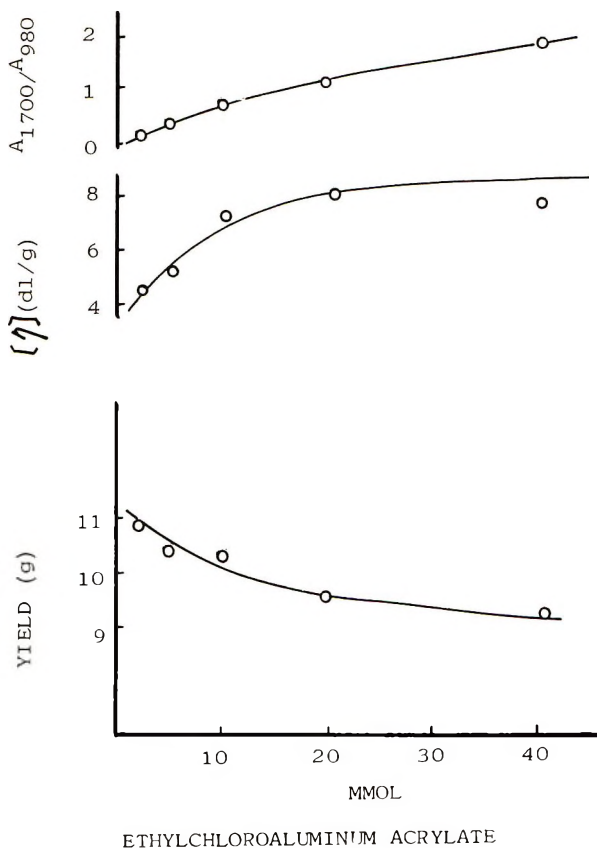


Fig. 3. Effect of ethylchloroaluminum acrylate on polymerization. Polymerization conditions: TiCl_3 , 2 mmole; $(\text{C}_2\text{H}_5)_3\text{Al}$, 2 mmole; benzene, 50 ml; 60°C ; time, 3 hr; initial propylene pressure, 3 atm. A_{1700}/A_{980} denotes an intense ratio of infrared bands at 1700 and 980 cm^{-1} .

Addition of excess acrylic acid over an equimolar amount of diethylaluminum chloride resulted in the formation of a white precipitate, which proved on chemical analysis to be chloroaluminum diacrylate. These findings indicate that acrylic acid reacts selectively with the ethyl group of diethylaluminum chloride to form ethylchloroaluminum acrylate.

Cryoscopic measurements (Table I) show ethylchloroaluminum acrylate is in the dimeric form.

Copolymerization of Propylene with Ethylchloroaluminum Acrylate

Polymerization of propylene with various amounts of ethylchloroaluminum acrylate was carried out in beverage bottles, and the reaction results

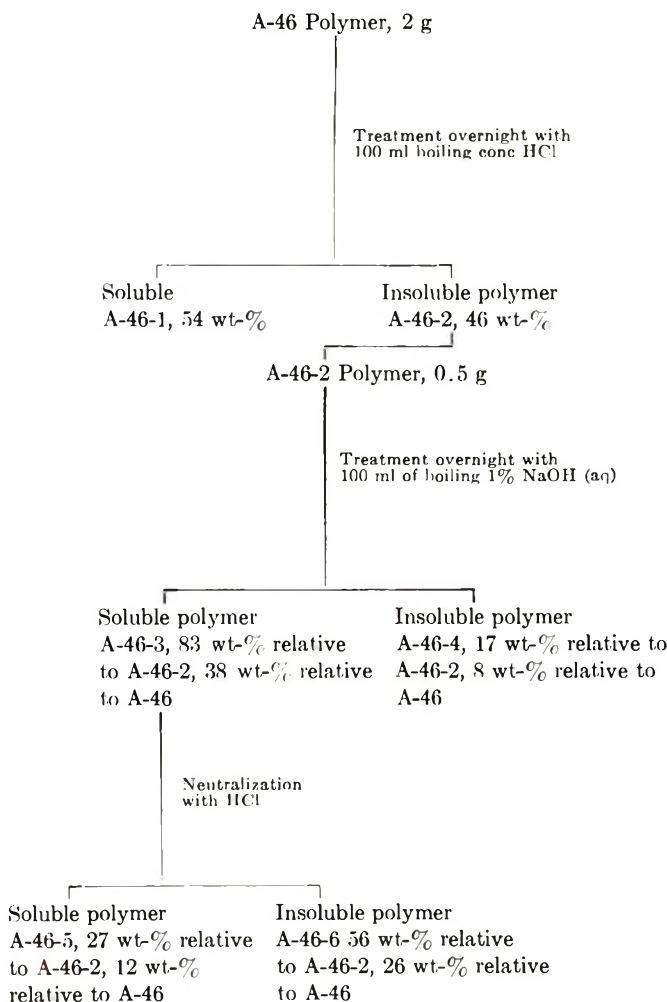


Fig. 4. Treatment of copolymer with HCl and aqueous NaOH. Polymerization conditions for A-46; TiCl_3 , 2 mmole; $(\text{C}_2\text{H}_5)_2\text{AlCl}$, 2 mmole; toluene, 40 ml; 60°C ; initial pressure, 3 atm; $\text{C}_2\text{H}_5\text{ClAlOOCCH}=\text{CH}_2$, 65 mmole; yield, 13 g.

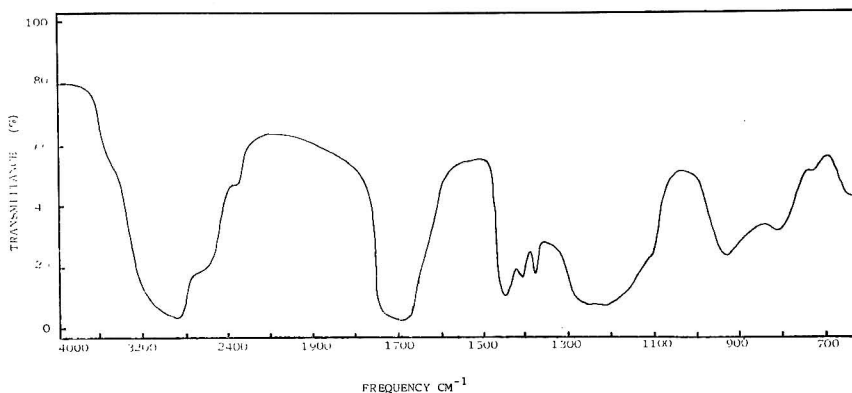


Fig. 5. Infrared spectrum of A-46-6 polymer in Fig. 4.

are shown in Figure 3. With increasing amount of ethylchloroaluminum acrylate, the yield of polymer decreases gradually, while the intrinsic viscosity increases. The infrared spectra of molded films of the polymer exhibit distinct absorption in the 1700 cm^{-1} region which is assigned to acid carbonyl groups. This clearly indicates that acrylate is polymerized with a Ziegler-Natta type catalyst. The ratio of absorption bands at 1700 cm^{-1} (carbonyl group) and 980 cm^{-1} (polypropylene) increases with increasing amount of ethylchloroaluminum acrylate.

In order to clarify whether or not acrylate is copolymerized with propylene, the polymer obtained was treated successively with hydrochloric acid and aqueous sodium hydroxide as shown in Figure 4. Of the original polymer A-46, 54% dissolved in hydrochloric acid. The soluble part is considered to contain both aluminum from ethylchloroaluminum acrylate and some soluble polymer comprising mainly poly(acrylic acid). Only a trace of aluminum was detected in the insoluble polymer, A-46-2, by chemical analysis. This indicates that all acrylic unit in the A-46-2 polymer is converted into the acid form during hydrochloric acid treatment. The polymer insoluble in hydrochloric acid, A-46-2, was treated overnight with aqueous sodium hydroxide at boiling temperature. Of the A-46-2 polymer, 83%, that is, 38.2 wt-% relative to the original polymer (A-46), was dissolved in aqueous sodium hydroxide. The content of acrylate in the original polymers (A-46) was calculated on assuming that all acrylate added to the polymerization system was polymerized and that the acrylic unit in the polymer was in the form of $\text{CH}_3\text{OClAlOOCCH}=\text{CH}_2$, which is formed during the treatment of the polymer with methanol after the polymerization. The result of the calculation is that the content of acrylic unit in the polymer A-46 is no more than 82 wt-%, and at least 18 wt-% of A-46 polymer must be propylene units. The total amount of the polymer soluble in hydrochloric acid or aqueous sodium hydroxide is 92.2 wt-% relative to A-46 polymer. This figure is higher than that of the calculated acrylic unit content in polymer A-46 and indicates that some propylene

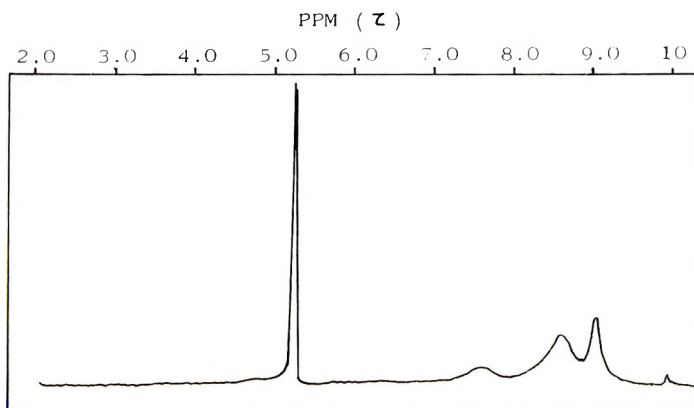


Fig. 6. NMR spectrum of A-46-6 polymer in Fig. 4.

unit in the polymer dissolved in hydrochloric acid and or in aqueous sodium hydroxide. Since, solid polypropylene is not soluble either in hydrochloric acid or in aqueous sodium hydroxide, propylene unit soluble in aqueous sodium hydroxide or in hydrochloric acid must be copolymerized with acrylic unit.

Neutralization of the sodium hydroxide solution by hydrochloric acid precipitated the polymer which amounts 56 wt-% relative to A-46-2 and 25.8 wt-% relative to original A-46 polymer. The precipitated polymer was molded into a transparent thin film. The infrared spectrum of the film is shown in Figure 5. There can be found clear differences between infrared spectrum of the precipitated polymer A-46-6 and that of poly-(acrylic acid) (Sadtlter Standard chart). The most significant difference is the presence of an absorption band at around 1380 cm^{-1} , which is assigned to methyl group, in the spectrum of the precipitated polymer A-46-6. This clearly indicates the presence of a propylene unit in this precipitated polymer. This is further evidence for the copolymerization of propylene with acrylate.

The A-46-6 fraction shown in Figure 4 was dissolved in heavy water containing sodium hydroxide and NMR spectrum was recorded. On the spectrum shown in Figure 6, there can be observed three broad peaks at around $\tau = 9.1\text{ ppm}$, 8.6 ppm , and 7.6 ppm . The peak at around 9.1 ppm can certainly be assigned to the methyl proton and the peak at around 8.6 ppm can be assigned to methylene and methyne proton judging from a standard spectrum of polypropylene (high-resolution NMR spectra, Japanese Electron Optics Laboratory Co., Ltd.). The peak at around 7.6 ppm may be assigned to the methyl proton of the acrylic unit, judging from a NMR spectrum of poly(methyl acrylate), although this assignment is not explicit. The clear presence of methyl group in the fraction soluble in aqueous sodium hydroxide indicates that propylene is copolymerized with the acrylic units.

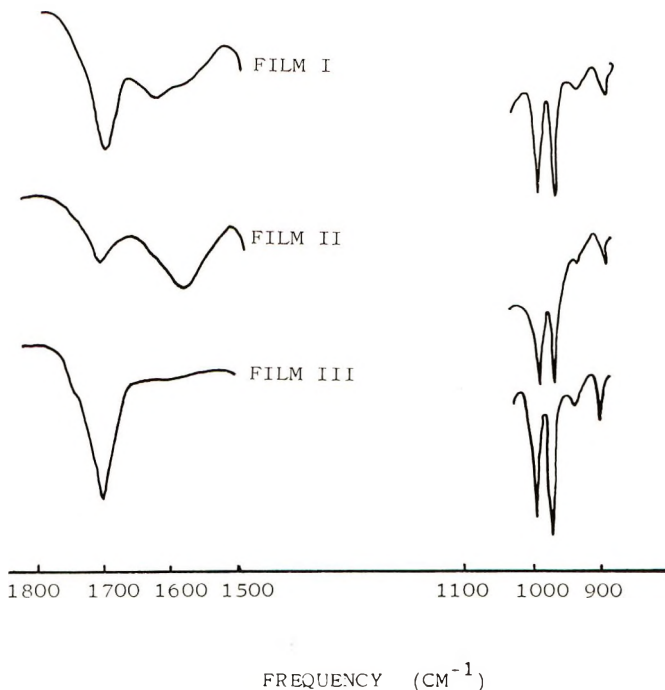


Fig. 7. Infrared spectra of A-46-4 copolymer shown in Fig. 4: (I) A-46-4 film; (II) after NaOH treatment of I, (III) after HCl treatment of II.

The polymer (A-46-4) insoluble in aqueous sodium hydroxide was molded into a thin film between sheets of aluminum foil and the aluminum foil was dissolved by hydrochloric acid. The transparent thin film thus obtained was treated successively with aqueous sodium hydroxide and hydrochloric acid. The infrared spectra of the film after each treatment were obtained and are shown in Figure 7. Absorption bands at around 1580 and 1700 cm^{-1} indicate clearly the presence of carboxyl group, which are reversibly interconvertible between acid and salt type by treatment with hydrochloric acid and aqueous sodium hydroxide. The presence of acrylic units in polymer which has been treated repeatedly with hydrochloric acid and aqueous sodium hydroxide is also evidence of the copolymerization of acrylate with propylene, since the poly(acrylic acid) is thought to be soluble in both hydrochloric acid and sodium hydroxide.

Polymer Characterization

Copolymerization of propylene with ethylchloroaluminum acrylate by $\text{TiCl}_3\text{-(C}_2\text{H}_5)_4\text{Al}_2\text{SO}_4$ system was carried out in an autoclave. The polymerization and purification conditions are detailed in Table II and the experimental section. The infrared spectrum of the copolymer before HCl-MeOH purification is shown in Figure 8. The absorptions at 620 and 1580 cm^{-1} indicate the presence of carbonyl group of salt type, and the

TABLE II
Copolymerization of Propylene with Ethylchloroaluminum Acrylate (AC-2)

Polymerization conditions	
Heptane, ml	500
TiCl ₃ (AA), mmole	10
(C ₂ H ₅) ₄ Al ₂ SO ₄ , mmole	5
C ₂ H ₅ ClAlOOCCH=CH ₂ in benzene, mmole/ml	400/510
H ₂ , ml NTP	300
Temperature, °C	60
Pressure, atm	6
Time, hr	6
Yield (after 3 hr purification with boiling HCl-CH ₃ OH) g	120
Polymer characterization	
Acrylic unit content, mole-% ^a	2
Tearing strength, gwt/cm ^b	60-100
Contact angle of water ^c	60-70°

^a Determined from elemental analyses of oxygen.

^b Determined for the film pasted with Arlon-S.

^c Determined by a goniometer.

absorption in the region of 3400 cm⁻¹ indicates a methoxy group bound to the copolymer through aluminum, the methoxy group being from the methanol used to deactivate the catalyst. The infrared spectrum of the polymer after having been purified with methanol containing hydrochloric acid is shown in Figure 9. A sharp absorption at 1720 cm⁻¹ appeared which can be assigned to ester carbonyl formed by an esterification reaction during purification of the crude polymer, while the absorptions at around 620, 1580, and 3400 cm⁻¹ disappeared. These findings indicate that the carboxylic salt in the copolymer is easily converted to an ester carbonyl. The esterified copolymer was found to contain 1.4 wt-% of oxygen, which corresponds to 2 mole-% of acrylic units.

The tear off strength of the pasted film of the copolymer was measured to be 60-100 gwt/cm, which is more than five times the tear strength of the

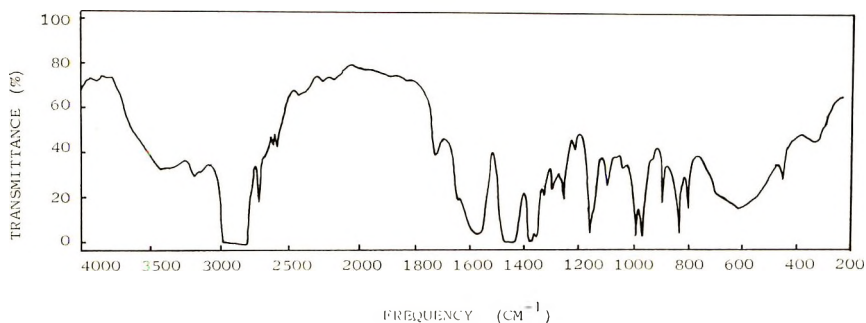


Fig. 8. Infrared spectrum of copolymer.

homopolymer. The contact angle of water on the copolymer film, which is a measure of the affinity of film to water was found to be 60–70°. This is almost the same value as that for polyamide or poly(vinyl acetate). The dyeing test on the copolymer (Table II) with the disperse dye Amacron

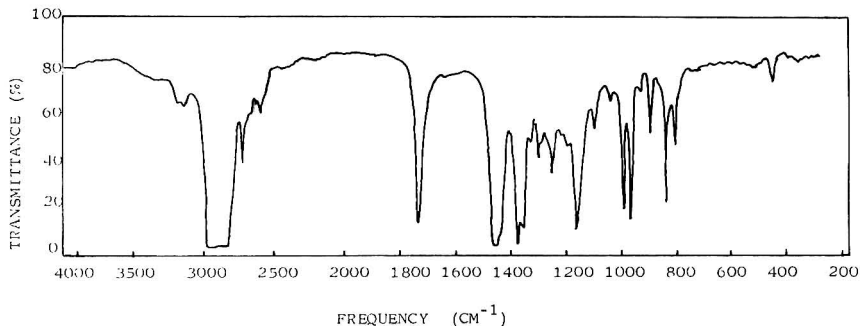


Fig. 9. Infrared spectrum of copolymer treated with $\text{CH}_3\text{OH-HCl}$.

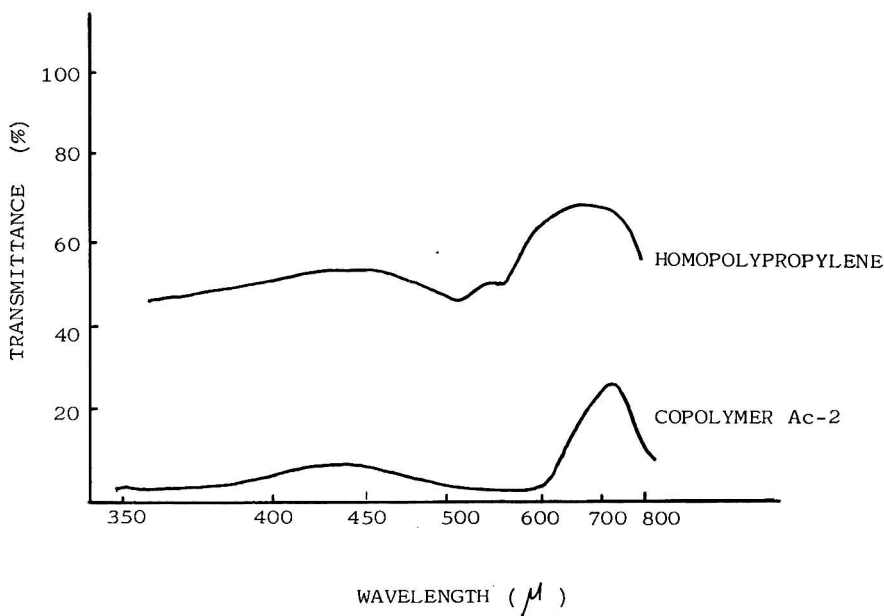


Fig. 10. Absorption spectra of polymer film ($180\ \mu$) dyed with Amacron Red FB.

Red FB was carried out, and the absorption spectrum of the film is shown in Figure 10. The figure indicates that the copolymer uptake of disperse dye is much greater than that of homopolymer. These experimental findings indicate that many shortcomings of the homopolymer due to the lack of polar groups are improved by copolymerization to a small extent with acrylate. In addition, it is worthy of mention that the copolymer contain-

ing 2 mole-% of acrylic units can be molded into a thin film of high transparency.

EXPERIMENTAL

Materials

Propylene was obtained from Mitsubishi Petrochemical Co. Analytical results showed that it contains 99.8% propylene, 0.2% propane, 5-6 ppm oxygen, and 10-20 ppm water. It was used without further purification.

Benzene and heptane were obtained commercially. They were shaken with sulfuric acid, washed with water, and dried by refluxing over sodium. They were carefully distilled at atmospheric pressure.

Diethylaluminum chloride was obtained from Ethyl Corp. and distilled under reduced pressure.

Bis(diethylaluminum) sulfate was synthesized by the reaction between diethylaluminum chloride and sodium sulfate.⁷

Titanium(III) chloride(AA) was obtained from Stauffer Chemical Co.

Methyl acrylate, 2-methyl-5-vinylpyridine, acrylic acid, and methacrylic acid were commercial products. They were dried over silica gel and distilled under reduced pressure.

Polymerization Procedure

Bottle Polymerization. The beverage bottle was baked overnight at 110-120°C and purged with nitrogen while hot. Solvent and titanium(III) chloride were added under a nitrogen atmosphere, and the bottle was capped immediately with the use of a nitrile rubber cap liner. After the bottle had been purged with propylene, alkylaluminum of the catalyst component and additive were added through a hypodermic needle. Propylene was then introduced up to the initial polymerization pressure. Polymerization was carried out by tumbling the bottle in a bath at suitable temperature. The catalyst was inactivated by adding methanol into the polymer suspension. After several minutes, the polymer was filtered off. Further purification was carried out by using hydrochloric acid when desired.

Autoclave Polymerization. A backed autoclave was purged with nitrogen. Heptane, titanium(II) chloride, bis(diethylaluminum) sulfate, and benzene solution of ethylchloroaluminum acrylate were added in that order to the autoclave under a nitrogen stream. The autoclave was closed and nitrogen was replaced with propylene. Hydrogen and then propylene were added to the polymerization pressure. Stirring was started and the temperature was raised to the desired temperature. The polymerization was carried out at constant pressure and temperature. Methanol was added to deactivate the catalyst and the reaction mixture was refluxed several hours. The slurry thus obtained was filtered and reslurried in the methanol containing hydrochloric acid and refluxed 3 hr at its boiling temperature, then filtered; the polymer obtained was dried.

Polymer Characterization

II Index. II index was taken as weight per cent of polymer which was not soluble in boiling *n*-heptane in 24 hr extraction with a Kumagawa extractor.

Intrinsic Viscosity. Measurements were made in tetralin containing 1% of Swanox [2,5-di-(*tert*-butyl)-3-methyl phenol] as antioxidant at 135°C with the use of a Fitz-Simons solution viscometer. The Huggins constant of 0.38 was used to calculate the intrinsic viscosity.⁸ No kinetic energy correction was applied.

Infrared Spectrum. The copolymer was molded into a thin film and the infrared spectrum of this film was run using Nihon Bunko spectrometer Model DS-402G and Shimadzu Model IR-27. A 1M benzene solution of ethylchloroaluminum acrylate was loaded into a KBr cell under nitrogen atmosphere and the spectrum was run immediately with the use of a Nihon Bunko Model DS-402G.

NMR Spectrum. A 6-mg portion of fraction A-46-6 was dissolved in 0.25 ml of heavy water containing sodium hydroxide. The NMR spectrum of this solution was obtained at room temperature with a Varian A-60 instrument, tetramethylsilane (TMS) being used as reference.

Ultraviolet Spectrum of the Dyed Polymer. A dye solution was prepared from 200 ml of distilled water, 0.2 g Amacron Red FB, and 0.16 g Nonipol (a nonionic detergent). The molded 180 μ film of the polymer was suspended in this solution, and the solution was stirred at 120°C in the autoclave for 2 hr. The film was separated from the dye solution and resuspended in a 1% aqueous solution of Nonipol and stirred at 60°C for 10 min. The ultraviolet spectrum of the dyed polymer thus obtained was obtained by use of a Hitachi spectrophotometer, Model EPS-2.

Tearing Strength of the Pasted Film. The polymer was molded into 200–300 μ thick film, and the film was cut into pieces 50 mm long and 10 mm wide. An Arlon-S, paste coating, comprising acrylic resin in toluene, was applied to a thickness of 0.1 mm on the film, and the film was dried at 80°C for 10 min. This film coated with paste was put on another film which was not coated with paste and the two films were pressed at 100°C by 30 kg/cm² weight for 10 min, allowed to stand at a room temperature overnight with 30 kg/cm² weight, and then further allowed to stand at a room temperature overnight without weight. The tearing strength of the pasted film was measured by using a Tensilon instrument at a tearing speed of 20 mm/min.

Contact Angle of Water on the Film. The contact angle of water on film is a measure of affinity of film to water. The polymer was molded into a thin film and one drop of water was placed on the film. The contact angle of the drop of water to film was measured with a goniometer.

Analyses of Ethylchloroaluminum Acrylate

The Ethyl group was determined by measuring ethane evolved by the reaction of the sample with water.

Chlorine was determined by conventional Mohr titration, after the sample had been decomposed with nitric acid.

Aluminum was determined by an EDTA method with the case of standard iron solution and salicylic acid as an indicator.

Acrylic group was determined from bromine number of the sample.

Molecular weight of ethylchloroaluminum acrylate was determined from cryoscopic measurements.

The authors wish to thank Toray Industries Inc. for permission to publish this paper, and Dr. H. Kobayashi, the director of Basic Research Laboratories, Dr. K. Nukushina, the former director of Central Research Laboratories, and Dr. Y. Atarashi, research associate of Basic Research Laboratories for their encouragement and support. The authors also wish to thank Mr. T. Nakae for his skillful assistance.

References

1. G. Natta, *J. Polym. Sci.*, **48**, 219 (1960).
2. E. A. H. Hopkins and M. L. Miller, *Polymer*, **4**, 75 (1963).
3. E. A. H. Hopkins and M. L. Miller, *Polymer*, **5**, 432 (1964).
4. O. F. Solomon, M. Dimonie, K. Ambrozh, and M. Tomesku, *J. Polym. Sci.*, **52**, 205 (1961).
5. R. Backskai, *J. Polym. Sci. A*, **3**, 2491 (1965).
6. N. Yamazaki and S. Maeda, *Kogyo Kagaku Zasshi*, **71**, 1549 (1968).
7. K. Matsumura and O. Fukumoto (to Toyo Rayon), Japanese Pat. Publication No. 42-4578, Pat. No. 499149 (1967).
8. Y. Atarashi, Thesis, Tokyo University, Tokyo, 1968.

Received June 16, 1970

Revised August 24, 1970

Polymerization of Propylene by the Three-Component System Comprising Titanium(III) Chloride, Ethylaluminum Sesquichloride, and Sodium Sulfate

KIICHIRO MATSUMURA, YUJI ATARASHI,* and
OSAMU FUKUMOTO,†
Kawasaki Plant, Toray Industries Inc., Kawasaki, Japan

Synopsis

Sodium sulfate increases the polymerization activity of the titanium(III) chloride (AA)-ethylaluminum sesquichloride system for the polymerization of propylene. The reaction of ethylaluminum sesquichloride with sodium sulfate at mild conditions isolates diethylaluminum chloride, which is responsible for the polymerization activity. The reaction of these components at severe conditions forms an organometallic compound containing sulfate, $(C_2H_5)_4Al_2SO_4$, and this compound is a powerful activator for titanium(III) chloride.

INTRODUCTION

Catalysts showing a great stereospecificity in the polymerization of propylene to solid polymer are the crystalline halides of transition metals, especially titanium(III) chloride and organometallic compound such as the trialkylaluminum or dialkylaluminum halides.^{1,2} Alkylaluminum sesquihalides in combination with titanium(III) chloride are scarcely effective for the polymerization of propylene to solid polymer. However, highly stereospecific catalysts for the polymerization of propylene can be obtained by using a suitable amount of a third component in combination with alkylaluminum sesquihalides and titanium(III) chloride.³

Ikegami and his co-workers⁴ studied some three-component systems containing di-*n*-butyl ether or pyridine as a third component and thought that diethylaluminum chloride formed from ethylaluminum sesquichloride by the action of the third component is responsible for the polymerization activity.

The present authors also investigated many kinds of inorganic third components and concluded that alkali metal sulfates are the most effective for increasing the polymerization activity of the ethylaluminum sesquichloride-titanium(III) chloride system. The present investigation was

* Present address: Basic Research Laboratories, Toray Industries Inc., Tebiro, Kamakura, Japan.

† Present address: Head Office, Toray Industries Inc., Muromachi, Nihonbashi, Tokyo, Japan.

undertaken to elucidate the three-component system containing sodium sulfate as a third component. No three-component system containing sodium sulfate has, to our knowledge, been reported.

EXPERIMENTAL

Materials

Propylene was obtained from Mitsubishi Petrochemical Co. Analytical results showed that it contained 99.8% propylene, 0.2% propane, 5–6 ppm oxygen, and 10–20 ppm water. It was used without further purification.

Titanium(III) chloride (AA) was obtained from Stauffer Chemical Co.

Sodium sulfate(G.R.) was obtained commercially and was pulverized. Powder of 350 Tyler mesh pass was calcined at 500°C for 2 hr and was stored over calcium chloride.

n-Heptane was a commercial product which was shaken with sulfuric acid, washed with water, and dried by refluxing over sodium. It was carefully distilled at atmospheric pressure.

Ethylaluminum sesquichloride, diethylaluminum chloride, and ethylaluminum dichloride were obtained from Texas Alkyls Co.

Polymerization

A typical polymerization was carried out as follows: *n*-Heptane, titanium(III) chloride, ethylaluminum sesquichloride, and sodium sulfate were added to an autoclave under nitrogen atmosphere in this order. The autoclave was closed and nitrogen was replaced with propylene. Stirring was started and the temperature was raised to the polymerization temperature, then propylene was charged. The polymerization was carried out at a constant pressure of propylene and constant temperature. Methanol was added to deactivate the catalyst, and the slurry thus obtained was refluxed for several hours, cooled to room temperature, and filtered. The polymer was dried at 60°C for 24 hr *in vacuo*.

Analyses

Aluminum. A sample was dissolved in aqueous hydrochloric acid and the solution was heated with excess EDTA at pH 6 to form a complex. The excess EDTA was then titrated with standard iron solution by using salicylic acid as an indicator.

Ethyl Group. A sample was introduced with a hypodermic syringe into a reactor containing a moist alundum shell suspended from the tip of a buret. Water vapor from the alundum shell decomposed the sample slowly with moderate evolution of the ethane. Dilute hydrochloric acid was added through the buret to complete the reaction. The gas evolved was measured in calibrated buret and the ethyl group content was calculated.

Chlorine. A sample was decomposed with water. Dilute nitric acid

was then added to dissolve the aluminum. The chlorine was determined by a conventional method (Mohr titration).

Sulfate. After the decomposition of a sample with dilute hydrochloric acid, the sulfate was determined as barium sulfate.

Sodium. Sodium was determined by the uranyl acetate method.

Insolubles. The insolubles content was taken as the weight per cent of polymer which was not soluble in boiling *n*-heptane in a Kumagawa extractor in a 24-hr extraction period.

Intrinsic Viscosity of the Polymer

Measurements were made in tetralin containing 1% Swanox (2,5-di-*tert*-butyl-3-methylphenol) as an antioxidant at 135°C by using Fitz-Simons solution viscometer. The Huggins relation was applied to calculate the intrinsic viscosity.

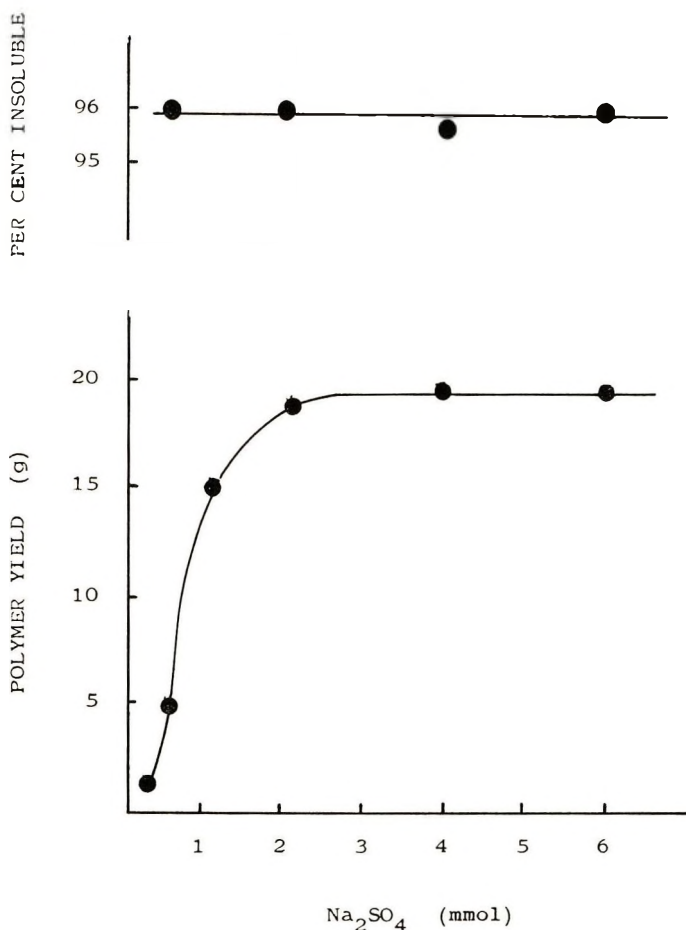


Fig. 1. Effect of sodium sulfate on polymerization activity. Polymerization conditions: *n*-heptane 130 ml; TiCl₃(AA) 4 mmole, (C₂H₅)₃Al₂Cl₃ 3.8 mmole, pressure 6 atm; 60°C; 60 min.

RESULTS

Effect of Sodium Sulfate

Polymerization of propylene was carried out to investigate the effect of sodium sulfate on the $\text{TiCl}_3\text{-(C}_2\text{H}_5)_3\text{Al}_2\text{Cl}_3$ system. The results are shown in Figures 1 and 2. The polymerization activity is very low in the absence of sodium sulfate, but it increases with increasing amount of sodium sulfate and then levels out at a $(\text{C}_2\text{H}_5)_3\text{Al}_2\text{Cl}_3/\text{Na}_2\text{SO}_4$ molar ratio of about 2. The effect of sodium sulfate is very remarkable.

When the concentration of ethylaluminum sesquichloride is varied, keeping concentration of sodium sulfate constant, the activity increases rapidly, passes through maximum at a $(\text{C}_2\text{H}_5)_3\text{Al}_2\text{Cl}_3/\text{Na}_2\text{SO}_4$ molar ratio of about 2, and decreases gradually with increasing amount of ethylaluminum sesquichloride. This shows that excess ethylaluminum sesquichloride decreases the activity. The molar ratio $(\text{C}_2\text{H}_5)_3\text{Al}_2\text{Cl}_3/\text{Na}_2\text{SO}_4$ of about 2 is critical.

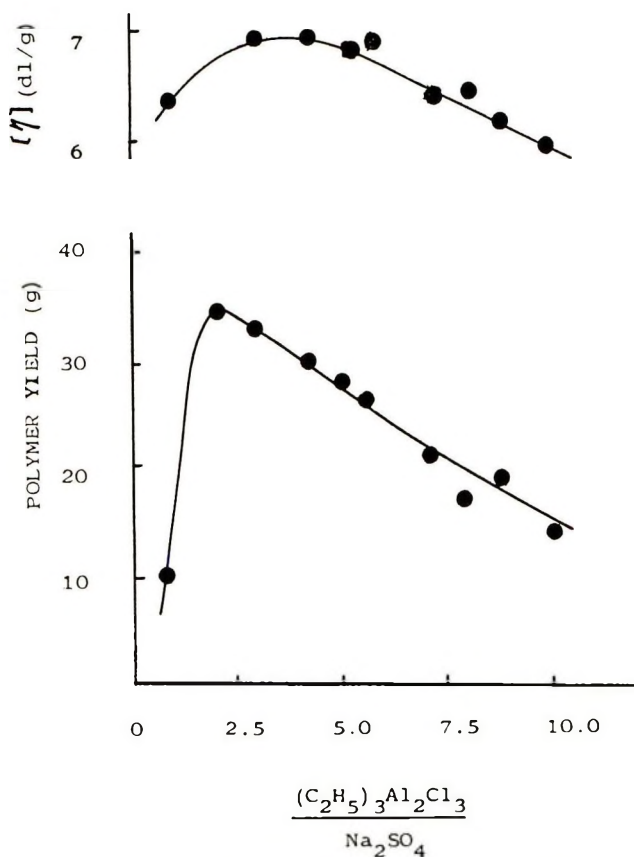


Fig. 2. Effect of molar ratio $(\text{C}_2\text{H}_5)_3\text{Al}_2\text{Cl}_3/\text{Na}_2\text{SO}_4$ on polymerization activity. Polymerization conditions: *n*-heptane 130 ml; $\text{TiCl}_3(\text{AA})$ 3 mmole, Na_2SO_4 1.5 mmole, $(\text{C}_2\text{H}_5)_3\text{Al}_2\text{Cl}_3$ 1.5–15 mmole, pressure 11 atm; 60°C ; 60 min.

The heptane-insoluble portion of the polymer remains at about 96% over the whole range of sodium sulfate concentrations; this value is almost equal to that usually observed for $\text{TiCl}_3-(\text{C}_2\text{H}_5)_2\text{AlCl}$ system. The intrinsic viscosity of the polymer ranges between 7 and 6 and decreases with increasing amount of ethylaluminum sesquichloride.

The marked effect of sodium sulfate on the $\text{TiCl}_3-(\text{C}_2\text{H}_5)_3\text{Al}_2\text{Cl}_3$ system seems to indicate that some reactions between sodium sulfate and ethylaluminum sesquichloride occur and that the reaction product activates titanium(III) chloride. Direct reaction between sodium sulfate and titanium(III) chloride is not probable because both components are solid.

Polymerizations with Titanium (III) Chloride and Reaction Product of Ethylaluminum Sesquichloride with Sodium Sulfate

The polymerization of propylene was carried out by using titanium(III) chloride and the reaction product of ethylaluminum sesquichloride with sodium sulfate, because it was suggested that reaction product from these components is responsible for activation of titanium(III) chloride. After addition of 40 mmole of sodium sulfate, the flask was purged with nitrogen and was sealed by a serum stopper. A 100-ml portion of heptane solution of ethylaluminum sesquichloride (1 mole/1000 ml) was added to the flask

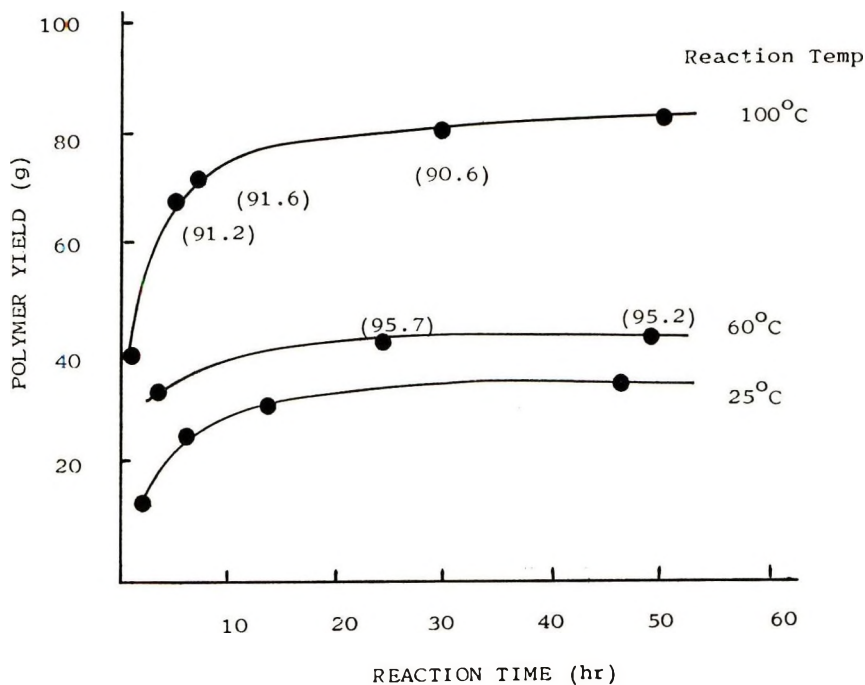


Fig. 3. Effect of reaction time of ethylaluminum sesquichloride with sodium sulfate on polymerization activity. Polymerization conditions: *n*-heptane 100 ml; $\text{TiCl}_3(\text{AA})$ 2 mmole; reaction product of ethylaluminum sesquichloride with sodium sulfate ($\text{Al}/\text{SO}_4 = 5$) 5 ml; pressure 9 atm; 60°C; 90 min. The figures in parentheses mean per cent insoluble.

by means of a syringe. The mixture was allowed to stand for a predetermined time at a given temperature. The polymerization of propylene was carried out by using 5 ml of the reaction product (liquid phase) thus obtained and 2 mmole of titanium(III) chloride. The activity and per cent insoluble of the polymer (in parentheses) are shown in Figure 3.

The polymerization activity increases with increasing reaction time of sodium sulfate and ethylaluminum sesquichloride and levels out at about 10 hr reaction time. The activity also increases with increasing reaction temperature of the two components. When a reaction temperature of 60°C is adopted, the activity is almost the same as, or slightly higher than that for the three-component system ($\text{TiCl}_3\text{-Et}_2\text{Al}_2\text{Cl}_3\text{-Na}_2\text{SO}_4$) at 60°C. The per cent insoluble of the polymer obtained by using the reaction product at 60°C is very similar to or slightly lower than that for polymers obtained with the three-component system and with the $(\text{C}_2\text{H}_5)_2\text{AlCl-TiCl}_3$ system at 60°C. These results show that in the three-component system, sodium sulfate and ethylaluminum sesquichloride first react, and the reaction product thus obtained activates titanium(III) chloride.

The polymerization activity is very high, even higher than that for the diethylaluminum chloride-titanium(III) chloride system, when the reaction product at 100°C is used with titanium(III) chloride. The per cent insoluble of the polymer obtained by using the reaction product obtained at 100°C is lower than that of the polymer formed with the three-component system and/or with the product reacted at 60°C. These results are enough to suggest that the high-temperature product is different from the low-temperature product. A very powerful activator for titanium(III) chloride must be formed by the reaction of ethylaluminum sesquichloride with sodium sulfate at higher temperature.

Analysis of the Reaction Product of Ethylaluminum Sesquichloride with Sodium Sulfate

The reaction product of ethylaluminum sesquichloride with sodium sulfate seems to activate titanium(III) chloride, as already mentioned. Hence, experiments were initiated to obtain some information on the reaction of these two components.

A 100-ml portion of a 1 *M* solution of ethylaluminum sesquichloride and 60 mmole of sodium sulfate were reacted under nitrogen at 25, 60, and 100°C for a predetermined time. Sodium sulfate was agglomerated with evolution of heat immediately after the reactants were mixed. The liquid phase of the reaction product was removed with a syringe and was submitted to analysis. The analytical results are shown in Table I. With increasing reaction temperature and time, (1) concentrations of aluminum, ethyl group, and especially chlorine decrease; (2) sulfate appears in the liquid phase and its concentration increases gradually; (3) the $\text{C}_2\text{H}_5/\text{Al}$ ratio increases and reaches 2; (4) on the contrary, the Cl/Al ratio decreases, and becomes less than 1; (5) sodium is not detected in the liquid phase; (6) $(\text{C}_2\text{H}_5 + \text{Cl} + 2\text{SO}_4)/\text{Al}$ is always 3. The analyses in Table I suggest a

TABLE I
Analyses of the Reaction Product (Liquid Phase) of Ethylaluminum Sesquichloride with Sodium Sulfate^a

No.	Reaction conditions							$\frac{C_2H_6}{Al}$	$\frac{Na,}{wt-\%}$	$\frac{C_2H_6}{Al}$	$\frac{Cl}{Al}$	$\frac{SO_4}{Al}$	$\frac{\Sigma^b}{Al}$
	Temp, °C	Time, hr	Al, wt-%	C_2H_6 , wt-%	Cl, wt-%	SO_4 , wt-%	Na , wt-%						
1	0		7.1	11.4	13.8	—	—	—	1.5	—	3.0		
2	25	1	5.5	10.7	8.4	0.0	—	—	1.8	0	3.0		
3	25	24	5.2	10.3	7.5	0.9	0.007	—	1.8	0.05	3.0		
4	60	24	5.1	10.3	6.0	2.1	—	—	1.9	0.1	3.0		
5	100	24	4.8	9.2	2.6	4.7	0.000	—	1.9	0.3	2.9		

^a Reaction conditions: $(C_2H_5)_2Al_2Cl_3 = 1$ mole/l. in heptane; $(C_2H_6)_2Al_2Cl_2/Na_2SO_4 = 5/3$.

^b $\Sigma = (C_2H_6 + Cl + 2SO_4)/Al$.

TABLE II
Analyses of the Reaction Product (Liquid Phase) of Ethylaluminum Dichloride
and Diethylaluminum Chloride with Sodium Sulfate^a

No.	Halide	Reaction conditions			Al, wt-%	C ₂ H ₅ , wt-%	Cl, wt-%	SO ₄ , wt-%	Na, wt-%	C ₂ H ₅ /Al	Cl/Al	SO ₄ /Al	Σ ^b /Al
		Temp, °C	Time, hr										
6	(C ₂ H ₅) ₂ AlCl	—	—	6.5	14.0	8.6	—	—	—	2.0	1.0	—	3.0
7		98	24	6.5	13.3	0.09	11.3	0.00	—	1.9	0.01	0.49	2.9
8	C ₂ H ₅ AlCl ₂	—	—	6.5	6.9	17.4	—	—	—	1.0	2.0	—	3.0
9		98	24	0.6	1.3	0.2	1.0	0.00	—	1.9	0.2	0.45	3.0

^a Na₂SO₄/Al = 1.

^b Σ = (C₂H₅ + Cl + 2SO₄)/Al.

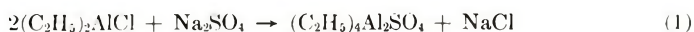
replacement reaction of chlorine with sulfate, and also the formation of heptane-insoluble compound. In order to clarify these points, reactions of sodium sulfate with diethylaluminum chloride and ethylaluminum dichloride were carried out as in the same way for ethylaluminum sesquichloride, since ethylaluminum sesquichloride can be regarded as an equimolar mixture of these two components.

The analytical results are shown in Table II. The decrease of aluminum concentration in the liquid phase in the course of the reaction is marked when ethylaluminum dichloride is used; on the contrary, the change in the aluminum concentration is slight for the reaction of diethylaluminum chloride. These findings suggest that the decrease of aluminum concentration in the course of the reaction of ethylaluminum sesquichloride with sodium sulfate is due mainly to the reaction between ethylaluminum dichloride and sodium sulfate. Ethylaluminum dichloride but not diethylaluminum chloride forms a heptane-insoluble complex with sodium chloride, as already reported by Ziegler et al.^{5,6} Ethylaluminum dichloride seems to react with sodium sulfate in the same way as with sodium chloride.

When diethylaluminum chloride is used as a reactant, sulfate appears in the liquid phase up to nearly half of the aluminum concentration, while chlorine decreases and C_2H_5/Al ratio remains constant. These results indicate that diethylaluminum chloride exchanges chlorine for sulfate with sodium sulfate.

With ethylaluminum dichloride, in addition to the remarkable decrease of aluminum from the heptane phase, C_2H_5/Al increases, Cl/Al decreases, and SO_4 also appears. These results suggest a dismutation reaction of ethylaluminum dichloride to diethylaluminum chloride,⁷ and also some displacement reaction between sulfate and probably chlorine of the diethylaluminum chloride formed. The extent of these reactions must be small, and 90% of ethylaluminum dichloride is fixed by sodium sulfate, on the basis of the results shown in Table II.

Two reactions can be suggested as the main reactions between ethylaluminum sesquichloride and sodium sulfate, on the basis of these experimental results:



Reaction (2) seems to be faster than reaction (1), judging from the data in Table I indicating that the C_2H_5/Al ratio increases even at mild reaction conditions, while sulfate can only appear at more severe reaction conditions.

The reaction product of ethylaluminum sesquichloride with sodium sulfate at 100°C for longer than about 5 hr shows very high activity for the polymerization of propylene, when used with titanium(III) chloride. Chemical analyses (Table I) indicate that the distinguished feature of the reaction product at 100°C is its higher content of sulfate and lower content

of chlorine compared with the reaction product at 60°C or 25°C, which can only give moderate activity. That is, when sulfate content is higher, the catalyst has the higher activity. This higher activity could be attributed to the compound containing sulfate $(C_2H_5)_3Al_2SO_4$, which is formed by reaction (1).

Infrared Spectrum of the Reaction Product of Ethylaluminum Sesquichloride and Sodium Sulfate

A 100-ml portion of a 1 *M* solution of ethylaluminum sesquichloride in *n*-heptane and 60 mmole of sodium sulfate were reacted under nitrogen atmosphere at 100°C for 24 hr. The reaction product was loaded into a KRS-5 cell (0.1 mm thickness of solution) under nitrogen atmosphere and the spectrum was run immediately by use of a Nihon Bunko Model DS-402G instrument. The spectrum is shown in Figure 4. The 1150–1200 cm^{-1} broad band can be assigned to sulfate,⁸ and the other bands are very similar to that of diethylaluminum chloride.⁹ This result indicates the presence of a heptane-soluble alkylaluminum compound having sulfate in its molecule.

DISCUSSION

The effect of sodium sulfate on the $(C_2H_5)_3Al_2Cl_3$ - $TiCl_3$ system can best be explained by assuming two main reactions, (1) and (2), mentioned already, between sodium sulfate and ethylaluminum sesquichloride. It is also assumed that the reaction (2) is faster than the reaction (1) and that the reaction product $(C_2H_5)_4Al_2SO_4$ is a powerful activator for $TiCl_3$.

Addition of ethylaluminum dichloride into the catalyst system consisting of diethylaluminum chloride and titanium(III) chloride, decreases the polymerization activity.¹⁰ This indicates that ethylaluminum dichloride is a catalyst poison. Hence, increase of the polymerization activity can be expected when ethylaluminum dichloride is removed from the $(C_2H_5)_3Al_2Cl_3$ - $TiCl_3$ system, since ethylaluminum sesquichloride can be regarded as the equimolar mixture of ethylaluminum dichloride and diethylaluminum chloride. In the three-component system used at about 60°C, reaction (2) takes place predominantly, and ethylaluminum dichloride, a catalyst poison, is removed, to yield diethylaluminum chloride. The polymerization activity is attributable to the diethylaluminum chloride thus formed. The similarity of per cent insolubles and intrinsic viscosity of the polymer obtained by three-component system to these of the polymer obtained with the $TiCl_3$ - $(C_2H_5)_2AlCl$ system lends some support to this explanation.

One mole of sodium sulfate seems to be able to fix only two moles of ethylaluminum dichloride under the experimental conditions, judging from the fact that a $(C_2H_5)_3Al_2Cl_3/Na_2SO_4$ ratio of about 2 is critical, as shown in Figures 1 and 2. Addition of ethylaluminum sesquichloride in excess, over a $(C_2H_5)_3Al_2Cl_3/Na_2SO_4$ ratio of about 2, leads to free ethylaluminum dichloride in the liquid phase, and this ethylaluminum dichloride acts as a catalyst poison, and hence the polymerization activity is lower. Excess

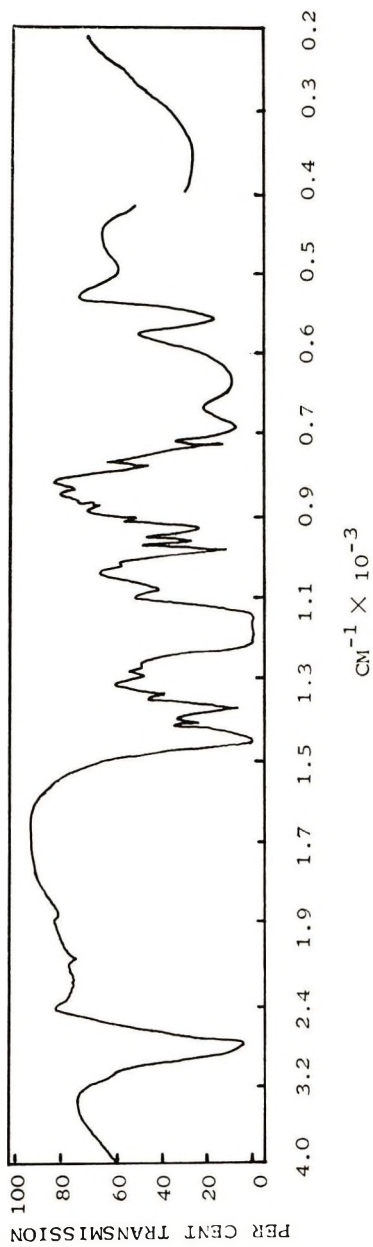


Fig. 4. Infrared spectrum of the reaction product of ethylaluminum sesquichloride and sodium sulfate in *n*-heptane.

addition of sodium sulfate, on the other hand, does not affect the polymerization activity because sodium sulfate is not a catalyst poison.

When ethylaluminum sesquichloride is reacted with sodium sulfate at 100°C for longer than about 5 hr, reaction (1) proceeds to a considerable extent to form $(C_2H_5)_4Al_2SO_4$, which is a powerful activator for the polymerization of propylene. The higher polymerization activity of the system comprising the reaction product at 100°C and the lower content of heptane-insoluble material of the polymer obtained can both be explained by a new activator containing sulfate, $(C_2H_5)_4Al_2SO_4$, which was first found in this study by the present authors.

When the temperature of reaction of ethylaluminum sesquichloride with sodium sulfate is 60 or 25°C, reaction (1) proceeds only to a lesser extent, hence the concentration of organometallic compound containing sulfate in the liquid phase is low. The main activator of the system comprising the reaction product at 60 and 25°C is diethylaluminum chloride. This is the reason why only a low activity can be shown by this catalyst system.

The authors wish to thank Toray Industries Inc. for permission to publish this paper and Dr. H. Kobayashi, the director of Basic Research Laboratories, and Dr. K. Nukushina, the former director of Central Research Laboratories, for their encouragement and support. The authors also wish to thank Mr. T. Nakae and Mr. M. Koike for their skillful assistance.

References

1. G. Natta, P. Pino, and G. Mazzanti, *Ital. Pat.* 526,101 (Dec. 3, 1954).
2. G. Natta, *Angew. Chem.*, **68**, 393 (1954).
3. Eastman Kodak Co., Japan Pats. 37-6989 and 37-6991; Sun Oil Co., Japan Pats. 36-20898 and 38-2386.
4. H. Ikegami, H. Kumura, and K. Machida, *Kogyo Kagaku Zasshi*, **69**, 321 (1966).
5. K. Ziegler, R. Köster, H. Lehmkuhl, and K. Reinert, *Ann. Chem.*, **629**, 33 (1960).
6. K. Ziegler and M. Martin, *Makromol. Chem.*, **18/19**, 186 (1956).
7. A. Zambelli, J. Dipietro, and G. Gatti, *J. Polym. Sci. A*, **1**, 407 (1963).
8. K. Nakamoto, *Infrared Spectra of Inorganic and Coordination Compounds*, Wiley, New York, 1962.
9. E. G. Hoffmann, *Z. Elektrochem.*, **64**, 616 (1950).
10. G. Natta, A. Zambelli, I. Pasquon, G. Gatti, and D. Deluca, *Makromol. Chem.*, **70**, 206 (1964).

Received May 18, 1970

Thermoplastic Elastomers via Radical Polymerization. II

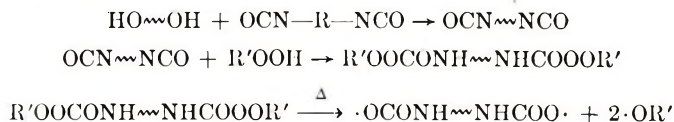
EMMANUEL J. ZAGANIARIS,* *Frick Chemical Laboratory,
Princeton University, Princeton, New Jersey 08540*

Synopsis

Simple models are used to study the formation of thermoplastic elastomers using a method for preparation of block copolymers introduced by Tobolsky and Rembaum. It was found that a small excess of isocyanate groups produce branched block copolymers with significantly reduced fractions of AB and B type molecules.

Introduction

Some time ago, Tobolsky and Rembaum¹ introduced a new method to prepare block copolymers. The reaction scheme is:



The free radicals initiate polymerization of a vinyl monomer. Further modification of this method² employs a bishydroxyl peroxide instead of the hydroperoxide, thus eliminating the vinyl homopolymer from the final product.

It was a challenge to try to use this method to synthesize thermoplastic elastomers, that is, block copolymers of ABA type, where A is a thermoplastic glassy material and B is an elastomer, in view of the attractive properties that this type of material possesses.³ Thus, a hydroxy-terminated polyester or polyether was chain-extended with a diisocyanate to form a high molecular weight polyurethane which was subsequently capped with a hydroperoxide. This polymeric peroxyurethane was used, under dead-end conditions⁴ to ensure highest possible block molecules formation, as initiator for vinyl polymerization.

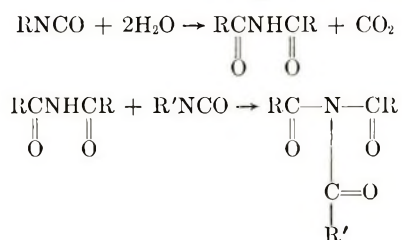
However experimental evidence as well as theoretical predictions suggest that there are two critical factors that limit the use of this method for preparation of thermoplastic elastomers. One is the efficiency of the peroxyurethane as initiator of vinyl polymerization and another is the extent of the condensation reaction. Because of these two factors, the product contained high fractions of polyester homopolymer and AB

* Present address: Rohm and Haas Company, Spring House, Pa. 19477.

type blocks along with the desired ABA. Since the strength of the thermoplastic elastomers decreases with even small portions of the above by-products, two approaches were employed to use this method.

One was to use aromatic diisocyanates so that the aromatic groups form blocks within the middle-block, thus capping both ends with vinyl polymer is no longer critical (see part I).⁵ The second approach was to use a branched middle block so that even if the extent of the reaction or the efficiency of the initiator is not 100% the reactions of AB and B type molecules are significantly decreased, a concept arrived at by discussion with Professor A. V. Tobolsky and P. C. Lue.

Branched polymeric peroxy-carbamates were made by using excess of isocyanate groups and a small amount of water molecules to create urea groups. The branches were formed through biuret links.



Linear Middle Block

In order to have most of the ends capped with peroxide, exactly equivalent amounts of OH and NCO groups was used. Since the allophanate formation goes much slower than the extension reaction,⁶ we neglect branching for low degrees of polymerization. So, starting, for example, with polyester glycol of \bar{m}_n about 3000, hexamethylene diisocyanate (HDI), cumene hydroperoxide (CHP), and T-8 catalyst, we describe this case by the system



where A = OH, B = NCO, and C = OOH groups.

Let N_A , N_B , and N_C be the moles of these reactants originally mixed together in proportions so that

$$N_C/N_A = \rho \quad (1)$$

If equivalent amounts are used, we also have

$$2N_A + N_C = 2N_B \quad (2)$$

The number of units N_0 is

$$\begin{aligned}
 N_0 &= N_A + N_B + N_C \\
 &= N_A(4 + 3\rho)/2 \quad (3)
 \end{aligned}$$

The number of ends N_e , except unreacted C, will be

$$N_c = N_A[2(1 - \alpha) + (2 + \rho)(1 - \beta) - \rho\gamma]$$

where α , β , and γ are the fractions of A, B, and C groups reacted. But we also have

$$2\alpha N_A + \gamma N_C = 2\beta N_B \quad (4)$$

$$2\alpha + \rho\gamma = (2 + \rho)\beta$$

or

$$\rho\gamma - 2\beta - \rho\beta = -2\alpha$$

Substituting, we obtain

$$N_c = N_A(4 - 4\alpha + \rho) \quad (5)$$

The number of molecules will be half the number of ends plus the number of unreacted C.

$$N = \frac{N_A}{2} [4 - 2\beta(2 + \rho) + 3\rho] \quad (6)$$

The number-average degree of polymerization, \bar{P}_n , is given by

$$\begin{aligned} \bar{P}_n &= \frac{\text{number of units}}{\text{number of molecules}} \\ &= (4 + 3\rho) / [4 - 2\beta(2 + \rho) + 3\rho] \end{aligned} \quad (7)$$

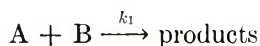
From γN_C peroxy endgroups, only a fraction f will be able to initiate vinyl polymerization. If dead-end conditions are employed, then all peroxy endgroups will decompose before the vinyl monomer is used up. The number of ends attached to vinyl polymer is then $N_C \gamma f$. The chance, therefore, of attachment of an end to a vinyl segment is

$$\begin{aligned} \chi &= N_C \gamma f / [N_A(4 - 4\alpha + \rho)] \\ &= \rho \gamma f / (4 - 4\alpha + \rho) \end{aligned} \quad (8)$$

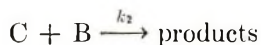
Since each molecule has two ends, the probability that n ends of the two are attached to vinyl polymer is

$$P_n(2) = \frac{2!}{n!(2-n)!} \chi^n (1 - \chi)^{2-n} \quad (9)$$

The relationship between α and γ is found by considering the kinetic scheme of the parallel reactions:



and



The result is that⁷

$$(1 - \alpha) = (1 - \gamma)^{k_1/k_2}$$

When $k_1 = k_2$, then $\alpha = \gamma$ and from eq. (4), $\alpha = \beta$. In that case \bar{P}_n can be obtained from⁸

$$\bar{P}_n = 1/[1 - (pf_n/2)] \quad (10)$$

where

$$f_n = \sum_i N_i f_i / \sum_i N_i \quad (11)$$

f_i being the functionality of species i and p the extent of the reaction.

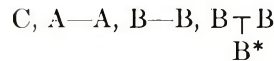
Branched Middle Block

If an excess of isocyanate groups is used, then except in the extension reaction, additional side reaction will take place, particularly allophanate or biuret formation. Assuming again side reactions to be much slower than extension reaction, we can use the following system to describe the case



C, A, and A* react with B; A* reacts after A has reacted; C = OOH, A = OH, A* = carbamate, and B = NCO. A* is equal to the excess of B groups.

A similar situation arises when an isocyanate of functionality greater than two is used. Then the system can be described by



C and A react with B and B*; C = OOH, A = OH, B = B* = NCO. We use this system to estimate the properties of the resulting polymer as follows.

Let N_A, N_B, N_{B^*}, N_C be the moles of A—A, B—B, B $\underset{\text{B}^*}{\text{T}}$ B, and C initially mixed together. From the condition of equivalent initial concentrations we have

$$N_C + 2N_A = 2N_B + 3N_{B^*} \quad (12)$$

Let

$$N_C/N_A = \rho \quad (13a)$$

and

$$N_B/N_{B^*} = \pi \quad (13b)$$


The number of units N_0 is

$$\begin{aligned}
 N_0 &= N_A + N_B + N_{B^*} + N_C \\
 &= N_A \left\{ 1 + \rho + [(\pi + 1)(2 + \rho)/(2\pi + 3)] \right\} \quad (14)
 \end{aligned}$$

The gel point for such a system has been presented by Case.⁹

The number of ends, except unreacted C, is

$$N_e = 2N_A(1 - \alpha) + 2N_B(1 - \beta) + 2N_{B^*}(1 - \beta) + N_{B^*}(1 - \beta^*) + N_C\gamma$$

where α , β , β^* , and γ are the fractions of A—A, B—B, B , and C, respectively, reacted.

By using eqs. (13) and (14) this becomes:

$$\begin{aligned}
 N_e &= N_A \left[2(1 - \alpha) + 2\pi \frac{(2 + \rho)}{(2\pi + 3)} (1 - \beta) \right. \\
 &\quad \left. + 2 \frac{(2 + \rho)}{(2\pi + 3)} (1 - \beta) + \frac{(2 + \rho)}{(2\pi + 3)} (1 - \beta^*) + \rho\gamma \right] \\
 &= N_A \left[2(1 - \alpha) + \frac{2(\pi + 1)(2 + \rho)}{(2\pi + 3)} (1 - \beta) \right. \\
 &\quad \left. + \frac{(2 + \rho)}{(2\pi + 3)} (1 - \beta^*) + \rho\gamma \right]
 \end{aligned}$$

We also have

$$2N_A\alpha + \gamma N_C = 2N_B\beta + 2N_{B^*}\beta + N_{B^*}\beta^*$$

or

$$\frac{2(\rho + 2)(\pi + 1)}{(2\pi + 3)} \beta + \frac{(2 + \rho)}{(2\pi + 3)} \beta^* = 2\alpha - \rho\gamma \quad (15)$$

On substituting, we obtain for N_e

$$N_e = N_A(4 - 4\alpha + \rho) \quad (16)$$

We have also that the number of ends is equal to twice the number of molecules plus the number of trifunctional units. Therefore the number of molecules N is

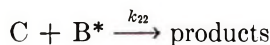
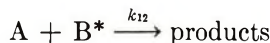
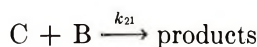
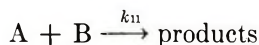
$$\begin{aligned}
 N &= [(N_e - N_{B^*})/2] + (1 - \gamma)N_C \\
 &= \frac{N_A}{2} (4 - 4\alpha + \rho) - \frac{(2 + \rho)N_A}{2(2\pi + 3)} + (1 - \gamma)\rho N_A \\
 &= N_A \left[2 - 2\alpha + \frac{\rho}{2} - \frac{(2 + \rho)}{2(2\pi + 3)} + (1 - \gamma)\rho \right] \\
 &= N_A \left[2 - 2\alpha - \gamma\rho + \frac{3\rho}{2} - \frac{(2 + \rho)}{2(2\pi + 3)} \right] \quad (17)
 \end{aligned}$$

The degree of polymerization is

$$\begin{aligned}
 P_n &= N_0/N \\
 &= \frac{N_A \{1 + \rho + [(\pi + 1)(2 + \rho)/(2\pi + 3)]\}}{N_A \{2 - 2\alpha - \gamma\rho + (3\rho/2) - [(2 + \rho)/2(2\pi + 3)]\}} \\
 &= \frac{1 + \rho + [(\pi + 1)(2 + \rho)/(2\pi + 3)]}{2 - 2\alpha - \gamma\rho + (3\rho/2) + [(2 + \rho)/2(2\pi + 3)]} \quad (18)
 \end{aligned}$$

When the reactivities are equal, P_n is again also given by eqs. (10) and (11).

The relationship between α and γ and between β and β^* is found from the kinetics of the parallel reactions:^{7,9}



If $k_{12}/k_{11} = k_{22}/k_{21}$, then

$$(1 - \alpha) = (1 - \gamma)^{k_{11}/k_{21}}$$

and

$$(1 - \beta) = (1 - \beta^*)^{k_{11}/k_{12}} \quad (19)$$

When the reactivities of the different groups are the same, then since we also have equivalent initial concentrations, using eq. (8) obtain

$$\alpha = \beta = \beta^* = \gamma$$

In that case, the gel point occurs when

$$\alpha^2 = (2\pi + 3)(\rho + 2)/4(\pi + 3) \quad (20)$$

The number of ends becomes

$$N_e = N_A(4 - 4\alpha + \rho) \quad (21)$$

The number of molecules is

$$N = N_A \{2 + (\rho/2) - 2\alpha - [(2 + \rho)/2(2\pi + 3)] + \rho(1 - \alpha)\} \quad (22)$$

and

$$P_n = \frac{N_0}{N} = \frac{(1 + \rho)(2\pi + 3) + (\pi + 1)(2 + \rho)}{4\pi + 5 + 4\rho - 4\alpha\rho - 6\alpha - 2\pi\rho\alpha} \quad (23)$$

We now have the number of peroxy endgroups as well as the total number of ends. We still need to know the fraction of molecules with 0, 1, 2, . . . , trifunctional units, that is with 2, 3, 4, . . . , ends. To find this we use

the so-called complexity distribution,¹⁰ which gives the number of molecules with n number of branch units irrespective of the number of the other monomer units. To derive this, one could sum over all m_i and n_j in Stockmayer's distribution formula,¹¹ for example. However another approach was used here, based on a similar derivation by Flory¹⁰ with minor modification to account for the monofunctional units, the equivalent amounts of A and B groups, and the different reactivities of the groups.

Let a be the probability of a branch unit to be connected through a sequence of two or more A—B bonds to another branch unit. Let also a^* be the probability of an unreacted A or B group or a reacted C group which leads to a branch unit through 0 or more A—B bonds. The probability of an unreacted A or B group or a reacted C group is part of a molecule with n branch units is

$$P_n = \omega_n a^* a^{n-1} (1 - a)^{(f-2)n-1} \quad n > 0$$

and

$$P_0 = 1 - a^* \quad n = 0 \quad (24)$$

where

$$\omega_n = \frac{(fn - n)!}{(fn - 2n + 1)n!}$$

The number of molecules with n branch units is

$$N_n = \frac{N_A(4 - 4\alpha + \rho)\omega_n a^* a^{n-1} (1 - a)^{fn-2n-1}}{fn - 2n + 2} \quad n > 0$$

$$N_{n=0} = N_A(1 - a^*)[2 - 2\alpha + (\rho/2)] \quad n = 0 \quad (25)$$

The mole fraction is obtained by dividing N_n by the total number of molecules N .

$$X_n = \frac{(4 - 4\alpha + \rho)\omega_n a^* a^{n-1} (1 - a)^{fn-2n-1}}{(fn - 2n + 2) \left(2 - 2\alpha - \rho\gamma + \frac{3\rho}{2} - \frac{(2 + \rho)}{2(2\pi + 3)} \right)} \quad n > 0$$

$$X_{n=0} = \frac{(1 - a^*)[2 - 2\alpha + (\rho/2)]}{2 - 2\alpha - \rho\gamma + \frac{3\rho}{2} - \frac{(2 + \rho)}{2(2\pi + 3)}} \quad n = 0 \quad (26)$$

The derivation of this complexity distribution is found in the Appendix.

To each fraction with a certain number of ends we distribute the vinyl end-blocks as before, using binomial distribution. The number of vinyl end blocks is γN_{cf} , where f is the efficiency of initiation of vinyl polymerization. The chance of an end to be attached to a vinyl segment is

$$\chi = \frac{\rho\gamma f}{4 - 4\alpha + \rho} \quad (27)$$

The probability that out of $(n + 2)$ ends there are k ends attached to vinyl segments is

$$P_k(n + 2) = \frac{(n + 2)!}{k!(n + 2 - k)!} \chi^k (1 - \chi)^{n+2-k} \quad (28)$$

The final composition of the product will be

$$X_k = \sum_n P_k(n + 2) X_n$$

where k is the number of vinyl endblocks, X_n is given by eq. (26), and $P_k(n + 2)$ by eq. (28).

Furthermore, from eq. (26) we can estimate the number of mid-chains in the physical network formed. Each B or AB type block molecule contributes nothing, each ABA contributes one, each AB_A^A contributes three, etc. chains. The modulus of the polymer would then be¹²

$$G = nRT \quad (29)$$

where n is the number of moles of network chains. G must be corrected for the filler effect of the vinyl polymer phase¹³

$$G = G_0(1 + 2.5\phi + 14.1\phi^2) \quad (30)$$

where ϕ is the volume fraction of the vinyl polymer and G_0 the modulus of the unfilled material. A further correction must be applied for the entanglements in the polyester phase. This number of chains must also be corrected for the dilution after the vinyl polymerization step.

At the second stage of vinyl polymerization, there are again several mechanisms involved. Of interest here is the termination mechanisms that can be either by disproportionation or by combination. Since we have dead-end conditions, the initiator is consumed up before the monomer.

We consider here two cases: that of PMMA where $k_{td} \gg k_{tc}$ and that of PS where $k_{tc} \gg k_{td}$.

In the first case the final product is described by the equations already derived. In the case of PS we can visualize the peroxy-carbamates as monomer units for condensation: AB type are monofunctional units, BA bifunctional, etc. In order that no gelation takes place it must be⁷

$$\bar{f}_w < 2$$

where

$$\bar{f}_w = \frac{\sum_i N_i f_i^2}{\sum_i N_i f_i}$$

and N_i denotes the number of molecules with functionality f_i . Since the properties of the final product do not depend on the number of blocks per molecule, no further consideration is required.

Experimental

The experimental conditions were the same as already described in part I;⁵ hexamethylene diisocyanate (HDI) was used as diisocyanate

and dibutyltin di(2-ethylhexoate), commercially known as T-8, was used as catalyst.

\bar{M}_n was measured with a Mechrolab vapor pressure osmometer (Model 301A).

Results

The \bar{M}_n of some polymeric peroxy-carbamates are given in Table I, along with the values calculated by using eq. (7) or (18). There is a fair agreement, although the range of the molecular weights is rather small.

TABLE I

π	ρ	β	\bar{M}_n	
			Calcd	Exptl
∞	0.2	0.97	17,000	15,000
∞	0.13	0.96	18,000	15,000
∞	0.08	0.96	20,000	20,000 ($\pm 5,000$)
23	0.5	0.97	10,000	8,100
120	0.1	0.97	20,000	25,000 ($\pm 5,000$)

The comparison of experimental with calculated modulus however was possible only in a very approximate degree.

The polyester phase is semicrystalline with melting temperature around 30–40°C. There is thus only limited temperature range remaining to the T_g of the glassy phase (about 100°C). In addition, there is no equilibrium modulus in this temperature region; possibly due to a certain degree of compatibility between the rubbery and the glassy phase, the modulus was continuously decreasing.

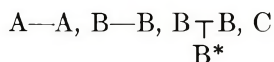
Qualitatively, however, the experimental values agree with those predicted (Table II). Linear block copolymers with $\rho < 0.2$ show no structure after the melting point of the rubbery phase; they flow at 30–40°C.

Linear block copolymers with $\rho > 0.2$ showed some structure but low modulus after 40°C. Branched block copolymers showed moduli in the 40–80°C region to increase in a predictable way, and those were samples with improved strength.

APPENDIX

Derivation of the Complexity Distribution

We have the system



where A and C react with B and B*. Originally N_A , N_B , N_{B^*} , and N_C moles of the above reactants were mixed together in such proportions that

$$N_C/N_A = \rho$$

TABLE II

PMMA, %	PS, %	(PMMA- co-PS), %	ρ	π	$\frac{\beta^* N_B^*}{N}$	G (calcd)	G $(1 + 2.5\phi + 14.1\phi^2)$ (exptl, 60°C)
38	—	—	0.18	50	0.17	4×10^5	6×10^5
46.5	—	—	0.20	10	1.0	3.5×10^5	6.5×10^5
46	—	—	0.20	∞	0	2.1×10^5	3.3×10^5
32	—	—	0.04	50	0.3	2.3×10^5	2.6×10^5
40	—	—	0.02	∞	0	6×10^3	0
—	40	—	0.20	∞	0	9×10^4	2×10^5
—	—	(25-75) 40	0.20	∞	0	1.2×10^5	3.1×10^5
—	—	(50-50)	0.20	∞	0	1.5×10^5	7×10^5

and

$$N_B/N_{B^*} = \pi \quad (\text{A-1})$$

Equivalent amounts of B and A + C groups were employed, so that

$$2N_A + N_C = 2N_B + 3N_{B^*} \quad (\text{A-2})$$

We also use the following notation:

$$N_C/(N_C + 2N_A) = \rho/(2 + \rho) = \mu$$

$$B/(B + B^*) = (2\pi + 2)/(2\pi + 3) = \xi$$

$$B \text{ (of } N_{B^*})/B \text{ (total)} = 1/(\pi + 1) = \nu$$

α , β , β^* , γ are the fractions of A—A, B—B, B \perp B, and C reacted, respectively.

tively.

The probability of a branch unit to be connected to another branch unit through $(i + 1)$ A—A and i B—B molecules is:

$$\begin{aligned} a &= \sum_{i=0}^{\infty} [\alpha\beta(1 - \mu)(1 - \nu)]^i \{ \alpha(1 - \mu)[\beta\nu + \beta^*(1 - \xi)] \}^2 \\ &= \frac{\{ \alpha(1 - \mu)[\beta\nu + \beta^*(1 - \xi)] \}^2}{1 - \alpha\beta(1 - \mu)(1 - \nu)} \end{aligned}$$

The probability of an unreacted A or B group or a reacted C group to be connected with a branch unit is found as follows. Starting with an unreacted A group:

$$a^* = \sum_{i=0}^{\infty} [\alpha\beta(1 - \mu)(1 - \nu)]^i (1 - \alpha)(1 - \mu)[\beta\nu + \beta^*(1 - \xi)]$$

Starting with an unreacted B group:

$$\begin{aligned} a^* &= \sum_{i=0}^{\infty} [\alpha\beta(1 - \mu)(1 - \nu)]^i (1 - \beta)(1 - \nu) \\ &\quad \times [\beta\nu + \beta^*(1 - \xi)] + (1 - \beta)\xi + (1 - \beta^*)(1 - \xi) \end{aligned}$$

Starting with a reacted C group:

$$a^* = \sum_{i=0}^{\infty} [\alpha\beta(1 - \mu)(1 - \nu)]^i \gamma\rho[\beta\nu + \beta^*(1 - \xi)]$$

The total probability is:

$$\begin{aligned} a^* &= \frac{\alpha(1 - \mu)[\beta\nu + \beta^*(1 - \xi)] \{ (1 - \alpha)(1 - \mu) + (1 - \beta)(1 - \nu) + \gamma\rho \}}{3[1 - \alpha\beta(1 - \mu)(1 - \nu)]} \\ &\quad + (1 - \beta)\xi + (1 - \beta^*)(1 - \xi) \end{aligned}$$

The probability that an unreacted A or B group or a reacted C group is part of a molecule having n branch units is:

$$P_n = a^* a^{n-1} (1 - a)^{fn-2n-1} \omega_n \quad n > 0$$

and

$$P_0 = 1 - a^* \quad n = 0 \quad (\text{A-3})$$

where

$$\omega_n = \frac{(fn - n)!}{(fn - 2n + 1)!n!}$$

We also have from the definition of P_n

$$\begin{aligned} P_n &= \frac{\text{ends on a molecule with } n \text{ branches}}{\text{total ends}} \\ &= \frac{N_n (fn - 2n + 2)}{\text{total ends}} \end{aligned} \quad (\text{A-4})$$

where N_n is the number of molecules with n branches.

From eqs. (A-3) and (A-4) we obtain, using also eq. (16)

$$N_n = \frac{N_A (4 - 4\alpha + \rho) \omega_n a^* a^{n-1} (1 - a)^{fn-2n-1}}{fn + 2n + 2} \quad n > 0$$

$$N_{n=0} = (1 - a^*) N_A [2 - 2\alpha + (\rho/2)] \quad n = 0 \quad (\text{A-5})$$

The author is indebted to Professor A. V. Tobolsky for his constructive discussions during this work.

The partial assistance of the Army Research Office (Durham) is also appreciated.

References

1. A. V. Tobolsky and A. Rembaum, *J. Appl. Polym. Sci.*, **8**, 307 (1964).
2. A. V. Tobolsky, U. S. Pat. 3,291,859 (1966).
3. J. T. Bailey, E. T. Bishop, W. R. Hendricks, G. Holden, and N. R. Legge, *Rubber Age*, **98**, No. 10, 69 (1966).
4. A. V. Tobolsky, *J. Amer. Chem. Soc.*, **80**, 5927 (1958).
5. E. J. Zaganariaris and A. V. Tobolsky, to be published.
6. J. H. Saunders and K. C. Frisch, *Polyurethanes* (High Polymers Series XVI, Pt. I), Interscience, New York, 1964.
7. A. W. Francis, A. J. Hill, and J. Johnston, *J. Amer. Chem. Soc.*, **47**, 2211 (1925).
8. H. Mark and A. V. Tobolsky, *Physical Chemistry of High Polymeric Systems* (High Polymers Series, II), Interscience, New York, 1950.
9. L. C. Case, *J. Polym. Sci.*, **26**, 333 (1957).
10. P. J. Flory, *Principles of Polymer Chemistry*, Cornell Univ. Press, Ithaca, N. Y., 1953, p. 395.
11. W. H. Stockmayer, *J. Polymer. Sci.*, **9**, 69 (1952); *ibid.*, **11**, 424 (1953).
12. A. V. Tobolsky, *Properties and Structure of Polymers*, Wiley, New York, 1962.
13. L. E. Nielsen, *Mechanical Properties of Polymers*, Reinhold, New York, 1962, p. 134.

Received February 17, 1970

Revised June 26, 1970

Polymerization of Asymmetric Polyfunctional Monomers. III. Ionic Polymerization of Acrylic and Methacrylic Esters of 2-Allylphenol

O. F. SOLOMON, *Laboratory of Macromolecular Chemistry, Polytechnic Institute, Bucharest, Rumania*, M. CORCIOVEI, *Petrochim Institute, Ploiești, Rumania*, I. GABE, *Petru Poni Institute, Iași, Rumania*, and E. BERAL, *Laboratory of Macromolecular Chemistry, Polytechnic Institute, Bucharest, Rumania*

Synopsis

The polymerization of acrylic and methacrylic esters of 2-allylphenol with different anionic, cationic and coordination catalysts was studied. The polymerization occurs exclusively or predominantly through (meth)acrylic C=C double bonds in all the studied cases. With anionic catalysts the allylic groups are not polymerizable and the polymers have linear structure. Polymerization with catalysts based on dialkylaluminum chloride (alone or associated with some metal salts) yields soluble or partially crosslinked polymers, depending on the reaction conditions. The crosslinking is due to the participation of allylic groups in the polymerization reactions. Copolymers of acrylic and methacrylic esters of 2-allylphenol with styrene, acrylonitrile, methyl methacrylate, *N*-vinylcarbazole and 1,3-pentadiene were synthesized by copolymerization in the presence of anionic catalysts and of systems based on dialkylaluminum chloride.

† Compounds containing two or more polymerizable groups which are different by their structure and reactivity were defined by Alfrey as polyfunctional asymmetric monomers.¹ Such monomers are the allylacrylic derivatives like acrylic and methacrylic esters of allyl alcohol, allylacrylamide, allylmethacrylamide, the acrylate and methacrylate of 2-allylphenol, etc.

The radical polymerization of allylacrylic monomers is usually accompanied by gelation at relatively low conversions.²⁻⁷ As an exception, it is possible to obtain soluble polymers by radical polymerization of allyl acrylate and allyl methacrylate in solvents like diallyl ether, which are able to hinder the polymerization of allylic groups.⁸ This was verified with satisfactory results in the case of 2-allyl phenylacrylate.

Anionic polymerization of allylacrylic monomers yields only linear polymers as a consequence of the high reactivity of acrylic and methacrylic groups and of the unreactivity of allylic groups in this system. This is the case with the *n*-butyllithium,⁹⁻¹¹ 1,1-diphenyl-*n*-hexyllithium,¹⁰ or naphthalenesodium¹¹ polymerization of allyl acrylate and allyl methacrylate.

Syntheses of linear copolymers of allyl acrylate and allyl methacrylate with styrene, acrylonitrile, and methyl methacrylate by anionic copolymerization have already been reported.¹¹

Attempts to polymerize allyl acrylate and allyl methacrylate using cationic catalysts lead to entirely crosslinked polymers.¹¹

In a previous paper we presented the possibility of obtaining soluble polymers, by polymerizing acrylic and methacrylic esters of 2-allylphenol with different ionic catalyst systems.¹²

In this paper we want to present some new results obtained by ionic polymerization of these two tetrafunctional asymmetric allylacrylic monomers and the attempts to synthesize some of their copolymers.

Experimental

2-Allylphenyl acrylate (AOAF), 2-allylphenyl methacrylate (MOAF) and 2,6-diallylphenyl acrylate (ADAF) were synthesized according to methods already described.^{5,7,13,14} Finally they were washed with dilute NaOH solution, washed with distilled water, and dried over CaH₂. They were vacuum-distilled before use under an inert atmosphere without inhibitors.

Physical constants of the monomers were AOAF, bp 88–90°C/0.9 mm Hg, n_D^{20} 1.5225; MOAF, bp 101–102°C/1.5 mm, n_D^{20} 1.5205; ADAF, bp 124–126°C/1.5 mm, 1.5379. The purity of the monomers was checked by chromatography.

The catalysts were stored in glass ampoules in the dark or in stainless steel cylinders. For use in the reaction, they were introduced in dried, argon-filled glass bulbs.

The solvents were refluxed over metallic Na or over CaH₂, fractionated, and finally distilled under an inert atmosphere and stored over 4 Å or 5 Å molecular sieves.

The polymerization and copolymerization experiments were carried out in glass ampoules or three-necked flasks equipped with a mechanical stirrer. The components were introduced in the following order: monomer, solvent, catalyst. When cocatalysts were used, they were weighed directly into the polymerization ampoules or flasks, before the other components were introduced.

All polymerization were carried out under a dry, inert atmosphere (argon).

The reactions were stopped by adding small amounts of methyl alcohol; the polymers were precipitated in methyl alcohol or petroleum ether, washed, dried *in vacuo*, and weighed.

Some AOAF and MOAF polymerization reactions with Al(C₂H₅)₂Cl and Al(C₂H₅)₂Cl + Me^{z+} catalysts were studied dilatometrically, by using a relatively simple dilatometer (Fig. 1) which permitted fairly good reproducibility. The final conversions were checked gravimetrically.

A special experimental method, which permitted a comparison of the

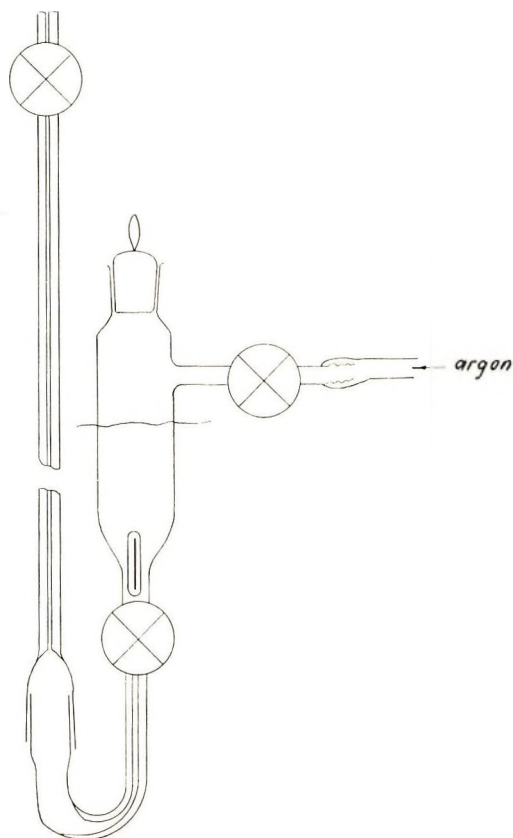


Fig. 1. Dilatometer.

activities of AOAF and MOAF by polymerization with $\text{Al}(\text{C}_2\text{H}_5)_2\text{Cl}$ and $\text{Al}(\text{C}_2\text{H}_5)_2\text{Cl} + \text{Me}^z+$, respectively, in different solvents (dichloroethane, toluene, and dimethylformamide), was employed. In this method, the components were introduced by molecular distillation into a previously dried, argon-purged glass apparatus; the whole system was then evacuated by repeated cycles of freezing—evacuating—thawing under argon. Finally the apparatus was sealed under vacuum (10^{-5} mm Hg). The components were then mixed in this closed system, thermostatted at 0°C . The polymerization yields were determined gravimetrically after a certain reaction time.

In order to establish the structure of the polymers, various methods,

TABLE I

Monomer	Total C=C double bonds/mole	Allylic double bonds/mole	
		Theoretical	Found
AOAF	2	1	0.99
MOAF	2	1	0.99-1.00
ADAF	3	2	2.02

like chemical analysis of the residual allyl groups,⁴ infrared spectroscopy (Unicam SP-100 and SP-200 spectrographs) and nuclear magnetic resonance (with a JEOL JNM-C-60 HL spectrograph), were used. The selectivity of the analytical method for determination of allyl double bonds was verified by applying it to the monomers (Table I).

The softening temperatures, viscosities of 5% solutions in $\text{CHCl}_3\text{-CCl}_4$ (1:1) at 20°C, and molecular weights of the polymers were determined by usual methods.

The compositions of some AOAF and MOAF copolymers were determined by elementary analysis.

Results and Discussion

AOAF and MOAF polymerize in the presence of several different catalysts, such as $n\text{-C}_4\text{H}_9\text{Li}$ (in aliphatic or aromatic hydrocarbons, in the presence or absence of tetrahydrofuran), $\text{CaZn}(\text{C}_2\text{H}_5)_4$, $\text{Al}(\text{C}_2\text{H}_5)_3 + \text{H}_2\text{O}$, $\text{Al}(\text{C}_2\text{H}_5)_2\text{Cl}$, $\text{Al}(\text{C}_2\text{H}_5)_2\text{Cl} + \text{Co}^{3+}$, $\text{Al}(\text{C}_2\text{H}_5)_2\text{Cl} + \text{Co}^{2+}$, $\text{Al}(\text{C}_2\text{H}_5)_2\text{Cl} + \text{Cu}^{2+}$. In Table II are presented data on ionic polymerization of AOAF and MOAF.

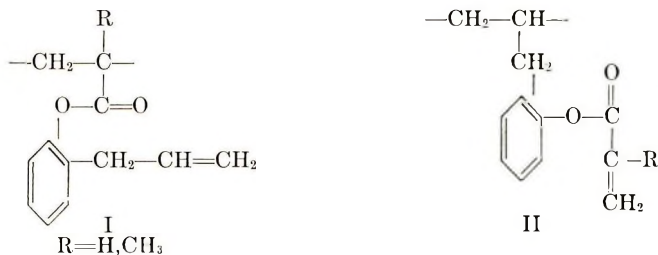
As can be seen, several catalyst systems permit high conversions to be reached in relatively short reaction times. The polymers are soluble or partially crosslinked. The reaction can be directed towards the formation of soluble polymers by selecting the type of catalyst and the reaction conditions. The catalysts which are specific for anionic polymerization (like $n\text{-C}_4\text{H}_9\text{Li}$) lead to the formation of linear polymers at any concentration of catalyst and monomer and over a large temperature range. The other catalysts tried could be also used for the synthesis of entirely soluble AOAF and MOAF polymers, but only if the reagent concentrations and the temperature do not exceed certain limits. By using catalytic systems based on alkylaluminum chloride or trialkylaluminum, the oxygen and moisture can favor crosslinking. By using diethylaluminum chloride at high monomer and catalyst concentration, a marked tendency to obtain relatively high crosslinked polymers was observed. This tendency disappears to a considerable extent if this catalyst is complexed with salts or complexes of metals like cobalt and copper.

It is difficult to explain the formation of soluble AOAF and MOAF polymers in the presence of catalysts as $\text{Al}(\text{C}_2\text{H}_5)_3 + \text{H}_2\text{O}$, $\text{Al}(\text{C}_2\text{H}_5)_2\text{Cl}$, and $\text{Al}(\text{C}_2\text{H}_5)_2\text{Cl} + \text{Me}^x+$, because it is well known that (meth)acrylic groups are not reactive in such conditions and, otherwise, there are very few indications of the polymerization of allylic groups with these catalytic systems. Consequently, we have considered it of great interest to establish the structure of AOAF and MOAF polymers (the nature of polymerized groups). For these polymers different structures could be imagined, but the most probable are those corresponding to the structures I and II and the copolymer of I and II.

TABLE II. Ionic Polymerization of AOAF and MOAF with Different Catalyst Systems

Run no	Mono-mer	[M], mole/l.	Solvent ^a	Catalyst	[Catalyst], mole/mole monomer	Cocatalyst	[Cocatalyst], mole/mole catalyst	Time, °C	Time, hr	Total	Polymer yield, %
1	AOAF	3.60	<i>n</i> -C ₇	<i>n</i> -C ₄ H ₉ Li	1.83 × 10 ⁻¹	—	—	20	22.5	24	0
2	AOAF	3.36	B + <i>n</i> C ₇ (2.5:1)	<i>n</i> -C ₄ H ₉ Li	2.02 × 10 ⁻¹	—	—	20	20	16.5	0
3	MOAF	3.60	<i>n</i> -C ₇	<i>n</i> -C ₄ H ₉ Li	1.90 × 10 ⁻¹	—	—	20	27	45	0
4	MOAF	0.88	THF + T + <i>n</i> C ₇ (0.93:11.4:1)	<i>n</i> -C ₄ H ₉ Li	1.99 × 10 ⁻¹	—	—	-50	1.5	91	0
5	MOAF	0.93	THF + T + <i>n</i> C ₇ (3.95:45.6:1)	<i>n</i> -C ₄ H ₉ Li	0.50 × 10 ⁻¹	—	—	-50	3.5	37	0
6	AOAF	4.60	L	Al(C ₂ H ₅) ₂ Cl	2.50 × 10 ⁻²	—	—	20	22	13.3	29
7	MOAF	3.84	L	Al(C ₂ H ₅) ₂ Cl	1.00 × 10 ⁻¹	—	—	20	11	99	38
8	MOAF	2.15	T + <i>n</i> -C ₇ + L (1:0.33:0.2)	Al(C ₂ H ₅) ₂ Cl	5.98 × 10 ⁻²	—	—	28	5.7	40	0
9	MOAF	2.66	B + L(1:1)	Al(C ₂ H ₅) ₂ Cl	1.45 × 10 ⁻¹	Co(C ₃ H ₇ O ₂) ₂ ^b	0.69 × 10 ⁻²	20	5.2	62	0
10	MOAF	2.40	B + L(1:0.32)	Al(C ₂ H ₅) ₂ Cl	1.16 × 10 ⁻¹	Co(C ₃ H ₇ O ₂) ₂	0.97 × 10 ⁻²	20	4.9	42	0
11	MOAF	3.15	B + L(1:0.75)	Al(C ₂ H ₅) ₂ Cl	0.92 × 10 ⁻¹	Cu(C ₃ H ₇ O ₂) ₂	0.75 × 10 ⁻²	20	4.8	52	0
12	MOAF	2.08	B (saturated with water at 20°C) + B (anhydrous) (1:5.4)	Al(C ₂ H ₅) ₂	1.66 × 10 ⁻¹	(H ₂ O)	—	20	0.1	63	0

^a Solvent mixture composition is given volumetrically: T = toluene; B = benzene; L = ligroin; *n*-C₇ = *n*-heptane; THF = tetrahydrofuran.
^b C₃H₇O₂ = acetylacetonate.



Other structures, for instance the polycyclic one, can not be taken into consideration because we observed a high residual unsaturation of all soluble polymers obtained.

In order to distinguish the real structure, the content of residual allylic groups was determined by a selective method. The results (Table III) show that with AOAF and MOAF, linear polymerization occurs exclusively or predominantly through the (meth)acrylic groups. Consequently, the structure I seems to be the most likely.

TABLE III

Run no. ^a	Monomer	Catalyst	Allyl groups/ structural unit ^b
1	AOAF	<i>n</i> -C ₄ H ₉ Li	1.05
4	MOAF	<i>n</i> -C ₄ H ₉ Li	1.10
6	AOAF	Al(C ₂ H ₅) ₂ Cl	0.95
7	MOAF	Al(C ₂ H ₅) ₂ Cl	1.00
11	MOAF	Al(C ₂ H ₅) ₂ Cl + Cu ²⁺	0.94
12	MOAF	Al(C ₂ H ₅) ₃ + H ₂ O	1.05

^a Run corresponds for number in Table II.

^b In the cases of partially crosslinked polymers (runs 6 and 7), the soluble fractions were analyzed.

As can be seen, the polymers obtained with Al(C₂H₅)₂Cl as catalyst have a lower residual allylic unsaturation in comparison with the other polymers. This could indicate crosslinking through allylic groups, but as differences between the values lie in the range of experimental error, they could not be considered as definite proof. In order to verify the role of the allylic groups in the crosslinking reaction, attempts were made to polymerize 2,6-diallylphenyl acrylate (ADAF), a hexafunctional monomer containing two allylic groups. The tendency of allyl phenyl ether (AFE) (used as model compound) to polymerize with Al(C₂H₅)₂Cl catalyst was also studied. The results of these experiments are presented in Table IV. The tendency of ADAF to crosslink by polymerization with catalysts based on alkyl-aluminum derivatives is considerably higher than in the cases of AOAF and MOAF. This behavior can be attributed to the higher allylic concentration and confirms the hypothesis of the role of the allylic groups in the crosslinking reaction. The reactivity of allylic groups in the presence of organoaluminum compounds is confirmed by results of polymerization of allyl phenyl ether.

TABLE IV

Mono- mer	[M], mole/l.	Catalyst	[Catalyst], mole/mole monomer	Solvent ^a	Tem- pera- ture, °C	Time, hr	Polymer yield, %	
							Total	Cross- linked (relative to total)
ADAF	1.92	$\left\{ \begin{array}{l} \text{Al}(\text{C}_2\text{H}_5)_3 \\ \text{H}_2\text{O} \end{array} \right.$	1.76×10^{-1}	B	20	48	60	15
			0.80×10^{-1}					
ADAF	4.00	$\text{Al}(\text{C}_2\text{H}_5)_2\text{Cl}$	5.4×10^{-2}	L	20	40	11	100
ADAF	2.76	$\left\{ \begin{array}{l} \text{Al}(\text{C}_2\text{H}_5)_2\text{Cl} \\ \text{Co}(\text{C}_5\text{H}_7\text{O}_2)_3 \end{array} \right.$	1.36×10^{-1}	T + L (1:1)	20	24	35	4
			0.93×10^{-3}					
AFE	3.84	$\text{Al}(\text{C}_2\text{H}_5)_2\text{Cl}$	5.76×10^{-2}	B + L (1:0.4)	25	24	36	0

^a See Table II.

Similar to the cases of AOAF and MOAF, in ADAF polymerization one can observe a marked decrease of the tendency to crosslink when a complex $\text{Al}(\text{C}_2\text{H}_5)_2\text{Cl} + \text{Me}^{x+}$ is employed instead of $\text{Al}(\text{C}_2\text{H}_5)_2\text{Cl}$. The weak crosslinking which however occurs, confirms that the crosslinking reaction is due to the allylic groups.

ADAF polymerization with $n\text{-C}_4\text{H}_9\text{Li}$ leads to formation of entirely soluble polymers, confirming the lack of reactivity of allylic C=C double bonds in the anionic mechanism. For instance, ADAF polymerization in a mixture of 91% toluene and 9% tetrahydrofuran ($[\text{M}] = 1.30$ mole/l.) with $n\text{-C}_4\text{H}_9\text{Li}$ (4.5×10^{-2} mole/mole ADAF), at -50°C , leads to a soluble polymer having 1.97 residual allyl groups/structural unit and a softening temperature of 83–85°C. The polymer yield reaches 45% in 65 min.

In order to check the conclusion that AOAF and MOAF polymerization with catalyst systems like $\text{Al}(\text{C}_2\text{H}_5)_2\text{Cl}$ or $\text{Al}(\text{C}_2\text{H}_5)_2\text{Cl} + \text{Me}^{x+}$ occurs through (meth)acrylic groups and that the soluble polymers have the preponderant structure I, high resolution infrared spectra and NMR spectra of the polymers were studied. In Figure 2 are given infrared spectra of MOAF, its polymers obtained with $n\text{-C}_4\text{H}_9\text{Li}$ and with $\text{Al}(\text{C}_2\text{H}_5)_2\text{Cl}$, and of the same polymer after bromination. As one can see, the methacrylic groups (3106 cm^{-1}) disappear on polymerization in both cases, while the allylic groups remain practically unchanged (3080 cm^{-1}). On bromination, allylic groups disappear too. The NMR spectra (Fig. 3) show a large group of low intensity signals at a δ value around 8.6 ppm, which indicates that CH_3 groups are bonded to quaternary carbon atoms. Consequently, the structure I of AOAF and MOAF polymers synthesized with $\text{Al}(\text{C}_2\text{H}_5)_2\text{Cl}$ catalyst is considered to be demonstrated.

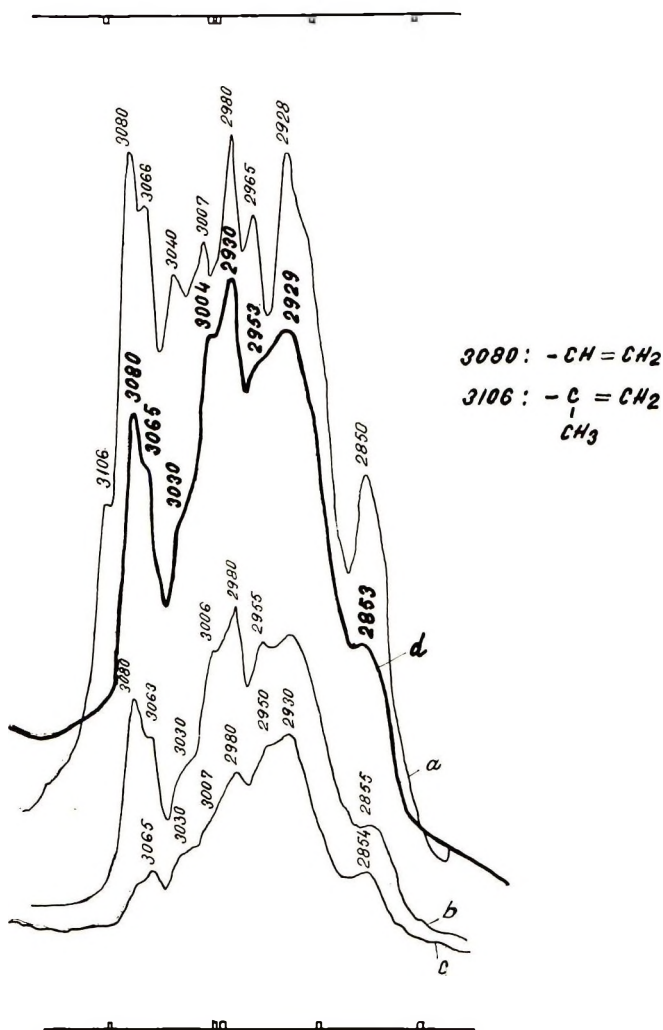


Fig. 2. Infrared spectra: (a) monomer; (b) polymer obtained with $n\text{-C}_4\text{H}_9\text{Li}$; (c) brominated polymer; (d) polymer obtained with $\text{Al}(\text{C}_2\text{H}_5)_2\text{Cl}$.

The structural identity of AOAF and MAOF polymers synthesized with anionic catalysts, such as $n\text{-C}_4\text{H}_9\text{Li}$, with those obtained with $\text{Al}(\text{C}_2\text{H}_5)_2\text{Cl}$ is a fact which poses a problem regarding the reaction mechanism in the second case. The data obtained to now do not permit anything to be ascertained about the mechanism; however, we considered it of interest to present the results of some experiments carried out to make a comparison between the activities of the studied monomers, by their polymerization in different solvents, with catalysts based on $\text{Al}(\text{C}_2\text{H}_5)_2\text{Cl}$. The solvents used were dimethylformamide (DMF), toluene (T), and dichloroethane (DCE). These results (Tables V and VI) indicate that in DMF the reaction is not favored, but the reactivity is high in T and in DCE.

AOAF and MAOF polymerization with $n\text{-C}_4\text{H}_9\text{Li}$ in toluene at temperatures between -60 and $+20$ °C is a slow reaction. The presence of rela-

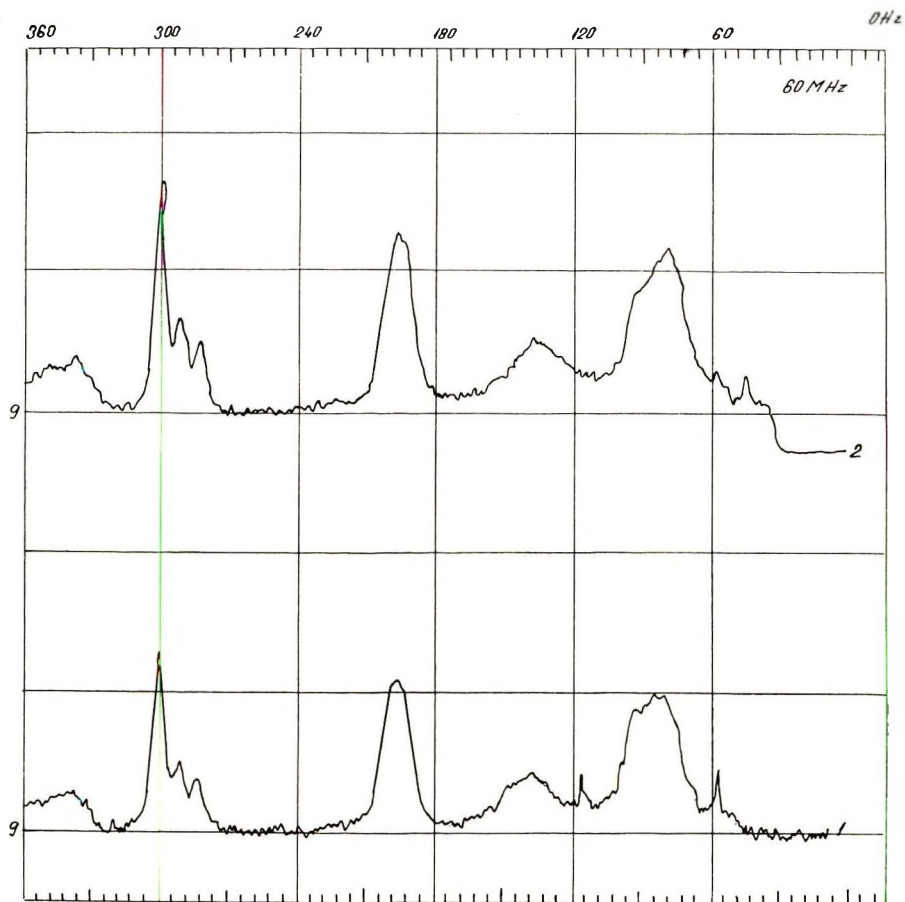


Fig. 3. Nuclear magnetic resonance spectra of MOAF polymers: (1) prepared with $n\text{-C}_4\text{H}_9\text{Li}$ catalyst; (2) prepared with $\text{Al}(\text{C}_2\text{H}_5)_2\text{Cl}$ catalyst.

TABLE V

Solvent	[AOAF], mole/l.	$[\text{Al}(\text{C}_2\text{H}_5)_2\text{Cl}]$, mole/mole monomer	Tempera- ture, $^\circ\text{C}$	Time, min	Polymer yield, %
DCE	1.21	3.8×10^{-2}	0	195	5
T	1.21	3.8×10^{-2}	0	195	4
DMF	1.21	3.8×10^{-2}	0	195	0

TABLE VI

Solvent	[MOAF], mole/l.	$[\text{Al}(\text{C}_2\text{H}_5)_2\text{Cl}]$, mole/mole monomer	$[\text{Co}(\text{C}_5\text{H}_7\text{O}_2)_3]$, mole/mole catalyst	Tem- pera- ture, $^\circ\text{C}$	Time, min	Polymer yield, %
DCE	1.36	5.1×10^{-2}	7.5×10^{-2}	0	180	38
T	1.36	5.1×10^{-2}	7.5×10^{-2}	0	180	82
DMF	1.36	5.1×10^{-2}	7.5×10^{-2}	0	180	7

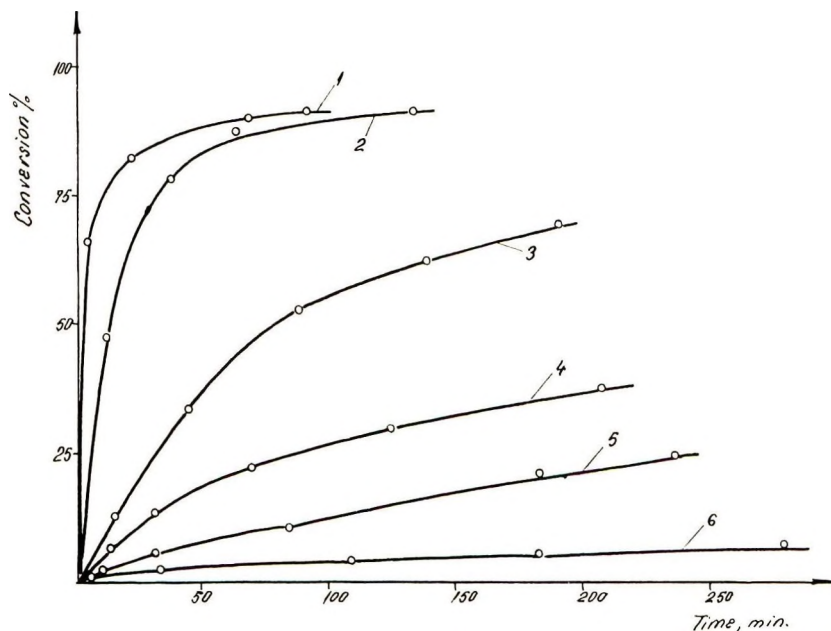


Fig. 4. MOAF and AOF polymerization with $n\text{-C}_4\text{H}_9\text{Li}$ in toluene and tetrahydrofuran at -50°C : (1) [MOAF] 0.90 mole/l., [catalyst] 0.200 mole/mole monomer, [THF] 0.79 mole/mole monomer; (2) [AOF] 0.88 mole/l., [catalyst] 0.200 mole/mole monomer, [THF] 0.79 mole/mole monomer; (3) [MOAF] 0.90 mole/l., [catalyst] 0.100 mole/mole monomer, [THF] 0.79 mole/mole monomer; (4) [MOAF] 0.94 mole/l., [catalyst] 0.050 mole/mole monomer, [THF] 0.85 mole/mole monomer; (5) [MOAF] 0.91 mole/l., [catalyst] 0.055 mole/mole monomer, [THF] 0.47 mole/mole monomer; (6) [MOAF] 0.98 mole/l., [catalyst] 0.050 mole/mole monomer, [THF] 0.20 mole/mole monomer.

tively small amounts of tetrahydrofuran in the reaction mixture strongly modifies the kinetics, accelerating the process considerably. Very high conversions can be reached in this way, even in short reaction times (about 60 min), at temperatures between -40 and -60°C . In Figure 4 are presented the curves of conversion versus reaction time for MOAF and AOF polymerization in toluene with various amounts of tetrahydrofuran, catalyzed by $n\text{-C}_4\text{H}_9\text{Li}$ at -50°C . As can be seen, the acrylic ester polymerizes at a lower rate than the methacrylic one. An increase in the catalyst concentration leads to an increase of the reaction rate. The increase of THF concentration is accompanied by an increase of the reaction rate, but only in certain ranges (from 0 to 1 mole THF/mole monomer) of THF concentration. At higher concentrations, increasing THF leads to a decrease in the reaction rate and beginning from certain THF/M values, the reaction does not occur any more. For instance, under the following conditions no polymer was formed: $[M] = 0.94$ mole/l., $n\text{-C}_4\text{H}_9\text{Li}/M = 10^{-2}$, $\text{THF}/M = 6$, -50°C , 10 hr.

The monomer concentration has a very marked influence on the polymerization rate. At concentrations higher than 1.5 mole/l. the rate was too high, and kinetical measurements were impossible.

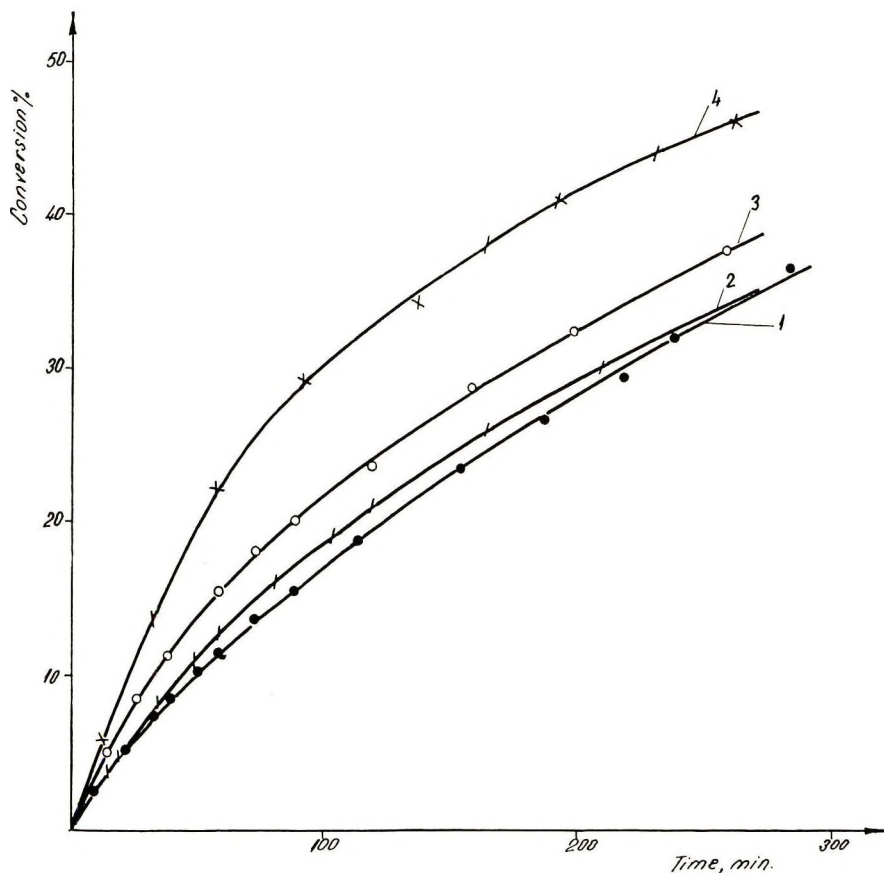


Fig. 5. Ionic polymerization of MOAF dilatometric curves for: (1) solvent T + $n\text{-C}_7$ + L (1:0.33:0.2), no cocatalyst; (2) solvent, B + $n\text{-C}_7$ + L (1:0.33:0.2), no cocatalyst; (3) solvent B + $n\text{-C}_7$ + L (1:0.33:0.2), cocatalyst Co^{2+} naphthenate, 8.1×10^{-5} g/mole catalyst; (4) solvent B + $n\text{-C}_7$ + L (1:0.33:0.2), cocatalyst Co^{3+} acetylacetone, 8.1×10^{-5} g/mole catalyst. Conditions for all runs 28°C ; catalyst $\text{Al}(\text{C}_2\text{H}_5)_2\text{Cl}$, 6 mole/mole MOAF; $[\text{M}] = 2.15$ mole/l.

As shown already, AOAF and MOAF polymerize in the presence of catalysts like $\text{Al}(\text{C}_2\text{H}_5)_2\text{Cl}$ and $\text{Al}(\text{C}_2\text{H}_5)_2\text{Cl} + \text{Me}^{\text{x}+}$. The dilatometric study of these reactions showed that in addition to their action to reduce crosslinking, the metal salts and complexes produce an increase in the polymerization rate. The curves presented in Figure 5 show that Co^{3+} has a more important influence upon the reaction rate than Co^{2+} . The reaction rate is the same in benzene and in toluene (curves 1 and 2, Fig. 5).

The experimental data allow us to confirm that MOAF is more reactive than AOAF in the ionic polymerization reactions, which is in agreement with the conclusions published by other authors¹¹ about anionic polymerization of allyl acrylate and allyl methacrylate.

Dilute solution viscosities (η_{sp}/c) of the polymers indicated in Table II varies from 0.04 to 0.09 dl/g for those obtained with $n\text{-C}_4\text{H}_9\text{Li}$ and from 0.10 to 0.55 dl/g for the others. The low molecular weights of the polymers

TABLE VII. Ionic Copolymerization of AOAF and MOAF with Different Monomers

Monomer (M ₁)	Comonomer (M ₂)	Molecular ratio M ₁ /M ₂	[M ₁ + M ₂], mole/l	Solvent ^a	Catalyst	[Catalyst], mole/l.	Cocatalyst	[Cocatalyst], mole/l.	Temp, °C	Time, hr	Co-polymer yield, % (relative to comonomer)	total position M _n , %
AOAF	Styrene	0.350	3.9	<i>n</i> -C ₆ + THF (21.5:1)	<i>n</i> -C ₄ H ₉ Li	0.25	—	—	-55	3	20	96
MOAF	Styrene	0.350	3.9	<i>n</i> -C ₆ + THF (21.5:1)	<i>n</i> -C ₄ H ₉ Li	0.25	—	—	-55	1	28	92
AOAF	Styrene	0.270	6.0	L	Al(C ₂ H ₅) ₂ Cl	0.38	—	—	^b	20	70 ^c	—
AOAF	Methyl methacrylate	0.260	5.9	<i>n</i> -C ₆	<i>n</i> -C ₄ H ₉ Li	0.50	—	—	-45	2.6	22	88
MOAF	Methyl methacrylate	0.260	5.9	<i>n</i> -C ₆	<i>n</i> -C ₄ H ₉ Li	0.49	—	—	-45	0.5	19	84
AOAF	Acrylonitrile	0.066 ^d	8.5	T + <i>n</i> -C ₆ (1.34:1)	<i>n</i> -C ₄ H ₉ Li	0.29	—	—	-60	2	8	53
MOAF	Acrylonitrile	0.066 ^d	8.5	T + <i>n</i> -C ₆ (1.34:1)	<i>n</i> -C ₄ H ₉ Li	0.29	—	—	-60	1	18	5
AOAF	Piperylene ^e	0.202	7.2	L	Al(C ₂ H ₅) ₂ Cl	0.26	Co ³⁺	0.37 × 10 ⁻²	20	3	21	58
AOAF	Piperylene ^e	0.101 ^f	7.9	L	Al(C ₂ H ₅) ₂ Cl	0.23	Co ³⁺	0.29 × 10 ⁻²	20	3	18	36
AOAF	<i>N</i> -Vinylcarbazole	7.6	2.1	T + L (3.6:1)	Al(C ₂ H ₅) ₂ Cl	0.25	—	—	-45	0.3	12	45
MOAF	<i>N</i> -Vinylcarbazole	7.6	2.1	T + L (3.6:1)	Al(C ₂ H ₅) ₂ Cl	0.24	—	—	-45	0.3	19	60

^a See Table II.^b The temperature was gradually increased from -65 to +25°C.^c Crosslinked copolymer.^d M₂ was added after the catalyst.^e Contained 69% *trans* isomer.^f M₁ was added after the catalyst.

synthesized with anionic catalysts (cryoscopic molecular weights between 2500 and 4000) are due to the secondary reactions between the catalyst and COO groups. Such reactions were demonstrated for the anionic polymerization of acrylic and methacrylic monomers and even for some allylacrylic compounds.¹⁰

MOAF polymers obtained with $n\text{-C}_4\text{H}_9\text{Li}$ in the presence of THF have softening temperatures between 70 and 100°C, whereas the catalysts based on $\text{Al}(\text{C}_2\text{H}_5)_2\text{Cl}$ produce polymers having higher softening points (95–140°C). Interesting behavior was observed in the case of MOAF polymers synthesized with $n\text{-C}_4\text{H}_9\text{Li}$ in the absence of electron-donors, which at values of $\eta_{sp}/c = 0.07\text{--}0.08$ dl/g have high softening points (150–160°C) in spite of their low molecular weights.

The polyfunctional asymmetric allylacrylic monomers can be copolymerized with various other monomers under the action of ionic catalytic systems. D'Alelio and Hoffend¹¹ described the synthesis of allyl acrylate and allyl methacrylate copolymers with styrene, acrylonitrile, and methyl methacrylate by anionic catalysis. They determined the copolymers compositions and calculated some copolymerization ratios.

In Table VII are presented the results of some attempts to synthesize copolymers of AOAF and MOAF with different monomers, using anionic catalysts ($n\text{-C}_4\text{H}_9\text{Li}$) and catalytic systems based on $\text{Al}(\text{C}_2\text{H}_5)_2\text{Cl}$. As can be seen, AOAF and MOAF anionic copolymerization with styrene leads to macromolecular compounds composed primarily of only the polyfunctional monomers (similarly to the copolymerization of allyl acrylate and allyl methacrylate with styrene¹¹). With $\text{Al}(\text{C}_2\text{H}_5)_2\text{Cl}$ there were obtained entirely crosslinked styrene-AOAF and styrene-MOAF copolymers having a good elasticity and swelling capacity.

Anionic copolymerization of the AOAF-MMA and MOAF-MMA systems yielded copolymers in whose composition the tetrafunctional monomers are preponderant.

The monomer ratios in AOAF-acrylonitrile and in MOAF-acrylonitrile copolymers are not the same; while acrylonitrile has a high reactivity in the copolymerization with MOAF, in the acrylonitrile-AOAF system the second monomer has the highest reactivity. These data are in agreement with those for anionic copolymerization of allyl acrylate and allyl methacrylate with acrylonitrile.¹¹

AOAF and MOAF give copolymers with *trans*-1,3-pentadiene (piperylene) in the presence of complex catalysts formed from $\text{Al}(\text{C}_2\text{H}_5)_2\text{Cl}$ and cobalt salts. These copolymers contain both monomers in considerable ratios. The reaction rate and copolymer composition are depending on the order of addition of components to the reaction mixture. The following order is preferable: solvent, cocatalyst, piperylene, catalyst, and (after 2–4 min) the allylacrylic monomer. In this way copolymers were obtained in which the majority of pentadienic units have a 1,4-*cis* structure.

With $\text{Al}(\text{C}_2\text{H}_5)_2\text{Cl}$ as catalyst, copolymers of AOAF and MOAF with *N*-vinylcarbazole having approximately equimolecular compositions could be synthesized.

References

1. T. Alfrey, D. Bohrer, and H. Mark, *Copolymerization*, Interscience, New York, 1952.
2. P. J. Flory, *Principles of Polymer Chemistry*, Cornell Univ. Press, Ithaca, N. Y., 1953.
3. L. Trossarelli, M. Guaita, and A. Priola, *Ric. Sci.*, **35**, 379, 429 (1965).
4. L. Trossarelli, M. Guaita, and A. Priola, *Makromol. Chem.*, **100**, 147 (1967).
5. V. V. Korshak, S. V. Vinogradova, and M. Corciovei, *Mater. Plastice* (Bucharest), **2**, 208 (1965).
6. O. F. Solomon, M. Corciovei, and V. Tararescu, *J. Appl. Polym. Sci.*, **11**, 1631 (1967).
7. M. Anghelina, M. Negoita, M. Corciovei, and O. F. Solomon, *Mater. Plastice* (Bucharest), **5**, 71 (1968).
8. J. P. Higgins and K. E. Weale (Imperial College, Department of Chemical Engineering and Chemical Technology), private communication.
9. M. Donati and M. Farina, *Makromol. Chem.*, **60**, 233 (1963).
10. S. Bywater, P. E. Black, and D. M. Wiles, *Can. J. Chem.*, **44**, 695 (1966).
11. G. F. D'Alelio and T. R. Hoffend, *J. Polym. Sci. A-1*, **5**, 323 (1967).
12. O. F. Solomon, M. Corciovei, and E. Beral, *J. Polym. Sci. B*, **6**, 507 (1968).
13. V. V. Korshak, S. V. Vinogradova, and M. Corciovei, USSR Pat. 172311 (1965).
14. O. F. Solomon and M. Corciovei, Rumanian Pat. 48382 (1966).

Received September 10, 1969

Revised June 2, 1970

Polymerization Studies on 1-Ferrocenyl-1,3-butadiene

DENNIS C. VAN LANDUYT, *Army Propulsion Laboratory and Center, Research & Engineering Directorate, U.S. Army Missile Command, Redstone Arsenal, Alabama 35809* and

SAMUEL F. REED, JR., *Rohm and Haas Company Redstone Research Laboratories, Huntsville, Alabama 35807*

Synopsis

The polymerization behavior of 1-ferrocenyl-1,3-butadiene has been investigated by using both free-radical and anionic initiation techniques. Polymerization occurred readily under the promoting action of butyllithium; however, no polymerization occurred when azobisisobutyronitrile (AIBN) or benzoyl peroxide was employed as initiator. Copolymerizations were carried out with methyl methacrylate and styrene. The behavior of 1-ferrocenyl-1,3-butadiene in the copolymerizations was followed by dilatometric rate measurements, solution viscosity determinations, and elemental analysis. The major effect observed was a severe reduction in the intrinsic viscosities of the copolymers. An explanation for the observed behavior of 1-ferrocenyl-1,3-butadiene in these reactions is advanced.

INTRODUCTION

Many polymers containing the ferrocene group have been described in recent years.¹⁻⁵ Included in these investigations have been studies involving the free-radical addition polymerization of alkenylferrocenes such as vinylferrocene⁶ and ferrocenylmethyl acrylate and methacrylate.⁷ With the rapidly advancing interest in charge-transfer polymers, we wish to report on the polymerization behavior of 1-ferrocenyl-1,3-butadiene (1-FB).

A study of the free-radical initiated polymerization of 1-FB was completed, azobisisobutyronitrile (AIBN) and benzoyl peroxide being used as the initiators. In addition, a thermal polymerization of 1-FB at 130°C was attempted. The anionic polymerization of 1-FB was examined with butyllithium as the initiator.

Copolymerization reactions of 1-FB with methyl methacrylate (MMA) and styrene were carried out to determine the effect of 1-FB on these reactions. The behavior of 1-FB in these reactions was determined from dilatometric rate measurements and from solution viscosities and elemental analyses of the copolymers.

EXPERIMENTAL

Materials

Methyl methacrylate and styrene were distilled just prior to the polymerization reactions. All solvents were reagent-grade, distilled materials. Azobisisobutyronitrile was recrystallized from methanol, mp 102–103°C with decomposition.

Techniques

Dilatometric polymerization rate determinations have been described elsewhere.⁸ Solution viscosities were determined in toluene at 30°C, with the use of Cannon dilution viscometers. Iron analyses were carried out on a Perkin-Elmer atomic absorption spectrophotometer, Model 303. The Mechrolab vapor-pressure osmometer was used for determinations of \bar{M}_n with benzene as solvent. A Waters Associates analytical instrument was employed for all GPC analyses. Degassed tetrahydrofuran flowing at the rate of 1 ml/min. was the eluting solvent. Four commercial Styragel columns in series (10⁴, 10³, 600, and 100 Å mean permeability) were used to fractionate the polymers for determining \bar{A}_n and \bar{A}_w values.

Polymerization Reactions

Homopolymerization. The free-radical polymerizations of 1-FB were carried out in degassed toluene solution at 67°C with AIBN as the initiator. Monomer/initiator mole ratios were varied from ¹⁵/₁ to ³/₁; however, each failed to produce any polymer over extended time periods. The only change occurring was the formation of a dimeric product in those reactions conducted with the higher AIBN concentrations.

Attempted free-radical polymerization of 1-FB in toluene using benzoyl peroxide (1 and 5 mole-%) at 125–130°C were unsuccessful. Bulk polymerization of 1-FB at 130°C (thermal initiation) in the melt stage gave a polymerlike product which appeared to be a dimer or other very low molecular weight polymer. Molecular weight analysis (VPO) gave an \bar{M}_n value of 530. This polymer contained 24.2% Fe (calculated 23.53% Fe).

The anionic polymerization of 1-FB was carried out in anhydrous toluene at ambient temperature. A glass vacuum line was employed to ensure the total maintenance of anhydrous condition and to avoid contact with the atmosphere. *n*-Butyllithium (1.46 *M* in hexane) was used as the initiator. A typical reaction may be described as follows: In a 250-ml round-bottomed flask fitted with magnetic stirrer and side delivery tube (septum covered) was placed 11.9 g (0.05 mole) of high-purity 1-FB, mp 97–98°C. The flask was connected to a vacuum manifold and deaerated. Toluene (50 ml) was transferred into the flask via vacuum manifold.* As the mixture

* Toluene used for solvent in the anionic polymerization was purified by distillation from sodium metal, treated with styrene monomer and *n*-butyllithium to give colored solution indicative of growing styryl anion, and transferred via vacuum line into the polymerization reactor.

reached ambient temperature, the desired quantity of *n*-butyllithium was added via syringe. An exothermic reaction occurred during the first hour of the reaction. The reaction time was 16 hr, followed by quenching with methanol. After thorough washing of the toluene solution with water and drying, the solvent was removed by evaporation to give a solid polymeric product. The polymer was redissolved in the minimum of methylene chloride and reprecipitated with excess hexane to give a yellow powder. All polymer characterization data were obtained on the purified material. Experimental and characterization data are shown in Table I.

TABLE I
Experimental and Characterization Data for Poly-1-FB
Prepared by Anionic Polymerization

No.	Mole ratio 1-FB/Bu Li	Reaction time, hr	\bar{M}_n	$[\eta]$	\bar{M}_w/\bar{M}_n
1	2.8/1	16	2890	0.0305	1.29
2	8.3/1	1	3350	0.0393	1.25
3	16.6/1	16	4010	0.0402	1.18

Copolymerization. All copolymerization reactions of 1-FB with MMA and styrene were carried out in toluene with AIBN as initiator (0.05 mole/l.) at 60°C in small-scale dilatometric studies. Reactions were carried to 10–12% completion and the copolymers isolated by precipitation, purified by reprecipitation, and each analyzed by solution viscosity and elemental analysis.

RESULTS

Homopolymerization

This study involving the free-radical polymerization of 1-FB has demonstrated that this diene monomer is reluctant to undergo polymerization under stated conditions. The only materials isolated were dimeric products obtained at high AIBN concentrations. Their structure will be reported on at a later time. Thermal initiated bulk polymerization gave a low-molecular-weight material represented as a probable dimer-trimer mixture ($M_n = 530$).

It was found that 1-FB could be polymerized by anionic polymerization to give polymers of relatively low molecular weight in good yields. Molecular weights varied from approximately 2800 to 4000 with corresponding ranges in intrinsic viscosities of 0.0305–0.0402. A GPC analysis of the polymers demonstrated that the molecular-weight distribution of each was quite low (1.2–1.3).

Copolymerization

Copolymerization of MMA and styrene with 1-FB was carried out in dilatometric reaction rate studies. The comonomer mole ratios (MMA or

TABLE II
Experimental Data for Copolymerizations^a

No.	[MMA], mole/l.	[Styrene], mole/l.	[1-FB], mole/l.	Mole ratio comonomers	R_p , %/min	R_p/R_{p0}	$[\eta]$	$[\eta]/[\eta]_0$
1	5.00	—	—	—	4.8×10^{-3}	1.000	1.090	1.000
2	4.75	—	0.105	45.27	1.0×10^{-4}	0.021	0.420	0.385
3	4.25	—	0.317	13.50	1.0×10^{-4}	0.021	0.120	0.110
4	3.75	—	0.525	7.15	1.1×10^{-4}	0.023	0.070	0.100
5	—	4.84	—	—	0.7×10^{-3}	1.000	0.260	1.000
6	—	4.57	0.105	43.50	1.8×10^{-4}	0.257	0.055	0.212
7	—	4.09	0.317	12.90	1.7×10^{-4}	0.243	0.044	0.169
8	—	3.60	0.525	6.90	1.5×10^{-4}	0.214	0.042	0.161

^a [AIBN] = 0.05 mole/l.

styrene/1-FB) were varied from approximately 45/1 to 7/1 (Table II). The R_{p0} values refer to the MMA or styrene polymerization rate in the absence of 1-FB with conditions approximating those of copolymerization. Similarly, the $[\eta]_0$ values are the intrinsic viscosity values for the homopolymers of MMA and styrene.

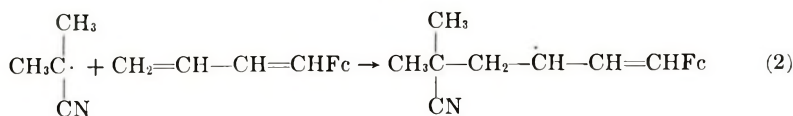
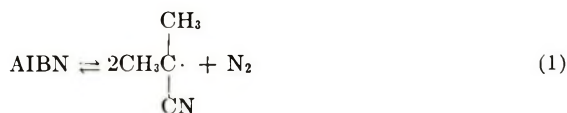
It is immediately obvious that 1-FB severely retards the rate of the free-radical polymerization of MMA and styrene as evidenced by the low R_p/R_{p0} values. A greater retardation was observed for MMA than for styrene. There was also a severe reduction in the intrinsic viscosity of the copolymers. The $[\eta]$ values decreased as the 1-FB concentration increased within the two copolymer series. The severity of the reduction in $[\eta]$ is shown by the low $[\eta]/[\eta]_0$ values between 0.4 and 0.1. Iron analyses showed that the copolymers prepared at the higher 1-FB concentrations contained higher iron contents (Table III) than were available in the respective comonomer mixtures. These results indicated that 1-FB enters the copolymer very readily during the initial stages (first 10%) of the reaction.

TABLE III
Elemental Analysis

No.	Calculated			Found		
	C, %	H, %	Fe, %	Fe, %	H, %	Fe, %
2	60.53	7.89	1.18	60.9	8.26	1.6
3	61.59	7.68	3.53	76.8	6.88	4.4
4	62.64	7.47	5.88	74.3	6.66	8.3
6	91.22	7.60	1.18	89.4	7.48	3.1
7	89.04	7.42	3.55	88.2	6.97	5.0
8	86.90	7.24	5.86	84.6	6.86	8.6

DISCUSSION

It was found that 1-FB does not polymerize under the influence of free-radical initiators. The failure of benzoyl peroxide to initiate polymerization may be attributed to the loss of the initiator radical via its attack on the ferrocene group, i.e., conversion of ferrocene to the ferricinium form; however, the limited success with AIBN is somewhat more difficult to explain. A brief explanation involving reduced radical activity is suggested. Following the initial decomposition of AIBN [reaction (1)], the 2-cyanoisopropyl radical



These results of rate retardation and low molecular weight products are typical of comonomer mixtures containing one monomer that is capable of undergoing degradative chain transfer, i.e., allylic monomers,¹⁰ or those that produce a chain radical of very low reactivity as evidence for 1-F'B. This type of behavior is vividly demonstrated by allyl alcohol, since small quantities of this monomer inhibit or retard the polymerization of other monomers in free-radical initiated reactions.

The fact that copolymerization did occur to a limited extent can be attributed to the presence of a high concentration of very reactive monomers (MMA, styrene, and 1-F'B). 1-F'B may be considered a reactive monomer in the copolymerizations because it would certainly enter into reaction with a chain radical terminated by an MMA or styrene unit. MMA and styrene apparently are sufficiently reactive to interact with growing polymer chains terminated by 1-F'B units to some extent. These assumptions are necessary to explain the relatively large ratios of 1-F'B found in the copolymers.

This study of the polymerization behavior of 1-F'B has demonstrated that this monomer is reluctant to undergo free-radical initiated polymerization because of the formation of inactive radical intermediates which display a propensity toward dimerization over monomer addition. 1-F'B was found to polymerize readily by use of butyl lithium. Copolymerization of 1-F'B with MMA and styrene occurred with drastic rate retardation and decrease in molecular weight of the copolymers. The composition of the copolymers was found to be rich in 1-F'B. These results are expected from a system containing reactive monomers, an intermediate radical of low reactivity, and a radical with dimerization tendencies.

References

1. P. L. Pauson, *Quart. Rev.*, **9**, 391 (1955).
2. C. U. Pittman, *J. Paint Technol.*, **39**, No. 513, 585 (1967).
3. H. Valot, *Double Liaison (France)*, **130**, 775 (1966).
4. M. Dub, *Compounds of the Transition Metals*, Vol. I, Springer-Verlag, Berlin, 1966.
5. E. W. Neuse, in *Advances in Macromolecular Chemistry*, W. M. Pasika, Ed., Academic Press, New York, 1968.
6. M. G. Baldwin and K. E. Johnson, *J. Polym. Sci. A-1*, **5**, 2091 (1967).
7. C. U. Pittman, J. C. Lai, and D. P. Vanderpool, *Macromolecules*, **3**, 105 (1970).
8. M. G. Baldwin and S. F. Reed, Jr., *J. Polym. Sci., A-1*, **7**, 1919 (1969).
9. D. C. Van Landuyt, in preparation.
10. R. C. Laible, *Chem. Rev.*, **58**, 807 (1958).
11. A. Terada and K. Murata, *J. Polym. Sci. A-1*, **5**, 2219 (1967).

Received June 30, 1970

Revised October 6, 1970

Influence of Monomer Concentration on the Structure of Poly(methyl Methacrylate) Polymerized by Butyllithium

Y. AMERIK,* W. F. REYNOLDS, and J. E. GUILLET,
*Department of Chemistry, University of Toronto, Toronto 181,
Ontario, Canada*

Synopsis

The polymerization of methyl methacrylate has been studied in toluene and tetrahydrofuran solution at -78°C using butyllithium as catalyst. The structure of the polymer produced was determined by analysis of the α -methyl groups using 100 MHz NMR. It is shown that in a noncomplexing solvent such as toluene, the number of isotactic triads increases from 70% to 93% as the monomer concentration during polymerization is reduced from 5 mole/l. to approximately zero. The value of P_{ss}/P_{is} depends strongly on monomer concentration, and hence any calculations regarding penultimate effects in such systems should be made at close to zero monomer concentration. In the THF solution the penultimate effect is nearly independent of monomer concentration, and both P_{ii}/P_{si} and P_{ss}/P_{is} are close to unity. The results may be explained in terms of a mechanism of the polymerization process in which toluene does not complex with the active site, while monomer and THF are weak and strong complexing agents, respectively.

The development of high resolution nuclear magnetic resonance instruments has made it possible to establish to a relatively high degree of accuracy the sequence of monomer configurations along a polymer chain and in principle one may use these data to test the various theories of stereoregular polymerization.¹⁻³ It is well known that in the anionic polymerization of methyl methacrylate for example, the degree of stereoregulation depends to a very large extent on both the catalyst and the solvent used.⁴

It has also been reported that the degree of stereoregularity depends upon the percentage conversion of monomer and upon initial monomer concentration.^{5,6} The importance of considering these effects has been commented upon⁷ but has largely been ignored by other workers in the field. In this paper we report the results of a more detailed investigation relating to the effect of monomer concentration upon the stereoregular polymerization of methyl methacrylate with the use of butyllithium as catalyst and toluene or tetrahydrofuran as solvent.

* Present address: Topchiev Petrochemical Institute, Academy of Science, Moscow V-71, U.S.S.R.

EXPERIMENTAL

Polymerization

The polymerizations were carried out in borosilicate glass vials sealed under high vacuum at -78°C . In order to obtain samples with relatively low molecular weight the butyllithium concentration was maintained in the range of 1.5–2.5%.

For polymerizing methyl methacrylate at approximately zero monomer concentration, the monomer was sealed into the side arm of a glass tube containing the catalyst and solvent. The catalyst and solvent were cooled at -78°C and the monomer allowed to distill slowly (less than 0.25 mole/l-hr) into the reaction tube, the monomer reservoir being kept at a temperature around 0°C . Under these conditions, it is estimated that the monomer concentration did not exceed 0.04 mole/l.

NMR Spectra

The NMR spectra of the polymer samples were determined by use of a Varian HA100 Spectrometer at 100 MHz. The polymers were dissolved in chloroform (10% w/v) containing a small amount of tetramethylsilane as an internal standard. The structure was determined from the areas under the three peaks obtained from the methyl ($\tau = 8.8\text{--}9.2$) resonances and are reported in terms of the per cent isotactic (I), heterotactic (H), or syndiotactic (S) triads in the polymer. Typical spectra for three polymers of different structure are shown in Figure 1.

RESULTS AND DISCUSSION

Experiments in Tetrahydrofuran Solutions

Data for the effect of monomer concentration on the stereoregularity of poly(methyl methacrylate) polymerized in tetrahydrofuran (THF) are shown in Figure 2. From the data it is clear that the polymer microstructure does not significantly depend upon initial monomer concentration in the range 0.6–5.0*M*.

Experiments in Toluene Solution

In this solvent, the polymer microstructure varies significantly with monomer concentration. Data for the fractional populations of isotactic, heterotactic, and syndiotactic triads (*I*, *H*, and *S*, respectively) are shown in Figure 3 and Table I. For complete conversion of monomer to polymer, *I* increases from 0.70 to 0.91 as the initial monomer concentration decreases from 4.75 to 0.3*M*. On this basis, the extrapolated value of *I* at zero monomer concentration should be approximately 0.92₅. In order to test this extrapolation, a polymer was synthesized at very low monomer concentration (see Experimental). The observed value of 0.93 for *I* represents the highest isotactic content which has been observed for this monomer-catalyst pair.

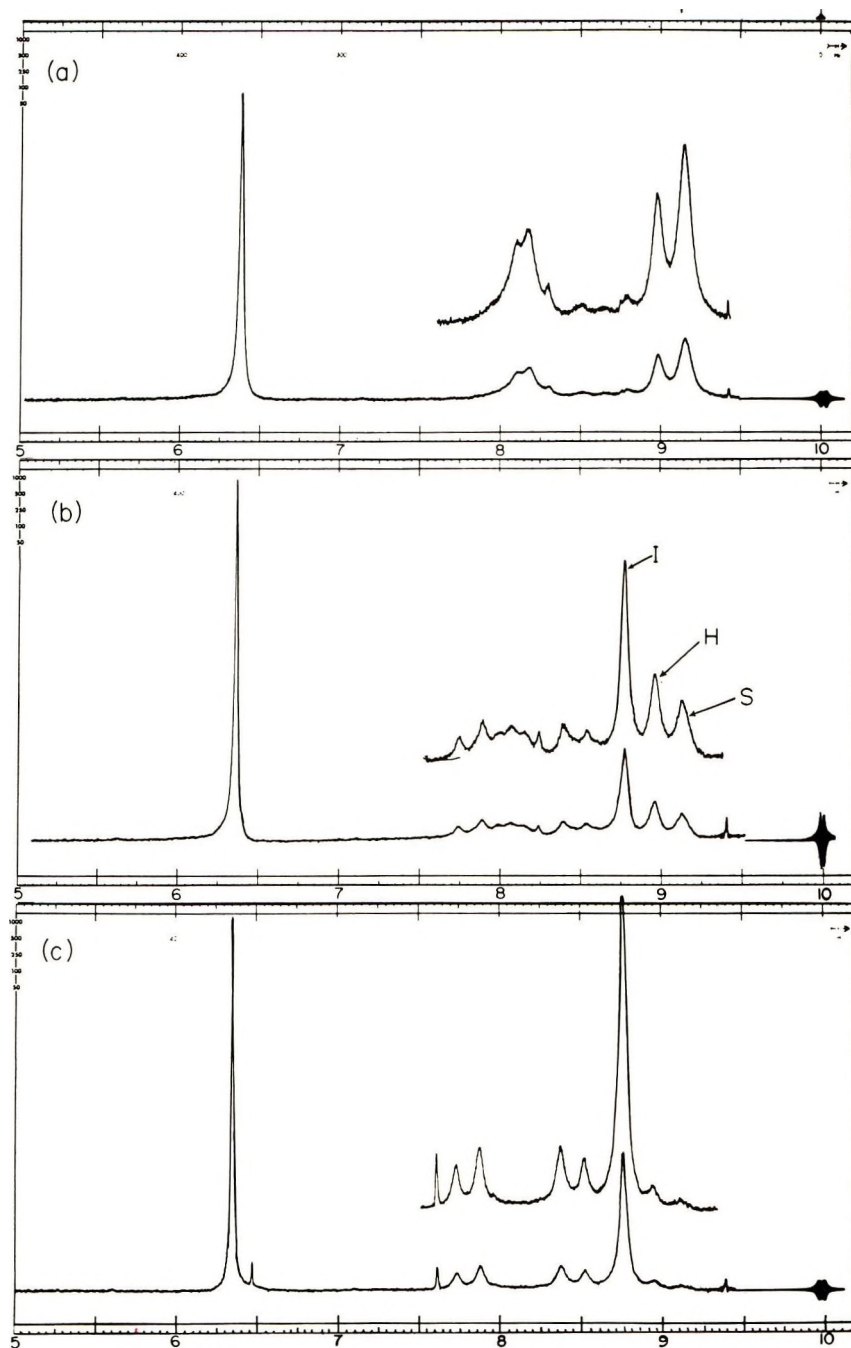


Fig. 1. Typical NMR spectra for poly(methyl methacrylate) in CDCl_3 solution (500 Hz sweep width, 1000 sec sweep time): (a) polymerized in THF solution ($I = 0.04$, $H = 0.34$, $S = 0.62$); (b) polymerized in toluene solution, $[M]_0 = 3.50$ mole/l. ($I = 0.70$, $H = 0.21_s$, $S = 0.08_s$); (c) polymerized in toluene solution, $[M]_0 < 0.04$ mole/l. ($I = 0.93$, $H = 0.05_s$, $S = 0.01_s$).

TABLE I
Effect of Initial Monomer Concentration Upon Tacticity Parameters

Monomer concn, <i>M</i>	<i>I</i>	<i>H</i>	<i>S</i>	<i>i</i>	<i>s</i>	<i>P_{ii}</i>	<i>P_{is}</i>	<i>F_{si}</i>	<i>F_{ss}</i>	<i>P_{ii}/P_{si}</i>	<i>P_{ss}/P_{is}</i>	ρ
	100% Conversion of Monomer to Polymer											
<0.04	0.93	0.05 ₅	0.01 ₅	0.95 ₈	0.04 ₃	0.97	0.03	0.65	0.35	1.5	12	1.5
0.29	0.91	0.07	0.02	0.94 ₅	0.05 ₅	0.96	0.04	0.64	0.36	1.5	9	1.5
1.90	0.87 ₅	0.09 ₅	0.03	0.92	0.08	0.95	0.05	0.62	0.38	1.5	8	1.6
2.75	0.81	0.13 ₅	0.05 ₅	0.87 ₈	0.12 ₃	0.92	0.08	0.55	0.45	1.7	6	1.6
3.50	0.74	0.18	0.08	0.83	0.17	0.89	0.11	0.53	0.47	1.7	4.3	1.6
4.75	0.70	0.20 ₅	0.09 ₅	0.80 ₈	0.19 ₈	0.87	0.13	0.52	0.48	1.7	3.7	1.5
Bulk (-25°C)	0.64 ₅	0.25	0.10 ₅	0.77	0.23	0.83	0.17	0.54	0.46	1.5	2.8	1.4
	15% Conversion of Monomer to Polymer											
1.90	0.86	0.10 ₅	0.03 ₅	0.91 ₃	0.08 ₈	0.94	0.06	0.60	0.40	1.6	7	1.5
2.75	0.79	0.15	0.06	0.86 ₅	0.13 ₅	0.91	0.09	0.56	0.44	1.6	4.4	1.6
3.50	0.70	0.21 ₅	0.08 ₅	0.80 ₈	0.19 ₃	0.87	0.13	0.56	0.44	1.6	3.4	1.4
4.75	0.65	0.24	0.11	0.77	0.23	0.84	0.16	0.52	0.48	1.6	3.0	1.5

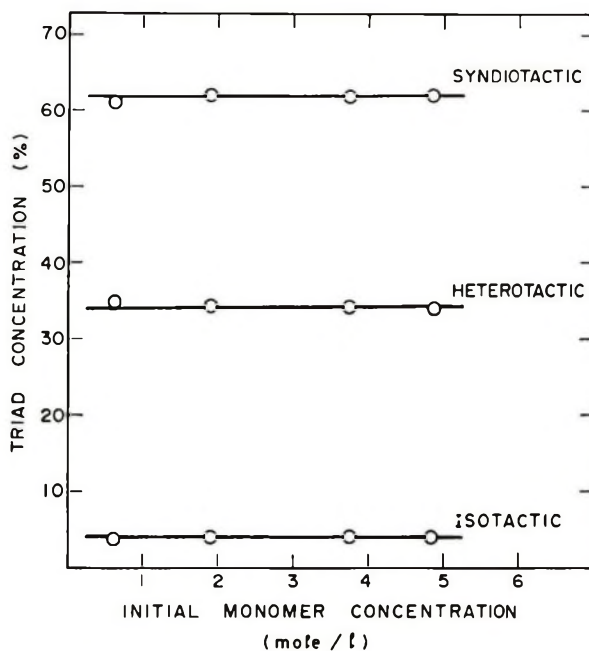


Fig. 2. Triad concentrations for poly(methyl methacrylate) as a function of initial monomer concentration; polymerized in THF at -78°C with butyllithium as catalyst.

Curves *a* in Figure 3 correspond to data obtained where polymerization was allowed to proceed to 100% conversion. During polymerization, the monomer concentration will decrease continuously from the initial value to zero. Consequently, one might expect to have a change in stereoregularity with conversion. A more correct estimate of the effect of monomer concentration would then be obtained from polymerization in which only low conversions are permitted to limit the change in monomer concentration. Such data are shown in curves *b* in Figure 3. These data were obtained at conversions not exceeding 15%. It is obvious that *I* increases slightly with conversion. A similar effect has previously been noted by Bywater et al.^{5,6}

The bulk polymerization of methyl methacrylate was also carried out at -25°C . (Data could not be obtained at -78°C since methyl methacrylate freezes at -50°C .) This polymer has a lower value for *I* (0.64_s) than those obtained in toluene.

From the values of *I*, *H*, and *S* one may calculate the fractional populations (*i* and *s*) of isotactic and syndiotactic diads and also the relative probabilities of formation of various types of triads from diads (P_{ii} , P_{is} , P_{si} , and P_{ss}) from the relations⁸ (1)–(6).

$$i = I + H/2 \quad (1)$$

$$s = S + H/2 \quad (2)$$

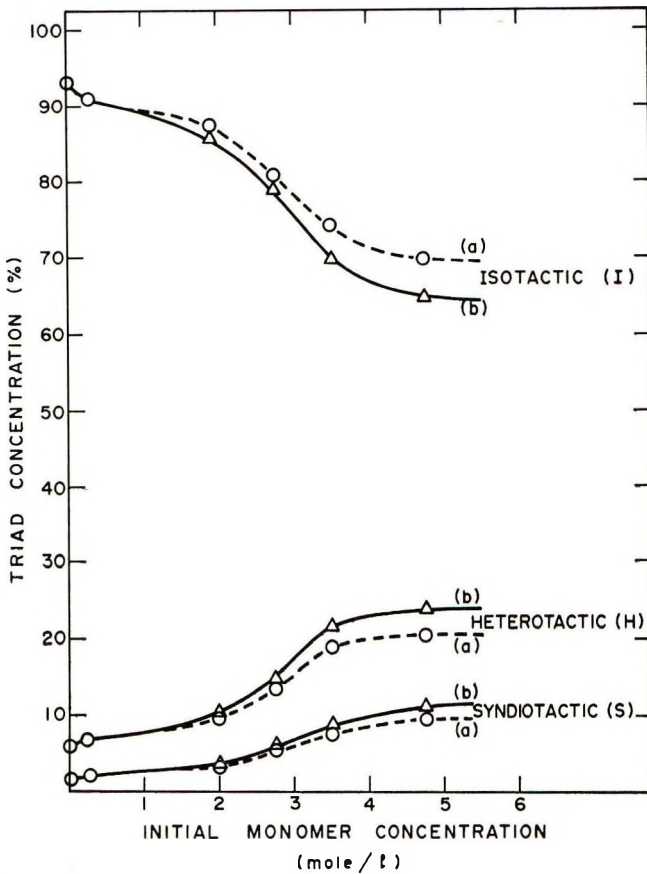


Fig. 3. Triad concentrations for poly(methyl methacrylate) as a function of initial monomer concentration; polymerized in toluene at -78°C with butyllithium as catalyst: (O) at 100% conversion; (Δ) at 15% conversion.

$$I = iP_{ii} \quad (3)$$

$$S = sP_{ss} \quad (4)$$

$$P_{is} = 1 - P_{ii} \quad (5)$$

$$P_{si} = 1 - P_{ss} \quad (6)$$

The calculated values are shown in Table I. The values of P_{ii}/P_{si} and P_{ss}/P_{is} characterize the dependence of polymer structure upon penultimate effects.⁸ While the value of P_{ii}/P_{si} is relatively independent of conversion and monomer concentration, the value of P_{ss}/P_{is} changes remarkably from 12 for a polymer produced at low monomer concentration to 3.0 for a polymer produced by 15% conversion of a 4.75M solution of monomer (see Table I). This difference is primarily due to an increase in the value of P_{is} , the probability of syndiotactic addition to an isotactic diad.

The data in Table I have also been used to calculate the persistence ratio

ρ , defined by $2(is/H)$.⁷ ρ is the ratio of the actual mean length of closed isotactic placements to the mean length one would calculate, assuming the distribution is Bernoullian. Therefore, one would expect $\rho = 1$ for a Bernoullian sequence distribution.

Finally, one can calculate the mean length of isotactic placements μ , defined by ρ/s .⁷ μ varies from 35 at low monomer concentration to 6 at high monomer concentration. This is further confirmation of the marked change in polymer microstructure with monomer concentration.

Possible Mechanism of Polymerization of Methyl Methacrylate

The first and most obvious conclusion which can be drawn from our results is that any attempt to deduce information about mechanisms of polymerization from measurements of penultimate effects or penpenultimate effects will be of doubtful reliability if the effect of monomer concentration is not considered. While this point has been made before,⁷ it has often been ignored by other workers.

The sequence distribution for poly(methyl methacrylate) obtained in THF is well described by a Bernoullian model at all monomer concentrations investigated. Taking a typical composition of $I = 0.04$, $H = 0.34$, and $S = 0.62$ (see Fig. 2), one obtains values of P_{ii}/P_{si} , P_{ss}/P_{is} , and ρ of 0.9, 1.0, and 1.0, respectively. All are in good agreement with the expected value of 1.0 in each case.

On the other hand, the sequence distribution for poly(methyl methacrylate) obtained in toluene does not fit Bernoullian statistics at any monomer concentration. This is in agreement with previously reported results.^{5,6} It is also possible to check our results against the two-parameter enantiomorphic site (EMS) model for polymerization which has recently been proposed by Sheldon.⁹ The equations derived by Sheldon can be represented on a triangular diagram which represents values of I , S , and H for different polymers simultaneously. Such a diagram is shown in Figure 4. On this diagram curve I corresponds to the Bernoullian model in which only the configuration of the chain end influences the configuration of the adding unit. The second straight line II corresponds to a simple EMS model in which the configuration of monomer addition is influenced only by the asymmetry of the catalyst sites. Curve III represents the lower limits for I , H , and S permissible from arithmetic considerations. Points falling in region 1 indicate that there is a tendency for persistence of configuration between the adding monomer and the chain end. Points falling in region 2 indicate a tendency for alternation of configuration. All of our data points lie in the area of region 1. This tendency for persistence of configuration is also indicated by the fact that $\rho > 1$ in all cases. The points lie relatively close to the line corresponding to the simple EMS model although the deviations at the lowest monomer concentration are considerable and bring the values much closer to the Bernoullian model. The EMS model predicts a ratio of $H/S = 2$ which is lower than the experimental value of 3.7 obtained at the lowest monomer concentration. H/S

approaches 2 at higher monomer concentrations. While the possible error in H/S is greatest at low monomer concentration (due to the very large fraction of isotactic triads), the observed deviations from the EMS model are believed to be experimentally significant.

We do not have sufficient data to check our results against other statistical models for polymerization. In order to carry out these comparisons it would be necessary to obtain accurate data for fractional populations of tetrad configurations and, if possible, pentad configurations. We have recently obtained access to a 220 MHz NMR spectrometer and hope to obtain the necessary data in the near future. In the mean time we have drawn certain tentative conclusions based upon the data obtained so far.

On the basis of these results, we favor a two (or higher) site model for the polymerization in toluene. As noted previously, there is a marked decrease in isotacticity with increasing monomer concentration (due pri-

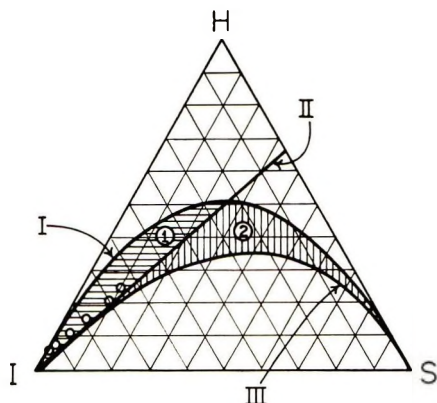


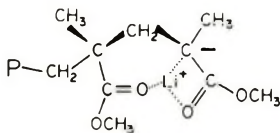
Fig. 4. Triangular diagram showing the relations between I , H , and S for experimental samples and for various statistical models.

marily to an increase in P_{is}). This suggests that at low monomer concentration the main polymerization site favors isotacticity while at high monomer concentration, a significant proportion of the polymerization occurs at one or more other sites which favor isotacticity less strongly. Polymerization at the other site(s), if present, apparently does not follow Bernoullian statistics, since the values of P_{ii}/P_{si} and ρ show no obvious tendency to approach unity at high monomer concentration.

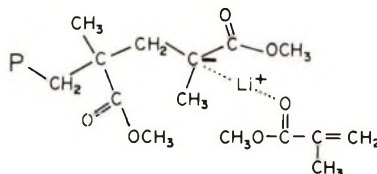
Bywater et al.^{5,6} have suggested a two-site mechanism to account for their results for the microstructure of poly(methyl methacrylate) produced in toluene with butyllithium. One site was believed to involve a normal ion pair, while the other site involved complexation of the anion by lithium methoxide produced by side reaction between butyllithium and monomer. An alternate explanation is presented below, involving the relative complexing abilities of solvent and monomer. In suggesting this mechanism, we do not claim to have disproved the mechanism of Bywater et al.^{5,6} or

to have rejected many other possible mechanisms, but simply to have offered another possible explanation.

Our data clearly indicate that in the polymerization of methyl methacrylate in a nonpolar medium the monomer concentration is important, while in a polar solvent such as tetrahydrofuran the effect of monomer concentration is insignificant. In order to explain these results, we suggest that in a nonpolar solvent such as toluene, two types of active site exist. In one of these the lithium counterion is complexed with the carbonyl of the penultimate methacrylate group in the polymer chain, and in the other the cation is complexed with a free monomer unit. These two structures are shown as structures I and II.



(I) Intramolecular Complex



(II) Intermolecular Complex

Structure I may be considered to involve an intramolecular coordination with the polymeric anion. Such a structure would be expected to be relatively rigid and to confer upon the catalyst the ability to add in a specific configuration. When the counterion is coordinated with the monomer carbonyl group as in structure II (intermolecular coordination) the transition state has greater rotational freedom. However, the active site may still have a preferred configuration leading to stereospecific addition of monomer, particularly since the most probable monomer to be added is the complexed monomer. Our results could then be explained if structure I has a strong tendency to produce isotactic linkages while structure II favors syndiotactic linkages.

The relative concentrations of structures I and II would depend on both the concentration of monomer and the relative complexing ability of monomer and the penultimate unit of the polymer chain. Low monomer concentration would clearly favor structure I, leading to increased isotacticity. The higher concentration of structure II at higher monomer concentration would account for the increased value of P_{is} . Addition of complexed monomer via structure II would tend to result in the reformation of an intramolecular complex. This could explain the high observed ratio of H/S at low monomer concentration since the polymer would tend to have a structure which may be represented as III:



where the pair $\begin{array}{|l} | \\ | \end{array}$ denotes isotactic diads and $\begin{array}{|l} | \\ | \end{array}$ denotes syndiotactic diads.

The observed increase in isotacticity with conversion and molecular weight could be due to two factors: a decrease in overall monomer concentration with conversion and a decrease in the local concentration of monomer since monomer may be partially excluded from the random coil of the polymer as the latter increases in size. Methyl methacrylate monomer appears, from solubility measurements, to be a less powerful solvent than toluene for isotactic poly(methyl methacrylate).

While both polymer and monomer would be expected to be stronger solvating agents for the counterion than toluene, this would no longer be true when the solvent is THF. Therefore, neither structure I or structure II would be expected to be present in appreciable concentrations in THF solutions. This would account for the totally different polymer microstructure in this solvent. It has been previously noted that addition of relatively small amounts of THF to toluene also leads to predominantly syndiotactic poly(methyl methacrylate).¹⁴

CONCLUSIONS

It is important to consider the effect of monomer concentration and per cent conversion if one wishes to obtain information concerning mechanisms of polymerization from polymer tacticity measurements.

The polymerization of methyl methacrylate in THF with butyllithium as catalyst obeys Bernoullian statistics, and the polymer microstructure is independent of monomer concentration in the concentration range investigated.

The polymerization of methyl methacrylate in toluene with butyllithium as catalyst does not obey Bernoullian statistics, and does not appear to fit an enantiomorphic site model. The polymer microstructure is strongly dependent upon monomer concentration.

One possible explanation for the above results involves a model for polymerization in which toluene does not complex the active site while monomer and THF are respectively weak and strong solvating agents.

The authors wish to acknowledge the generous financial assistance of the National Research Council of Canada and the helpful comments of a referee.

References

1. H. L. Frisch, C. L. Malloes, and F. A. Bovey, *J. Chem. Phys.*, **45**, 1565 (1966).
2. B. D. Coleman and T. Fox, *J. Chem. Phys.*, **38**, 1065 (1963).
3. J. Furukawa, Paper presented at ACS meeting, held at Miami Beach, April 1967, *Polym. Preprints*, **8**, 39 (1967).
4. T. G. Fox, W. E. Goode, S. Gratch, R. M. Nuggett, J. F. Kincaid, A. Spell, and J. D. Stroupe, *J. Polym. Sci.*, **31**, 173 (1958).
5. D. M. Wiles and S. Bywater, *Polymer*, **3**, 175 (1962).
6. B. J. Cottam, D. M. Wiles, and S. Bywater, *Can. J. Chem.*, **41**, 1905 (1963).
7. B. D. Coleman and T. Fox, in *Macromolecular Chemistry, Paris 1963* (*J. Polym. Sci. C*, **4**), M. Magat, Ed., Interscience, New York, 1963, p. 345.

8. Y. Ohsumi, T. Higashimura, and S. Okamura, *J. Polym. Sci. A*, **3**, 3729 (1965).
9. R. Sheldon, Paper presented at ACS meeting, held at San Francisco, April 1968, *Polym. Preprints*, **9**, 142 (1968).
10. K. Hatada, K. Ota, and H. Yuki, *J. Polym. Sci. B*, **5**, 225 (1967).

Received August 14, 1969

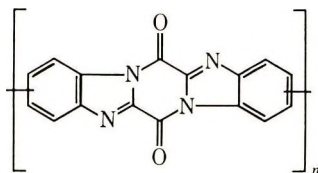
Revised July 22, 1970

NOTES

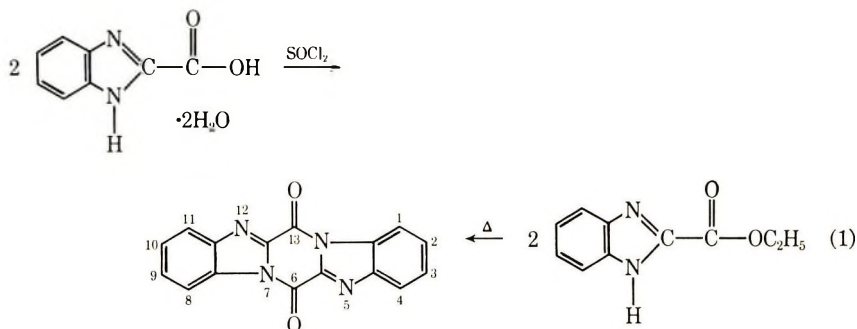
**Preparation and Characterization of a
Pyrazinobisbenzimidazole Polymer**

INTRODUCTION

In a search for new, thermally stable polymers, considerable effort has been directed toward the preparation of novel, aromatic-heterocyclic polymer systems. This note describes the preparation and characterization of an aromatic-heterocyclic polymer of the general structure:

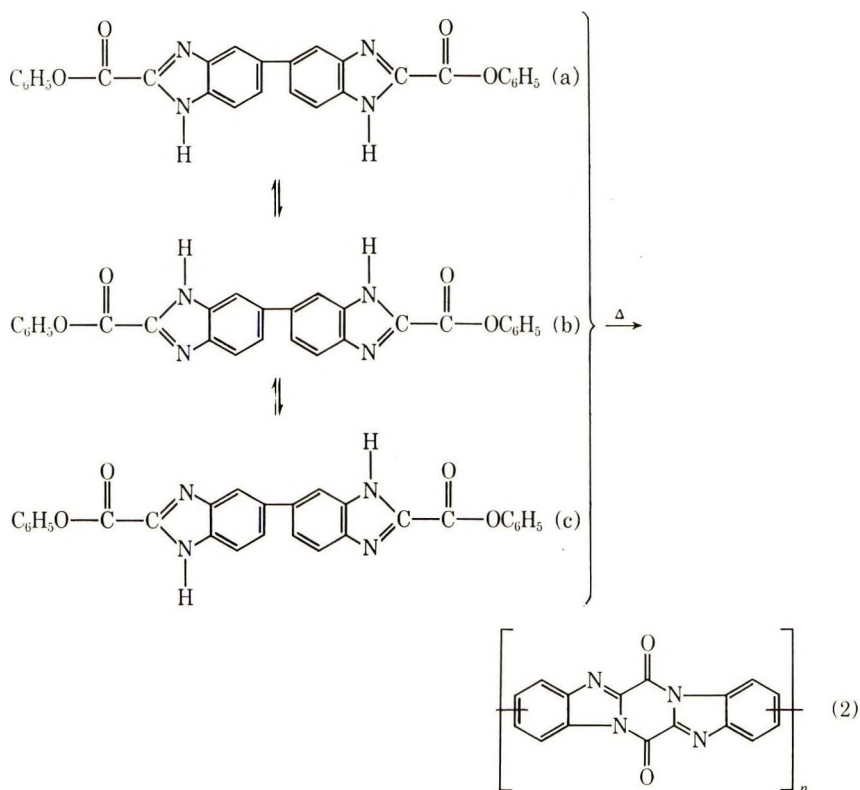


The polymer contains a 6*H*-13*H*-pyrazino[1,2-*a*:4,5-*a'*]bisbenzimidazole-6,13-dione ring system as the repeating unit in the polymer backbone. This ring system is reported in the literature as having been prepared by the condensation of 2-carboxybenzimidazole dihydrate in thionyl chloride.¹



In the course of this investigation, it was shown that this model compound could also be prepared in high yield and purity by the thermal condensation of 2-carbophenoxybenzimidazole. Consequently, it was considered that the desired polymer could be readily prepared via the reaction scheme (2), shown on page 544.

The requisite monomer is referred to in this note as 2,2'-bis(carbophenoxy)-5,5'-bibenzimidazole (a), although it also probably exists in the tautomeric forms, 2,2'-bis(carbophenoxy)-6,6'-bibenzimidazole (b) and 2,2'-bis(carbophenoxy)-5,6'-bibenzimidazole (c). The polymerization of this monomer could thus lead to a polymer with isomeric 2,9-, 2,10-, and 3,11-(6*H*,13*H*-pyrazino[1,2-*a*:4,5-*a'*]bisbenzimidazole-6,13-dione) repeating units in the polymer chain. For this reason, the polymer is represented as a general structure possessing uncertain stereochemistry. The exact name of a polymer containing, for example, exclusively the 2,10-isomer as a repeating unit would be



poly(6,13-dioxo-6*H*,13*H*-pyrazino[1,2-*a*:4,5-*a'*]bisbenzimidazole-2,10-diyl).^{*} Since this nomenclature is cumbersome, the polymer will be referred to as a pyrazinobisbenzimidazole polymer. The preparation and characterization of this polymer is described below.

DISCUSSION

Preparation of Polymer

2,2'-Bis(carbophenoxy)-5,5'-bibenzimidazole was subjected to melt polymerization. Evolution of phenol began below 250°C and became quite vigorous at 300°C with the formation of a red melt which rapidly resolidified to a bright orange solid. Solid-phase reactions at 350 and 400°C under reduced pressure yielded orange-brown powders which were over 95% soluble in cold concentrated sulfuric or methanesulfuric acid. Inherent viscosities of greater than 0.20 were not obtained.

Subsequent efforts were directed toward the solution polymerization of the monomer in tetramethylene sulfone. Appreciable reaction did not occur until the reaction temperature reached 270–275°C. After 15–30 min at this temperature, precipitation of polymer occurred. An inherent viscosity of 0.28 was recorded. Several additional runs were made under almost identical conditions. In these cases, the molecular weights of the polymers were further advanced by secondary solid phase reactions at 350°C. Inherent viscosities of 0.51 and 0.62 were realized.

A summary of the above polymerization reactions is given in Table I.

^{*} Polymer name was provided through the courtesy of Kurt L. Loening, Nomenclature Director, American Chemical Society, Chemical Abstracts Service.

TABLE I
Polymerization of 2,2'-Bis(carbophenoxy)-5,5'-bibenzimidazole

Trial no.	Reaction medium	Total reaction time, hr	Maximum reaction temp, °C	η_{inh} dl/g (solvent) ^a
1	Melt	1.5	400	0.15 (H ₂ SO ₄)
2	Melt	3.5	350	0.20 (H ₂ SO ₄)
3	TMS ^b	1.5	280	0.28 (CH ₃ SO ₃ H)
4	TMS ^b	6.5 ^c	350	0.62 (CH ₃ SO ₃ H)
5	TMS ^b	8.0 ^d	350	0.51 (CH ₃ SO ₃ H)

^a Values determined at a solution concentration of 0.2 g/dl at 25°C.

^b Tetramethylene sulfone.

^c Includes thermal treatment for 3 hr; prepolymer had $\eta_{inh} = 0.27$ (CH₃SO₃H, 25°C.)

^d Includes thermal treatment for 4.5 hr.

Physical Properties of the Polymer

The polymer samples from the various reactions were bright orange to orange-brown powders which were insoluble in all organic solvents tested. The low molecular weight samples ($\eta_{inh} = 0.20$) were almost completely soluble in cold concentrated sulfuric or methanesulfonic acid. At higher molecular weights, the samples were appreciably soluble only in methane sulfonic acid with gentle warming (to 60°C) being necessary, in some cases, to effect solution. The inherent viscosities of all the polymer samples were determined in concentrated sulfuric or methane sulfonic acid and ranged from 0.15 to 0.62. Since the model compound was somewhat unstable toward warm mineral acid, there was some concern as to any deleterious effect the acidic solvents might have upon the degree of polymerization of the polymer samples. The relationship between the inherent viscosity and the age of a methane sulfonic acid solution of polymer was, therefore, studied. The polymer sample (No. 4) upon gentle warming in pure methanesulfonic acid (mp ~ 20°C) was found to be 80% soluble with an initial inherent viscosity of 0.60. Aging at 25°C for 3, 6, and 20 hr resulted in solution viscosities of 0.58, 0.55, and 0.52, respectively. Aging of the solution at 60°C for 3 hr resulted in little change in solution viscosity. If a slightly wet solvent sample was used, the polymer was 85% soluble and had an inherent viscosity of 0.62. After 16 hr at 25°C, the inherent viscosity had decreased to 0.29. The use of methanesulfonic acid from a bottle which had been opened for some time and appeared to have a considerable water content resulted in immediate dissolution of the polymer at room temperature. An initial inherent viscosity of 0.10 was recorded. These tests pointed out the necessity of using pure methanesulfonic acid for the viscosity determinations. The relatively slow rate of decrease of the inherent viscosity in pure methanesulfonic acid both at 25°C and 60°C would seem to indicate that only limited hydrolysis of the polymer sample had occurred during dissolution. The inherent viscosity values obtained would thus appear to be indicative of the true degree of polymerization of the polymer.

The hydrolytic stability of the polymer in the presence of strong base was also investigated. A finely ground sample (No. 4) was slurried in 1N sodium hydroxide at both room temperature and 60°C. Dissolution to a light yellow solution occurred almost immediately at 60°C and over the course of a few minutes at room temperature. Careful acidification of the solution yielded a white solid which from its infrared spec-

TABLE II
Physical Properties of the Pyrazinobisbenzimidazole Polymer

Property	
Physical appearance	Orange-brown, amorphous powder
Solubility	Insoluble in dimethyl sulfoxide, <i>N,N'</i> -dimethylacetamide, hexamethylphosphoramide, formic acid, <i>m</i> -cresol Slightly soluble in concentrated sulfuric acid Soluble (82%) in methanesulfonic acid
Inherent viscosity dl/g	0.62 (0.2 at 25°C)
Elemental analysis	
Calcd, %	C, 67.12; H, 2.10; N, 19.58; O, 11.19
Found, %	C, 66.98; H, 3.11; N, 19.07; O, 10.84*
Thermogravimetric analysis	
In nitrogen	Initial breakdown at 475°C Inversion point of curve at 625°C Weight loss at 900°C = 32%
In air	Initial breakdown at 375°C Inversion point of curve at 525°C Weight loss at 900°C = 96%
Softening behavior	No softening up to 450°C
Differential thermal analysis:	No transitions noted

* By difference.

trum appeared to be fairly pure 2,2'-bis(carboxy)-5,5'-bibenzimidazole dihydrate. Base hydrolysis appeared to have been both rapid and complete.

The various polymer samples were, in general, characterized by their elemental analyses, infrared spectra, and thermogravimetric analyses (TGA). Most of the polymer characterization, however, centered on the polymer sample from trial 4 which was used in the above solution stability studies. Its properties are summarized in Table II. It was a powdery, orange-brown material which was only slightly soluble in sulfuric acid but 82% soluble in methanesulfonic acid. It could be reprecipitated without apparent change if methanesulfonic acid-methanol was used as the solvent-nonsolvent system. A finely pulverized sample was found to be completely amorphous by x-ray diffraction techniques and to have a softening point higher than 450°C, the limiting temperature of the test apparatus.² No transitions could be detected by differential thermal analyses. TGA under nitrogen indicated that initial breakdown begins at 475–500°C with 32% weight loss at 900°C. In an air atmosphere, TGA indicated catastrophic breakdown commencing at 375°C with essentially no residue at 900°C. The TGA curves are shown in Figure 1. Little difference was noted in comparing these TGA results with those from lower molecular weight samples ($\eta_{inh} = 0.20$ and 0.28).

The structure of the bisbenzimidazopyrazine polymer was established by elemental analysis and by comparison of its infrared absorption characteristics with those of the model compound, 6*H*,13*H*-pyrazino[1,2-*a*:4,5-*a'*]bisbenzimidazole-6,13-dione. The elemental analysis results for the polymer agreed fairly well with the calculated values for the proposed polymer structure. Despite thorough drying of the analytical samples at elevated temperatures and reduced pressures, the hydrogen determination yielded results higher than the theoretical value. Elemental analysis for nitrogen by the Kjeldahl method gave low and unreproducible results. Ordinary Dumas techniques, however, proved to be more satisfactory and gave results which compared fairly well with the theoretical value.

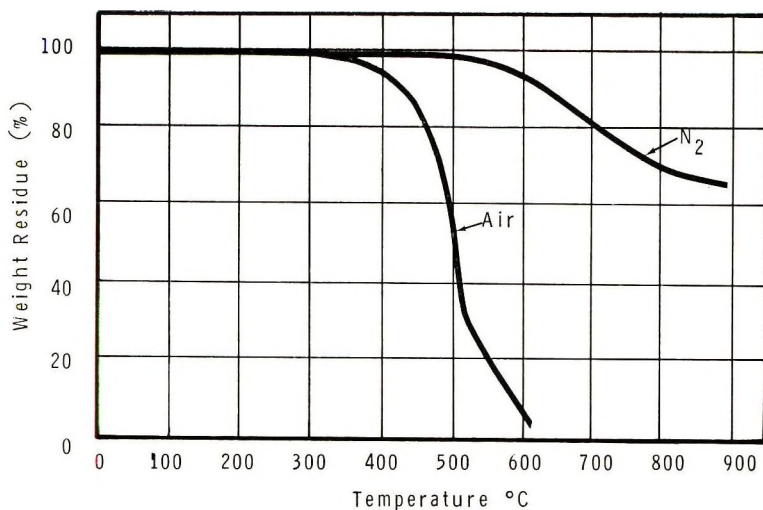


Fig. 1. TGA curves of the pyrazinobisbenzimidazole polymer ($\Delta T = 180^\circ\text{C/hr}$).

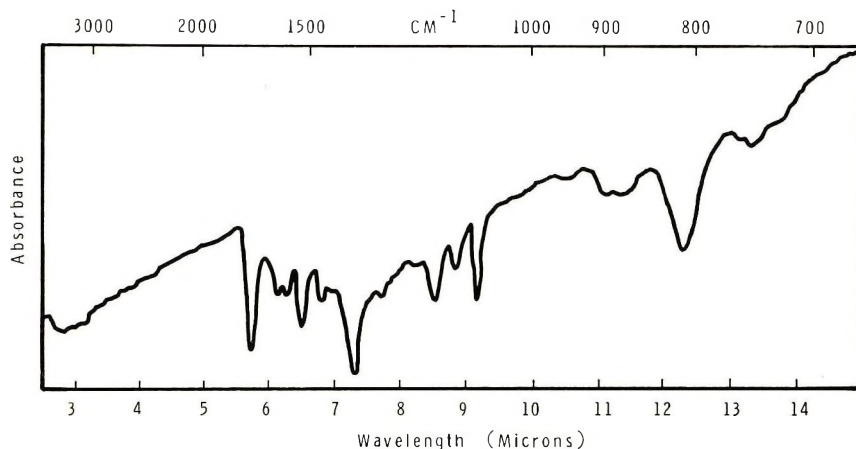


Fig. 2. Infrared spectrum of the pyrazinobisbenzimidazole polymer (KBr pellet).

Comparison of the polymer infrared spectrum with that of the model compound disclosed a number of correlations. Both spectra exhibited the expected carbonyl bands in the $1740\text{--}1745\text{ cm}^{-1}$ region.³ Also present in both spectra were prominent bands at $1530\text{--}1535$, $1355\text{--}1360$, $1160\text{--}1170$, and $1085\text{--}1090\text{ cm}^{-1}$, the nature of which is not fully understood. Absent in both spectra were absorptions at 1200 and 1775 cm^{-1} which were present in the spectrum of the monomer, 2,2'-bis(carbophenoxy)-5,5'-bibenzimidazole. These absorptions are attributable, respectively, to the C—O and C=O stretching vibrations of the carbophenoxy group.³ Only the monomer spectrum exhibited a fairly strong band at 3400 cm^{-1} , attributable to the N—H stretching vibration of the benzimidazole ring. It must be noted, however, that mechanical grinding of the polymer samples with potassium bromide led to atmospheric water contamination of the potassium bromide pellets. Absorptions due to water thus appeared in the $3300\text{--}3700\text{ cm}^{-1}$ region and may have masked any other absorptions in this region.

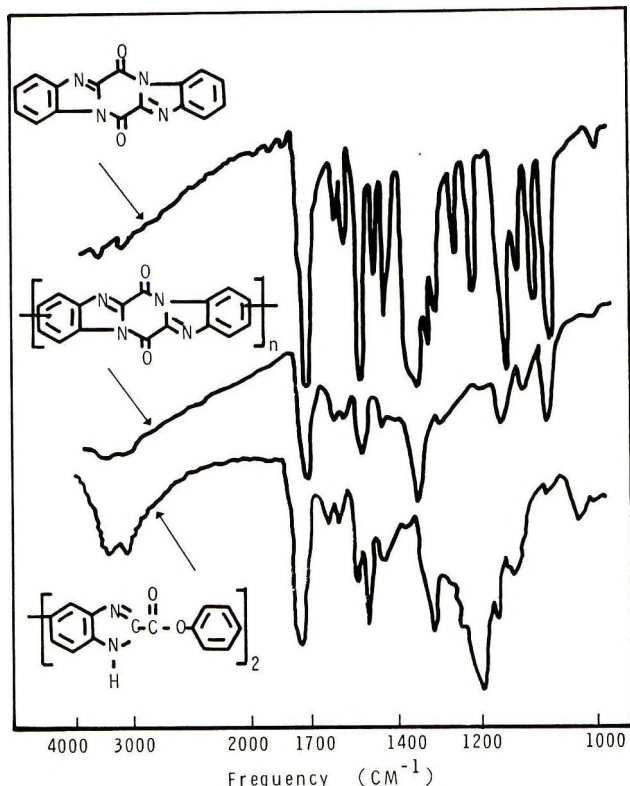


Fig. 3. Infrared spectra in the 4000–1000 cm^{-1} region.

The infrared spectrum of the polymer can be seen in Figure 2. A comparison of the infrared spectra of the polymer, model compound, and monomer in the 4000–1000 cm^{-1} region is shown in Figure 3.

EXPERIMENTAL

Preparation of Solvents and Intermediates

Tetramethylene sulfone was obtained from standard commercial sources and was purified by vacuum distillation over phosphorus pentoxide. Only the center fraction was retained. The purified material was stored over freshly dried molecular sieves in amber colored bottles.

3,3'-Diaminobenzidine was obtained from Burdick and Jackson Laboratories, Inc. It was used without further purification.

2-Carbophenoxybenzimidazole was prepared by the following procedure. Phenol (16 g) and phosphorus oxychloride (200 ml) were stirred together at room temperature to form a clear solution. 2-Carboxybenzimidazole dihydrate (8 g) (as prepared according to the method of Bistrzycki and Przeworski⁴) was added, and the resultant yellow slurry was warmed to reflux with stirring being maintained. The reaction mixture gradually cleared and a clear reddish solution resulted. After 90 min, the excess phosphorus oxychloride was drawn off under reduced pressure and the residue dissolved in 75 ml of acetone. The insolubles (1 g) were filtered off and the acetone solution added to 300 ml of ice water which was kept slightly alkaline by the addition of saturated sodium carbonate solution. The precipitate was isolated by filtration.

The tan solid was recrystallized once from an ethanol-water solution and twice from a dioxane-water solution. The yield was 3 g (32%) of white platelets, mp 205-206°C.

ANAL. Calcd: C, 70.59%; H, 4.20%; N, 11.76%. Found: C, 70.35, 70.67%; H, 4.62, 4.66%; N, 11.78, 11.99%.

Preparation of 6H,13H-Pyrazino[1,2-a:4,5-a']bisbenzimidazole-6,13-dione

From 2-Carboxybenzimidazole Dihydrate and Thionyl Chloride. The procedure of Copeland and Day was followed. 2-Carboxybenzimidazole dihydrate (10 g) was powdered and added slowly with stirring to thionyl chloride (60 ml). The yellow mixture was refluxed with stirring for 3 hr and the excess thionyl chloride drawn off under reduced pressure. The yellow, powdery residue was slurried in cold water and then filtered. It was washed on the filter with dilute sodium carbonate solutions, dried, and then extracted in a Soxhlet with methanol until the extract was colorless. About 6.4 g (87% yield) of a yellow powder was obtained. It started to discolor at 370°C and finally melted with decomposition at 430-440°C. (lit. mp >300°C).

From 2-Carbophenoxybenzimidazole. 2-Carbophenoxybenzimidazole (1.5 g) was heated under nitrogen in a polymer tube at 300°C for 30 min. A vigorous evolution of phenol resulted. This phenol was drawn off by further heating at 300°C/0.01 mm for 15 min. The crude product (0.85 g, 91% yield) was recrystallized from *N,N*-dimethylacetamide, a few milliliters of water being added to induce crystallization. It was isolated by filtration and washed on the filter with hot water and methanol. The dense yellow crystals started to discolor at 370°C and finally melted with decomposition at 440°C. This product had an infrared spectrum identical to that of the product obtained from 2-carboxybenzimidazole dihydrate and thionyl chloride.

ANAL. Calcd: C, 66.66%; H, 2.78%; N, 19.44%; MW, 288. Found: C, 66.74, 66.46%; H, 2.99, 2.85%; N, 19.20, 18.88%; MW 288 (mass spectroscopy).

Preparation of Monomer

2,2'-Bis(α -hydroxymethyl)-5,5'-bibenzimidazole. 3,3'-Diaminobenzidine (10.70 g, 0.05 mole) and glycolic acid (11.40 g, 0.15 mole) were dissolved with stirring in 200 ml of hot 4*N* hydrochloric acid. The resultant clear red solution was refluxed for 3 hr, at which time it was treated with charcoal and filtered. The warm filtrate was treated with 50% ammonium hydroxide solution until basic to litmus. The suspension was stirred for 1 hr, cooled, and filtered. About 12 g (82% yield) of pale orange material resulted. An analytical sample was recrystallized from a 60-40 dimethyl sulfoxide-water solution. The fine, pale orange crystals melted at 335-337°C to form a red liquid which resolidified almost immediately to a reddish-brown solid.

ANAL. Calcd: C, 65.30%; H, 4.76%; N, 19.05%. Found: C, 65.38, 65.48%; H, 4.86, 4.93%; N, 19.01, 19.09%.

2,2'-Bis(carboxy)-5,5'-bibenzimidazole Dihydrate. 2,2'-Bis(α -hydroxymethyl)-5,5'-bibenzimidazole (26.46 g, 0.09 mole) was placed in 450 ml of hot water which was made basic by the addition of several milliliters of concentrated sodium carbonate solution. Powdered potassium permanganate (41.72 g, 0.26 mole) (10% excess) was added portionwise with stirring so as to avoid excessive boiling and foaming. The resultant brown suspension was refluxed with stirring for an additional 45 minutes and then filtered hot. The residue was dried, finely powdered, and boiled with 500 ml of hot water to remove any product adhering to the manganese dioxide. This suspension was filtered and the extract added to the original filtrate. The combined solutions were cooled and neutralized with 50% acetic acid. The creamy white precipitate was isolated by filtration, redissolved in warm sodium carbonate, and again precipitated by the addition of acetic acid. The product was isolated by filtration, washed with methanol and ether, and dried for several hours at 70°C in a vacuum oven. About 15 g (46% yield) of product with mp 188-191°C was isolated.

ANAL. Calcd for $C_{16}H_{10}N_4O_4$: C, 59.63%; H, 3.11%; N, 17.39%. Calcd for $C_{16}H_{10}$ -

$N_4O_4 \cdot 2H_2O$: C, 53.63%; H, 3.91%; N, 15.64%. Found: C, 53.01, 53.80%; H, 4.40, 4.00%; N, 15.42, 15.10%.

Alternatively, reduction in volume of the original filtrate by boiling off water until crystallization was imminent resulted in isolation of the dipotassium salt of 2,2'-bis-(carboxy)-5,5'-bibenzimidazole as long, white needles, mp $>300^\circ C$ (dec.).

ANAL. Calcd for $C_{16}H_8N_4O_4K_2$: C, 48.24%; H, 2.01%; N, 14.07%. Found: C, 48.02, 48.02%; H, 2.26, 2.38%; N, 13.88, 13.92%.

2,2'-Bis(carboxy)-5,5'-bibenzimidazole. 2,2'-Bis(carboxy)-5,5'-bibenzimidazole dihydrate as isolated by the above procedure (8 g) was slurried in a cooled solution of phenol (16 g) in phosphorus oxychloride (200 ml). The reaction mixture was saturated with dry hydrogen chloride gas and the temperature then slowly raised to reflux. After several hours, a clear, light red solution was formed. The excess phosphorus oxychloride was stripped off under reduced pressure and the gummy residue treated with cold sodium carbonate solution. The crude product was isolated by filtration and then refluxed in benzene. Any occluded water was removed in the benzene-water azeotrope. The residue was isolated by filtration. It was recrystallized twice from water-ethanol and three times from dioxane-water (charcoal) to give about 1 g (10% yield) of snow-white product, mp $>165^\circ C$ (dec.).

ANAL. Calcd: C, 70.89%; H, 3.80%; N, 11.81%. Found: C, 70.59, 70.71%; H, 3.80, 3.99%; N, 11.76, 11.58%.

Preparation of Polymer

The following examples are typical procedures for the polymerization of 2,2'-bis-(carboxy)-5,5'-bibenzimidazole.

Melt Polymerization. The monomer (1.0 g) was heated at $300^\circ C$ under nitrogen in a polymer tube. Evolution of phenol occurred with subsequent solidification of the polymerization mixture after about 30 min. After 1 hr, the polymer tube was allowed to cool and the bright orange solid finely crushed. The polymer was placed in a rotating 30-ml flask containing several small ball bearings to facilitate mixing. Heating was resumed at $350^\circ C/0.1$ mm for 1 hr. The final product was an orange-brown powder which was 95% soluble in cold sulfuric acid and had an inherent viscosity of 0.20 in that solvent at $25^\circ C$.

ANAL. Calcd: C, 67.13%; H, 2.10%; N, 19.58%. Found: C, 68.34%; H, 2.98%; N, 20.68%.

Solution Polymerization. The monomer (1.65 g) was dissolved under nitrogen at $80^\circ C$ in tetramethylene sulfone (70 ml). The temperature of the resultant water-white solution was gradually increased. At $180^\circ C$, a slight yellow color developed which deepened as the temperature was increased further. After 30 min at $260^\circ C$, the solution had taken on a deep orange color but no precipitation of polymer had occurred. Precipitation of an orange solid occurred, however, after 15 min of heating at 270 – $275^\circ C$. After being heated at $280^\circ C$ for an additional 3 hr, the polymerization mixture was cooled and added to a tenfold excess of methanol. The bright orange product (0.76 g, 76% yield) was isolated by filtration, washed well with methanol, and dried at $150^\circ C$ under reduced pressure. It was only partially soluble in cold sulfuric acid. An inherent viscosity of 0.27 in methane sulfonic acid at $25^\circ C$ was recorded. The finely powdered polymer was heated in a rotating flask at $350^\circ C$ for 3 hr to give an orange-brown powder which was 82% soluble in methanesulfonic acid. It had an inherent viscosity in that solvent of 0.62 at $25^\circ C$.

ANAL. Calcd: C, 67.13%; H, 2.10%; N, 19.58%. Found*: C, 66.98%; H, 3.11%; N, 19.07%.

* Values found for the combined soluble and insoluble portions.

References

1. R. A. B. Copeland and A. R. Day, *J. Amer. Chem. Soc.*, **65**, 1073 (1943).
2. G. F. L. Ehlers and W. M. Powers, *Materials Res. Stds.*, **4**, 298 (1964).
3. L. J. Bellamy, *The Infrared Spectra of Complex Molecules*, 2nd ed., Methuen, London, 1958.
4. A. Bistrzycki and G. Przeworski, *Ber.*, **45**, 3483 (1912).

ROBERT C. EVERS

Polymer Branch
Air Force Materials Laboratory
Wright-Patterson Air Force Base,
Ohio 45433

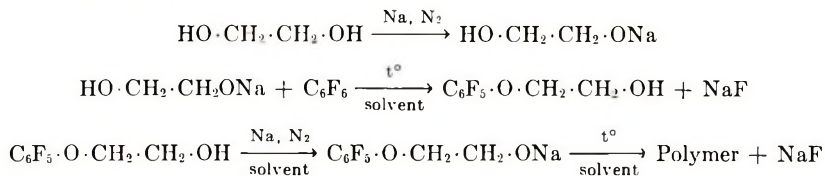
Received May 11, 1970

Synthesis and Study of $(-C_6F_4OCH_2CH_2O)_n^*$

Although perfluoroaromatic polyethers in general have been reported¹⁻⁵ in the past, the subject is by no means exhausted.

Polyethers of the type $(-C_6F_4 \cdot O \cdot CH_2 \cdot CH_2 \cdot O)_n$ were synthesized in the present work by what is believed to be the repeated stepwise attack of the anion $C_6F_5 \cdot CH_2 \cdot CH_2 \cdot O^-$ at the *para*-position of a molecule of undissociated alcohol to give the polymer. Although there has been no proof that this reaction proceeds through displacement of the fluorine atom *para*- to the functional group, theoretical considerations as well as experimental data^{2,6} have shown that apart from extreme cases, the position *para* to the functional group in pentafluorophenyl compounds is the most susceptible towards nucleophilic attack.

The general route employed in the synthesis of the polyether can be roughly illustrated by the following sequence of reactions:



The monomer 1-hydroxy-2-pentafluorophenoxyethane was a colourless liquid soluble in most organic solvents and its purity was established by gas-liquid chromatography, which showed the presence of only one component. The infrared spectrum of this alcohol showed the characteristic absorption of the perfluorinated benzene ring at 1510 cm^{-1} and the hydroxyl stretching vibration at 3390 cm^{-1} .

The polymerization of 1-hydroxy-2-pentafluorophenoxyethane was studied in two series of experiments and these are described in the last section. In the first series, the initial concentration of the monomer was kept constant (ca. 5% w/w) while the refluxing period varied from 80 min to 32 hr. In the second series, the refluxing time was kept constant (32 hr) while the initial monomer concentration was varied from 5.3% to 22.6% w/w.

Information regarding the degree of polymerization was obtained from comparison of the intensities of the O-H stretching vibration (3340 cm^{-1}) in the infrared spectra of the polymers. (Purified samples in CS_2 solution for the liquid polymers. Mull for the solid polymer.) Since these reactions were designed to produce polymers with hydroxyl end-groups, the percentage of -OH present in the polymer chain should decrease as the degree of polymerization increased.

Polymer I obtained in a 75% yield after a polymerization time of 80 min was a yellow liquid whose infrared spectrum indicated a rather low degree of polymerization. A polymerization time of four hours gave polymer II (yield 84%) more viscous than the previous one and with a higher degree of polymerization. The best results were obtained, however, with a reaction time of 32 hr at the end of which two types of polymer had been produced. Polymer III was a very viscous liquid or semisolid (56% yield) soluble in ether and acetone like the previous ones, yet polymer IV was an amorphous off-white powder (26% yield) insoluble in all solvents tested, whose infrared spectrum showed no absorption whatsoever in the region above 3000 cm^{-1} . This polymer would not melt and it was stable towards acids and alkalis for many days. (See Table I.)

It was thought at this point that the yield of the solid polymer IV could be improved at the expense of the liquid one III by increasing the initial concentration of the monomer instead of a further increase in the refluxing time. A second series of experiments was carried out, therefore, under the same experimental conditions as those of the first series.

* Part of a Ph.D. Thesis submitted to the University of Manchester (1965).

TABLE I
Thermal Decomposition on Thermobalance^a

Temperature, °	Loss of weight, %
305	0.8
355	4.2
390	17.5
485	29.2

^a Rate of temperature increase 6.5°/min.

TABLE II
Polymerization of 1-Hydroxy-2-Pentafluorophenoxyethane in Various Initial Concentrations^a

1-Hydroxy-2-pentafluorophenoxyethane	Iso-propyl ether, g	%	Liquid polymer, g		Solid polymer, g		Over-all yield, %	
			w/w	%	%	%	%	%
5.8 g, 25.4 m mole	108	5.3	3.22	60	1.21	23	83	
4.0 g, 17.5 m mole	50	7.4	1.10	31	2.12	58	89	
4.1 g, 17.6 m mole	26	13.3	0.91	25	2.51	68	93	
3.5 g, 15.3 m mole	12	22.6	0.51	13	2.83	77	90	

^a Experimental conditions as in the section, Synthesis of Polymers.

Four experiments were included in this series, with initial monomer concentrations of 5.3, 7.4, 13.3, and 22.6%, and the results of these experiments are listed in Table II. It is important to emphasize that at an initial monomer concentration of 5.3% the ratio of solid to liquid polymer yields was approximately 1:3. This ratio, however, was more than reversed at an initial monomer concentration of 22.6%, when it became 6:1.

Although, as already mentioned above, nucleophilic attack on pentafluorophenyl compounds leads almost invariably to *para* isomers, attempts were made to cleave the polymer so that the structure would be verified by the cleavage products. Such attempts, however, employing the use of hydrazine hydrate⁷ and constant b.p. hydriodic acid failed to cleave solid polymer IV. More drastic conditions such as heating the polymer together with 80% sulphuric acid for many hours at temperatures up to 110° did not prove more fruitful; but when the temperature was raised to 140° for 40 hr, 66% of the polymer was turned to intractable tars. The failure to obtain any small molecules as products of this cleavage must be due to the extremely drastic conditions required for the reaction to take place. Indeed, the free electron pairs of the ethereal oxygen atom must be strongly delocalized by the inductive effect of the perfluorinated benzene ring as well as by the usual mesomeric interaction with the ring, with the result that protonation of the ether is very difficult. The difficulty of protonation is further enhanced by the insolubility of the polyether in the protonation solvent.

EXPERIMENTAL

1-Hydroxy-2-pentafluorophenoxyethane

A solution of hexafluorobenzene (39.0 g, 0.21 mole) in ethylene glycol (50 ml) was heated under reflux to 85–90°, while a 10% solution of the monosodium derivative of ethylene glycol (19.5 g, 0.23 mole) in ethylene glycol was added dropwise and the heating was continued for one hour after the hexafluorobenzene had stopped refluxing (total

6 hr). The sodium fluoride was then removed by filtration and the filtrate was poured into water and was left overnight. The oily layer under the water was dissolved in ether, dried and distilled under reduced pressure to give 1-hydroxy-2-pentafluorophenoxyethane (25.5 g, 53%) (Found: C, 42.2; H, 2.3%. Calculated for $C_8H_5F_5O$: C, 42.1; H, 2.2%), b.p. $98^\circ/11$ mm. G.L.C. gave only one peak.

Synthesis of Polymers

Sodium (0.50 g, 29.8 m mole) was added in small pieces under nitrogen to a solution of 1-hydroxy-2-pentafluorophenoxyethane (4.8 g, 21.0 m mole) in anhydrous isopropyl ether and the mixture was heated under reflux for 32 hr. The precipitate formed was separated by filtration, treated with dilute hydrochloric acid, and repeatedly boiled with water to remove the inorganic salts; it was then dried *in vacuo* to leave a powder characterized as polymer IV (1.1 g, 26%) [Found: C, 46.0; H, 2.5%. $(C_8F_4H_4O_2)_n$ requires: C, 46.1; H, 2-2.4%]. This polymer would not melt up to a temperature of 350° ; it was insoluble in organic solvents and was not affected by sodium hydroxide or hydrochloric acid at room temperature for 15 days. The filtrate (after removal of the solvent) was treated with 2N sulphuric acid, redissolved in ether, dried, and the solvent was distilled off to leave a very viscous liquid polymer III (2.4 g, 56%) [Found: C, 46.0; H, 2.7%. $(C_8F_4H_4O_2)_n$ requires: C, 46.1; H, 2.0-2.4%].

Refluxing periods of 80 min and four hours in other experiments gave only viscous liquid polymers I and II, characterized by elemental analysis.

Variation of Monomer Concentration

The results of experiments carried out with different initial monomer concentrations are listed in Table II.

References

1. Birchall and Haszeldine, *J. Chem. Soc.*, 3719 (1961).
2. J. Nikokavouras, PhD. thesis, University of Manchester, 1965.
3. Pummer and Wall, *J. Res.*, N.B.S., **68A**, 277 (1964).
4. Robson, Stacey, Stephens, and Tatlow, *J. Chem. Soc.*, 4754 (1960).
5. M. Stacey, *J. Roy. Inst. Chem.*, **84**, 11 (1960).
6. Tatlow, *Endeavour*, **22**, 89 (1963).
7. Forbes, Richardson, Stacey, and Tatlow, *J. Chem. Soc.*, 2019 (1959).

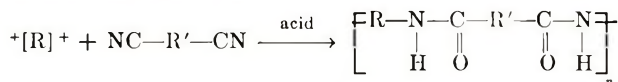
J. NIKOKAVOURAS

Nuclear Research Center
DEMOCRITOS
Aghia Paraskevi Attikis
Athens, Greece

Received April 21, 1970

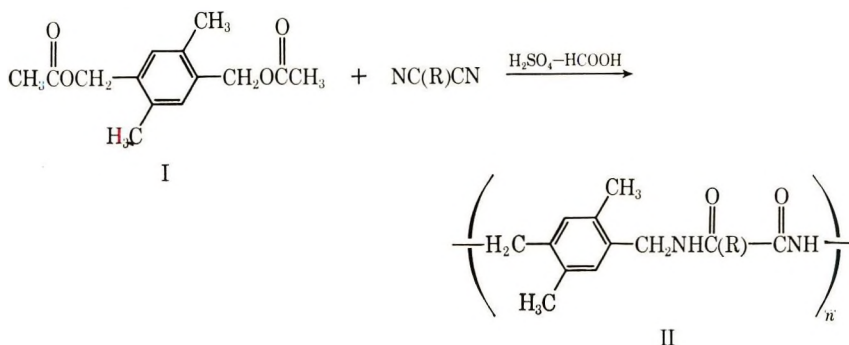
New Polyamides via Ritter Reaction

The condensation between nitriles and olefins or their derivatives in aqueous acidic media to form amides has been described by Ritter and co-workers.¹ Extension of this reaction to the preparation of linear polyamides has been achieved by the condensation of dinitriles with diolefins,² glycols,² diesters,² dihalides,² and formaldehyde;³



Because the Ritter reaction proceeds by a carbonium ion mechanism, the alkylating compounds are ordinarily restricted to those which can form a secondary or tertiary carbonium ion in an acidic medium. An exception to this trend are the primary systems of the benzyl⁴ and allyl⁵ type which can be readily *N*-alkylated under mild Ritter conditions. It has also been shown by Ramp⁶ that linear polyamides can be obtained by the condensation of dinitriles with bis(acetoxymethyl)durene in sulfuric acid. However, his attempts to extend the reaction to other alkylated benzenes failed.

To further study polymeric extensions of the Ritter reaction, a series of new polyamides were prepared by the condensation reaction between 2,5-dimethyl-1,4-bis(acetoxymethyl)benzene (I) with various dinitriles in sulfuric-formic acid mixture.



The diacetate I is prepared from 2,5-dimethyl-1,4-bis(chloromethyl)benzene (III) and silver acetate according to the procedures for preparing bis(acetoxymethyl)durene by Rhoad and Flory.⁷ The dichloro (III) compound is prepared by a modification of Braun's method⁸ using *p*-xylene and formaldehyde in hydrogen chloride solution. The diacetate I is readily soluble in chloroform to form a homogeneous solution with dinitriles. The well-dispersed mixture, therefore, can gradually form a high molecular weight polyamide upon contact with the acidic surface. This has some resemblance to an interfacial polymerization. The benzyl-type carbonium ion generated in this manner can apparently react readily with dinitriles to form amide before it can rearrange or decompose or become insolubilized. This is supported experimentally by the finding that high molecular weight polyamide can not be made from the 2,5-dimethyl-1,4-bis-(hydroxymethyl)benzene and dinitriles without using an interfacial solvent.

A number of polyamides were prepared from the 2,5-dimethyl-1,4-bis(acetoxymethyl)benzene and various dinitriles as shown in Table I. The structure of these polyamides were established by elemental analysis and infrared and NMR spectra. The glass transition temperatures of these polyamides were in the range of 70–225°C as determined by differential thermal analysis. In most cases, the polymers had good thermal stability as measured by thermogravimetric analysis (Fig. 1). Weight losses were less than 5% at a temperature of 350°C. The melting point of the polyamides obtained, except for that prepared from terephthalonitrile, were lower than 300°C.

TABLE I
Polyamides Based on 2,5-Dimethyl-1,4-bis(acetoxymethyl)benzene

Dinitriles	Inherent viscosity, dl/g	T_g , °C	T_m , °C	Calculated			Found			Yield, %	Weight loss at 350°C, %
				C, %	H, %	N, %	C, %	H, %	N, %		
Adiponitrile	0.47	70	283	69.06	7.92	10.14	68.06	8.04	10.62	92	2.1
Terephthalonitrile	0.82	225	>400	72.48	6.13	9.36	72.52	6.24	8.70	98	2.0
β,β -Oxydipropionitrile	0.39	80	248							88	5.0
Suberonitrile	0.50	78	270	72.50	8.33	8.98	71.80	8.72	8.97	95	3.5

^a Measured by TGA.

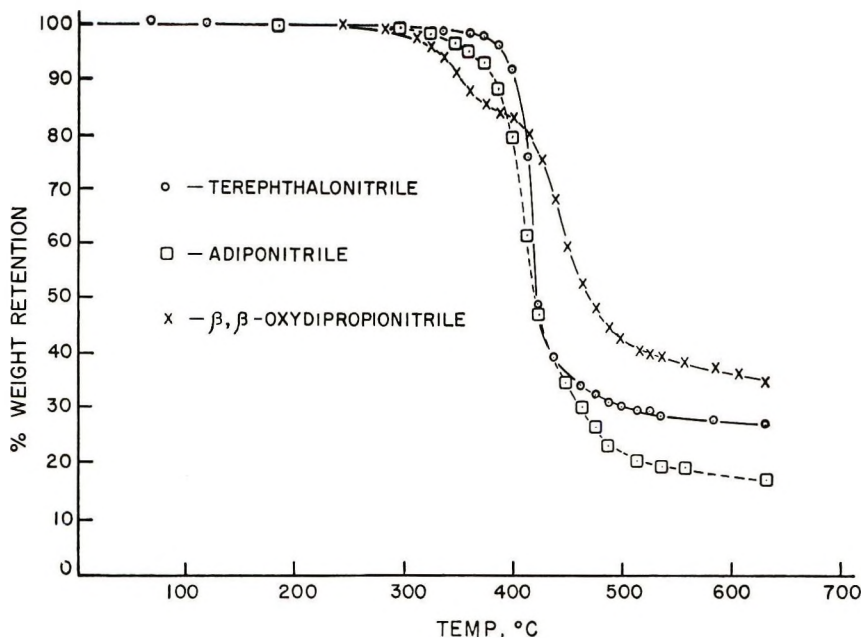


Fig. 1. TGA thermograms of polyamides based on 2,5-dimethyl-1,4-bis(acetoxymethyl)-benzene and various dinitriles.

Substituents on the aromatic moiety seem to have an important effect on the polymerization. The unsubstituted benzene, 1,4-bis(acetoxymethyl)benzene, gave oligomers only when reacted with dinitriles under Ritter conditions similar to those used to prepare high polymer from I. The number of methyl groups on the ring also had some effect on the properties of the resulting polyamides, as shown in Table II. The trend seems to indicate that the higher the number of substituents on the ring, the higher the glass transition temperature and the lower the solubility. The melting point did not show any effect. This substituent effect on glass transition temperature was previously reported by McCall and co-authors,⁹ where the polyamides made from the 5-*tert*-butyl-*m*-xylenediamine had T_g 's 8–48°C higher than the corresponding unsubstituted polymer.

The effect of the acid catalyst system on the resulting polyamide was also investigated. The following acids, or mixtures of them, were used as the Ritter catalysts—sulfuric acid, formic acid, acetic acid, phosphoric acid, and polyphosphoric acid. Concentrated sulfuric acid with formic acid as a diluent was found to be the best catalyst and was used throughout this study.

EXPERIMENTAL

Preparation of 2,5-Dimethyl-1,4-bis(chloromethyl)benzene (III)

The modified procedure of Braun⁸ was adopted. *p*-Xylene (53 g, 0.50 mole) was mixed with 400 ml concentrated HCl in a 1-liter, three-necked flask, and then mixed with 39.5 g of formaldehyde (1.30 mole). The mixture was stirred at 68–72°C for 24 hr. Anhydrous hydrogen chloride gas was introduced into the solution during this period. After cooling to room temperature, the white solid was filtered and then recrystallized from hot *n*-hexane to yield 25 g of white crystals (III). The *n*-hexane was cooled to 0°C and yielded another 13.70 g of III. The oily layer in the reaction vessel was separated from

TABLE II
 Effect of Substituents on Polyamide Properties

Polyamide	T_g , °C ^a	T_m , °C ^a	Viscosity	Solubility
Poly-2,5-dimethyl- <i>p</i> -xylyleneadipamide	70	283	0.47 ^b	In <i>m</i> -cresol at 25°C
Poly-1,2,4,5-tetramethyl- <i>p</i> -xylyleneadipamide ^c	—	>300	(7300) ^d	In <i>m</i> -cresol at 50°C
Poly-5- <i>tert</i> -butyl- <i>m</i> -xylyleneadipamide ^c	109	179–193	0.64 ^t	—
Poly- <i>p</i> -xylyleneadipamide ^c	—	330–333	—	—
Poly-2,5-dimethyl- <i>p</i> -xylene- β,β -oxydipropionamide	80	248	0.39 ^b	In <i>m</i> -cresol at 25°C
Poly-1,2,4,5-tetramethyl- <i>p</i> -xylylene- β,β -oxydipropionamide ^c	191 ^b	246	0.1 ^b	—

^a Measured by DTA unless otherwise stated.

^b At 0.5% concentration in 98% formic acid at 25°C.

^c Data obtained by Ramp.⁶

^d The number-average molecular weight was obtained by Ramp⁶ in *m*-cresol at 110°C with the use of 55-08 membranes.

^e Polymer was prepared by McCall⁹ from salt of 5-*tert*-butyl-*m*-xylylenediamine and adipic acid.

^t Inherent viscosity was determined using a 60/40 phenol/tetrachloroethane mixture as solvent in 0.23 g/100 ml.

^{*} Data obtained by Frunze et al.¹⁰

^b Data obtained by Ramp⁶ using Dynamic extrusion valve.

the liquid layer and subjected to fractional distillation. After the liquid portion was removed at 35°C/5 mm and 85°C/5 mm, the white residue was recrystallized from *n*-hexane to yield an additional 39 g of 2,5-dimethyl-1,4-bis(chloromethyl)benzene, mp of the solid is 132–133°C (lit.¹ 133°C). Both infrared and NMR spectra agreed with the proposed structure III. The overall yield is 77.70 g or 77%.

ANAL. Calcd. for C₁₀H₁₂Cl₂: C, 59.30%; H, 5.92%; Cl, 34.78%. Found: C, 59.07%; H, 5.99%; Cl, 34.80%.

Preparation of 2,5-Dimethyl-1,4-bis(acetoxymethyl)benzene (I)

The method of Rhoad and Flory⁷ was used. The 2,5-dimethyl-1,4-bis(chloromethyl)benzene (12.0 g, 5.93 mmoles) in 150 ml of glacial acetic acid was added to a stirred slurry of 27.6 g (16.5 mmole) of silver acetate in 200 ml of glacial acetic acid. The mixture was refluxed for 3 hr. Purple solids formed gradually during this period. The silver chloride was removed by filtration from the hot solution. The unreacted silver acetate was filtered out after the solution was cooled to 70°C. Further cooling to room temperature gave a white filterable solid which was recrystallized from methanol, dried, and gave 4.70 g of (I). The liquid filtrate was slowly neutralized with dilute sodium carbonate to yield additional (I) which was also recrystallized from methanol (yield 6.40 g). Total yield of (I) was 11.10 g or 76%, mp 64–65°C (lit.⁷ 65°C).

General Procedure for Polyamide Synthesis

The polyamide was synthesized by interfacial method similar to the procedures described by Ramp.⁶ The general procedure can be exemplified by using the reaction of diacetate with adiponitrile. The 2,5-dimethyl-1,4-bis(acetoxymethyl)benzene (4.40

g, 17.4 mmole) and adiponitrile (1.89 g, 17.4 mmoles) in 70 ml of chloroform was added to a stirred solution containing 30 ml of concentrated sulfuric acid (80%) and 8 ml of formic acid. The solution was kept below 30°C during the addition. After stirring for a total of 5 hr, the chloroform was removed by separation, and the solvent residue was removed by vacuum distillation. The aqueous solution was poured into 300 ml of an ice-water mixture. The white polymer which precipitated was stirred in the aqueous solution for 1 hr, then filtered, and washed until neutral, then dried to constant weight. The polymer has a melting point of 283°C measured by DTA. Infrared and NMR spectra both agreed with the proposed polyamide structure. The inherent viscosity (0.50% concentration in 95% formic acid) was 0.47 dl/g.

Physical Properties

Infrared measurements were obtained on the Perkin-Elmer Model 21 infrared spectrophotometer. Inherent viscosities were determined at 25°C on a 0.5% solution of the polymer in *m*-cresol. These values are expressed in units of deciliters/gram. Glass transition temperatures (T_g) were measured with a differential thermal analyzer (DuPont Model 900), or Perkin-Elmer DSC-1B with the calorimeter attachment. T_g was taken as the point at which a change in heat capacity was first observed during the heating cycle, while T_m was taken as the peak temperature of the endotherm. The analysis was carried out in N₂ at a heating rate of 10°C/min and with 25-mg samples.

Thermogravimetric analysis (TGA) was carried out on the Ainsworth balance in N₂ and in air, at a heating rate of 10°C/min and with 10-mg samples.

We wish to acknowledge the contributions of Mrs. E. Turi for obtaining and interpreting the TGA and DTA data and Dr. John Sibilis and Mrs. L. Komarowski for obtaining and interpreting the IR and NMR spectra.

References

1. J. J. Ritter and P. P. Mincer, *J. Am. Chem. Soc.*, **70**, 7048 (1948).
2. E. E. Magat, U.S. Pats. 2,628,216-2,628,219.
3. J. T. Mowry and E. L. Ringwald, *J. Am. Chem. Soc.*, **72**, 4439 (1950).
4. C. L. Parris and C. M. Christenson, *J. Org. Chem.*, **25**, 331 (1960).
5. H. Christal and A. Laurent, *Bull. Soc. Chim. France*, **1958**, 920.
6. F. L. Ramp, *J. Polym. Sci., A-1*, **3**, 1877 (1965).
7. M. J. Rhoad and P. J. Flory, *J. Am. Chem. Soc.*, **72**, 2218 (1950).
8. J. V. Braun and J. Nelles, *Chem. Ber.*, **67B**, 1094 (1934).
9. M. A. McCall, J. R. Caldwell, H. G. Moore, and H. M. Beard, paper presented at American Chemical Society Meeting, September 1968; *Polym. Preprints*, **9**, 1644, (1968).
10. T. M. Frunze, V. V. Korshak, and E. A. Krasnyanskaya, *Polym. Sci. USSR*, **1**, 495 (1959).

LESTER T. C. LEE
ELI M. PEARCE

Corporate Chemical Research Laboratory
Allied Chemical Corporation
Morristown, N. J. 07960
Received May 25, 1970

Reactivity Ratios in the Cationic Polymerization of Styrene and Isoprene

INTRODUCTION

The copolymerization of styrene and isoprene has been investigated by numerous workers. Reactivity ratios are readily available for the free-radical, anionic, and γ -radiation-induced copolymerization.^{1,2} Quite a bit of work has been done utilizing a cationic initiator, but to the knowledge of the authors, information suitable for comparison was not available at 22°C. Workers have obtained interesting results at other temperatures, finding the product of the monomer reactivity ratios to be abnormally low.³ Kraus-erova et al.⁴ have observed the copolymerization in both hexane and benzene at this temperature, but their conversions were too high to permit accurate calculation of reactivity ratios.

It was further considered of interest to compare the reactivity ratios obtained cationically to those obtained by using γ -radiation. The γ -radiation-induced copolymerization has shown evidence of a free-radical nature, but evidence for an ionic mechanism in radiation-induced polymerization has been obtained in studies of isoprene⁵ and styrene.⁶

Triethylaluminum-based cationic catalysts have been described in the literature⁷ and are usually used in conjunction with one or more cocatalysts. These catalyst compositions proved to be either inactive or overactive for the styrene-isoprene system, so that it became necessary to develop a suitable catalyst. The conversion of monomer to polymer was held low so that the monomer feed ratios could be considered constant throughout any individual run.

EXPERIMENTAL

The isoprene and styrene were both purified by vacuum distillation and the center cut retained. The 2-methyl-2-chloropropane, dichloromethane, and *n*-hexane were obtained from Eastman Chemical Co. and used without further purification. The triethylaluminum was obtained from Columbia Organic Chemical Co. and used without further purification. The benzene was spectral grade.

The catalyst blend that proved most effective is shown in Table I.

TABLE I
Catalyst Composition

Reagent	Volume, ml
Dichloromethane	5.00
<i>n</i> -Heptane	1.50
Triethylaluminum	2.00
<i>tert</i> -Butyl chloride	1.56
Water	0.26

The reactants were added in the following order: *n*-heptane, dichloromethane, triethylaluminum, *tert*-butyl chloride, and water. Both the *tert*-butyl chloride and the water were added dropwise from a syringe. The *tert*-butyl chloride was added over a 45-min period, while addition of the water required an additional 30 min. The mixture was stirred vigorously throughout since the reaction was very exothermic. The triethylaluminum was transferred from the cylinder to the reaction vessel without permitting it to come in contact with the atmosphere.

After all of the components of the catalyst were added it was necessary to age the

catalyst for 90 min while stirring continuously in the ice bath. During this time some of the solid, which was formed when water was added, appeared to dissolve.

The amount of benzene needed to control the rate and prevent a temperature rise varied from 5 ml for low styrene monomer blends to 13 ml for blends with a high styrene content. Quinone (0.002 g) was also added to each run. Reaction times were 3 min for all runs.

A total of about 1.5 g of monomer was used in each run. The molar feed ratio of styrene to isoprene varied from 0.4 to 1.9.

A 0.4-ml portion of catalyst was introduced into the diluted monomer blends at room temperature. The monomers turned a light violet color upon initial contact with the catalyst, but faded in a few seconds to a grey color. Polymerization was terminated by the addition of 5 ml of dilute hydrochloric acid. Water alone would destroy the catalyst, but would form insoluble aluminum hydroxide in the process.

The samples were then centrifuged and the aqueous layer removed. After washing twice with 5-ml portions of water the polymer solution was next frozen to the walls of the centrifuge tube and the solvent removed by freeze-drying. It was not possible to precipitate the polymer with methanol when even a few drops of dichloromethane were present. After drying, the polymer was dissolved in 2 ml of benzene and then precipitated with methanol. This was repeated three times, and then the copolymer was frozen and freeze-dried again.

The copolymer samples were dissolved in a small quantity of benzene, and transferred to small preweighed rolls of filter paper. The samples were dried in a vacuum oven at 80°C for several hours and then weighed on a Cahn M-10 electrobalance. Sensitivity of the balance was about 0.01% of the total sample load. After weighing, the paper cylinders were oxidized in the Fisher combustion train. The vibrating reed electrometer analyses were performed in a manner similar to that already described.⁸ The amount of radioactivity present in the paper itself was found to yield a specific charge per milligram of 0.00402.

Results and Discussion

The conversion of monomer to polymer was held below 12% in all runs. There was no observable heat effect, the appearance of a solid phase, or any rapid increase in viscosity indicating that gelation had occurred. The data obtained are summarized in Table II. Solution of the copolymer equation gives reactivity ratios for styrene and isoprene respectively as 0.46 and 0.50.

Other investigators have observed somewhat similar reactivity ratios with these two monomers.^{4,9} The reactivity ratios seem quite dependent on solvent and catalyst. It has been shown that the addition of isoprene units is not a simple process.⁹ It has also

TABLE II
Copolymerization of Styrene and Isoprene in Benzene by Cationic Initiation

Run	Monomer feed ratio styrene/isoprene	Conversion, %	Copolymer molar ratio isoprene/styrene
1	4.0760	11.70	0.3996
2	2.3994	6.33	0.5750
3	2.3994	6.33	0.5664
4	1.0733	11.70	1.0054
5	1.0733	11.70	0.9717
6	0.6987	8.78	1.2590
7	0.6987	8.78	1.2615
8	0.4607	6.76	1.8383
9	0.4607	6.76	1.9151

been observed that phenyl groups from the solvent can be found in the polymer when benzene is used as solvent.¹⁰ A further complication is the possibility of crosslinking of any isoprene links by a 1,2 or 3,4 mechanism. In spite of these complications, however, it appears likely that some type of alternation mechanism is present.

References

1. R. H. Wiley and B. Davis, *J. Polym. Sci. A*, **1**, 2819 (1963).
2. S. K. Mansour, Thesis, University of Louisville, Louisville, Kentucky, 1965.
3. S. Medvedev and A. R. Gantmakher, in *Macromolecular Chemistry, Paris 1963* (*J. Polymer Sci. C*, **4**), M. Magat, Ed., Interscience, New York, 1964, p. 173.
4. H. Krauserova, I. Kössler, B. Matyska, and N. G. Gaylord, in *Macromolecular Chemistry, Tokyo-Kyoto 1966*, (*J. Polymer Sci. C*, **23**), I. Sakurada and S. Okamura, Eds., Interscience, New York, 1968, p. 327.
5. W. J. Burlant and D. H. Green, *J. Polym. Sci.*, **31**, 227 (1958).
6. A. Chapiro, *Radiation Chemistry of Polymeric Systems*, Interscience, New York, 1962.
7. T. Saegusa, H. Imai, and J. Furukawa, *Makromol. Chem.*, **79**, 207 (1964).
8. J. B. Niederl and V. V. Niederl, *Organic Quantitative Microanalysis*, Wiley, New York, 1948.
9. T. E. Lipatova, A. R. Gantmakher, and S. S. Medvedev, *Dokl. Akad. Nauk SSSR*, **100**, 925 (1955).
10. N. G. Gaylord, D. S. Hoffenberg, B. Matyska, and K. Mach, *J. Polym. Sci. A-1*, **6**, 269 (1968).

N. THORNTON LIPSCOMB

WALTER K. MATTHEWS

Department of Chemistry
College of Arts and Sciences
University of Louisville
Louisville, Kentucky 40208
Department of Chemistry
Georgia Southwestern College
Americus, Georgia 31709

Received June 9, 1970

NMR Studies on Terpolyesters

Introduction

Since the development of NMR spectroscopy, sequence distributions of many copolymers have been studied.¹ Copolyesters are especially suitable for studies of sequences by NMR, and the present authors² studied NMR spectra of many copolyesters and their sequence distributions by NMR.

Terpolymers have received the attention of many investigators and their reactivity ratios were studied on many systems,³⁻⁷ but their sequence distributions have not yet been found experimentally, although they are quite important in determining the reactivity ratios in terpolymerization. These relationships were found in some binary copolymers.

In present paper, sequence distributions in some terpolyesters were determined by NMR spectroscopy.

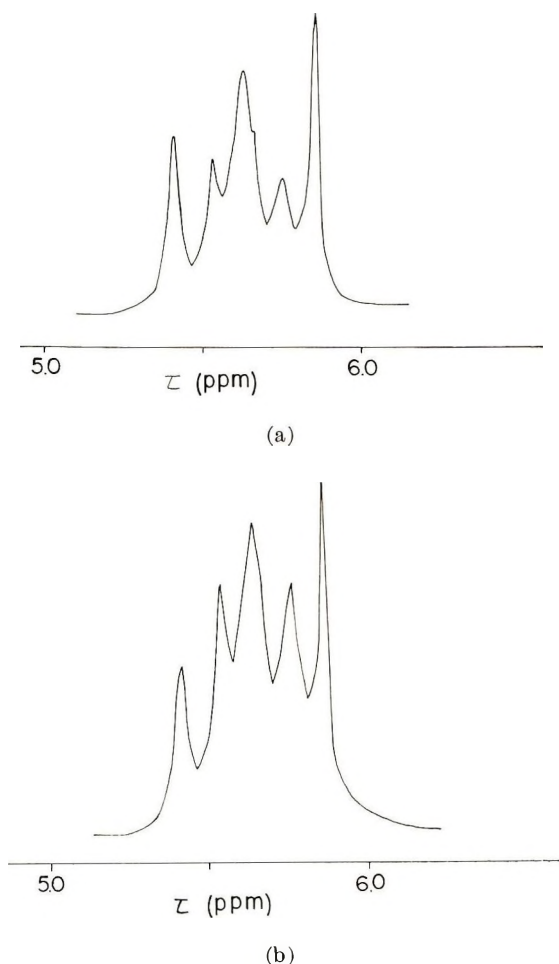


Fig. 1. Ethylene glycol proton resonance spectra (60 MHz) of PET/S/F terpolymers in chloroform at 70°C: (a) 40/40/20; (b) 35/35/30.

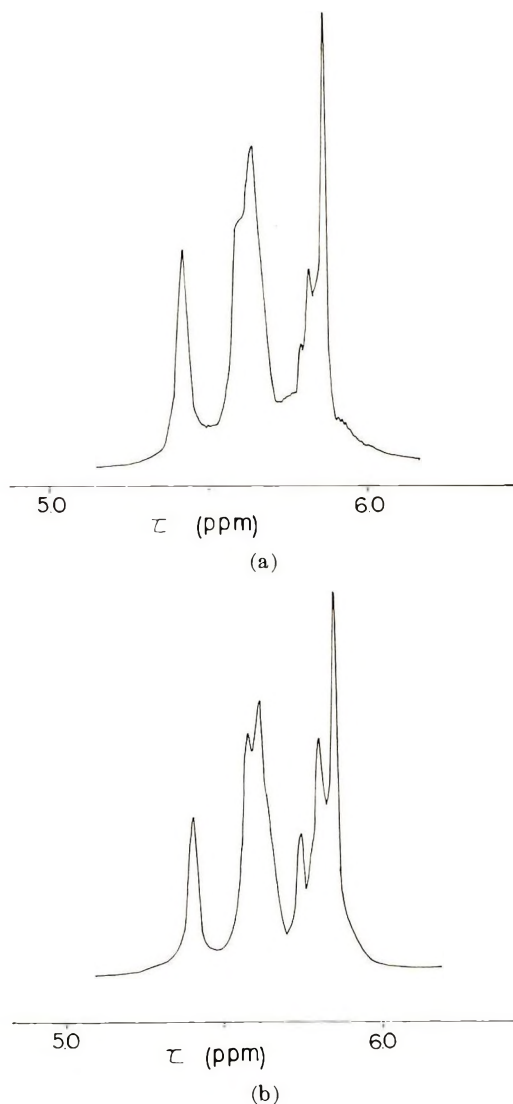


Fig. 2. Ethylene glycol proton resonance spectra (60 MHz) of PET/S/M terpolymers in chloroform at 70°C: (a) 40/40/20; (b) 35/35/30.

Experimental

Poly(ethylene terephthalate sebacate fumarate) (PET/S/F), poly(ethylene terephthalate sebacate malonate) (PET/S/M), and poly(ethylene terephthalate sebacate phthalate) (PET/S/Ph) were obtained from ethylene glycol and dimethyl esters of the corresponding acids by ordinary melt polycondensation under reduced pressure at 195°C. The corresponding binary copolymers and each homopolyesters were also prepared.

NMR spectra were measured in chloroform solution (0.05 g/ml) at 70°C with a Varian A-60 spectrometer.

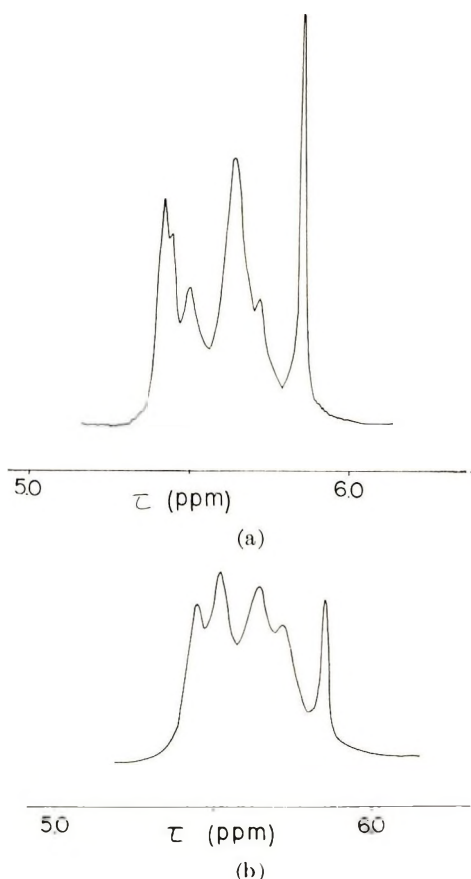


Fig. 3. Ethylene glycol proton resonance spectra (60 MHz) of PET/S/Ph terpolymers in chloroform at 70°C: (a) 40/40/20; (b) 30/30/40.

Results and Discussion

As found in our previous paper,² ethylene glycol units are sensitive to the linking acid units, and they have three resonance peaks in the case of binary copolymers. If we take poly(ethylene terephthalate sebacate) as an example, it has three peaks corresponding to T-E-T, T-E-S, and S-E-S linkages, where T, S, and E represent terephthalate, sebacate, and ethylene glycol units, respectively.

In the case of a terpolymer, consisting of A, B, and C monomers, there should be nine kinds of dyad sequences, A-A, A-B, A-C, B-A, B-B, B-C, C-A, C-B, and C-C. But if we use ethylene glycol in the terpolyester, A-B, B-C, and C-A linkages have the same chemical shifts as B-A, C-B, and A-C, respectively, and there are six resonance peaks of ethylene glycol units.

In Figure 1, NMR spectra of PET/S/F terpolymers are shown. They have six resonance peaks in the ethylene glycol region. These six peaks coincide with the resonance peaks in the binary copolymers of PET/S, PES/F, and PEF/T, and they can be assigned to T-E-T, T-E-F, T-E-S, F-E-F, S-E-F, and S-E-S linkages from the low field. These assignments were confirmed with samples having different feed ratios and 100 MHz spectra.

Figure 2 shows the NMR spectra of PET/S/M terpolymers; they also have six peaks in ethylene glycol resonance. These peaks can be assigned to T-E-T, T-E-M, T-E-S,

M-E-M, M-E-S, and S-E-S linkages from the low field, and they coincide with those in the binary copolymers of PET/S, PIS/M, and PEM/T.

Figure 3 shows the NMR spectra of PET/S/Ph terpolymers and they also show six peaks of ethylene glycol units, which are assigned to T-E-T, T-E-Ph, Ph-E-Ph, T-E-S, S-E-Ph, and S-E-S linkages from the low field.

It is quite important to measure these sequences in studying the sequence distributions of terpolymers and reactivity ratios in terpolymerization.

These results will be published in full in the near future.

References

1. R. C. Ferguson, *J. Amer. Chem. Soc.*, **82**, 2416 (1960).
2. R. Yamadera and M. Murano, *J. Polym. Sci., A-1*, **5**, 2259 (1967).
3. T. Alfrey, Jr. and G. Goldfinger, *J. Chem. Phys.*, **12**, 322 (1944); *ibid.*, **14**, 115 (1946).
4. G. E. Ham, *Copolymerization*, Interscience, New York, 1964, p. 1.
5. S. Iwatsuki and Y. Yamashita, *Makromol. Chem.*, **104**, 263 (1967).
6. H. J. Harwood, N. W. Johnston, and H. Piotrowski, in *The Computer in Polymer Science (J. Polym. Sci. C, 25)*, J. B. Kinsinger, Ed., Interscience, New York, 1968, p. 23.
7. N. W. Johnston and H. J. Harwood, *Macromolecules*, **2**, 221 (1969).

MASAO MURANO

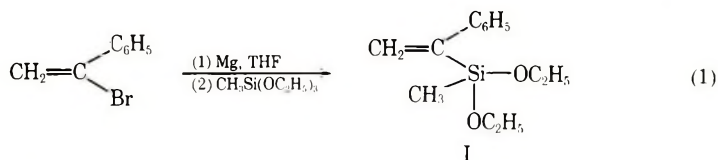
Textile Research Institute
Toyobo Company, Ltd.
Katata, Otsu, Japan

Received May 4, 1970
Revised June 8, 1970

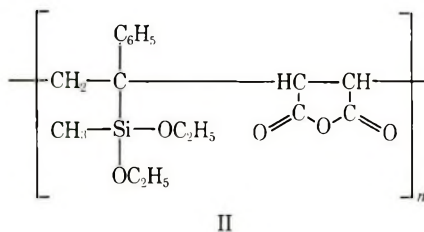
Preparation of Some Unsaturated Silanes

In the course of work concerning the synthesis of thermally stable polymers, we had occasion to synthesize some silicon containing monomers and polymers which we report here.

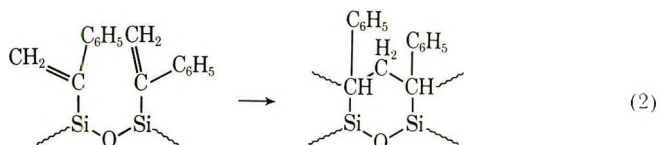
Methyldiethoxy- α -styrylsilane(I) was synthesized in 55% yield as shown in eq. (1).



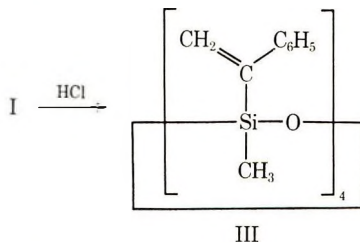
Compound I is a highly hindered 1,1-disubstituted olefin and as was anticipated did not homopolymerize with radical or low-temperature cationic initiators. However, compound I did copolymerize in the presence of benzoyl peroxide with maleic anhydride to form a nearly 1:1 copolymer (II).



If one prepared a high molecular weight polysiloxane from I, a partial ladder structure could possibly be achieved by polymerization of the residual styryl groups [eq. (2)].

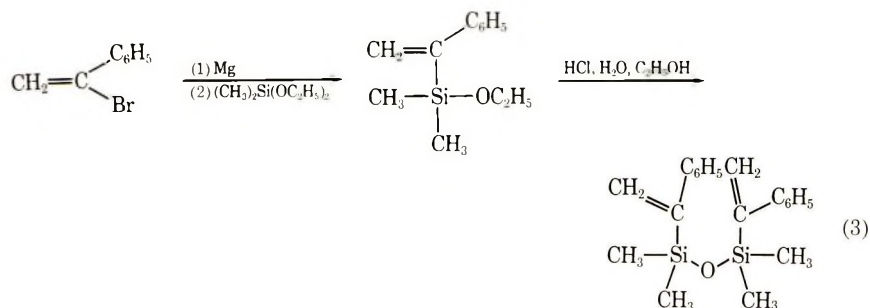


Hydrolysis of I with dilute hydrochloric acid in methyl isobutyl ketone resulted in the formation of largely cyclic tetramer(III).



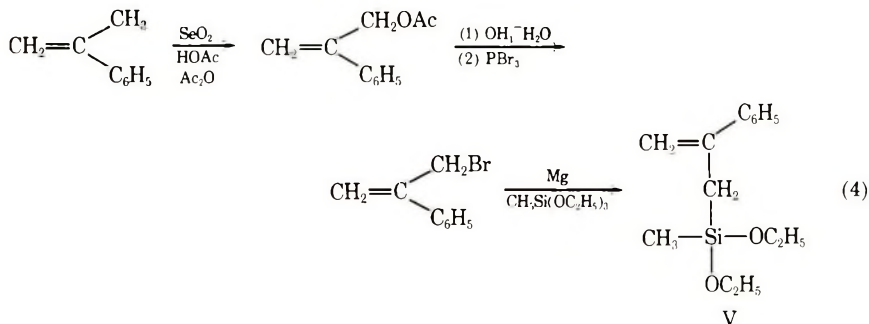
However, attempted equilibration of III by using a number of acidic or basic catalysts including the base-dimethyl sulfoxide system recently reported to be extremely effective¹ did not result in any significant molecular weight increase.

Bis(dimethyl- α -styryl) disiloxane (IV) was also synthesized, as indicated, in the hope that it would undergo cyclopolymerization through the styryl units.



In our hands, however, this compound did not polymerize with radical or cationic initiators.

In order to determine whether the introduction of an additional methylene group would enable vinyl polymerization to occur, methyldiethoxy- β -phenallylsilane (V) was prepared. Although one might expect the precursor, α -bromomethylstyrene to be prepared by the radical bromination of α -methylstyrene, it has been shown that this procedure leads to the formation of a difficultly separable mixture of the desired product and 1-bromo-2-phenylpropene.² Therefore V was prepared as shown in eq. (4).



Dropwise addition of α -bromomethylstyrene to magnesium and methyltriethoxysilane in ether suppressed the normal allylic Grignard coupling reaction and resulted in a 40% yield of V, which was also quite resistant to homopolymerization.

Experimental

Microanalyses and molecular weight determinations were performed by Micro-Tech Laboratories, Skokie, Illinois.

Diethoxymethyl- α -styrylsilane (I). α -Bromostyrene² (26.7 g, 0.146 mole) in 175 ml of THF was added dropwise over a 4-hr period to 3.9 g (0.16 mole) of magnesium turnings in 50 ml of THF which was maintained at 25–30°C according to the procedure of Normant.³ The mixture was stirred for an additional hour, filtered to remove magnesium and added dropwise over a 90-min period to a stirred solution of triethoxymethylsilane (44.5 g, 0.250 mole) in 50 ml of THF under anhydrous conditions and a nitrogen atmosphere. The resulting solution was stirred for an additional 10 hr, heated at reflux for 2 hr, filtered after adding acetone to remove magnesium salts, dried with anhydrous magnesium sulfate, stripped of solvent under reduced pressure and distilled through a Vigreux column at 75–85°C/0.5 torr to yield 19 g (55%) of I. Redistillation at 67–71°C/0.3 torr yielded 15 g (44%) of a clear colorless liquid; n_D^{25} 1.4843. The NMR spectrum (CCl₄) showed τ 2.7 (*m*, 5, phenyl), 4.0 (*d*, 1, $J = 3$ Hz, vinylidene H *cis* to phenyl), 4.2 (*d*, 1, $J = 3$ Hz, vinylidene H *trans* to phenyl), 6.2 (quartet, 4, $J = 7$ Hz, CH₂—CH₃), 8.8 (*t*, 6, $J = 7$ Hz, CH₃—CH₂) and 9.8 (*s*, 3, methylsilane). The infrared spectrum showed absorption at 1605 (vinyl) and 1260 and 763 cm⁻¹ (methylsilane).

ANAL. Calcd for $C_{13}H_{20}O_2Si$: C, 66.05%; H, 8.53%; Si, 11.88%. Found: C, 65.75%; H, 8.49%; Si, 11.63%.

Copolymerization of Diethoxymethyl- α -styrylsilane (I) and Maleic Anhydride. A solution of I (4.0 g, 17 mmole), maleic anhydride (4.0 g, 41 mmole) and azobisisobutyronitrile (0.04 g, 0.2 mmole) was polymerized for 1 day at 55°C, 4 days at 70°C, and 14 days at 85°C. Benzoyl peroxide (0.04 g, 0.2 mmole) was added at the start of the 70°C period and after 10 hr at 85°. The viscous solution was precipitated from benzene into anhydrous ether to yield 0.5 g (8%) of II, η_{inh} (30°C, benzene) 0.18. The infrared spectrum (KBr) showed absorptions at 1860 and 1790 (anhydride carbonyl) and 1265 cm^{-1} (methylsilane).

ANAL. Calcd for $C_{17}H_{22}O_5Si$ (1:1 copolymer): Si, 8.40%. Found: Si, 8.35%.

Preparation of Cyclic Trimers and Tetramers (III) of Diethoxymethyl- α -styrylsilane (I). A mixture of (I) (58 g, 0.25 mole), water (5.9 g, 0.35 mole), 0.4 ml of 12N hydrochloric acid, and 100 ml of 4-methyl-2-pentanone was heated at reflux for 4 days under nitrogen. Water, hydrochloric acid, and 4-methyl-2-pentanone were removed under reduced pressure to yield 41.0 g (100%) of III. Distillation through a Vigreux column yielded 34 g (83%), bp 190–270°C/1.5 torr. The NMR spectrum (CCl_4) showed τ 2.7 (*m*, 5, phenyl), 4.1 (*m*, 1, vinylidene H *cis* to phenyl), 4.2 (*m*, 1, vinylidene H *trans* to phenyl) and 9.7, two at 9.8 and 9.9 (*s*, 3, methyl silanes). The infrared spectrum (neat) showed absorptions at 1600 (vinyl), 1260 (methylsilane), 1080 broad (tetramer) and 1020 cm^{-1} shoulder (trimer). The molecular weight by cryoscopy (CCl_4) was 580 and 685, tetramer (calcd 650), trimer (calcd 490). The ultraviolet maximum (methanol) was at 242 $m\mu$ (ϵ , 7600).

ANAL. Calcd for $C_9H_{10}OSi$: C, 66.60%; H, 6.22%; Si, 17.31%. Found: C, 67.10%; H, 6.30%; Si, 17.30%.

Equilibration of Cyclic Trimers and Tetramers (III) of Diethoxymethylstyrylsilane. A mixture of III (10 g, 15 mmole based on tetramer), cesium hydroxide (5.0 mg, 0.034 mmole), and dimethyl sulfoxide (0.2 ml, 3 mmole) was prepared in a nitrogen-filled dry box, degassed by freeze-thawing, purged with nitrogen, heated to 85°C and ca. $\frac{1}{4}$ -ml samples removed at various times. The samples were stirred in an ether-water mixture for ca. 30 min. The ether layer was dried over anhydrous sodium sulfate and ether was removed under vacuum. Inherent viscosities were determined in 0.5 g/dl benzene solutions nine times between time zero and 13 hr and were observed not to change from 0.02.

Similar treatment of III with cesium hydroxide at 100°C for 45 min and 150°C for 20 min also resulted in a material with an inherent viscosity of 0.03. Treatment of III with catalytic amounts of potassium hydroxide at 150°C, silver oxide at 100°C or concentrated sulfuric acid at 60°C resulted in material of lower viscosity.

Ethoxydimethyl- α -styrylsilane. α -Bromostyrene (117 g, 0.640 mole) in 120 ml of anhydrous diethyl ether, magnesium (30.0 g, 1.25 mole) in 125 ml of anhydrous diethyl ether, and diethoxydimethylsilane (250 g, 1.70 mole) in 100 ml of anhydrous diethyl ether were allowed to react and worked up as was I to yield 50 g of product (38%) after distillation at 94–99°C/3.2 torr, 42 g (32%) after redistillation at 70–72°C/1.3 torr, of a pale yellow liquid; n_D^{25} 1.4988. The NMR spectrum (CCl_4) showed τ 2.8 (*s*, 5, phenyl), 4.1 (*d*, 1, $J = 7$ Hz, vinylidene H *cis* to phenyl), 4.3 (*d*, 1, $J = 3$ Hz, vinylidene H *trans* to phenyl), 6.4 (quartet, 2, $J = 7$ Hz, $\underline{CH_2-CH_3}$), 8.9 (*t*, 3, $J = 7$ Hz, $\underline{CH_3-CH_2}$) and 9.8 (*s*, 6, methylsilane). Infrared absorptions (CCl_4), were at 1603 (vinyl) and 1260, 855, and 800 cm^{-1} (methylsilane).

Bis(dimethyl- α -styryl)disiloxane (IV). Ethoxydimethyl- α -styrylsilane (20 g, 0.097 mole), water (7 g, 0.4 mole) containing 1 ml of 2N hydrochloric acid was stirred for 14 hr, extracted with ether, dried with anhydrous magnesium sulfate, stripped of volatile material under reduced pressure, and distilled through a Vigreux column at 141–145°C/0.7 torr to yield 10 g (61%) of a yellow liquid; bp 136°C/0.6 torr; n_D^{27} 1.5333. The NMR spectrum (CCl_4) showed τ 2.8 (*s*, 5, phenyl), 4.2 (*d*, 1, $J = 3$ Hz, vinylidene H *cis* to phenyl), 4.4 (*d*, 1, $J = 3$ Hz, vinylidene H *trans* to phenyl), 9.8 (*s*, 6, methyl-

silane). Infrared absorptions (CCl_4), were at 1600 (vinyl), 1260, 855, and 800 cm^{-1} (methylsilane).

ANAL. Calcd for $\text{C}_{20}\text{H}_{26}\text{OSi}_2$: C, 70.94%; H, 7.74%; Si, 16.59%. Found: C, 70.93%; H, 7.69%; Si, 16.28%.

β -Phenallyl Bromide. A solution of 3-hydroxy-2-phenylpropene (63.2 g, 0.472 mole), pyridine (7.5 g, 0.095 mole), and 40 ml of anhydrous ether was added dropwise over a 2-hr period to a solution of phosphorus tribromide (56.0 g, 0.207 mole) and pyridine (9 g, 0.1 mole) in 100 ml of anhydrous ether, which was maintained at -3 to -20°C under anhydrous conditions and a nitrogen atmosphere. The reaction mixture was allowed to warm to room temperature over a 1-hr period and stirred for an additional 22 hr. Volatile material was removed under vacuum, and 79.6 g (85.7%) of β -phenallyl bromide was obtained after distillation at $68\text{--}74^\circ\text{C}/1.5$ torr. Redistillation at $65\text{--}68^\circ\text{C}/1.3$ torr produced a pale yellow liquid; n_D^{27} 1.5901. The NMR spectrum (CCl_4) showed τ 2.6 (*m*, 5, phenyl), 4.5 (*d*, 1, $J = 1$ Hz, vinylidene H *cis* to phenyl), 4.6 (*d*, 1, $J = 1$ Hz, vinylidene H *trans* to phenyl), and 5.7 (*s*, 2, methylene).

ANAL. Calcd for $\text{C}_9\text{H}_9\text{Br}$: C, 54.85%; H, 4.60%; Br, 40.55%. Found: C, 54.92%; H, 4.50%; Br, 40.82%.

Diethoxymethyl- β -phenallylsilane (V). β -Phenallyl bromide (102 g, 0.518 mole) in 800 ml of anhydrous ether was added dropwise at a rate of one drop/3 sec to a mixture of magnesium turnings (30 g, 1.2 mole) (which had been activated with 0.1 g of iodine), triethoxymethylsilane (173 g, 0.973 mole) and 160 ml of anhydrous ether under a nitrogen purge and anhydrous conditions. The reaction mixture was periodically refluxed during the addition period. Next the mixture was heated at reflux for 5 min and stirred for an additional 6 hr at room temperature. Anhydrous acetone (50 ml) was added, the solution filtered and dried over anhydrous sodium sulfate. Volatile material was removed under vacuum. Distillation through a Vigreux column at $98\text{--}117^\circ\text{C}/0.5$ torr yielded 50 g (mainly V). A higher-boiling fraction of $117\text{--}190^\circ\text{C}/3.5$ torr yielded 22 g (mainly 2,5-diphenyl-1,5-hexadiene). Redistillation through a spinning band column at $114\text{--}115.5^\circ\text{C}/2.2$ torr at a 10:1 reflux ratio yielded 47.0 g (39%) of combined fractions of V, n_D^{25} 1.4930. The NMR (CCl_4) showed τ 2.7 (*m*, 5, phenyl), 4.8 (*d*, 1, $J = 2$ Hz, vinylidene H *cis* to phenyl), 5.0 (*d*, 1, $J = 2$ Hz, vinylidene H *trans* to phenyl), 6.4 (quartet, 4, $J = 7$ Hz, $\text{CH}_2\text{--CH}_3$), 8.0 (*s*, 1, $\text{CH}_2\text{--Si}$), 9.0 (*t*, 6, $J = 7$ Hz, $\text{CH}_3\text{--CH}_2$), and 10.2 (*s*, 3, methylsilane).

ANAL. Calcd for $\text{C}_{14}\text{H}_{22}\text{O}_2\text{Si}$: C, 67.15%; H, 8.85%; Si, 11.21%; mol. wt. 250. Found: C, 67.41%; H, 8.60%; Si, 10.49%; mol. wt. 255.

We wish to acknowledge support of this research by the U.S. Army Research Office, Durham, under Contract DA-31-124-ARO-D-232.

References

1. G. D. Cooper and J. R. Elliot, *J. Polym. Sci. A-1*, **4**, 603 (1966).
2. H. Pines, H. Alul, and M. Kolobielski, *J. Org. Chem.*, **22**, 1113 (1957).
3. F. Ashworth and G. N. Burkhardt, *J. Chem. Soc.*, **1928**, 1791.
4. H. Normant, in *Advances in Organic Chemistry*, Vol. 2, R. A. Raphael, E. C. Taylor, and H. Wynberg, Eds., Interscience, New York, 1960, pp. 1-65.

H. G. GOLLMAR
J. E. MULVANEY

Department of Chemistry
The University of Arizona
Tucson, Arizona 85721

Received June 12, 1970

ERRATUM

Four-Center Type Photopolymerization in the Solid State. IV. Polymerization of α,α' -Dicyano-*p*-benzenediacylic Acid and Its Derivatives

FUSAE NAKANISHI and MASAKI HASEGAWA

[article in *J. Polym. Sci. A-1*, 8, 2151 (1970)]

In Table I, the yield of *n*-propyl ester ($R=COO-n-C_3H_7$) was described as "qualitative." It should be "quantitative."

Contents (continued)

DENNIS C. VAN LANDUYT and SAMUEL F. REED, JR.: Polymerization Studies on 1-Ferrocenyl-1,3-butadiene.....	523
Y. AMERIK, W. F. REYNOLDS, and J. E. GUILLET: Influence of Monomer Concentration on the Structure of Poly(methyl Methacrylate) Polymerized by Butyllithium.....	531
NOTES	
ROBERT C. EVERS: Preparation and Characterization of a Pyrazinobisbenzimidazole Polymer.....	543
J. NIKOKAVOURAS: Synthesis and Study of $-(C_6F_4OCH_2CH_2O)_n-$	553
LESTER T. C. LEE and ELI M. PEARCE: New Polyamides via Ritter Reaction....	557
N. THORNTON LIPSCOMB and WALTER K. MATTHEWS: Reactivity Ratios in the Cationic Polymerization of Styrene and Isoprene.....	563
MASAO MURANO: NMR Studies on Terpolyesters.....	567
H. G. GOLLMAR and J. E. MULVANEY: Preparation of Some Unsaturated Silanes.....	571
ERRATUM.....	575

The *Journal of Polymer Science* publishes results of fundamental research in all areas of high polymer chemistry and physics. The *Journal* is selective in accepting contributions on the basis of merit and originality. It is not intended as a repository for unevaluated data. Preference is given to contributions that offer new or more comprehensive concepts, interpretations, experimental approaches, and results. Part A-1 *Polymer Chemistry* is devoted to studies in general polymer chemistry and physical organic chemistry. Contributions in physics and physical chemistry appear in Part A-2 *Polymer Physics*. Contributions may be submitted as full-length papers or as "Notes." Notes are ordinarily to be considered as complete publications of limited scope.

Three copies of every manuscript are required. They may be submitted directly to the editor: For Part A-1, to C. G. Overberger, Department of Chemistry, University of Michigan, Ann Arbor, Michigan 48104; and for Part A-2, to T. G. Fox, Mellon Institute, Pittsburgh, Pennsylvania 15213. Three copies of a short but comprehensive synopsis are required with every paper; no synopsis is needed for notes. Books for review may also be sent to the appropriate editor. Alternatively, manuscripts may be submitted through the Editorial Office, c/o H. Mark, Polytechnic Institute of Brooklyn, 333 Jay Street, Brooklyn, New York 11201. All other correspondence is to be addressed to Periodicals Division, Interscience Publishers, a Division of John Wiley & Sons, Inc., 605 Third Avenue, New York, New York 10016.

Detailed instructions in preparation of manuscripts are given frequently in Parts A-1 and A-2 and may also be obtained from the publisher.

New Titles in the Polymer Sciences from Wiley-Interscience

ENCYCLOPEDIA OF POLYMER SCIENCE AND TECHNOLOGY

Plastics, Resins, Rubbers, Fibers

Volume 13: Step-Reaction Polymerization to Thermoforming

Executive Editor: NORBERT M. BIKALES, *Consultant*
Editorial Board: HERMAN F. MARK, (*Chairman*),
Polytechnic Institute of Brooklyn
NORMAN G. GAYLORD, *Gaylord Associates, Incorporated*

In recent years, the polymer concept has fused plastics, resins, rubber, fibers, and biomolecules into one body of knowledge. The *Encyclopedia of Polymer Science and Technology* presents the developments, both academic and industrial, that are a result of this fusion.

This latest volume, like the previous, is a collection of authoritative and original articles that were written and reviewed by specialists from all over the world. It comprehensively treats all monomers and polymers, their properties, methods, and processes, as well as theoretical fundamentals.

1970 843 pages (est.) Subscription: \$40.00
Single copy: \$50.00

VINYL AND DIENE MONOMERS

Parts One, Two, and Three

Edited by EDWARD C. LEONARD, *Kraftco Corporation, Glenview, Illinois*

Volume 24 of High Polymers, edited by H. Mark, C. S. Marvel, H. W. Melville, and P. J. Flory

Vinyl and Diene Monomers provides a comprehensive, systematic, and uniform treatment of vinyl and diene monomers.

- Part One describes the manufacture, chemical and physical properties, purification and polymerization behavior of some of the commercially important vinyl monomers. These include acrylonitrile, acrylamides, methacrylic acid and the related esters, vinyl acetate and the higher vinyl esters, and vinyl ethers.
- Part Two parallels the format of Part One, discussing styrene, ethylene, isobutylene, butadiene, isoprene, and chloroprene.
- Part Three similarly treats vinyl and vinylidene chloride, the fluorocarbon monomers, and certain miscellaneous monomers such as N-vinyl compounds, vinyl sulfur compounds, vinylfuran, and certain substituted styrenes.

Part One: 1970 477 pages \$19.95
Part Two: 1971 704 pages \$37.50
Part Three: 1971 432 pages \$24.95

MOLECULAR WEIGHT DISTRIBUTION IN POLYMERS

by LEIGHTON H. PEEBLES, JR., *Chemstrand Research Center, Inc., Durham, North Carolina*

Volume 18 of Polymer Reviews, edited by H. F. Mark and E. H. Immergut

Molecular Weight Distribution in Polymers deals with the question, "How do changes in the manufacturing process affect the molecular weight distribution of the polymers?" Special features include—

- distribution functions that are presented mainly without derivation and with a minimum of commentary on the assumptions used
- standardization of the nomenclature for equations which are illustrated with many examples based on computer calculations
- distributions, derived for polymers with a number-average molecular weight of 100, which may be compared with any other degree of polymerization to a good approximation
- references to the original literature that enable the reader to examine the derivation

1971 352 pages \$17.50

PHYSICAL CHEMISTRY OF ADHESION

By DAVID H. KAEUBLE, *Science Center, North American Rockwell Corporation*

This comprehensive treatment of adhesion phenomena covers thermodynamics, surface chemistry, polymer physics and rheology, as well as specialized topics in the mechanics of fracture.

Physical Chemistry of Adhesion is divided into three major sections. The first section, on surface chemistry, emphasizes the analysis of contact angle experiments. The second section, on rheology, presents the significance of thermal expansivity and compressibility measurements in defining the polymer physical state. The third section, on fracture mechanics, analyzes six basic rheological operations, and deals directly with the phenomenological and engineering aspects of adhesion and cohesion phenomena.

1971 528 pages \$27.50

wiley

WILEY-INTERSCIENCE

a division of JOHN WILEY & SONS, Inc.
605 Third Avenue, New York, New York 10016

In Canada:
22 Worcester Road, Rexdale, Ontario